universität wien

DISSERTATION / DOCTORAL THESIS

Titel der Dissertation / Title of the Doctoral Thesis

'Kinetic Modelling of Colonies of Myxobacteria'

verfasst von / submitted by

Laura Kanzler, BSc MSc

angestrebter akademischer Grad / in partial fulfillment of the requirements for the degree of

Doktorin der Naturwissenschaften (Dr. rer. nat.)

Wien, 2021 / Vienna 2021

Studienkennzahl lt. Studienblatt / degree programme code as it appears on the student record sheet:	A 796 605 405
Studienrichtung lt. Studienblatt / degree programme as it appears on the student record sheet:	Mathematik
Betreut von / Supervisor:	Univ.-Prof. Dr. Christian Schmeiser

'Remember, everything is right until it's wrong. You'll know when it's wrong.'
'You think so?'
'I'm quite sure. If you don't, it doesn't matter. Nothing will matter then.'

Ernest Hemingway ('The Garden of Eden')

Danksagungen/Acknowledgements

My first an greatest thanks belong to my supervisor Prof. Christian Schmeiser and this not only for his patient guidance through my PhD. Indeed, I was lucky to have him as a teacher and mentor already during my undergraduate studies. Starting with his lecture "Enführung in die Analysis" during my first semester and followed by several other courses and seminars he inspired and supported me in finding and pursuing my mathematical interests and in the end gave me the the opportunity to work with him on this very beautiful subject, matter of this thesis. From the beginning, he guided me to become the mathematician I am today.

Further, I want to thank my collaborators Sabine Hittmeir and Angelika Manhart for our (not only) scientific discussions, which were a huge help in orienting myself in the academic world, especially at the beginning of my PhD. Also I want to express my gratefulness to Amic Frouvelle for collaborating with us, which resulted in very fruitful scientific input to be found in a part of this thesis. Moreover, I want to thank Veronica Tora on one hand for our scientific exchange, which's outcome also forms a chapter of this manuscript, but as well for many discussions about several other things.

I also thank Axel Klar and Barbara Niethammer for agreeing to be reviewers of this thesis.

Furthermore, I want to show my gratitude to Prof. Radu Ioan Boţ not only for introducing and guiding me to the world of optimization, another research field I found great passion in, but -above all- for being a mentor on who's support and advice I could always count.

During my years at the University of Vienna I had the chance to meet many interesting and inspiring people, who somehow took part in my journey to the PhD. Some accompanied me longer, some just for a short -not less important- time and some stayed until the end. I therefore especially want to mention my former fellow students and friends Manveer and Annemarie, accompanying and supporting me during all the years of my undergraduate and -even though our mathematical interests lead us in totally different directions- graduate studies. Further, many thanks to my study-, teaching-, office-, climbing- and drinking-buddy Paul. Thinking back to the first semester of our undergraduate studies: Who would have thought that we end up as office mates during the PhD!?

I would further like to express my thanks to the friends and colleagues I got to know during my doctoral studies. On one hand for all the scientific and political discussions, but on the other hand also for a lot of fun and precious moments during coffee breaks, lunches and summer/winter schools, which delighted my working days every time. Thank you, Axel, Michael, Max, Bea, Pietro, Annalisa, Gianluca, Gaspard, Lara, Alexandra, Helene, David and Melanie! Also I'm grateful for all the administrative help from Matteo and Bettina.

Among the people I got to know during my doctoral studies, I am especially grateful to have met my PhD sister and also friend Julia right at the beginning of my doctoral studies so that we could go through the PhD together. No other person made me feel so much understood and supported in all my concerns. Further, I am deeply indebted to my dear friend Giulia, who managed to open my view of the world, being able to now seeing it in a lot more different facets. I am grateful for all of our (math- and nonmath-) conversations, Yoga-sessions, climbing- as well as travel- adventures and, above all, for our friendship.

Also, I am very thankful for finding in Michi a colleague and friend, with whom I enjoy the perfect combination of fruitful scientific exchange and having also a lot of fun beside work. (Moreover, thank you for often pushing me out of my comfort zone, highly needed sometimes!) Last, I want to express special thanks to Idriss for his support, patience, advice, help and actually just for being there, when-

ever needed, during the final phase of my doctoral studies. *Merci beaucoup!*

All of this would not have been possible without the endless support I received from my family and friends away from university, embracing and me and cheering me up in the "real world", whenever I had to face difficulties in my professional one. I specially want to thank my lifetime-friends:

Philipp, für die die moralische Unterstützung und unsere langen und intensiven Gedankenaustausche, die mich immer wieder zur Selbstreflexion bringen und die auch großen Einfluss auf meinen Zugang zum wissenschaftlichen Arbeiten haben.

Meiner besten Kaffee-/Tattoo-Schwester Lisa, für die vielen verrückten, unvergesslichen Momente, nicht nur im Jahr 2018 ;) ¡Chicas Austriacas locas para siempre!

Marion, die meine Ansprechpartnerin für einfach wirklich alles ist, und das um jede Tages- und Nachtzeit. Seien es politische, wissenschaftliche, pferdige oder sentimentale Themen, sie hat immer ein offenes Ohr und das schon seit vielen, vielen Jahren. Auf viele weitere gemeinsame Erlebnisse, wo es uns auch immer hinziehen mag ;)

Last, I want to thank the ones, who kept me sane during the most difficult times: My family. *Besonders dabei den wunderbaren Pferden Honey und Sweety, die mich sprichwörtlich durch mein gesamtes Studium getragen haben. Und natürlich meinen Eltern, denen ich diese Dissertation widme. Mama & Papa, danke für so vieles, aber vor allem, dass ihr ohne eine Sekunde zu zögern immer für mich da seid, auch wenn es nicht immer leicht für euch ist!*

Kurzfassung

Myxobakterien sind stäbchenförmige sich auf flachen Oberflächen durch Gleiten fortbewegende Einzeller. Durch ihr kollektives Verhalten sind sie in Paradebeispiel, wie einfache Interaktionen zwischen einzelnen Bakterien zu emergenten, makroskopischen Bewegungsmustern führen können. Von Biologen beobachtetes Bewegungsverhalten einzelner Zellen ist einerseits das Gleiten mit annähernd konstanter Bewegungsgeschwindigkeit und Bewegungsrichtung, sofern das Bakterium nicht in Interaktion mit einem anderen Individuum steht. Andererseits, wenn es zu Kollision zwischen Individuen kommt, dann wurden Umkehrung der Bewegungsrichtung sowie das sich einander Ausrichten der involvierten Bakterien beobachtet. Diese Dissertation lässt sich in vier Abschnitte unterteilen.

Einerseits wird in dieser Doktorarbeit ein neues kinetisches Modell für Kolonien von Myxobakterien hergeleitet und untersucht, das Ähnlichkeit zur Boltzmanngleichung hat. Es wird Existenz und Eindeutigkeit, sowie, in einem speziellen Setting, exponentielles Abklingen zum Equilibrium für die räumlich homogene Version der Gleichung gezeigt.

Weiters, wird eine Modellerweiterung mit zusätzlicher Brown'scher Bewegung der Individuen während der Phase des freien Gleitens betrachtet. Auf dem kinetischen Level drückt sich dies durch einen Diffusionsterm, lediglich in Bewegungsrichtung, aus. Auch hier wird Existenz und Eindeutigkeit einer Lösung gezeigt, sowie das Bifurkationsverhalten bezüglich des Diffusionsparameters bestimmt.

Ferner ist die kinetische Gleichung, die lediglich die Umkehrreaktionen zwischen zwei Bakterien separat modelliert, Gegenstand der Untersuchung. Auch hier konnte neben Existenz einer Lösung, exponentielles Abklingen dieser zu einem symmetrischen Equilibrium bewiesen werden. Dieses Resultat konnte für eine große Klasse an metrischen Räumen mit einer gewisser Symmetriestruktur abstrahiert werden.

Die Modellannahme, dass die Zweibakterien-Stöße instant passieren, ist, obwohl Standard in der kinetischen Modellierung, biologisch nicht ganz korrekt. Dies war Inspiration, eine kinetische Gleichung für nicht-instante Interaktionen zwischen Partikel herzuleiten, was ein komplett neuer Zugang in der kinetischen Modellierung ist. Das Modell besteht aus zwei Gleichungen: Eine beschreibt die Dynamik der Teilchen, die sich gerade in der Freiflug-Phase befinden. Die zweite gibt Information über das Verhalten von Paaren von Partikel, die sich in einem Kollisionsprozess befinden, in dem sie sich einander ausrichten. Auch hier wurden Existenz einer Lösung des Systems, sowie Konvergenz zu einem Equilibirum gezeigt. Ferner wurde das Model im instanten Limes untersucht, d.h. das Verhalten des Systems, wenn man die Kollisionszeit gegen Null konvergieren lässt.

Abstract

Myxobacteria are rod-shaped, social bacteria that are able to move on flat surfaces by „gliding“ and form a fascinating example of how simple cell-cell interaction rules can lead to emergent, collective behavior. Observed movement patterns of individual bacteria include straight runs with approximately constant velocity, alignment interactions and velocity reversals.

In this doctoral thesis a new kinetic model of Boltzmann-type for colonies of myxobacteria will be derived and investigated. An existence and uniqueness result is shown for the spatially homogeneous equation as well as exponential decay to an equilibrium in a special setting.

Further, the model extension with additional consideration of Brownian forcing to the free flight phase of single bacteria, which then gives rise to a directional diffusion term at the level of the kinetic equation, is matter of investigation. Besides an existence result, bifurcation behavior with respect to the diffusion parameter is characterized.

Considering the model with just reversal interactions between agents, existence as well as exponential convergence to a symmetric equilibrium is proved. This result could be generalized to an abstract setting for reversal dynamics on a broad class of metric spaces equipped with a suitable symmetry structure.

Moreover, the urge to overcome the simplification of instantaneous binary bacterial collisions, standard in kinetic modelling, was inspiration to introduce a kinetic model for time-resolved binary interactions between individuals, a completely novel approach in kinetic theory. The proposed model consists of a system of two equations, one for the distribution of particles in free flight, one for the distribution of pairs of particles in an alignment collision process. Existence of solutions as well as convergence to equilibrium are shown. Further, the instantaneous limit is performed, from which a kinetic equation modelling instantaneous alignment collisions between particles is recovered and investigated.

Contents

1 General Introduction **1**
- 1.1 Biological Motivation: Myxobacteria as an example for emergent phenomena . . . 3
- 1.2 Mathematical Framework: Kinetic Theory . . . 5
  - 1.2.1 Derivation of the kinetic equation . . . 5
  - 1.2.2 Entropy methods . . . 7
- 1.3 Main Contribution of this Thesis . . . 9
  - 1.3.1 Kinetic Model for Colonies of Myxobacteria . . . 9
  - 1.3.2 Kinetic Model for Myxobacteria with Directional Diffusion . . . 13
  - 1.3.3 Reversal Collision Dynamics in a General Domain . . . 16
  - 1.3.4 A Kinetic Model for Non-instantaneous Binary Collisions . . . 18
- 1.4 Declaration of Authorship . . . 22

2 Kinetic Modelling of Colonies of Myxobacteria **27**
- 2.1 Introduction . . . 27
- 2.2 Model derivation . . . 29
- 2.3 Properties of the collision operator . . . 35
- 2.4 The spatially homogeneous problem . . . 37
- 2.5 Numerical Simulations . . . 42
- 2.6 Formal macroscopic limit . . . 44

3 Kinetic Model for Myxobacteria with Directional Diffusion **53**
- 3.1 Introduction . . . 53
- 3.2 Decay to the uniform equilibrium . . . 56
  - 3.2.1 Spectral stability by hypocoercivity . . . 56
  - 3.2.2 Nonlinear stability of the uniform equilibrium . . . 60
- 3.3 Existence and Stability of Equilibria for the Spatially Homogeneous Equation . . . 62
  - 3.3.1 Bifurcation Analysis . . . 62
  - 3.3.2 Existence of Equilibria for Small Diffusivity . . . 66
- 3.4 Numerical Simulations . . . 69

4 Reversal Collision Dynamics **81**
- 4.1 Introduction . . . 81
- 4.2 Properties of the collision operator . . . 82
- 4.3 Asymptotic behavior . . . 83
- 4.4 Reversal collisions on the torus $\mathbb{T}^1$ . . . 90
- 4.5 Numerical simulations . . . 91

5 A Kinetic Model for Non-instantaneous Binary Collisions **95**
- 5.1 Introduction . . . 95

5.2 Kinetic Equation for Time-resolved Alignment Collisions with Stochastic Collisions Dynamics . . . 96
5.2.1 Conservation laws and equilibria . . . 98
5.2.2 Existence and uniqueness of solutions . . . 101
5.2.3 Convergence to equilibrium . . . 103
5.2.4 Instantaneous limit . . . 105
5.3 Kinetic Equation for Time-resolved Alignment Collisions with Deterministic Collisions Dynamics . . . 113
5.3.1 Conservation laws and equilibria . . . 115
5.3.2 Instantaneous limit . . . 116

1 General Introduction

> I begin with an idea and then it becomes something else.
>
> Pablo Picasso

Contents

1.1 Biological Motivation: Myxobacteria as an example for emergent phenomena . . . 3
1.2 Mathematical Framework: Kinetic Theory . . . 5
1.2.1 Derivation of the kinetic equation . . . 5
1.2.2 Entropy methods . . . 7
1.3 Main Contribution of this Thesis . . . 9
1.3.1 Kinetic Model for Colonies of Myxobacteria . . . 9
1.3.2 Kinetic Model for Myxobacteria with Directional Diffusion . . . 13
1.3.3 Reversal Collision Dynamics in a General Domain . . . 16
1.3.4 A Kinetic Model for Non-instantaneous Binary Collisions . . . 18
1.4 Declaration of Authorship . . . 22

This thesis is dedicated to the derivation and study of mathematical models describing the movement behavior of colonies of myxobacteria on flat substrates. Proved to be an accurate modelling approach for such biological phenomena, we choose the kinetic setting as a mathematical framework. Trying to encompass as many biological aspects as possible, we study four nonlinear kinetic partial differential equations arising from our considerations.

The first model, which is the subject of Section 1.3.1 in this introduction, resp. Chapter 2 of the manuscript, is a *kinetic transport equation of Boltzmann-type* for the distribution function $f(x, \varphi, t)$ for bacteria at position $x \in \mathbb{R}^2$, moving in direction $\varphi \in \mathbb{T}^1$ at time $t \geq 0$, and has the form

$$\partial_t f + \omega(\varphi) \cdot \nabla_x f = 2 \int_{\mathbb{T}^1_{AL}} b(\tilde{\varphi}, \varphi_*) \left(\tilde{f} f_* - f \tilde{f}_* \right) d\varphi_* + \int_{\mathbb{T}^1_{REV}} b(\varphi^{\downarrow}, \varphi^{\downarrow}_*) \left(f^{\downarrow} f^{\downarrow}_* - f f_* \right) d\varphi_* \,, \tag{1.1}$$

where $\omega(\varphi) = (\cos\varphi, \sin\varphi)$, $\tilde{\varphi} = 2\varphi + \varphi_*$, $\varphi^{\downarrow} = \varphi + \pi$ and $\mathbb{T}^1$ denotes the one-dimensional flat torus of length 2π. The model describes motion along straight lines with fixed speed in direction φ, interrupted by instantaneous binary collisions with collision cross-section $b(\varphi, \varphi_*)$, giving information about the collision frequency. As usual, sub- and super-scripts on f indicate evaluation at φ with the same sub- and super-scripts. The two different collision terms on the right hand side correspond to the two different types of bacterial collisions considered: Alignment and Reversal. $\mathbb{T}^1_{AL} \subset \mathbb{T}^1$ and $\mathbb{T}^1_{REV} \subset \mathbb{T}^1$ denote the sets of alignment- resp. reversal- collision partners of bacteria moving in direction φ.

In the second problem, corresponding to Section 1.3.2 of the general introduction and Chapter 3 of the thesis, we study a model extension of (1.1) featuring *Brownian forcing* in the free flight phase of

bacteria. This results as a directional diffusion term in the kinetic equation, which then has the form

$$\partial_t f + \omega(\varphi)\cdot\nabla_x f = \mu\partial_\varphi^2 f + 2\int_{\mathbb{T}^1_{AL}} b(\tilde{\varphi},\varphi_*)\left(\tilde{f}f_* - f\tilde{f}_*\right)d\varphi_* + \int_{\mathbb{T}^1_{REV}} b(\varphi^\downarrow,\varphi_*^\downarrow)\left(f^\downarrow f_*^\downarrow - f f_*\right)d\varphi_*\,. \quad (1.2)$$

The constant $\mu > 0$ in (1.2) describes the diffusion intensity.

The third equation, detailed out in Section 1.3.3 and further in Chapter 4, we analyze is of the following shape

$$\partial_t f = \int_{x*\in\mathcal{C}[x]} b(x,x_*)\left(f^\downarrow f_*^\downarrow - f f_*\right)dx_*\,, \quad (1.3)$$

which describes the evolution of the distribution function $f = f(x,t)$ of the dynamical states of individual particles x in a probably abstract metric space $\mathcal{S}$ at time $t > 0$, undergoing reversal collisions

$$(x,x_*) \longrightarrow (x^\downarrow, x_*^\downarrow).$$

We assume $\mathcal{S}$ to be equipped with a symmetric structure that allows to define an *inclusion* $x^\downarrow$ for all $x \in \mathcal{S}$. Also here we use the notation $f^\downarrow = f(x^\downarrow,t)$ and $f_* = f(x_*,t)$. By $\mathcal{C}[x] \subset \mathcal{S}$ we denote the set of collision partners for a particle $x \in \mathcal{S}$. For the case $\mathcal{S} = \mathbb{T}^1$ equation (1.3) corresponds to the spatially homogeneous model (1.1) with just the reversal collision operator on the right hand side, where it was inspired from.

The forth and last problem, corresponding to Section 1.3.4 in this introduction and Chapter 5 of the manuscript, we consider the following system of two coupled equations:

$$\begin{aligned}
&\partial_t f + \omega(\varphi)\cdot\nabla_x f(\varphi) = 2\Big(\gamma\int_{\mathbb{R}} g(\varphi,\varphi_*)\,\mathrm{d}\varphi_* - \lambda f(\varphi)\int_{\mathbb{R}} b(\varphi,\varphi_*)f(\varphi_*)\,\mathrm{d}\varphi_*\Big)\,,\\
&\partial_t g + \nabla\cdot(V(\varphi,\varphi_*)g(\varphi,\varphi_*)) = \lambda b(\varphi,\varphi_*)f(\varphi_*)f(\varphi) - \gamma g(\varphi,\varphi_*)\,,
\end{aligned} \quad (1.4)$$

where $f = f(x,\varphi,t)$ describes the distribution function of single particles in free flight at position $x \in \mathbb{R}^2$, time $t > 0$ and moving with constant speed and velocity ω depending on their property $\varphi \in \mathbb{R}$. While $b(\varphi,\varphi_*)$ again describes the collision cross section, the constant $\lambda > 0$ stands for the rate at which binary collisions between individuals happen. The function $g(x,\varphi,\varphi_*,t)$ stands for pairs of particles with properties φ and φ_*, which are in a collision process given by the potential $V(\varphi,\varphi_*)$. Pairs separate with rate $\gamma > 0$. Equation (1.4) therefore models dynamics of an ensemble of particles undergoing *non-instantaneous binary collisions*, a fairly new approach in kinetic theory.

Main objectives and organization of the manuscript: Once derived or stated, the main driving question regarding these models (1.1)-(1.4) is on one hand the one of *well-posedness* of these problems. On the other hand we aim to qualify the *asymptotic behavior* of solutions and compare it to the biological observations in order to to give validation of the proposed models.
The organization of this introductory Chapter is the following: In Section 1.1 we give an overview over the considered biological phenomenon -myxobacteria- and further about emergence phenomena in general. The following Section 1.2 is dedicated to introducing the mathematical framework -kinetic theory- these models are set in, where methods and tools are motivated and explained. In Section 1.3 the equations (1.1)-(1.4) are explained in more detail with emphasis on their mathematical difficulties and tools to handle them.

1.1 Biological Motivation: Myxobacteria as an example for emergent phenomena

Biological phenomenon myxobacteria: Myxobacteria, from Greek 'myxo' (slime), are rod-shaped, social bacteria that live in cultivated soil and feed on insoluble organic substances including bacteria and eukaryotic microbes. Acting as scavengers cleaning up biological detritus makes them play an important role in maintaining balance in the environment. They have a fascinating life cycle, similar to certain amoebae, called cellular slime molds (with *Dictyostelium discoideum* as the best known example). During their vegetative growth phase they move as predatory swarms searching and killing prey collectively, while under starvation conditions they aggregate and form fruiting bodies, which produce spores that are more likely to survive until nutrients are more plentiful again.

Myxobacteria are specially known for their *gliding* movement on flat substrates, which was observed in laboratory conditions (e.g. on agar-agar) [35], leaving a slime-trail behind them. This behavior was eponymous for these kind of bacteria. The physical mechanism as well as the genetic basis are still partly a puzzle to microbiologists and have already challenged them for several decades [24, 36, 44, 46].

During their vegetative growth phase, while hunting and killing pray collectively, as well as during their aggregation phase, bacteria form organized mono- or multi-layered groups called *swarms*. During the swarming process the so-called *rippling* phenomenon is observed, i.e., macroscopic patterns due to propagating waves of aligned bacteria [27, 28]. From a macroscopic point of view such waves of aligned bacteria seem to travel unaffectedly through each other when colliding frontally. However, it was revealed by tracking individual bacteria [40, 45] that most cells reverse their direction in the collision process, while preserving a nematic alignment order. In other words: Locally myxobacteria are oriented and move in the same or in opposite directions.

Large scale pattern formation requires signaling between individual cells on a microscopic level. The signaling mechanism for myxobacteria, which is most important for cell aggregation and rippling is called *C-signaling* [40]. Unlike many other signaling mechanism based on diffusing chemical substances, C-signaling relies on the *C-factor,* a protein bound to the cell surface. These protein is interchanged between individuals, where it has been observed that direct cell-cell contact is necessary for C-signaling [29, 30].

Emergence phenomena: Myxcobacteria are a fascinating example how simple individual based interactions can lead to large scale collective behavior. This phenomenon is known as *emergence* (from Latin 'emergere' meaning 'to surface', 'to emerge') and corresponds to the appearance of macroscopic structures caused by underlying microscopic dynamics of a huge assemble of individuals. Emergence is ubiquitous in nature and occurs for example in collective dynamics of bird flocks, fish schools [38], crowds of pedestrians [23], but also can be seen in network formation [25], opinion dynamics [19] or tissue growth [37]. All these examples have in common that at the microscopic level single individuals or agents (e.g. cells, animals, etc.) interact with each other following intrinsic rules. These microscopic fluctuations lead to macroscopic structures, which, however, are not encoded directly in these individual based dynamics. The main challenge therefore is given by finding an explanation how the macroscopic or observable dynamics emerge from the microscopic ones.

The *kinetic or mesoscopic description* of such an assemble often serves as mathematical tool forming the bridge between the transition from microscopic scale at the level of each agent to the large scale realized at the level of the whole group. Applying this methodology of kinetic theory to describe self-organization phenomena in life sciences is still a fairly young discipline, which gained popularity over the last years. One of the earliest approaches to capture such emergence phenomena on the

microscopic level is the Vicsek model [41] introduced in 1995 as well as variations of it, which have received much attention over the years. Although being of minimal structure it gives an accurate description for a wide range of phenomena in life sciences. The time-dependent Vicsek model describes motion of self-propelled agents along straight lines with constant speed, interrupted by adjustment of the agent's direction towards the mean direction of the individuals in its neighborhood at specific time steps, subject to some random perturbation. In 2006 a Boltzmann-like model has been proposed as a kinetic description of the Vicsek particle model [5]. Starting from a microscopic bidimensional model of self-propelled particles with noisy and local interaction rules tending to align the velocities the authors analytically performed the phase-transition to hydrodynamic equations for the density and velocity fields within a Boltzmann approach. Also this model gained much attention in the last years [4, 5, 10, 13] due to its ubiquitousness in its application.

Also the emergence phenomenon specifically in colonies of myxobacteria has been motivation to formulate kinetic theories for interacting self-propelled rods [2, 3]. In [14] a kinetic model has been formulated, which produces relaxation to nematically aligned states. The model is of mean field type, i.e., cell-cell signaling is modeled as a nonlocal process. Simulations with the macroscopic limit do not produce the rippling phenomenon. Including a waiting time until an individual can reverse again seems to be necessary to observe the desired behavior [15, 26, 27, 28].

1.2 Mathematical Framework: Kinetic Theory

A typical way to describe dynamics of a many agents-system is by stating ordinary differential equations for the evolution of the time-dependent state $z = z(t), t \geq 0$ of each individual. With Γ we denote the state-space for the assemble of N agents, which includes usually a *non-overlapping constrain*. For example in the situation of physical particles, where the states $z = (x, v)$ are usually given by position $x \in \mathbb{R}^d$ and velocity $v \in \mathbb{R}^d, d = 2, 3$, this *microscopic description* of the system is governed by *Newton's laws of motion*. Although very precise, the disadvantage of this approach is the enormous number of involved particles, which makes the state of the huge system practically intractable with respect to time. From a numerical point of view it would involve high computational costs, hardly performable by modern super computers. On the other hand, the *macroscopic description* of particles consists of observable quantities, often position-dependent as the density, mean velocity or in the case of physical systems also temperature and pressure, which has the disadvantage of loosing precision. The link between the microscopic laws and the macroscopic behavior is often difficult to establish.

As indicated in Section 1.1 the mathematical tools for studying emergence with aim to overcome the just mentioned difficulties come from *kinetic theory*. This builds the bridge between the microscopic and the macroscopic description of the dynamics of an assemble of particles by stating a *statistical description* of the particle system. This *kinetic* or also called *mesoscopic* description was originally developed in the field of mathematical physics, more precisely in the field of gas dynamics. Being introduced first by *Boltzmann* [7], in his study of gas dynamics, and *Maxwell* [33], while investigating the stability of Saturn's Rings. After being established, this statistical description of many particle systems gained popularity soon, although it also was matter of great discussion, criticized mostly by opponents of the atomic theory in the late 19th century.

1.2.1 Derivation of the kinetic equation

The main concept of kinetics is to introduce a (probability) distribution function $f(z, t) \geq 0$ of a single agent (interpreted as particle), which encodes the density at a state z in the state space (usually a position-velocity space), at time $t \geq 0$. The quantity $f(z, t)dz$ then represents the number of particles in the volume element dz.

One way to derive an equation for such a quantity f starting from microscopic interaction rules is following Boltzmann in his formal derivation of the *Boltzmann equation for hard sphere dynamics* [7], which is also the method we chose to derive the kinetic model for myxobacteria dynamics (1.1), see section 1.3.1 of this introduction, or Chapter 2 in the manuscript. In the following we explain the main ideas in a general framework. In order to place ourselves in an appropriate setting for this demonstration, we assume a (probably very huge) number of N particles with states of the form $\Gamma \ni z_i = (x_i, v_i), i \in \{1, \dots, N\}$, given by a particle's position x_i and its velocity v_i, both from a position- resp. velocity space, which are subsets of $\mathbb{R}^d$. The individual based dynamics shall be given by

$$\frac{dx_i}{dt} = v_i, \quad \frac{dv_i}{dt} = 0,$$

interrupted by *instantaneous binary collisions* which cause velocity jumps subject to invertible collision rules. Let further the state space Γ be such that *no overlapping* in position between agents is allowed. Introducing a time-dependent probability density function $P(z_1, \dots, z_N, t) \geq 0$ and deriving P with respect to time we obtain the following *Liouville equation*

$$\partial_t P(z_1, \dots, z_N, t) + \sum_{i=1}^{N} v_i \cdot \nabla_{x_i} P(z_1, \dots, z_N, t) = 0. \tag{1.5}$$

Integrating (1.5) over $\Gamma^1(z) := \{(z_2, \dots, z_N) : (z, z_2, \dots, z_N) \in \Gamma\}$ gives an evolution equation for the one-particle distribution function

$$P_1(z,t) := \int_{\Gamma^1(z)} P(z, z_2, \dots, z_N, t) \prod_{i=2}^{N} dz_i \,,$$

the first marginal of P. Important to mention here is the *indistinguishability property*-assumption we take on the assemble of particles, which means that interchanging two individuals doesn't effect the dynamics of the whole system. Therefore, the choice of the particle's index, with respect to which we define the first marginal, is insignificant. After additional use of the *divergence theorem* the equation for P_1 is of the form

$$\partial_t P_1 + v \cdot \nabla_x P_1 = Q(P_2), \tag{1.6}$$

where $Q(P_2)$ denotes an integral over the boundary of Γ, where particles overlap due to a collision. Since the boundary of Γ consists of an ingoing (post-collisional) and an outgoing (pre-collisional) part, $Q(P_2) = G(P_2) - L(P_2)$ can be separated into a gain-term $G(P_2)$ and a loss-term $L(P_2)$. Therefore, in the gain-term $G(P_2)$ the integrand P_2 is evaluated at post-collisional states and in the loss-term $L(P_2)$, P_2 is evaluated at pre-collisional states. The unknown P_2 is defined as the second marginal of P:

$$P_2(z, z_*, t) := \int_{\Gamma^2(z,z_*)} P(z, z_*, z_3, \dots, z_N, t) \prod_{i=3}^{N} dz_i \,,$$

where $\Gamma^2(z, z_*) := \{(z_3, \dots, z_N) : (z, z_*, z_3 \dots, z_N) \in \Gamma\}$. This makes (1.6) a not closed problem. An attempt to close this equation by deriving an equation for the two-particle probability density P_2 would include P_3, the three-particle probability density, on its right-hand-side, the same way as an evolution equation for P_k includes P_{k+1}, $k \in \{3, \dots, N-1\}$. This results in a completely coupled system for the marginals $P_k, k \in \{1, \dots, N\}$, known as the *BBGKY-hierarchy* [11]. After rewriting the post-collisional evaluation of P_2 in the gain-term $G(P_2)$ in terms of pre-collisional states, which is possible since we assume invertible collisions, and a proper rescaling of (1.6), we perform the *Boltzmann-Grad limit* [20].

Remark 1.1. *We may note here, that the representation of G in terms of pre-collisional states is essential, since otherwise the right-hand-side would formally go to zero in the limit. The question why this is the correct choice is fairly nontrivial, for further insights we refer the reader to [11].*

The Boltzmann-Grad limit is characterized by letting the number of particles go to infinity, i.e. $N \to \infty$, the size of the particles go to zero, while the ratio of the interaction-range to the *mean free path* (average travel-distance between collisions) of particles remains fixed. The derivation of the Boltzmann equation further involves the *molecular chaos assumption*, first introduced by Maxwell in [34], stating that in the limit two colliding particles are uncorrelated, which yields that P_2 becomes a product of the one-particle densities:

$$P_1(z,t) \longrightarrow f(z,t), \quad P_2(z, z_*, t) \longrightarrow f(z,t) f(z_*, t).$$

Finally, formally performing the limit, equation (1.6) becomes

$$\partial_t f + v \cdot \nabla_x f = Q(f, f), \tag{1.7}$$

a kinetic equation, similar to the Boltzmann equation for hard sphere dynamics, and describing the evolution of the expected particle density function $f = f(x, v, t)$. While the left-hand-side of (1.7) describes transport of particles with their velocity v, the operator Q on the right-hand-side is an integral operator and accounts for the interaction between particles, therefore also quadratic in f.

It should be emphasized here that molecular chaos is an assumption, which cannot be produced by the dynamics of the system of particles itself, since a collision would imply correlation between the two interacting particles. One major step in performing the above illustrated limit rigorous, is proving *propagation of chaos*, i.e. that for an initially chaotic state this property is conserved in time, where a first result was obtained by Lanford in [31].

For further insight into the derivation of the Boltzmann equation, also in a rigorous manner, including several aforesaid remarks, we refer the reader to [11].

1.2.2 Entropy methods

Entropy (from Greek 'entropía' meaning 'transformation'), describes a measure for energy dispersal or molecular disorder. Its concept was first introduced by *Claudius* in 1865 as physical quantity in a thermodynamcal context measuring the amount of energy no longer usable for work (second law of thermodynamics) in [9]. Few years later, in the 1870s, statistical descriptions were proposed by *Boltzmann, Gibbs* and *Maxwell*. In 1877 [8] *Boltzmann's* statistical interpretation for the second law of thermodynamics, given by the famous formula

$$S = k \log W,$$

combined the thermodynamical and the statistical interpretations of entropy. It states that the entropy S of a system is proportional to the logarithm of W, the number of ways the distribution of particles can be constructed,

Other than in physics, where the molecular chaos can only increase in time, the *mathematical entropy* is defined as a nonincreasing function, the negative physical entropy. This concept gained interest as mathematical tool starting in the mid/end of the 20th century by, e.g., *Lax* in 1971 who defined entropy solutions for hyperbolic conservation laws [32], by *Bakry* and *Émry* in 1985 for the large time behavior in stochastic processes [1] and, in the kontext of kinetic equations, Boltzmann's $\mathcal{H}$-functional is used for obtaining a priori estimates for solutions of the Boltzmann equation by *DiPerna* and *Lions* in 1989 [17] and for large time behavior of its solutions by *Desvillettes* [16], just to name a few.

Decay to equilibrium: In order to characterize the asymptotic behavior of the proposed models (1.1)-(1.4) the crucial ingredients are *entropy* and *entropy/entropy-dissipation inequalities*, which in this section will be presented in a quite general framework. These ideas will be applied in several aspects and situations to all problems described in this thesis.

The main task is given by finding convex quantities connected to some intrinsic properties of the considered model, which are nonincreasing along solutions of the corresponding equation or system of equations. In the optimal case they will serve as Lyapounov functional for the differential equation, from which decay to a steady state, in a suitable topological framework can be deduced. This can be optimized by finding explicit decay-rates. To be more precise, for a differential equation of a general form

$$\partial_t f = F(f), \quad t \geq 0, \tag{1.8}$$

where the right-hand-side F can be thought of being a sum of differential- and integral-operators, we are searching for functionals $\mathcal{E}(t) = \mathcal{E}[f(t)] \to \mathbb{R}$, such that for the *entropy dissipation* we have

$$\frac{d}{dt}\mathcal{E}[f(t)] =: -\mathcal{D}[f(t)] \leq 0,$$

along solutions $f(t)$ to (1.8). Let further f_∞ be a unique *equilibrium* of (1.8), i.e. $F(f_\infty) = 0$, then we may further ask for the condition $\mathcal{E}[f_\infty] \leq \mathcal{E}[f(t)]$, for all $t \geq 0$. Interpreting the *relative entropy* $\mathcal{E}\left[f(t)|f_\infty\right] := \mathcal{E}[f(t)] - \mathcal{E}[f_\infty]$ as a measure for distance (in an appropriate topological setting the problem is posed) between the solution f and the steady state f_∞, the relation

$$\frac{d}{dt}\mathcal{E}[f(t)|f_\infty] = -\mathcal{D}[f(t)] \leq 0,$$

already shows that a trajectory $f(t)$ can not move further away from the equilibrium than it was initially. The optimal situation would be to find an inequality of the form

$$\mathcal{D}[f(t)] \geq \kappa \left(\mathcal{E}[f(t)] - \mathcal{E}[f_\infty]\right), \tag{1.9}$$

for a constant $\kappa > 0$. Exponential decay of $\mathcal{E}[f(t)|f_\infty]$ to zero with rate κ then follows immediately from (1.9). In a situation where the relative entropy even controls the distance of f to f_∞ in the norm $\|\cdot\|$ of the space equation (1.8) is set in, i.e.

$$\|f - f_\infty\| \leq c \left(\mathcal{E}[f(t)] - \mathcal{E}[f_\infty]\right), \quad c > 0,$$

inequality (1.9) can be seen as *coercivity* property of the entropy dissipation $\mathcal{D}$, also called *Poincaré inequality* in analogy to diffusion processes. In this case $\mathcal{E}[f(t)|f_\infty]$ serves as Lyapunov functional, from which decay of $f(t)$ to equilibrium f_∞ can be concluded.

Even in absence of this coercivity property of the entropy dissipation some situations allow decay to equilibrium, a concept which is known as *hypocoercivity*. This concept, after being first introduced in [22, 42], recently became matter of high interest in the kinetic community, e.g. see [18], [21]. We may now demonstrate a standard, but quite general situation of a hypocoercive differential equation. We write F of the right-hand-side in equation (1.8) as

$$F = F_D + F_I,$$

sum of a *dissipate operator* F_D, fulfilling

$$\mathcal{D}[f(t)] = -\mathcal{E}'[f]F_D(f)$$

and an *invariant operator* F_I with

$$\mathcal{E}'[f]F_I(f) = 0,$$

where $\mathcal{E}'[f]$ denotes the Fréchet-derivative of the entropy $\mathcal{E}$. Further we assume that the stationary state f_∞ is a global equilibrium, meaning that it is in the nullspace of both F_D and F_I, i.e. $F_D(f_\infty) = F_I(f_\infty) = 0$. This implies that the entropy $\mathcal{E}[f]$ already stops decaying if f reaches $\mathcal{N}(F_D)$, the nullspace of the dissipative part F_D, also called the set of local equilibria of (1.8). The information for convergence to the global equilibrium f_∞ therefore also has to come from the invariant part F_I, supposed that $\mathcal{N}(F_D)$ is not invariant under F_I. The basic idea is that once the solution f reaches the nullspace of F_D it is transported out of it again by action of F_I, unless the global equilibrium f_∞ is reached. Therefore, the main aim in such a hypocoercivity situation is to find a modification $\tilde{\mathcal{E}}$ of the 'natural' entropy $\mathcal{E}$ by adding terms having their origin in F_I, which are acting on $\mathcal{N}(F_D)$. More precisely, we want

$$\frac{d}{dt}\tilde{\mathcal{E}}[f(t)] = -\tilde{\mathcal{D}}[f(t)] \leq 0, \quad \text{with} \quad \tilde{\mathcal{D}}[f] = 0 \Leftrightarrow f \equiv f_\infty.$$

Exponential decay of f to equilibrium follows then, if $\tilde{\mathcal{E}}$ controls $\|f - f_\infty\|$ and $\tilde{\mathcal{D}}$ is coercive.

1.3 Main Contribution of this Thesis

This thesis is divided into five Chapters. The second consists of a published article, the third of an article close to submission. The forth chapter contains first results form an ongoing project and the fifth chapter again consists of an article close to submission and further results of an ongoing project. Notation might therefore be slightly inconsistent across chapters. The corresponding list of literature can be found at the end of each chapter separately.

1.3.1 Kinetic Model for Colonies of Myxobacteria

Chapter 2 is a collaboration with *S. Hittmeir*, *A. Manhart* and *C. Schmeiser* in which we formally derive the main model (1.1) for the movement behavior of colonies of myxobacteria and perform first steps in its analysis.

Model assumptions: We make the following model assumptions based on the biological behavior explained in Section 1.1.

- We consider N identical bacteria moving in $\mathbb{R}^2$, each being idealized as a rod of thickness zero and of length l.
- For $i = 1, \dots, N$ $x_i \in \mathbb{R}^2$ describes the center and $\omega_i = \omega(\varphi_i) = (\cos\varphi_i, \sin\varphi_i)$ the direction of movement with direction angle $\varphi_i \in \mathbb{T}^1$ of bacterium i.
- *Between interactions*, bacterium number i glides with constant speed s_0 in its longitudinal direction ω_i, i.e.

$$\begin{aligned} dx_i &= s_0\omega_i dt, \\ d\varphi_i &= 0. \end{aligned} \tag{1.10}$$

- The free flight is interrupted by *instantaneous, binary collisions* of bacteria, where we distinguish two types of interactions between agents (x, φ) and (x_*, φ_*):
  - **Alignment** of the two agents, if $\omega \cdot \omega_* > 0$ (collision with pre-collisional angles less than $\pi/2$ apart) given by:

$$(x, \varphi),\ (x_*, \varphi_*) \quad \to \quad (x', \varphi'),\ (x', \varphi') \qquad \text{with } x' = \frac{x + x_*}{2},\ \varphi' = \frac{\varphi + \varphi_*}{2}.$$

  - **Reversal** of both bacteria, if $\omega \cdot \omega_* < 0$ (collision with pre-collisional angles greater than $\pi/2$ apart) given by the collision rule:

$$(x, \varphi),\ (x_*, \varphi_*) \quad \to \quad (x, \varphi + \pi),\ (x_*, \varphi_* + \pi).$$

These model assumptions involve some simplifications, which causes the mathematical description to be not completely accurate compared to biological observations. This, on one hand is the assumption that bacteria move with constant velocity in the time between collisions. An attempt to overcome this simplification can be found in Section 1.3.2 of this introduction, corresponding to Chapter 3 of the manuscript. On the other hand, the proposal of instantaneous binary collisions between bacteria corresponds to an adaptation of our setting to the one for hard sphere dynamics. The concept of *noninstantaneous* collisions between particles describes, to our best knowledge, a new concept in kinetic theory, which will be discussed in Section 1.3.4 in the general introduction and Chapter 5 of the complete thesis.

Model Derivation: In order to perform the phase transition from the above described individual based dynamics to the mesoscopic scale, we use the Boltzmann's method [7] described in Section 1.2.1 and adapted to our setting. The main specialty in our setting is that the alignment collisions are not invertible. This causes the procedure not to be directly applicable, since a pre-collisional representation of the right-hand-side in (1.6) is needed to be able to perform the Boltzmann-Grad limit correctly. (See Remark 1.1.) Therfore, a regularization of the alignment collisions is needed:

$$(x,\varphi),\,(x_*,\varphi_*) \quad \to \quad (x'_\varepsilon,\varphi'_\varepsilon),\,(x'_{*\varepsilon},\varphi'_{*\varepsilon})$$

with

$$\varphi'_\varepsilon = \frac{1-\varepsilon}{2}\varphi + \frac{1+\varepsilon}{2}\varphi_*\,, \qquad \varphi'_{*\varepsilon} = \frac{1+\varepsilon}{2}\varphi + \frac{1-\varepsilon}{2}\varphi_*\,, \quad \varepsilon \ll 1,$$

i.e. bacteria are drifting slightly apart from each other after the collision. The post-collisional centers x'_ε and $x'_{*\varepsilon}$ are determined accordingly such that the post-collisional states are on the ingoing boundary of Γ. The resulting equation is of the form

$$\begin{aligned}\partial_t f + \omega\cdot\nabla_x f = \frac{2}{1-\varepsilon}\int_{\mathbb{T}^{AL}_{\to\varphi}} b(\tilde\varphi,\varphi_*) f(x,\tilde\varphi) f(x,\varphi_*) d\varphi_* + \int_{\mathbb{T}^{REV}_{\varphi}} b(\varphi,\varphi_*) f(x,\varphi^\downarrow) f(x,\varphi_*^\downarrow) d\varphi_* \\ - \int_{\mathbb{T}^1} b(\varphi,\varphi_*) f(x,\varphi) f(x,\varphi_*) d\varphi_*\,,\end{aligned}$$

with $b(\varphi,\varphi_*) = |\omega_*\cdot\omega^\perp| = |\sin(\varphi-\varphi_*)|$ and

$$\mathbb{T}^{REV}_{\varphi} = \left(\varphi+\frac{\pi}{2}, \varphi+\frac{3\pi}{2}\right), \qquad \mathbb{T}^{AL}_{\to\varphi} = \left(\varphi-\frac{\pi}{4}, \varphi+\frac{\pi}{4}\right),$$

$$\tilde\varphi = \frac{2\varphi-(1+\varepsilon)\varphi_*}{1-\varepsilon}\,, \qquad \varphi^\downarrow = \varphi+\pi\,, \qquad \varphi_*^\downarrow = \varphi_*+\pi\,.$$

Removing the regularization in the alignment collisions, i.e. performing the limit $\varepsilon\to 0$, we obtain the *kinetic model for myxobacteria*:

$$\begin{aligned}&\partial_t f + \omega\cdot\nabla_x f = Q(f,f) := G_{AL}(f,f) + G_{REV}(f,f) - L(f,f) \\ &= 2\int_{\mathbb{T}^{AL}_{\to\varphi}} b(\tilde\varphi,\varphi_*)\tilde f f_* d\varphi_* + \int_{\mathbb{T}^{REV}_{\varphi}} b(\varphi,\varphi_*) f^\downarrow f_*^\downarrow d\varphi_* - \int_{\mathbb{T}^1} b(\varphi,\varphi_*) f f_* d\varphi_*\,,\end{aligned} \tag{1.11}$$

with now $\tilde\varphi = 2\varphi-\varphi_*$, subject to initial condition $f(x,\varphi,0) = f_I(x,\varphi)$. If we also split up the loss-term in its reversal- and alignment part, we obtain the following representation of the collision operator:

$$\begin{aligned}Q(f,f) &= Q_{AL}(f,f) + Q_{REV}(f,f) \\ &:= 2\int_{\mathbb{T}^1_{AL}} b(\tilde\varphi,\varphi_*)\left(\tilde f f_* - f\tilde f_*\right) d\varphi_* + \int_{\mathbb{T}^1_{REV}} b(\varphi^\downarrow,\varphi_*^\downarrow)\left(f^\downarrow f_*^\downarrow - f f_*\right) d\varphi_*\,.\end{aligned}$$

Basic properties of (1.11) are the two conservation laws: *Conservation of the number of bacteria,*

$$\partial_t\rho + \nabla_x\cdot(\rho u) = 0\,, \tag{1.12}$$

with the usual definition of *number density* $\rho(x,t) := \int_{\mathbb{T}^1} f(x,\varphi,t)d\varphi$ and *flux* $\rho u(x,t) := \int_{\mathbb{T}^1}\omega(\varphi) f(x,\varphi,t)d\varphi$, and the second one given by

$$\partial_t\int_{\mathbb{T}^1}\varphi f\,d\varphi + \nabla_x\cdot\int_{\mathbb{T}^1}\varphi\,\omega f\,d\varphi = 0\,. \tag{1.13}$$

Equilibria of Q are of the form

$$f_\infty(\varphi) = \rho_+\delta(\varphi - \varphi_+) + \rho_-\delta(\varphi - \varphi_+^\downarrow)\,, \tag{1.14}$$

with arbitrary $\rho_\pm \geq 0$, $\varphi_+ \in \mathbb{T}^1$. The factor $b(\varphi, \varphi_*) = |\omega_* \cdot \omega^\perp| = |\sin(\varphi - \varphi_*)|$ in the collision integrals is a consequence of the rod shape of the bacteria. It gives the rate of collisions between bacteria with the directions φ and φ_*. Assuming instead bacteria with circular shape makes the collision rate independent from the movement direction. By analogy to a similar simplification in the Boltzmann equation for the gas dynamics [11], we use the name *Maxwellian myxos* for this imagined species, modeled by (1.11) with $b(\varphi, \varphi_*) \equiv 1$.

Main goals concerning the analysis of (1.11): The two main objectives in the study of (1.11) are

1. to show its *well-posedness*
2. and characterize its *asymptotic behavior*.

The task of proving an existence result for the full model (1.11) can be compared to the case of the original Boltzmann equation [17], but with the lack of an logarithmic entropy, due to the singularity of the alignment collisions. This is therefore still an open problem. Investigating the asymptotic behavior, we face the difficulty that there are three free parameters, ρ_+, ρ_-, φ_+, in the equilibrium distribution (1.14) as opposed to only two conservation laws (1.12) and (1.13). In order to overcome the aforesaid difficulties we investigate the spatially homogeneous version of (1.11) and place ourselves in a special setting of initial conditions.

Analysis of the spatially homogeneous case: We consider the spatially homogeneous initial value problem of (1.11):

$$\begin{aligned} &\partial_t f = Q(f, f), \qquad \text{in } \mathbb{T}^1 \times (0, \infty) \\ &f(\varphi, 0) = f_I(\varphi)\,, \qquad \varphi \in \mathbb{T}^1. \end{aligned} \tag{1.15}$$

Concerning goal 1, we were able to prove the following result:

Theorem (see Chapter 2, Theorem 2.1)**.** *For $f_I \in L^1_+(\mathbb{T}^1)$ the initial value problem (1.15) has a unique global solution $f \in C\left([0, \infty), L^1_+(\mathbb{T}^1)\right)$.*

The main tool of this proof is a *fixed-point argument via Lipschitz-estimates in L^1* on the collision operator Q. We want to emphasize at this point that the boundedness of the collisional cross section $b(\cdot, \cdot) \leq 1$ plays an important role. In contrast to the case of the spatially homogeneous version of the original Boltzmann equation, where first truncation of the collision kernel is needed to establish existence of a solution as weak limit of the solutions of the truncated equations via compactness arguments.

For the long-time behavior, goal 2, we restrict ourselves to a certain class of initial conditions:

$$f(x, \varphi, 0) = f_I(x, \varphi)\,, \quad \text{satisfying} \quad \operatorname{supp}(f_I(x, .)) \subset \mathbb{T}^1_+ \cup \mathbb{T}^1_-, \qquad \forall x \in \mathbb{R}^2\,, \tag{1.16}$$

where $\mathbb{T}^1_+ := (\pi/4,\, 3\pi/4)$ and $\mathbb{T}^1_- := (-3\pi/4,\, -\pi/4)$, which means that initially the colony of bacteria is already grouped into two parts, one moving up in a direction with angle between $(\pi/4,\, 3\pi/4)$, the

other moving down with an angle on the opposite part of the torus. Property (1.16) is propagated by (1.15), which causes *mass conservation within each group*

$$\rho_+ =: \int_{\mathbb{T}^1_+} f\, d\varphi, \quad \rho_- =: \int_{\mathbb{T}^1_-} f\, d\varphi.$$

Further, with the third conserved quantity

$$\varphi_+ = \frac{1}{\rho_+ + \rho_-}\left(\int_{\mathbb{T}^1_+} \varphi f_I\, d\varphi + \int_{\mathbb{T}^1_-} \varphi^{\downarrow} f_I\, d\varphi\right) \in \mathbb{T}^1_+,$$

we are now able to characterize the equilibrium (1.14) completely. In order to achieve decay to f_∞ we used *entropy methods* described in Section 1.2.2. Since the alignment operator Q_{AL} causes concentration of direction angles, a natural guess for finding a decaying quantity for the system (1.15) would be

$$\mathcal{V}[f] = \int_{\mathbb{T}^1_+} (\varphi - \varphi_+)^2 f\, d\varphi + \int_{\mathbb{T}^1_-} (\varphi - \varphi_+^{\downarrow})^2 f\, d\varphi\,,$$

i.e. the relative variance from the conserved angle φ_+ in each group. It's time derivative along solutions of (1.15) is given by

$$\begin{aligned}\frac{d}{dt}\mathcal{V}(f) \quad &= \quad -\frac{1}{4}\int_{\mathbb{T}^1_+}\int_{\mathbb{T}^1_+} b(\varphi,\varphi_*) f f_* (\varphi-\varphi_*)^2 d\varphi_* d\varphi \\ &\quad -\frac{1}{4}\int_{\mathbb{T}^1_-}\int_{\mathbb{T}^1_-} b(\varphi,\varphi_*) f f_* (\varphi-\varphi_*)^2 d\varphi_* d\varphi \le 0\,.\end{aligned}$$

Note that the reversal collisions do not contribute to the right hand side, which vanishes whenever concentration is reached in both groups, even when the two concentration angles are not opposite each other. Therefore it is not possible to derive a differential inequality for $\mathcal{V}(f)$ as in (1.9), additional information from the in this context invariant operator Q_{REV} is needed. Since the reversal collisions cause symmetry, a natural extension of $\mathcal{V}$ would be the term

$$\rho_+(\bar\varphi_+ - \varphi_+)^2 + \rho_-(\bar\varphi_- - \varphi_+^{\downarrow})^2,$$

measuring the quadratic distance between the time-depending mean angles

$$\bar\varphi_+ := \int_{\mathbb{T}^1_+} \varphi f\, d\varphi, \quad \bar\varphi_- := \int_{\mathbb{T}^1_-} \varphi f\, d\varphi.$$

The entropy $\mathcal{H}$ is defined as the sum of these two contributions

$$\mathcal{H}[f] := \int_{\mathbb{T}^1_+} (\varphi - \varphi_+)^2 f\, d\varphi + \int_{\mathbb{T}^1_-} (\varphi - \varphi_+^{\downarrow})^2 f\, d\varphi + \gamma\rho_+(\bar\varphi_+ - \varphi_+)^2 + \gamma\rho_-(\bar\varphi_- - \varphi_+^{\downarrow})^2,$$

which, for $\gamma > 0$ suitably chosen, can be shown to control the *2-Wasserstein distance* of the solution f to equilibrium f_∞, i.e. $W_2^{\mathbb{T}^1}(f(\cdot,t), f_\infty) \le \mathcal{H}[f]$, which will be the topological framework of our convergence result. *For deeper insights in the concept of Wasserstein spaces we refer the reader to Chapter 2, Section 2.4, or to [43].*

With this preparation, we were able to prove the following result, concerning point 2 of the main questions:

Theorem (see Chapter 2, Theorem 2.6)**.** *Let $f_I \in L^1_+(\mathbb{T}^1)$ with $\mathrm{supp}(f_I) \subset \mathbb{T}^1_+ \cup \mathbb{T}^1_-$, and let f be a solution of (1.15). Then for Maxwellian myxos, i.e. $b(\varphi, \varphi_*) \equiv 1$, there exists $C > 0$, such that*

$$W_2^{\mathbb{T}^1}(f(\cdot,t), f_\infty) \leq Ce^{-\lambda t}, \qquad \forall\, t \geq 0,$$

with f_∞ defined in (1.14) and $\lambda > 0$ explicitly computable.

Numerical simulations for (1.11) (see Chapter 2, Section 2.5) give evidence for the above result, even showing the expected behavior for the general case without restrictions on f_I as well as $b(\varphi, \varphi_*) = |\sin(\varphi - \varphi_*)|$. Further, assuming again two group initial data (1.14), a *formal macroscopic limit* in (1.11) reveals equations for the three quantities ρ_+, ρ_- and φ_+, who resemble the ones obtained in [14], although having its origin in different microscopic dynamics.

1.3.2 Kinetic Model for Myxobacteria with Directional Diffusion

In Chapter 3, a collaboration with *C. Schmeiser*, we study a model for the in Section 1.3.1 described behavior of bacteria with additional consideration of Brownian drift in velocity direction during the free-flight phase of bacteria. This describes an attempt to overcome the simplification of assuming that bacteria move on straight lines between interactions, which turned out to be not completely accurate in biological observations. The microscopic dynamics stated in (1.10) are changed to

$$\begin{aligned} dx_i &= s_0 \omega_i dt, \\ d\varphi_i &= \sqrt{2\mu} dB_t, \end{aligned}$$

where $\mu > 0$ describes the diffusion constant and B_t is the standard *Brownian motion*. On the kinetic scale, this leads to a diffusion term just in velocity direction. Therefore, the model considered in this section of the introduction, corresponding to Chapter 3 of the thesis, is of the form

$$\begin{aligned} &\partial_t f + \omega \cdot \nabla_x f = \mu \partial_\varphi^2 f + Q(f,f) \\ &= \mu \partial_\varphi^2 f + 2 \int_{\mathbb{T}^{AL}_{\to\varphi}} b(\tilde{\varphi}, \varphi_*) \tilde{f} f_* d\varphi_* + \int_{\mathbb{T}^{REV}_{\varphi}} b(\varphi, \varphi_*) f^{\downarrow} f_*^{\downarrow} d\varphi_* - \int_{\mathbb{T}^1} b(\varphi, \varphi_*) f f_* d\varphi_*, \quad (1.18) \\ &f(x, \varphi, 0) = f_I(x, \varphi) \end{aligned}$$

using the same notation as in (1.11), but now assuming a bounded velocity- and position-space: $(x, \varphi) \in \mathbb{T}^2_x \times \mathbb{T}^1_\varphi$. Also for this model the total mass is conserved and denoted by

$$M := \int_{\mathbb{T}^1 \times \mathbb{T}^2} f(x, \varphi, t)\, \mathrm{d}\varphi \mathrm{d}x.$$

Therefore, the *uniform distribution* is given by

$$f_0 := \frac{M}{2\pi},$$

and defines an equilibrium for both this model (1.18) and for the no-diffusion case (1.11). The theorem stated in the last section (corresponding to Theorem 2.6 in Chapter 2) above as well as numerical simulations suggest the instability of f_0 in absence of directional diffusion.

Main goals concerning the analysis of (1.18): Regarding the analysis of (1.18) we aim to answer the following questions:

1. Does a unique *solution to* (1.18) *exist*?
2. How does the stability behavior of the equilibrium f_0 change with varying diffusivity μ? Are there other equilibira?

Existence and uniqueness in L^2: Due to the regularizing effect of the directional diffusion term the higher regularity and integrability than in the no-diffusion case (1.11) can be expected. Concerning objective 1, we managed to prove the following result:

Theorem (see Chapter 3, Theorem 3.1)**.** *Let $f_I \in H^2_{x,\varphi}(\mathbb{T}^2 \times \mathbb{T}^1)$, $f_I \geq 0$, and let μ/M be large enough with $M = \int_{\mathbb{T}^2\times\mathbb{T}^1} f_I \mathrm{d}\varphi\mathrm{d}x$. Let furthermore $\|f_I - f_0\|_{H^2_{x,\varphi}(\mathbb{T}^2\times\mathbb{T}^1)}$ be small enough with $f_0 = M/(2\pi)$. Then equation (1.18) subject to the initial condition $f(t=0) = f_I$ has a unique global solution $f \in C([0,\infty), H^2_{x,\varphi}(\mathbb{T}^2 \times \mathbb{T}^1))$, satisfying*

$$\|f(t) - f_0\|_{H^2_{x,\varphi}(\mathbb{T}^2\times\mathbb{T}^1)} \leq Ce^{-\lambda t}\|f_I - f_0\|_{H^2_{x,\varphi}(\mathbb{T}^2\times\mathbb{T}^1)}\,, \qquad C, \lambda > 0\,.$$

The proof of this result consists of two steps: First, we show spectral stability of f_0 regarding the linearization around the uniform equilibrium of (1.18)

$$\partial_t f + \omega(\varphi)\cdot\nabla_x f = \mu\partial^2_\varphi f + Q(f_0, f) + Q(f, f_0),$$

by applying the L^2-*hypocoercivity method* established by *Dolbeault, Mouhot and Schmeiser* in 2015 [18]. Here, the main goal is to find a *Lyapunov function*, which provides enough control over f and the involved operators such that existence and exponential decay to f_0, with an explicite rate, depending on the diffusivity μ, can be concluded. More precisely, we will first show that there exist constants $C > 0$ and $\lambda > 0$, such that

$$\|e^{t(L+Q_M-T)} f_I\| \leq Ce^{-\lambda t}\|f_I\|\,, \quad \forall t > 0,$$

where the following notation

$$L := \mu\partial^2_\varphi, \quad T := \omega(\varphi)\cdot\nabla_x, \quad Q_M := Q(f_0, \cdot) + Q(\cdot, f_0)$$

for the involved operators was used. The second step involves including the nonlinear remainder of the collision operator $Q(f, f)$, which is quadratic in f. In order to include Q into the estimates, control up to second order derivatives of f is needed, which is achieved by applying the same method as for the linear equation in f iteratively for all derivatives up to order two of f. The obtained decay of f, its derivatives and, due to regularity estimates, also $Q(f, f)$, will be used to find time independent estimates of the mild formulation for the original problem (1.18), form which global existence of a solution and exponential decay to equilibrium can be concluded.

Bifurcation analysis: The following considerations addressing objective 2 correspond to Chapter 3, Section 3.3.1.

Inspired by the results for the equation without diffusion (1.11), we expect the uniform steady state f_0 to remain unstable for sufficiently small μ and hope to find stable, non-uniform equilibria in this collision dominating regime. On the other hand, in an regime with large enough diffusion, f_0 is expected to be stable. Therefore, we aim to determine a concrete diffusion parameter μ^*, at which

the uniform equilibrium changes its stability, i.e. where a *bifurcation* happens. *For further insights into the concept of bifurcation analysis, we refer the reader to [12].*

We perform a *linear stability analysis* for the spatially homogeneous version of (1.18)

$$\begin{aligned} &\partial_t f = \mu \partial_\varphi^2 f + Q(f,f), \quad \varphi \in \mathbb{T}^1,\ t > 0, \\ &f(\varphi, 0) = f_I(\varphi), \quad \varphi \in \mathbb{T}^1. \end{aligned} \tag{1.19}$$

We linearize (1.19) around the uniform equilibrium f_0 and obtain

$$\begin{aligned} \partial_t f^* &= \mu \partial_\varphi^2 f^* + Q_M f^*, \\ \int_{\mathbb{T}^1} f^* \, \mathrm{d}\varphi &= 0, \end{aligned}$$

for the perturbation f^*, which's average over $\mathbb{T}^1$ vanishes to be consistent with mass conservation. Existence of a solution in $L^2(\mathbb{T}^1_\varphi)$ motivates the *Fourier series* ansatz

$$f^*(\varphi, t) = \sum_{n \geq 1} a_n(t) \cos(n\varphi) + \sum_{n \geq 1} b_n(t) \sin(n\varphi).$$

Indeed, it turns out that the operator $\mu \partial_\varphi^2 \cdot + Q_M \cdot$ is diagonal in $L^2(\mathbb{T}^1)$ with respect to the basis $\{\cos(n\,\cdot), \sin(n\,\cdot)\}_{n \geq 0}$. We obtain the following evolution equations for the Fourier modes

$$\begin{pmatrix} \dot{a}_n \\ \dot{b}_n \end{pmatrix} = \lambda_n(\mu, f_0) \begin{pmatrix} a_n \\ b_n \end{pmatrix},$$

where $\{\lambda_n(\mu, f_0)\}_{n \geq 1}$ describe the eigenvalues to the eigenfunctions $\{\sin(n\cdot)\}_{n \geq 1}$ resp. $\{\cos(n\cdot)\}_{n \geq 1}$, which can be computed explicitly. Quantitatively the following properties are important:

$$\lambda_n(\mu, f_0) < 0, \quad \text{for all } n \neq 2, \text{ for all } \mu > 0, f_0 > 0,$$

and

$$\lambda_2(\mu, f_0) \begin{cases} > 0, & \text{for } \mu < \mu^*, \\ < 0, & \text{for } \mu > \mu^*, \end{cases}$$

with critical value $\mu^* = \frac{f_0}{6}$. Therefore, we formally proved that f_0 is *linearly stable* for $\mu > \mu^*$, while for $\mu < \mu^*$ it becomes an unstable equilibrium, since the critical eigenvalue λ_2 is positive. The point (μ^*, f_0) is a *bifurcation point*, where a branch of new stationary solutions emerge, which close left to the bifurcation point is of the form

$$f(\varphi) = f_0 + \varepsilon f^*(\varphi) = f_0 + \varepsilon a_2 \sin(2\varphi + \pi/2) + \varepsilon b_2 \sin(2\varphi),$$

for some small parameter $\varepsilon << 1$. Determining the bifurcation behavior further, i.e. determining the Fourier modes a_2, b_2 reveals the occurrence of a *supercritical pitchfork bifurcation*, see Figure 3.1 in Chapter 3, Section 3.3.1, which is already indicated by the *flip-symmetry* in our equation (1.19).

Remark 1.2. *The above described bifurcation analysis can also be carried out with the total mass $M = 2\pi f_0$ as bifurcation parameter, depending on the initial condition. The linear stability result gained in the considerations above can then be interpreted in the following way: If the total mass stays below the critical threshold $M_* := 12\pi\mu$, i.e. $M < M_*$, then the uniform equilibrium is linearly stable. For $M > M_*$ the equilibrium f_0 becomes unstable. This means, that a certain amount of bacteria has to be present such that sufficiently enough collisions take place to overcome the diffusivity, which causes uniformization.*

Further, for the small diffusion regime, i.e. $\mu \ll 1$, existence of symmetric solutions of an approximation of the stationary version of (1.19) is shown. This indicates the existence of nonuniform equilibira for small diffusion, smooth approximations of the equilibirum (1.14). *Numerical simulations* for (1.19) (see Chapter 3, Section 3.4) give evidence for the bifurcation result.

1.3.3 Reversal Collision Dynamics in a General Domain

Chapter 4 is joint work with *A. Frouvelle* and *C. Schmeiser*, in which we investigated the dynamics of Q_{REV}, the reversal-part of the collision operator on the right-hand-side of the main model (1.11). We lifted the framework to higher abstraction and consider Q_{REV} acting on a general *compact metric space* $\mathcal{S}$, which is endowed with a symmetric structure that allows to define an *inclusion* $x^{\downarrow}$ for all $x \in \mathcal{S}$ as well as a symmetric measure dx. As the *set of collision partners* for $x \in \mathcal{S}$ we define

$$\mathcal{C}[x] := \left\{ x_* \in \mathcal{S} : \, x_* \in B_\alpha(x^{\downarrow}) \right\},$$

for a constant $\alpha > 0$. Additionally, we assume a more general collision kernel $b = b(x, x_*)$, but bounded away from zero, $0 < b_0 < b(x, x_*)$, and being consistent with the symmetry structure of the metric space, i.e. $b(x, x_*) = b(x^{\downarrow}, x_*) = b(x, x_*^{\downarrow}) = b(x^{\downarrow}, x_*^{\downarrow})$. The problem describing the evolution of the distribution function $f = f(x, t)$ of the dynamical states of individual particles $x \in \mathcal{S}$, undergoing reversal collisions

$$(x, x_*) \longrightarrow (x^{\downarrow}, x_*^{\downarrow})$$

is therefore stated as

$$\begin{aligned} &\partial_t f = \int_{x_* \in \mathcal{C}[x]} b(x, x_*) \left(f^{\downarrow} f_*^{\downarrow} - f f_* \right) dx_*, \quad x \in \mathcal{S},\, t > 0 \\ &f(x, 0) = f_I(x), \quad x \in \mathcal{S}, \end{aligned} \tag{1.20}$$

where the notation $f^{\downarrow} = f(x^{\downarrow}, t)$ and $f_* = f(x_*, t)$ is used. One can immediately deduce *mass conservation*:

$$\int_{\mathcal{S}} f \, \mathrm{d}x = \int_{\mathcal{S}} f_I \, \mathrm{d}x \equiv 1,$$

which we assume to be normalized, as well as conservation of the average distribution $\tilde{f}$, defined as

$$\tilde{f}(x) := \frac{f(x) + f(x^{\downarrow})}{2}, \tag{1.21}$$

and therefore symmetric by its definition. Due to the symmetrizing effect of the reversal collisions, $\tilde{f}$ will be the candidate for the equilibirum the solution f is expected to approach asymptotically in time.

Main goals concerning the analysis of (1.20): We aim to answer the following questions regarding 1.20:

1. In which framework do *solutions to* (1.18) *exist*?
2. Can we prove *decay to a symmetric equilibrium*?

Existence and uniqueness in L^1: Question 1 is answered by the following result:

Theorem (Chapter 4, Theorem 4.2)**.** *Let $b \in L^\infty(\mathcal{S}\times\mathcal{S})$ and $f_I \in L^1(\mathcal{S})$. Then (1.20) has a unique global solution $f \in C([0,\infty), L^1_+(\mathcal{S}))$.*

Also in this framework *Picard iteration* is the basic tool to prove existence and uniqueness of the solution, since under the assumption of a bounded collision kernel, Q_{REV} can be shown to be Lipschitz continuous on $\mathcal{S}$.

Asymptotic behavior: Concerning objective 2, we aim to show exponential convergence to the *symmetric equilibrium* (1.21). Therefore, we first introduce

$$h(x) := \frac{f(x)-\tilde{f}(x)}{\tilde{f}(x)}, \quad \text{for } x \in \mathcal{K},$$

where the compact set $\mathcal{K}$ denotes the measure theoretical support of $\tilde{f}$, defined as

$$\mathcal{K} := \operatorname{supp}(\tilde{f}) := \left\{ x \in \mathcal{S} : \int_{B_\varepsilon(x)} \tilde{f}\, dx > 0,\ \forall \varepsilon > 0 \right\}.$$

With setting

$$\mathcal{H}[f] := \frac{1}{2}\int_{\mathcal{S}} h^2 \tilde{f}\, dx = \frac{1}{2}\int_{\mathcal{S}}\int_{\mathcal{S}} \tilde{f}\tilde{f}'(h-h')^2\, dx'dx, \tag{1.22}$$

which encodes the distance from f to $\tilde{f}$, we found a functional, decaying along solutions f to (1.20). Indeed, taking the time-derivative, we obtain

$$\frac{\mathrm{d}}{\mathrm{d}t}\mathcal{H}[f] = -\int_{\mathcal{S}}\int_{\mathcal{C}[x]} b(x,x_*)(h+h_*)^2 \tilde{f}\tilde{f}_*\, dx_* dx := -\mathcal{D}[f]. \tag{1.23}$$

For the dissipation $\mathcal{D}[f]$ we make the following observation:

$$\mathcal{D}[f] = 0 \quad \Leftrightarrow \quad h(x) + h(x_*) = 0, \quad \text{for a.e. } x, x_* \in \mathcal{K} \text{ s.t. } x_* \in \mathcal{C}[x],$$

which implies that once the dissipation is zero, h has the same value for two elements $x, x_* \in \mathcal{S}$, who have at least one common collision partner. Indeed, we have

$$h(x) - h(x_*) = h(x) + h(\bar{x}) - h(\bar{x}) - h(x_*) = 0,$$

for a.e. $\bar{x} \in \mathcal{C}[x] \cap \mathcal{C}[x_*]$. This motivates the following definition of a *graph associated to the initial conditions f_I* (see also Chapter 4, Definition 4.5):

Definition 1.3. *Let $x, y \in \mathcal{K}$. We say x and y are* connected *and write*

$$x \longleftrightarrow y \quad :\Leftrightarrow \exists x_* \in \mathcal{K},\ \exists \gamma > 0 \text{ s.t. : } B_\gamma(x_*) \subset \mathcal{C}[x] \cap \mathcal{C}[y].$$

This relation defines a graph $\Gamma = \{\mathcal{V}, E\}$ associated to the initial conditions with vertices $\mathcal{V} := \mathcal{K}$ and edges $E := \{(x,y) \in \mathcal{K}\times\mathcal{K} : \ x \longleftrightarrow y\}$. By Γ^i, $i = 1,\dots,N$, we denote its connected components, with corresponding set of vertices $\mathcal{V}^i$. The crucial property of this graph is that for every $i = 1,\dots,N$ and arbitrary two points y and z in $\mathcal{V}^i$ there exists a path $\{y = x_1, x_2, \dots, x_n = z\}$, such that for $l = 1,\dots,n$ each pair x_{l-1} and x_l is connected and therefore has at least one common collision partner. This property together with a *telescopic sum* argument will be the key ingredient to estimate

the right-hand-side of (1.22) further in order to bring it to a shape similar as $\mathcal{D}[f]$ (1.23), from which exponential decay of $\mathcal{H}$ can be deduced via *Grönwall's estimate*.

More precisely, we split the representation of $\mathcal{H}$ which involves integrals over $\mathcal{S} \times \mathcal{S}$ (1.22) into several parts. In each of these terms the integration is over subsets $\mathcal{T}_1^i, \mathcal{T}_2^i \subset \mathcal{V}^i$ of the set vertices corresponding to a connected component of Γ, such that $x \longleftrightarrow x_*$ for all $x \in \mathcal{T}_1^i, x_* \in \mathcal{T}_2^i$ and

$$(\mathcal{C}[x] \cap \mathcal{C}[x_*]) \cap \mathcal{K} \neq \emptyset \quad \forall x \in \mathcal{T}_1^i, x_* \in \mathcal{T}_2^i,$$

i.e. there exists at least one element in set of common collision partners, which is also part of the support of $\tilde{f}$. For such a contribution of (1.22) we have

$$\begin{aligned}&\int_{\mathcal{T}_1^i}\int_{\mathcal{T}_2^i} \tilde{f}\tilde{f}'(h-h')^2\,dx'dx = \int_{\mathcal{T}_1^i}\int_{\mathcal{T}_2^i} \tilde{f}\tilde{f}'(h+h_*-h_*-h')^2\,dx'dx\\ &\leq 2\max\{\rho_1^i,\rho_2^i\}\int_{\mathcal{T}_1^i\cup\mathcal{T}_2^i}\tilde{f}(h+h_*)^2\,dx\,,\end{aligned}$$

for an arbitrary $x_* \in \mathcal{C}[\mathcal{T}_1^i \cup \mathcal{T}_2^i]$, with $\rho_j^i := \int_{\mathcal{T}_j^i} \tilde{f}\,dx$. Integration over $\mathcal{C}[\mathcal{T}_1^i \cup \mathcal{T}_2^i]$ and denoting $\rho_* := \int_{\mathcal{C}[\mathcal{T}_1^i\cup\mathcal{T}_2^i]} \tilde{f}\,dx$ gives

$$\int_{\mathcal{T}_1^i}\int_{\mathcal{T}_2^i} \tilde{f}\tilde{f}'(h-h')^2\,dx'dx \leq \frac{2}{\rho_*}\max\{\rho_1^i,\rho_2^i\}\int_{\mathcal{T}_1^i\cup\mathcal{T}_2^i}\int_{\mathcal{C}[x_*]}\tilde{f}\tilde{f}'(h+h_*)^2\,dx_*dx\,,$$

which resembles, up to the lack of the collision kernel b, the corresponding contribution of the integral defining the dissipation $\mathcal{D}$. The collision kernel b can be estimated by its lower bound b_0, which leaves us just to use Grönwall's estimate in order to obtain exponential decay of $\mathcal{H}$.

For the proof that we can always find such a partition of $\mathcal{S}$ such that we can split up the integrals on the right-hand-side of (1.22) in a way described before, we refer the reader to Chapter 4, Lemma 4.7. In the case, where Γ is connected, the result stating exponential decay of the solution f to $\tilde{f}$ is stated in Chapter 4, Corollary 4.8. For the situation, where Γ has more than one connected component, decay to the average, although not symmetric, but weighted accordingly on each connected component, can be proved (see Chapter 4, Corollary 4.12).

Numerical Simulations (see Chapter 4, Section 4.5) for the special setting $\mathcal{S} = \mathbb{T}^1$, $\alpha = \frac{\pi}{2}$, corresponding to the spatially homogeneous kinetic model for myxobacteria (1.15) including just reversal collisions

$$\partial_t f = \int_{d(\varphi,\varphi_*)>\frac{\pi}{2}} b(\varphi,\varphi_*)\left(f^{\downarrow}f_*^{\downarrow} - f f_*\right)\,d\varphi_*,$$

give evidence to the above discussed results.

1.3.4 A Kinetic Model for Non-instantaneous Binary Collisions

Chapter 5 is a collaboration with *C. Schmeiser* and *V. Tora*, in which we introduce and investigate two kinetic models describing *non-instantaneous alignment collisions* between two agents. The inspiration for proposing a kinetic model with time-resolved binary collisions was the fact that assuming instantaneous interactions between bacteria (see Section 1.3.1) is a huge simplification in biological context.

For the first variant of this model, we assume an assemble of particles each equipped with a specific property $\varphi \in \mathbb{R}$, who undergo *binary collisions*. We suppose that the times at which a collision between two particles happen as well as the times at which two colliding particles separate again are modeled

by *Poisson processes*. On a kinetic scale, the dynamics of these assemble of particles are governed by the following system of equations:

$$\begin{aligned} \partial_t f &= 2\Big(\gamma \int_{\mathbb{R}} g(\varphi,\varphi_*)\,\mathrm{d}\varphi_* - \lambda f(\varphi)\int_{\mathbb{R}} b(\varphi,\varphi_*) f(\varphi_*)\,\mathrm{d}\varphi_*\Big)\,, \\ \partial_t g + \nabla\cdot(V(\varphi,\varphi_*)g(\varphi,\varphi_*)) &= \lambda b(\varphi,\varphi_*) f(\varphi_*) f(\varphi) - \gamma g(\varphi,\varphi_*)\,, \end{aligned} \tag{1.24}$$

where $f = f(\varphi,t)$ describes the distribution function for the single particles, while $g = g(\varphi,\varphi_*,t)$ stands for the pairs of particles in collision. The constant $\lambda > 0$ is the rate at which collisions take place, while $\gamma > 0$ stands for the rate at which a pair of colliding particles split up. The *collision potential* V is chosen to model an alignment collision, i.e. two colliding particles φ, φ_* approach their midpoint $\frac{\varphi+\varphi_*}{2}$, and is of the form

$$V(\varphi,\varphi_*) := \frac{1}{2}\begin{pmatrix}\varphi_* - \varphi \\ \varphi - \varphi_*\end{pmatrix}.$$

It should be noted that (1.24) allows two conservation laws: Conservation of *total mass*

$$M = M_f(t) + 2M_g(t) := \int_{\mathbb{R}} f\,d\varphi + 2\int_{\mathbb{R}^2} g\,d\varphi_* d\varphi,$$

and of the *total mean value*

$$M\varphi_\infty := I_f(t) + 2I_g(t) := \int_{\mathbb{R}} \varphi f\,d\varphi + 2\int_{\mathbb{R}^2} \varphi g\,d\varphi_* d\varphi. \tag{1.25}$$

Main goals concerning the analysis of (1.24): The main objectives in the analysis of (1.24) are

1. proving *existence and uniqueness of solutions to* (1.24),
2. showing *convergence to equilibrium*,
3. and performing the *instantaneous limit* in (1.24), i.e. letting the collision time go to zero.

Existence and uniqueness in L^1: Objective 1 could be achieved by carrying out a *fixed-point argument* after rewriting (1.24) in *mild formulation* (Peano-formulation) by incorporating the drift. Time-independent estimates of the fixed-point mapping gave global existence of a solution in $L^1(\mathbb{R}\times\mathbb{R}^2)$. More precisely, we proved the following result:

Theorem (see Chapter 5, Theorem 5.1)**.** *Let $f_0 \in L^1_+(\mathbb{R})$, $g_0 \in L^1_+(\mathbb{R}\times\mathbb{R})$. Then (1.24) has a unique global solution $(f,g) \in C([0,\infty);\, L^1(\mathbb{R})\times L^1(\mathbb{R}\times\mathbb{R}))$.*

Convergence to equilibrium: Concerning the 2nd of our main goals, we again have to face a *hypocoercivity situation*. Indeed, searching for equilibria of (1.24) we have to take into account the two different effects governing the dynamics. One one hand, we have an exchange between single and and pairs of particles. Functions being uneffected by these exchange dynamics can be described by the set of local equilibria

$$Eq := \Big\{(\bar f,\bar g):\ \ \lambda \bar f \bar f^* = \mu \bar g\ \Big\}. \tag{1.26}$$

One can see immediately that, if the system arrives at the set (1.26), it will not remain there, but instead will be transported away by the drift-term in the g-equation, which produces concentration of mass at a single point, namely the mean value φ_∞ defined in (1.25). The interplay between the transport towards concentration $\nabla \cdot (Vg)$ and the exchange dynamics is needed to arrive at the *global equilibrium*, given by

$$(f_\infty, g_\infty) := (M_{f_\infty}\delta_{\varphi_\infty}, M_{g_\infty}\delta_{(\varphi_\infty,\varphi_\infty)}),$$

where M_{f_∞} and M_{g_∞} can be determined explicitely (see Chapter 5, equation (5.5)). Combining both the effects of the exchange and the drift we found with

$$\mathcal{E}[f,g,t] := \mathcal{V}[f,g] + \mathcal{H}[f,g,t],$$

consisting of the *total variance*

$$\mathcal{V}[f,g] := \int_{\mathbb{R}} (\varphi - \varphi_\infty)^2 f \, d\varphi + 2\int_{\mathbb{R}^2} (\varphi - \varphi_\infty)^2 g \, \mathrm{d}\varphi_* \mathrm{d}\varphi,$$

and the *logarithmic-type entropy*

$$\mathcal{H}[f,g,t] := \int_{\mathbb{R}} (\ln(f) - 1) f \, \mathrm{d}\varphi + \int_{\mathbb{R}^2} \left(\ln\left(\frac{\mu g}{\lambda}\right) - 1\right) g \, \mathrm{d}\varphi_* \, \mathrm{d}\varphi - \int_0^t M_g(s) \, \mathrm{d}s,$$

an *entropy*, with nonpositive *dissipation*

$$\frac{\mathrm{d}}{\mathrm{d}t}\mathcal{E}[f,g,t] = -\iint_{\mathbb{R}^2} (\varphi - \varphi_*)^2 g \, \mathrm{d}\varphi_* \mathrm{d}\varphi - \int_{\mathbb{R}^2} (\lambda f f_* - \mu g) \ln\left(\frac{\lambda f f_*}{\mu g}\right) \mathrm{d}\varphi_* \mathrm{d}\varphi \leq 0$$

with the property

$$\frac{\mathrm{d}}{\mathrm{d}t}\mathcal{E}[f,g,t] \equiv 0 \Leftrightarrow (f,g) = (f_\infty, g_\infty).$$

using these results, *weak convergence to equilibirum* could be shown (see Chapter 5, Theorem 5.2).

Instantaneous limit: Objective 3 refers to the question about deriving an instantaneous collision model from (1.24) by performing the limit where the average collision-time goes to zero. After the rescaling

$$g \mapsto \varepsilon g, \ \mu \mapsto \varepsilon^{-1}\mu, \ V \mapsto \varepsilon^{-1} V$$

for $\varepsilon \ll 1$ of (1.24) we obtain a singular perturbed problem of the form

$$\begin{aligned} \partial_t f &= 2\Big(\mu \int_{\mathbb{R}} g \, \mathrm{d}\varphi_* - \lambda M_f f\Big), \\ \varepsilon \partial_t g + \nabla \cdot (Vg) &= \lambda f f^* - \mu g. \end{aligned}$$

The formal limit $\varepsilon \to 0$ of this singular perturbed problem yields, after reformulating everything in terms of the distribution function f (for details see Chapter 5, Section 5.2.4),

$$\partial_t f = 4\mu\lambda \int_0^\infty \int_0^\infty |u - v|^{\mu - 1} |u + v|^{-\mu} f(\varphi + u) f(\varphi - v) \mathrm{d}u \, \mathrm{d}v - 2\lambda f \int_{\mathbb{R}} f^* \, \mathrm{d}\varphi_*. \tag{1.27}$$

Analysis of (1.27) reveals the usual behavior of an *instantaneous kinetic midpoint* model, which can also be found in Chapter 5, Section 5.2.4. The instantaneous limit can be performed *rigorously*, which is done via *compactness arguments* (Prokhorov's theorem, [39]).

Chapter 5 further contains considerations regarding a non-instantaneous alignment model with *deterministic collision dynamics*, i.e. there is no randomness in the duration of the collision process and the collision only ends once the mean $\frac{\varphi+\varphi_*}{2}$ of the pre-collisional states φ and φ_* is reached. An instantaneous limit of this model reveals a kinetic equation with collision operator of the same form as the alignment terms on the right-hand-side of (1.11). Details can be found in Chapter 5, Section 5.3 of this manuscript.

1.4 Declaration of Authorship

Chapter 2 is joint work with Sabine Hittmeir (University of Vienna), Angelika Manhart (University College London) and Christian Schmeiser and it has been published in *Kinetic and Related Models*, **14** (2021), pp. 1-24. Chapter 3 contains an article, joint work with Christian Schmeiser, which is close to submission. Furthermore, Chapter 4 consists of results, which arose from an ongoing collaboration with Amic Frouvelle (CEREMADE, Université de PARIS - DAUPHINE) and Christian Schmeiser. Finally, Chapter 5 summarizes the outcome from joint work with Christian Schmeiser and Veronica Tora (University of Vienna), where the first part (Chapter 5, Section 5.2) consists of an article close to submission. All of these works are based on discussions and exchange of ideas with my co-authors.

Bibliography

[1] D. Bakry and M. Émery, *Diffusions hypercontractives,* Séminaire de probabilités, XIX, 1983/84, Lecture Notes Math., Springer, Berlin, 1123, 177–206, 1985.

[2] A. Baskaran, M.C. Marchetti, *Enhanced Diffusion and Ordering of Self-Propelled Rods,* Phys. Rev. Lett. 101 (2008), 268101.

[3] A. Baskaran, M.C. Marchetti, *Nonequilibrium statistical mechanics of self propelled hard rods,* J. Stat. Mech. 2010 (2010), P04019.

[4] E. Ben-Naim, P.L. Krapivsky, *Alignment of rods and partition of integers,* Phys. Rev. E Stat. Nonlin. Soft Matter Phys. 73 (2006), 031109.

[5] E. Bertin, M. Droz, G. Grégoire, *Boltzmann and hydrodynamic description for self-propelled particles.* (2006-08-02), Physical Review E. 74 (2): 022101.

[6] E. Bertin, M. Droz, G. Gregoire, *Hydrodynamic equations for self-propelled particles: microscopic derivation and stability analysis,* J. Phys. A: Math. Theor. 42 (2006), 445001.

[7] L. Boltzmann, *Weitere Studien über das Wärmegleichgewicht unter Gasmolekülen,* Sitzungsberichte Akad. Wiss., Vienna, part II, 66 (1872), pp. 275–370.

[8] L. Boltzmann, *Über die Beziehung zwischen dem zweiten Hauptsatz der mechanischen Wärmetheorie und der Wahrscheinlichkeitsrechnung respektive den Sätzen über das Wärmegleichgewicht.* In: Sitzungsber. d. k. Akad. der Wissenschaften zu Wien II 76, S. 428 (1877).

[9] R. Clausius, *Über verschiedene für die Anwendung bequeme Formen der Hauptgleichungen der mechanischen Wärmetheorie,* Annalen der Physik, 125 (7): 353–400, 1865

[10] E. Carlen, M. C. Carvalho, P. Degond, B. Wennberg, *A Boltzmann model for rod alignment and schooling fish,* Nonlinearity 28 (2015), pp. 1783–1804.

[11] C. Cercignani, R. Illner, M. Pulvirenti, *The Mathematical Theory of Dilute Gases*, Springer-Verlag, New York, 1994.

[12] M. G. Crandall, P. H. Rabinowitz, *Bifurcation from simple eigenvalues*, Journal of Functional Analysis, Vol 8, Issue 2, October 1971, pp 321–340.

[13] P. Degond, A. Frouvelle, G. Raoul, *Local stability of perfect alignment for a spatially homogeneous kinetic model,* J. Stat. Phys. 157 (2014), pp. 84–112.

[14] P. Degond, A. Manhart, H. Yu, *A continuum model of nematic alignment of self-propelled particles,* DCDS-B 22 (2017), pp. 1295–1327.

[15] P. Degond, A. Manhart, H. Yu, *An age-structured continuum model for myxobacteria,* M3AS 28 (2018), pp. 1737–1770.

[16] L. Desvillettes, *Convergence to equilibrium in large time for Boltzmann and B.G.K. equations.* Arch. Rational Mech. Anal. 110, 73–91 (1990)

[17] R. J. DiPerna and P. L. Lions, *On the Cauchy Problem for Boltzmann Equations: Global Existence and Weak Stability*, Annals of Mathematics, Second Series, Vol. 130, No. 2 (Sep., 1989), pp. 321-366

[18] J. Dolbeault, C. Mouhot, C. Schmeiser, *Hypocoercivity for linear kinetic equations conserving mass,* Trans. Amer. Math. Soc., 367(6): 3807-3828, 2015.

[19] B. Düring and M.-T. Wolfram, *Opinion dynamics: inhomogeneous boltzmanntype equations modelling opinion leadership and political segregation.* Proc. R. Soc. A, 471(2182):20150345, 2015.

[20] H. Grad, *Principles of the kinetic theory of gases,* Handbuch Physik , 12 , Springer (1958) pp. 205–294

[21] M. P. Gualdani, S. Mischler, C. Mouhot, *Factorization for non-symmetric operators and exponential Htheorem,* Mémoire de la Société Mathématique de France 153 (2017)

[22] F. Hérau, *Hypocoercivity and exponential time decay for the linear inhomogeneous relaxation Boltzmann equation,* Asymptot. Anal., 46(3-4):349-359, 2006.

[23] D. Helbing, I. Farkas, & T. Vicsek, *Simulating dynamical features of escape panic.* Nature 407, 487–490 (2000).

[24] J. Hodgkin, D. Kaiser, *Genetics of gliding motility in Myxococcus xanthus (Myxobacterales): two gene systems control movement,* Mol. Gen. Genet. 171 (1979), pp. 177–191.

[25] J. Haskovec, P. Markowich & B. Perthame, *Mathematical Analysis of a PDE System for Biological Network Formation,* (2015) Communications in Partial Differential Equations, 40:5, 918-956

[26] O. A. Igoshin, A. Mogilner, R. D. Welch, D. Kaiser, G. Oster, *Pattern formation and traveling waves in myxobacteria: Theory and modelling,* PNAS December 18, 2001 98 (26) 14913-14918

[27] O. A. Igoshin, G. Oster, *Rippling of myxobacteria,* Math. Biosci. 188 (2004), pp. 221–233.

[28] O. A. Igoshin, R. Welch, D. Kaiser, and G. Oster, *Waves and aggregation patterns in myxobacteria*, PNAS 101 (2004), pp. 4256–4261.

[29] L. Jelsbak, L. Sogaard-Andersen, *The cell surface-associated intercellular C-signal induces behavioral changes in individual Myxococcus xanthus cells during fruiting body morphogenesis,* PNAS 96 (1999), pp. 5031–5036.

[30] S. Kim, D. Kaiser, *C-factor: A cell-cell signaling protein required for fruiting body morphogenesis of M. xanthus,* Cell 61 (1990), pp. 19–26.

[31] O. E. Lanford, *Time evolution of large classical systems,* Dynamical systems, theory and applications, 1975, pp. 1–111.

[32] P. Lax, *Shock Waves and Entropy,* Contributions to Nonlinear Functional Analysis Proceedings of a Symposium Conducted by the Mathematics Research Center, the University of Wisconsin–Madison, April 12–14, 1971 1971, Pages 603-634

[33] J. C. Maxwell, *On the Stability of the Motion of Saturn's Rings; an Essay which obtained the Adams' Prize for the Year 1856, in the University of Cambridge,* Monthly Notices of the Royal Astronomical Society, Volume 19, Issue 8, June 1859, Pages 297–304

[34] J. C. Maxwell (1867). *On the Dynamical Theory of Gases.* Philosophical Transactions of the Royal Society of London. 157: 49–88.

[35] E. M. F. Mauriello, T. Mignot, Z. Yang, D. R. Zusman, *Gliding Motility Revisited: How Do the Myxobacteria Move without Flagella?,* Microbiol. Mol. Biol. Rev. 74 (2010), pp. 229–249.

[36] B. Nan, D. R. Zusman, *Uncovering the Mystery of Gliding Motility in the Myxobacteria,* Annu. Rev. Genet. 45 (2011), pp. 21–39.

[37] D. Peurichard, F. Delebecque, A. Lorsignol, C. Barreau, J. Rouquette, X. Descombes, L. Casteilla, and P. Degond. *Simple mechanical cues could explain adipose tissue morphology.* Journal of theoretical biology, 429:61–81, 2017.

[38] J.K. Parrish and W.M. Hamner (Eds.), *Three Dimensional Animals Groups,* Cambridge University Press (Cambridge, 1997).

[39] Y. V. Prokhorov, (1956). *Convergence of random processes and limit theorems in probability theory.* Theory of Probability & Its Applications. 1 (2): 157–214.

[40] B. Sager, D. Kaiser, *Intercellular C-signaling and the traveling waves of Myxococcus,* Genes Dev. 8 (1994), pp. 2793–2804.

[41] T. Vicsek, A. Czirok, E. Ben-Jacob, I. Cohen, and O. Shochet. *Novel type of phase transition in a system of self-driven particles.* Phys. Rev. Lett., 75(6):12261229, 1995.

[42] C. Villani, *Hypocoercivity,* Mem. Amer. Math. Soc., 202(950): iv+141, 2009

[43] C. Villani, *Topics in Optimal Transportation,* Graduate Studies in Math. 58, AMS, 2003.

[44] D. Wall, D. Kaiser, *Type IV pili and cell motility,* Mol. Microbiol. 32 (1999), pp. 1–10.

[45] R. Welch, D. Kaiser, *Cell behavior in traveling wave patterns of myxobacteria,* PNAS 98 (2001), pp. 14907–14912.

[46] C. Wolgemuth, E. Hoiczyk, D. Kaiser, G. Oster, *How myxobacteria glide,* Curr. Biol. 12 (2002), pp. 369–377.

2 Kinetic Modelling of Colonies of Myxobacteria

Eleganz sei die Sache der Schuster und Schneider.

Ludwig Boltzmann

Contents

2.1 Introduction **27**
2.2 Model derivation **29**
2.3 Properties of the collision operator **35**
2.4 The spatially homogeneous problem **37**
2.5 Numerical Simulations **42**
2.6 Formal macroscopic limit **44**

Sabine Hittmeir, Laura Kanzler, Angelika Manhart and Christian Schmeiser

Published in *Kinetic and Related Models*, **14** (2021), pp. 1-24.

2.1 Introduction

The goal of this work is the derivation of a new model for the dynamics of myxobacteria colonies on flat substrates, as well as first steps in its analysis. The model is a kinetic transport equation for the distribution function $f(x,\varphi,t)$, $x\in\mathbb{R}^2$, $\varphi\in\mathbb{T}^1$, $t\geq 0$, and has the form

$$\partial_t f+\omega(\varphi)\cdot\nabla_x f=2\int_{\mathbb{T}^{AL}_{\to\varphi}} b(\tilde\varphi,\varphi_*)\tilde f f_* d\varphi_*+\int_{\mathbb{T}^{REV}_{\varphi}} b(\varphi^\downarrow,\varphi_*^\downarrow)f^\downarrow f_*^\downarrow d\varphi_*-\int_{\mathbb{T}^1} b(\varphi,\varphi_*)f f_* d\varphi_*\,, \tag{2.1}$$

where $\omega(\varphi)=(\cos\varphi,\sin\varphi)$, $\mathbb{T}^1$ denotes the one-dimensional flat torus of length 2π. For given φ the integration intervals in the gain terms are given by

$$\mathbb{T}^{REV}_{\varphi}=\left(\varphi+\frac{\pi}{2},\varphi+\frac{3\pi}{2}\right),\qquad \mathbb{T}^{AL}_{\to\varphi}=\left(\varphi-\frac{\pi}{4},\varphi+\frac{\pi}{4}\right),$$

and the precollisional directions are defined by

$$\tilde\varphi=2\varphi-\varphi_*\,,\qquad \varphi^\downarrow=\varphi+\pi\,,\qquad \varphi_*^\downarrow=\varphi_*+\pi\,.$$

The model describes motion along straight lines with fixed speed in direction φ, interrupted by hard binary collisions with collision cross-section $b(\varphi,\varphi_*)$, which quantifies the collision frequency and depends on the shape of the bacteria. As usual, sub- and super-scripts on f indicate evaluation at φ with the same sub- and super-scripts. The two different gain terms describe two different types of collisions:

- *Alignment:* $(\tilde{\varphi}, \varphi_*) \to (\varphi, \varphi)$ with $\varphi = (\tilde{\varphi} + \varphi_*)/2$, if two myxobacteria moving in directions $\tilde{\varphi}$ and φ_* meet at an angle smaller than $\pi/2$. The factor 2 is due to the fact that an alignment collision produces 2 myxobacteria with the same direction. The set $\mathbb{T}^{AL}_{\to\varphi}$ describes all angles φ_*, which can produce the angle φ upon collision.

- *Reversal:* $(\varphi, \varphi_*) \to (\varphi^{\downarrow}, \varphi_*^{\downarrow})$, if two myxobacteria with directions φ and φ_* meet at an angle larger than $\pi/2$. The set $\mathbb{T}^{REV}_{\varphi}$ describes all angles φ_* such that a collision involving φ can produce the angle $\varphi^{\downarrow}$.

Myxobacteria are rod-shaped bacteria that live in cultivated soil. They feed on living and dead decaying material including bacteria and eukaryotic microbes, which makes them play an important role as scavengers cleaning up biological detritus in the environment. They have an interesting life cycle, similar to certain amoebae, called cellular slime molds (with *Dictyostelium discoideum* as the best known example). During their vegetative phase they move as predatory swarms searching and killing prey collectively, while under starvation conditions they aggregate and form fruiting bodies, which produce spores that are more likely to survive until nutrients are more plentiful again.

Myxobacteria are able to move on flat surfaces by *gliding* [30], leaving a slime–trail behind them. The physical mechanism as well as the genetic basis are still partly a puzzle to microbiologists and have already challenged them for several decades [21, 33, 38, 40].

Moving on solid surfaces, bacteria form organized mono- or multi-layered groups called *swarms*. During the swarming process *rippling* is observed, i.e., macroscopic patterns due to propagating waves of aligned bacteria. The formation of these waves can be seen during collective hunting as well as in the aggregation phase [23]. From a macroscopic point of view colliding waves seem to travel unaffectedly through each other, while tracking of individual bacteria [34, 39] has revealed that most cells reverse their direction in the collision process preserving, however, a nematic alignment order, i.e. locally myxobacteria are oriented and move in the same or in opposite directions.

Pattern formation requires signaling between cells. The signaling mechanism most important for aggregation and rippling is called *C-signaling* [34]. It relies on the *C-factor,* a protein bound to the cell surface and interchanged between individuals. It has been observed that direct cell-cell contact is necessary for C-signaling [27, 28].

The dynamics of myxobacteria has been one of the motivations to formulate kinetic theories for interacting self-propelled rods [6, 10]. In [18] a kinetic model has been formulated, which produces relaxation to nematically aligned states. The model is of mean field type, i.e., cell-cell signaling is modeled as a nonlocal process. Simulations with the macroscopic limit do not produce the rippling phenomenon. It turns out to be necessary to include a waiting time between reversals [19, 22, 23].

The model (2.1) is based on local interactions to take into account the experimental evidence on C-signaling. As a consequence it is structurally similar to the *Boltzmann equation* of gas dynamics [13,16]. In the following section we present a formal derivation from a stochastic many-particle model, following the lines of [16] (see [15] for a rigorous derivation of a similar spatially homogeneous equation). The derivation is facilitated by an approximate version of the alignment collisions, with slightly different post-collisional directions, allowing inversion of the collisional rules. The final step is the removal of the approximation. The model with approximate alignment collisions has similarities with the *dissipative Boltzmann equation* for granular gases [35], whereas after removal of the approximation it corresponds to the extreme case of *sticky particles*. A model with approximate alignment, motivated by microtubule dynamics, has already been formulated in [4], and the sticky particles case, regularized by diffusion in the angular direction, has been analyzed in [8].

The theory for the dissipative Boltzmann equation is much less developed than for its conservative counterpart, mainly because of the lack of an entropy estimate. Global existence results are only

known for small data (see, e.g., [1], [36]) or in the one-dimensional situation, where grazing collisions are almost elastic [7]. The rigorous macroscopic limit towards pressureless gas dynamics has been carried out in the one-dimensional case [25].

In Section 3 formal properties of the collision operator are collected, by separately considering the reversal and the alignment collisions. It is shown that the set of equilibria is three-dimensional, whereas in general there are only two independent collision invariants, which does not allow to identify equilibria uniquely from initial data. A remedy is to make assumptions on the support of the initial data, such that the bacteria are split into two groups with alignment collisions only within the groups and reversal collisions only between members of different groups. In this case the sizes of the groups are invariant, which provides the missing third collision invariant.

Section 4 is dedicated to the spatially homogeneous case which, for the inelastic Boltzmann equation, is much better understood than the spatially inhomogeneous case, see for example [12, 31, 32]. In our case a global existence and uniqueness result in L^1 for the spatially homogeneous equation is proved. By the boundedness of the collision cross-section the proof is rather straightforward. A possible extension to measure solutions as in [2] does not seem feasible because of the jumps from alignment to reversal collisions. Convergence to equilibrium is only considered for special initial data as described above, since only in this case we are able to identify the equilibrium in terms of the initial data. It is shown that a variance type functional, which can be interpreted as the Wasserstein-2 distance from the equilibrium, is dissipated as an effect of the alignment collisions. However, the dissipation is not definite, since the convergence to equilibrium also requires the reversal collisions. A full decay result to equilibrium is only obtained for circular myxobacteria, termed *Maxwellian myxos,* since in this case the collision cross-section is constant. Under this assumption a second decaying functional can be combined with the first, providing exponential decay to equilibrium with respect to the Wasserstein-2 metric, a result similar to [17] (see also [12] for the long time behavior of the inelastic Boltzmann equation for Maxwellian molecules). For rod shaped myxobacteria convergence could only be shown for an even smaller set of initial conditions supported in an interval of length $\pi/2$ such that only alignment collisions occur. In this case convergence cannot be expected to be exponential, since the collision cross-section degenerates close to equilibrium. An algebraic decay estimate is shown as in *Haff's law* [20] for the dissipative Boltzmann equation. Haff's law has been proved rigorously in the 3-dimensional homogeneous case for constant restitution in [32]. Further results for the one dimensional dissipative Boltzmann equation can be found in [2] as well as for viscoelastic hard-spheres in [3]. In these works it has been shown that the algebraic decay rates are sharp by methods, which do not seem to be applicable in our situation.

In Section 5 numerical simulations of the spatially homogeneous model are presented, illustrating the results of Section 4 as well as the conjecture that they remain valid without special assumptions on initial data and bacteria shape. Finally, a short discussion of the formal macroscopic limit of (2.1) is presented in Section 6. In a special case the structure of the macroscopic equations is that of pressureless gas dynamics as for the dissipative Boltzmann equation [25]. A more regular macroscopic limit including a temperature equation has been formally derived in [11] under the assumption of weak inelasticity.

2.2 Model derivation

The individual based model: We consider N identical bacteria moving in $\mathbb{R}^2$. Each of them is idealized as a rod of thickness zero and of length l, represented by the parametrization $B_i = \{x_i + \alpha\,\omega_i : -l/2 \le \alpha \le l/2\}$ with center $x_i \in \mathbb{R}^2$, direction $\omega_i = \omega(\varphi_i) = (\cos\varphi_i, \sin\varphi_i)$, and direction angle $\varphi_i \in \mathbb{T}^1$, $i = 1, \dots, N$. As usual in kinetic theory, sub- and superscripts on functions of

the direction angle indicate evaluation at φ with the same sub- and superscripts. Between interactions, bacterium number i is gliding with constant speed s_0 in its longitudinal direction ω_i, i.e. its velocity is given by $v_i = s_0\,\omega_i$.

The state space is given by $\Gamma_N \subset (\mathbb{R}^2 \times \mathbb{T}^1)^N$, defined such that the bacteria do not overlap:

$$\Gamma_N := \{(x_1, \varphi_1, \ldots, x_N, \varphi_N) : (x_i, \varphi_i, x_j, \varphi_j) \in \Gamma_2 \quad \forall (i,j)\} ,$$

with

$$\Gamma_2 := \left\{ (x, \varphi, x_*, \varphi_*) : \max\{|\alpha|, |\alpha_*|\} > \frac{l}{2} , \quad \text{for } \alpha = \frac{(x_* - x)\cdot \omega_*^\perp}{\omega \cdot \omega_*^\perp} , \, \alpha_* = \frac{(x - x_*)\cdot \omega^\perp}{\omega_* \cdot \omega^\perp} \right\} ,$$

with $\omega = \omega(\varphi)$, $\omega_* = \omega(\varphi_*)$, $(a_1, a_2)^\perp = (-a_2, a_1)$. Note that α and α_* are determined such that $x + \alpha\omega = x_* + \alpha_*\omega_*$.

The collision rules are derived from the biological observations mentioned above. We assume that collisions between two bacteria B and B_* with pre-collisional states (x, φ) and, respectively, (x_*, φ_*) are instantaneous and can either lead to

- **Alignment**, if $\omega \cdot \omega_* > 0$ (collision with pre-collisional angles less than $\pi/2$ apart), or to
- **Reversal** of both bacteria, if $\omega \cdot \omega_* < 0$ (collision with pre-collisional angles greater than $\pi/2$ apart).

Only *binary collisions* are considered. As usual in kinetic theory, collisions between three or more bacteria at the same time are much less likely than binary collisions and are therefore neglected. By the same argument we neglect the limiting case $\omega \cdot \omega_* = 0$.

For a precise formulation of the *collision rules* we introduce the set of *pre-collisional* states,

$$\partial\Gamma_2^{out} := \left\{ (x, \varphi, x_*, \varphi_*) \in \partial\Gamma_2 : \exists\, \alpha \in \left[-\frac{l}{2}, \frac{l}{2}\right] : x + \alpha\omega = x_* + \frac{l}{2}\omega_* \quad \text{or} \right.$$
$$\left. \exists\, \alpha_* \in \left[-\frac{l}{2}, \frac{l}{2}\right] : x + \frac{l}{2}\omega = x_* + \alpha_*\omega_* \right\} ,$$

and of *post-collisional* states, $\partial\Gamma_2^{in} := \partial\Gamma_2 \setminus \partial\Gamma_2^{out}$, of a pair of bacteria.

Alignment between (x, φ) and (x_*, φ_*) happens, if $(x, \varphi, x_*, \varphi_*) \in \partial\Gamma_2^{out}$ and

$$\varphi_* \in \mathbb{T}^{AL}_{\varphi\rightarrow} := \{\psi \in \mathbb{T}^1 : \omega(\varphi)\cdot\omega(\psi) > 0\} = \left(\varphi - \frac{\pi}{2}, \varphi + \frac{\pi}{2}\right) .$$

The alignment collision rule is (see Fig. 2.1 (a)):

$$(x, \varphi),\, (x_*, \varphi_*) \quad \rightarrow \quad (x', \varphi'),\, (x', \varphi') \qquad \text{with } x' = \frac{x + x_*}{2},\, \varphi' = \frac{\varphi + \varphi_*}{2}.$$

Note that the representation of $\mathbb{T}^{AL}_{\varphi\rightarrow}$ as an interval around φ is necessary for the above formula for the post-collisional angle φ' to provide the direction $\omega(\varphi')$ lying between the pre-collisional directions $\omega(\varphi)$ and $\omega(\varphi_*)$.

Reversal between (x, φ) and (x_*, φ_*) happens, if $(x, \varphi, x_*, \varphi_*) \in \partial\Gamma_2^{out}$ and

$$\varphi_* \in \mathbb{T}^{REV}_{\varphi} := \{\psi \in \mathbb{T}^1 : \omega(\varphi)\cdot\omega(\psi) < 0\} .$$

The reversal collision rule is (see Fig. 2.1 (b)):

$$(x, \varphi),\, (x_*, \varphi_*) \quad \to \quad (x, \varphi + \pi),\, (x_*, \varphi_* + \pi).$$

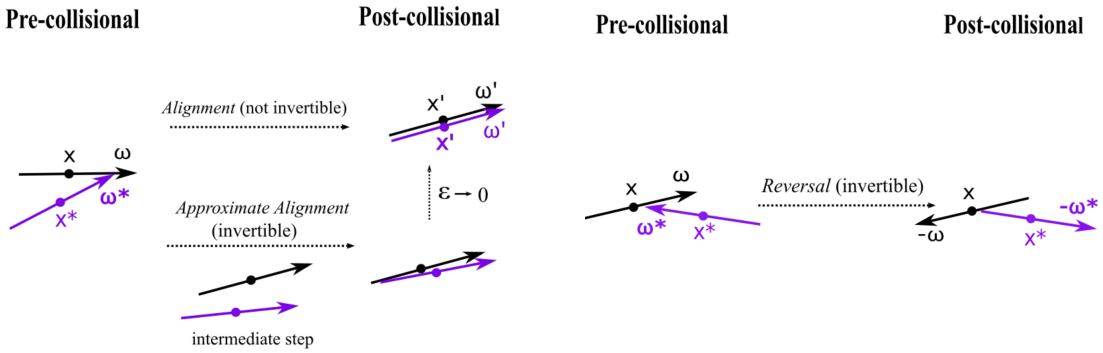

(a) Alignment collisions

(b) Reversal collisions

Figure 2.1: Graphic illustration of the collision rules. (a): *Alignment collisions* with two-step geometric algorithm to regularize it. (b): Already invertible *reversal collisions*.

Regularization of the alignment collisions: In both types of collisions the pair of post-collisional states is in $\partial\Gamma_2^{in}$. After an alignment event its state space velocity does, however, not point into the interior of Γ_2. Also the collision rule for alignment is obviously not invertible. Since we intend to formulate a kinetic model following the standard derivation of the *Boltzmann equation for hard spheres* [13, 16], where the inverse of the collision rule is used, we shall introduce a regularization of the alignment collisions, which will be removed again after the derivation. The *post-collisional* angles are reformulated such that the bacteria drift slightly apart after the collision:

Regularized alignment: Let $(x, \varphi, x_*, \varphi_*) \in \partial\Gamma_2^{out}$ with $\varphi_* \in \mathbb{T}^{AL}_{\varphi\to}$. With a small parameter $\varepsilon > 0$, the regularized collision rule is given by $(x, \varphi), (x_*, \varphi_*) \quad \to \quad (x', \varphi'), (x'_*, \varphi'_*)$, with the rule

$$\varphi' = \frac{1-\varepsilon}{2}\varphi + \frac{1+\varepsilon}{2}\varphi_*\,, \qquad \varphi'_* = \frac{1+\varepsilon}{2}\varphi + \frac{1-\varepsilon}{2}\varphi_*\,, \tag{2.2}$$

for the angles. The post-collisional centers are determined such that the post-collisional states are in $\partial\Gamma_2^{in}$, according to the following algorithm: First the bacteria are turned to the post-collisional directions around the pre-collisional centers, and then the centers are shifted towards each other, until the trailing end of one of them touches the other (see Fig. 2.1 (a)).

This leads to

$$x' = \frac{1+\varepsilon A}{2}x + \frac{1-\varepsilon A}{2}x_*\,, \qquad x'_* = \frac{1-\varepsilon A}{2}x + \frac{1+\varepsilon A}{2}x_*\,, \tag{2.3}$$

with $0 < A = O(1)$ as $\varepsilon \to 0$, depending on the pre-collisional state. There are two different versions for the formula for A covering the cases where the pre-collisional leading end of B is touching B_* (and the post-collisional trailing end of B_* is touching B) or vice versa.

The inversion of the collision rule is easy for the angles:

$$\varphi = \frac{1+\varepsilon}{2\varepsilon}\varphi'_* - \frac{1-\varepsilon}{2\varepsilon}\varphi'\,, \qquad \varphi_* = \frac{1+\varepsilon}{2\varepsilon}\varphi' - \frac{1-\varepsilon}{2\varepsilon}\varphi'_*\,.$$

For the cell centers it can be described by a geometric algorithm as above: First the bacteria are turned around their post-collisional centers to the pre-collisional directions given above, leading to a forbidden state, where they cross each other. Then the centers are shifted apart until the leading end of one of them touches the other.

Probabilistic description: To derive the kinetic equation, we now reformulate the problem in terms of a probability density $P(\cdot, t)$ on Γ_N at time $t \geq 0$. We assume *indistinguishability* of the bacteria, i.e. P is invariant under permutations of the labels of the bacteria. It satisfies the *Liouville equation*

$$\partial_t P + \sum_{i=1}^{N} v_i \cdot \nabla_{x_i} P = 0\,,$$

where $v_i = s_0\omega_i$, subject to boundary conditions, which are determined by the collision rules:

$$P(\ldots, x', \varphi', \ldots, x'_*, \varphi'_*, \ldots, t) = F_{in} P(\ldots, x, \varphi, \ldots, x_*, \varphi_*, \ldots, t) \tag{2.4}$$
$$\text{for} \quad (x, \varphi, x_*, \varphi_*) \in \partial\Gamma_2^{out}, \quad \omega \cdot \omega_* > 0\,,$$
$$P(\ldots, x, \varphi^{\downarrow}, \ldots, x_*, \varphi_*^{\downarrow}, \ldots, t) = P(\ldots, x, \varphi, \ldots, x_*, \varphi_*, \ldots, t) \tag{2.5}$$
$$\text{for} \quad (x, \varphi, x_*, \varphi_*) \in \partial\Gamma_2^{out}, \quad \omega \cdot \omega_* < 0\,,$$

where $\varphi^{\downarrow} = \varphi + \pi$, $\varphi_*^{\downarrow} = \varphi_* + \pi$, and the relations between $(x, \varphi, x_*, \varphi_*)$ and $(x', \varphi', x'_*, \varphi'_*)$ in (2.4) are given by (2.2) and (2.3). The factor F_{in} in (2.4) is determined such that

$$P(\ldots, x', \varphi', \ldots, x'_*, \varphi'_*, \ldots, t)|{v_*}' \cdot {\omega'}^{\perp}|d\sigma' = P(\ldots, x, \varphi, \ldots, x_*, \varphi_*, \ldots, t)|v_* \cdot \omega^{\perp}|d\sigma\,,$$

where $d\sigma$ and $d\sigma'$ are the 5-dimensional surface measures on $\partial\Gamma_2^{out}$ and, respectively, $\partial\Gamma_2^{in}$. This guarantees particle conservation. No such factor is needed in (2.5) since the reversal collisions preserve the surface area as well as the normal component $|v_* \cdot \omega^{\perp}|$ of the flux.

We shall need a formula for F_{in} for the situation, where the leading end of bacterium B hits bacterium B_* in an alignment collision. The corresponding part of $\partial\Gamma_2^{out}$ can be parametrized by $(x, \varphi, \varphi_*, \alpha)$ with

$$x_* = x + \frac{\ell}{2}\omega - \alpha\omega_*\,.$$

Similarly, the parameters along the corresponding part of $\partial\Gamma_2^{in}$ can be taken as $(x', \varphi', \varphi'_*, \alpha')$ with

$$x'_* = x' + \alpha'\omega' + \frac{\ell}{2}\omega'_*\,.$$

A straightforward computation then gives

$$F_{in} = \frac{|\omega_* \cdot \omega^{\perp}|}{\varepsilon|\partial_\alpha \alpha'||\omega'_* \cdot {\omega'}^{\perp}|}\mathbb{1}_{\omega\cdot\omega_*>0}\,.$$

Since $|\varphi' - \varphi'_*| = \varepsilon|\varphi - \varphi_*|$, the inflow data vanish, whenever $\varepsilon\pi/2 < |\varphi' - \varphi'_*| < \pi/2$.

The k-bacteria marginals ($1 \leq k \leq N$) of the distribution will be denoted by

$$P_k(x_1, \varphi_1, \ldots, x_k, \varphi_k, t) := \int_{\Gamma_{N-k}^N(x_1,\varphi_1,\ldots,x_k,\varphi_k)} P(x_1, \varphi_1, \ldots, x_N, \varphi_N, t) \prod_{j=k+1}^{N} dx_j d\varphi_j\,,$$

with

$$\Gamma_{N-k}^N(x_1, \varphi_1, \ldots, x_k, \varphi_k) = \{(x_{k+1}, \varphi_{k+1}, \ldots, x_N, \varphi_N) : (x_1, \varphi_1, \ldots, x_N, \varphi_N) \in \Gamma_N\}$$

In order to obtain an evolution equation for the one-bacterium marginal $P_1(x,\varphi,t)$, we integrate the Liouville equation (2.2) over $\Gamma_{N-1}^N(x,\varphi)$, which gives

$$\partial_t P_1 + v\cdot\nabla_x P_1 + \sum_{j=2}^N \int_{\Gamma_{N-1}^N(x,\varphi)} v_j\cdot\nabla_{x_j} P \prod_{i=2}^N \mathrm{d}x_i \mathrm{d}\varphi_i = 0\,.$$

By the indistinguishability property, all the terms in the sum are identical, leading to

$$\partial_t P_1 + v\cdot\nabla_x P_1 = -(N-1)\int_{\Gamma_1^2(x,\varphi)} v_*\cdot\nabla_{x_*} P_2(x,\varphi,x_*,\varphi_*,t)dx_*d\varphi_*\,. \tag{2.6}$$

An application of the divergence theorem gives an integration over

$$(x_*,\varphi_*)\in\partial\Gamma_1^2(x,\varphi) \quad\Longleftrightarrow\quad (x,\varphi,x_*,\varphi_*)\in\partial\Gamma_2\,,$$

where the splitting

$$\begin{aligned} G-L \;:=\; & (N-1)\int_{\mathbb{T}^1}\int_{-\ell/2}^{\ell/2}|v_*\cdot\omega^\perp| P_2\left(x,\varphi,x+\alpha\omega+\frac{\ell}{2}\omega_*,\varphi_*\right)d\alpha\,d\varphi_* \\ & -(N-1)\int_{\mathbb{T}^1}\int_{-\ell/2}^{\ell/2}|v_*\cdot\omega^\perp| P_2\left(x,\varphi,x+\alpha\omega-\frac{\ell}{2}\omega_*,\varphi_*\right)d\alpha\,d\varphi_* \end{aligned}$$

of the right hand side of (2.6) into a *gain term* and a *loss term* corresponds to a splitting into post-collisional states ($(x,\varphi,x_*,\varphi_*)\in\partial\Gamma_2^{in}$) and pre-collisional states ($(x,\varphi,x_*,\varphi_*)\in\partial\Gamma_2^{out}$). Note that only those post-collisional states contribute, where the trailing end of bacterium B_* touches bacterium B, i.e. $x_*-\frac{\ell}{2}\omega_* = x+\alpha\omega$, and only those pre-collisional states, where the leading end of B_* touches B, i.e. $x_*+\frac{\ell}{2}\omega_* = x+\alpha\omega$.

The next step is to write the gain term in terms of pre-collisional states. In the part originating from reversal collisions it is straightforward to use the boundary conditions (2.5) to obtain

$$G_{REV}(x,\varphi) = (N-1)s_0\int_{\mathbb{T}^{REV}_\varphi}\int_{-\ell/2}^{\ell/2}|\omega_*\cdot\omega^\perp| P_2\left(x,\varphi^\downarrow,x+\alpha\omega-\frac{\ell}{2}\omega_*,\varphi_*^\downarrow\right)d\alpha\,d\varphi_*\,,$$

where also the coordinate change $\alpha\to-\alpha$ has been carried out. For the alignment collisions a little more care is necessary. For easier use of our earlier notation we write

$$\begin{aligned} G_{AL,\varepsilon}(x',\varphi') &= (N-1)s_0\int_{\mathbb{T}^{AL}_{\varphi'\to}}\int_{-\ell/2}^{\ell/2}|\omega_*'\cdot\omega'^\perp| P_2\left(x',\varphi',x'+\alpha'\omega'+\frac{\ell}{2}\omega_*',\varphi_*'\right)d\alpha'\,d\varphi_*' \\ &= (N-1)s_0\int_{\mathbb{T}^{AL}_{\varphi'\to}}\int_{-\ell/2}^{\ell/2}|\omega_*'\cdot\omega'^\perp| F_{in} P_2\left(x,\varphi,x+\frac{\ell}{2}\omega-\alpha\omega_*,\varphi_*\right)d\alpha'\,d\varphi_*' \\ &= \frac{2(N-1)s_0}{1-\varepsilon}\int_{\mathbb{T}^{AL}_{\to\varphi'}}\int_{-\ell/2}^{\ell/2}|\omega_*\cdot\omega^\perp| P_2\left(x,\varphi,x+\frac{\ell}{2}\omega-\alpha\omega_*,\varphi_*\right)d\alpha\,d\varphi_*\,, \end{aligned}$$

where in the last line $\mathbb{T}^{AL}_{\to\varphi'} = \{\varphi_* : |\varphi'-\varphi_*|\leq(1-\varepsilon)\pi/4\}$ denotes the set of all angles φ_* which, after an alignment collision with collision partner

$$\varphi = \frac{2\varphi'-(1+\varepsilon)\varphi_*}{1-\varepsilon}$$

(as a consequence of (2.2)) produce the post-collisional angle φ'. Also x can be expressed in terms of x', φ', α, and φ_*, satisfying $x = x'+O(\ell)$ for small ℓ. Note that this representation is sufficient for the Boltzmann-Grad limit, which we will perform next and where ℓ is assumed to be small compared to a reference length. The computations have involved the use of the boundary conditions (2.4) and the coordinate change $(\alpha',\varphi_*')\to(\alpha,\varphi_*)$, according to the rules for the regularized alignment collisions.

Scaling and Boltzmann-Grad limit: We choose as macroscopic length scale the total length of $N-1$ bacteria, $\mathcal{L} = (N-1)\ell$, and introduce the nondimensionalization

$$x \to \mathcal{L}x\,, \quad t \to \frac{\mathcal{L}}{s_0}t\,, \quad P_k \to \mathcal{L}^{-2k}P_k\,, \quad \alpha \to \ell\alpha\,,$$

leading to the dimensionless version of the equation for the one-bacterium marginal:

$$\partial_t P_1 + \omega\cdot\nabla_x P_1 = G_{AL,\varepsilon} + G_{REV} - L\,,$$

where

$$\begin{aligned}
L(x,v) &= \int_{\mathbb{T}^1}\int_{-1/2}^{1/2} |\omega_*\cdot\omega^\perp| P_2(x,\varphi,x+\delta(\alpha\omega-\omega_*/2),\varphi_*)d\alpha\,d\varphi_*\,,\\
G_{REV}(x,\varphi) &= \int_{\mathbb{T}^{REV}_\varphi}\int_{-1/2}^{1/2} |\omega_*\cdot\omega^\perp| P_2\left(x,\varphi^\downarrow,x+\delta(\alpha\omega-\omega_*/2),\varphi_*^\downarrow\right)d\alpha\,d\varphi_*\,,\\
G_{AL,\varepsilon}(x,\varphi) &= \frac{2}{1-\varepsilon}\int_{\mathbb{T}^{AL}_{\to\varphi}}\int_{-1/2}^{1/2} |\omega_*\cdot\tilde\omega^\perp| P_2(\tilde x,\tilde\varphi,\tilde x+\delta(\tilde\omega/2-\alpha\omega_*),\varphi_*)d\alpha\,d\varphi_*\,,
\end{aligned}$$

with

$$\delta = \frac{\ell}{\mathcal{L}}\,, \qquad \tilde\varphi = \frac{2\varphi-(1+\varepsilon)\varphi_*}{1-\varepsilon}\,, \qquad \tilde x = x + O(\delta) \quad \text{as } \delta\to 0\,.$$

The Boltzmann-Grad limit is the large particle number limit $N\to\infty$, i.e. $\delta\to 0$. As usual, the *molecular chaos* assumption [16] will be used. Roughly speaking, it amounts to assuming that initially the probability distributions of the bacteria are pairwise independent and that any pair of bacteria collides at most once, such that the independence is still valid for each pre-collisional state. This is the reason for writing the collision integrals in terms of pre-collisional states. As a consequence, assuming $P_1\to f$ implies $P_2\to f\otimes f$ as $N\to\infty$, wherever it occurs in the equation. In the limit, we obtain the Boltzmann-type equation

$$\begin{aligned}
&\partial_t f + \omega\cdot\nabla_x f = G_{AL,\varepsilon}(f,f) + G_{REV}(f,f) - L(f,f)\\
&= \frac{2}{1-\varepsilon}\int_{\mathbb{T}^{AL}_{\to\varphi}} b(\tilde\varphi,\varphi_*)f(x,\tilde\varphi)f(x,\varphi_*)d\varphi_* + \int_{\mathbb{T}^{REV}_\varphi} b(\varphi,\varphi_*)f(x,\varphi^\downarrow)f(x,\varphi_*^\downarrow)d\varphi_*\\
&- \int_{\mathbb{T}^1} b(\varphi,\varphi_*)f(x,\varphi)f(x,\varphi_*)d\varphi_*\,,
\end{aligned}$$

with $b(\varphi,\varphi_*) = |\omega_*\cdot\omega^\perp| = |\sin(\varphi-\varphi_*)|$. The collision integrals are now written as bilinear operators where, abusing notation, we have kept the same names.

Alignment limit: It is now straightforward to remove the regularization of the alignment collisions, i.e. to carry out the limit $\varepsilon\to 0$, leading to our *kinetic model for myxobacteria:*

$$\begin{aligned}
&\partial_t f + \omega\cdot\nabla_x f = Q(f,f) := G_{AL}(f,f) + G_{REV}(f,f) - L(f,f)\\
&= 2\int_{\mathbb{T}^{AL}_{\to\varphi}} b(\tilde\varphi,\varphi_*)\tilde f f_* d\varphi_* + \int_{\mathbb{T}^{REV}_\varphi} b(\varphi,\varphi_*)f^\downarrow f_*^\downarrow d\varphi_* - \int_{\mathbb{T}^1} b(\varphi,\varphi_*)f f_* d\varphi_*\,,
\end{aligned} \tag{2.7}$$

with

$$\mathbb{T}^{REV}_\varphi = \left(\varphi+\frac{\pi}{2},\varphi+\frac{3\pi}{2}\right)\,, \qquad \mathbb{T}^{AL}_{\to\varphi} = \left(\varphi-\frac{\pi}{4},\varphi+\frac{\pi}{4}\right)\,,$$

$$\tilde\varphi = 2\varphi-\varphi_*\,, \qquad \varphi^\downarrow = \varphi+\pi\,, \qquad \varphi_*^\downarrow = \varphi_*+\pi\,.$$

Note that $\varphi_*\in\mathbb{T}^{AL}_{\to\varphi}$ satisfies $\omega(\tilde\varphi)\cdot\omega(\varphi_*)>0$ and that $\mathbb{T}^{REV}_\varphi$ is a representation of the set of all $\varphi_*\in\mathbb{T}^1$ satisfying $\omega(\varphi)\cdot\omega(\varphi_*)<0$.

'Maxwellian myxos': The factor $b(\varphi,\varphi_*) = |\omega_* \cdot \omega^\perp| = |\sin(\varphi-\varphi_*)|$ in the collision integrals is a consequence of the rod shape of the bacteria. It gives the rate of collisions between bacteria with the directions φ and φ_*. Assuming instead bacteria with circular shape makes the collision rate independent from the movement direction. By analogy to a similar simplification of the gas dynamics Boltzmann equation [16], we use the name *Maxwellian myxos* for this imagined species, modeled by (2.7) with $b(\varphi,\varphi_*) \equiv 1$.

2.3 Properties of the collision operator

Collision invariants and conservation laws: In the following it will be convenient to also split the loss term of the collision operator into alignment and reversal parts:

$$\begin{aligned} Q(f,f) &= Q_{AL}(f,f) + Q_{REV}(f,f) \\ &= \int_{\mathbb{T}^1} \left(2b(\tilde\varphi,\varphi_*)\mathbb{1}_{\varphi_*\in\mathbb{T}^{AL}_{\to\varphi}} \tilde f f_* - b(\varphi,\varphi_*)\mathbb{1}_{\varphi_*\in\mathbb{T}^{AL}_{\varphi\to}} f f_* \right) d\varphi_* \\ &\quad + \int_{\mathbb{T}^{REV}_\varphi} b(\varphi,\varphi_*)(f^\downarrow f_*^\downarrow - f f_*) d\varphi_* \,, \end{aligned}$$

A weak formulation of the alignment operator is obtained by integration against a test function $\psi(\varphi)$, the coordinate change $\tilde\varphi = 2\varphi - \varphi_* \to \varphi$, and subsequent symmetrization:

$$\int_{\mathbb{T}^1} Q_{AL}(f,f)\psi\, d\varphi = \int_{\mathbb{T}^1}\int_{\mathbb{T}^{AL}_{\varphi\to}} b(\varphi,\varphi_*) f f_* \left(\psi\left(\frac{\varphi+\varphi_*}{2}\right) - \frac{\psi(\varphi)+\psi(\varphi_*)}{2} \right) d\varphi_*\, d\varphi \qquad (2.9)$$

This shows that the space of collision invariants of Q_{AL} is two-dimensional and spanned by $\psi = 1$ and $\psi = \varphi$. Furthermore, with $\psi = \varphi^2$, we obtain

$$\int_{\mathbb{T}^1} Q_{AL}(f,f)\varphi^2\, d\varphi = -\frac{1}{4}\int_{\mathbb{T}^1}\int_{\mathbb{T}^{AL}_{\varphi\to}} b(\varphi,\varphi_*) f f_* (\varphi-\varphi_*)^2 d\varphi_*\, d\varphi \le 0\,.$$

Therefore $Q_{AL}(f,f) = 0$ implies that for $f(\varphi) \neq 0$, $f(\varphi_*)$ vanishes for all $\varphi \neq \varphi_* \in \mathbb{T}^{AL}_{\varphi\to}$. As a consequence, equilibria are concentrated at isolated angles with a pairwise distance bigger than $\pi/2$, implying that there are at most three of them. Thus, every equilibrium distribution f of Q_{AL} can be written as

$$f(\varphi) = \rho_1\delta(\varphi-\varphi_1) + \rho_2\delta(\varphi-\varphi_2) + \rho_3\delta(\varphi-\varphi_3)\,,$$

with $\rho_j \ge 0$ and $\mathrm{dist}_{\mathbb{T}^1}(\varphi_i,\varphi_j) > \pi/2$, $i \neq j$, where

$$\mathrm{dist}_{\mathbb{T}^1}(\varphi,\varphi_*) := \min_{k\in\mathbb{Z}} |\varphi - \varphi_* + 2k\pi| \le \pi\,.$$

The weak formulation of the reversal operator can be written as

$$\begin{aligned} \int_{\mathbb{T}^1} Q_{REV}(f,f)\psi\, d\varphi &= \frac{1}{2}\int_{\mathbb{T}^1}\int_{\mathbb{T}^{REV}_\varphi} b(\varphi,\varphi_*) f f_* \left(\psi^\downarrow + \psi_*^\downarrow - \psi - \psi_*\right) d\varphi_*\, d\varphi \\ &= \frac{1}{2}\int_{\mathbb{T}^1}\int_{\mathbb{T}^{AL}_{\varphi\to}} b(\varphi,\varphi_*) f f_*^\downarrow \left(\psi^\downarrow + \psi_* - \psi - \psi_*^\downarrow\right) d\varphi_*\, d\varphi\,, \end{aligned}$$

where the first equality is obtained analogously to the treatment of the alignment operator, and the second equality is due to the coordinate change $\varphi_* \leftrightarrow \varphi_*^\downarrow$. Both forms show that all π-periodic functions are collision invariants. However, the second representation reveals the additional collision invariant

$\psi(\varphi) = \varphi$. It is obvious that all π-periodic functions are equilibria of Q_{REV}. However, the set of equilibria is larger: Let $g : (\pi/4, 3\pi/4) \to \mathbb{R}_+$ be arbitrary, $\lambda \geq 0$, and let

$$f(\varphi) := \begin{cases} g(\varphi) & \text{for } \varphi \in \mathbb{T}^1_+ := (\pi/4, 3\pi/4)\,, \\ \lambda g(\varphi + \pi) & \text{for } \varphi \in \mathbb{T}^1_- := (-3\pi/4, -\pi/4)\,, \\ 0 & \text{else.} \end{cases} \tag{2.11}$$

Then it is easily checked that $Q_{REV}(f, f) = 0$. We see that the set of functions unaffected by reversal collisions contains functions describing bacteria colonies which can be separated into two groups, one moving upwards with direction $\varphi \in \mathbb{T}^1_+$, the other downwards with $\varphi \in \mathbb{T}^1_-$ and whose distribution in each group is equal up to a proportionality constant $\lambda \geq 0$. It is important to note that the boundary angles of $\mathbb{T}^1_+$ and $\mathbb{T}^1_-$ are $\pi/2$ apart, so that reversal collisions can only occur between two individuals from different groups.
The question of a characterization of the whole set of equilibria of Q_{REV} seems rather difficult and is left open.

Since the collision invariants of Q_{AL} are also collision invariants of Q_{REV}, solutions of (2.7) satisfy two conservation laws, *conservation of the number of bacteria,*

$$\partial_t \rho + \nabla_x \cdot (\rho u) = 0\,, \tag{2.12}$$

with the usual definition of *number density* and *flux:*

$$\rho(x,t) := \int_{\mathbb{T}^1} f(x,\varphi,t) d\varphi\,, \qquad \rho u(x,t) := \int_{\mathbb{T}^1} \omega(\varphi) f(x,\varphi,t) d\varphi\,,$$

and

$$\partial_t \int_{\mathbb{T}^1} \varphi f \, d\varphi + \nabla_x \cdot \int_{\mathbb{T}^1} \varphi\, \omega f \, d\varphi = 0\,. \tag{2.13}$$

Note that this second conservation law depends on the representation of $\mathbb{T}^1$. However, the differences are only up to adding a multiple of the bacteria number.

The only equilibria of Q_{AL}, which are also equilibria of Q_{REV}, are of the form

$$f_\infty(\varphi) = \rho_+ \delta(\varphi - \varphi_+) + \rho_- \delta(\varphi - \varphi_+^{\downarrow})\,, \tag{2.14}$$

with arbitrary $\rho_\pm \geq 0$, $\varphi_+ \in \mathbb{T}^1$. This raises the problem that there are three free parameters, ρ_+, ρ_-, φ_+, in the equilibrium distribution as opposed to only two conservation laws (2.12) and (2.13).

Two group initial data: The form (2.11) of reversal equilibria suggests to consider initial conditions

$$f(x, \varphi, 0) = f_I(x, \varphi)\,,$$

satisfying

$$\operatorname{supp}(f_I(x, .)) \subset \mathbb{T}^1_+ \cup \mathbb{T}^1_-, \qquad \forall x \in \mathbb{R}^2\,, \tag{2.15}$$

i.e., with angles in the opposite groups $\mathbb{T}^1_+$ and $\mathbb{T}^1_-$ (see Fig. 2.2). It is easily seen that the property (2.15) is propagated by (2.7). Indeed, *alignment collisions* are only possible between two individuals from the same group, producing post-collisional angles in the same group. *Reversal interactions* can only occur between bacteria from different groups, causing the two individuals to swap groups. These

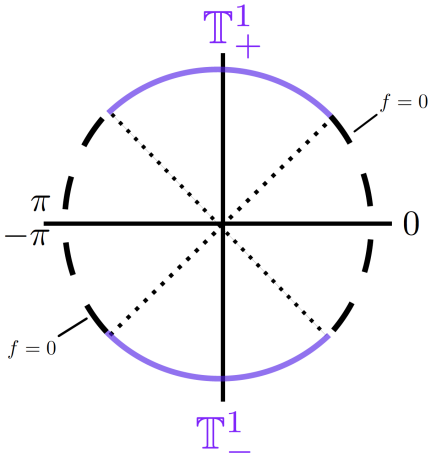

Figure 2.2: Support of two group data (solid lines, purple).

observations imply that in this special situation the bacteria numbers in each group are conserved. With the notation

$$\rho_\pm = \int_{\mathbb{T}^1_\pm} f\, d\varphi\,, \qquad \rho_\pm u_\pm = \int_{\mathbb{T}^1_\pm} \omega f\, d\varphi\,,$$

we have

$$\partial \rho_\pm + \nabla_x \cdot (\rho_\pm u_\pm) = 0\,,$$

where the sum gives (2.12), of course. Thus, there is one additional conservation law, bringing the total number up to three, the dimension of the set of equilibria. This will allow us to perform the (formal) macroscopic limit in Section 6.

2.4 The spatially homogeneous problem

Existence and uniqueness of solutions: We consider the initial value problem

$$\begin{aligned} &\partial_t f = Q(f,f), \qquad \text{in } \mathbb{T}^1 \times (0,\infty) \\ &f(\varphi,0) = f_I(\varphi)\,, \qquad \varphi \in \mathbb{T}^1, \end{aligned} \tag{2.16}$$

with the collision operator as in (2.7) and no restriction on f_I. Existence and uniqueness in $L^1(\mathbb{T}^1)$ will be shown by the Picard theorem since, by the boundedness of the collision cross-section b, the collision operator can be shown to be Lipschitz continuous.

Theorem 2.1. *Let $b \in L^\infty(\mathbb{T}^1 \times \mathbb{T}^1)$ and $f_I \in L^1_+(\mathbb{T}^1)$. Then (2.16) has a unique global solution $f \in C\left([0,\infty), L^1_+(\mathbb{T}^1)\right)$.*

Proof. Let $f, g \in L^1(\mathbb{T}^1)$ with $\|f\|_{L^1(\mathbb{T}^1)}, \|g\|_{L^1(\mathbb{T}^1)} \leq \rho$, and $\bar{b} := \|b\|_{L^\infty(\mathbb{T}^1\times\mathbb{T}^1)}$. We split the collision operator as in (2.7):

$$\|G_{AL}(f,f) - G_{AL}(g,g)\|_{L^1(\mathbb{T}^1)} \leq 2\bar{b} \int_{\mathbb{T}^1} \int_{\mathbb{T}^{AL}_{\to\varphi}} |\tilde{f} f_* - \tilde{g} g_*| d\varphi_* d\varphi = \bar{b} \int_{\mathbb{T}^1} \int_{\mathbb{T}^{AL}_{\varphi\to}} |f f_* - g g_*| d\varphi_* d\varphi\,,$$

with the change of variables $\tilde{\varphi} \to \varphi$ as in the previous section. Further estimation gives

$$\begin{aligned} \|G_{AL}(f,f) - G_{AL}(g,g)\|_{L^1(\mathbb{T}^1)} &\leq \bar{b} \int_{\mathbb{T}^1} \int_{\mathbb{T}^{AL}_{\varphi\to}} \left(|f|\,|f_* - g_*| + |f-g|\,|g_*|\right) d\varphi_* d\varphi \\ &\leq 2\bar{b}\rho\, \|f-g\|_{L^1(\mathbb{T}^1)} \end{aligned}$$

For the reversal term we have

$$\begin{aligned}\|G_{REV}(f,f) - G_{REV}(g,g)\|_{L^1(\mathbb{T}^1)} &\leq \bar{b}\int_{\mathbb{T}^1}\int_{\mathbb{T}^{REV}_\varphi} |f^\downarrow f_*^\downarrow - g^\downarrow g_*^\downarrow| d\varphi_* d\varphi \\ &= \bar{b}\int_{\mathbb{T}^1}\int_{\mathbb{T}^{REV}_\varphi} |f f_* - g g_*| d\varphi_* d\varphi \leq 2\bar{b}\rho \|f-g\|_{L^1(\mathbb{T}^1)},\end{aligned}$$

with $(\varphi^\downarrow, \varphi_*^\downarrow) \to (\varphi, \varphi_*)$. An analogous estimate for the loss term finally gives

$$\|Q(f,f) - Q(g,g)\|_{L^1(\mathbb{T}^1)} \leq 6\bar{b}\rho \|f-g\|_{L^1(\mathbb{T}^1)}.$$

Therefore a unique local solution exists by Picard iteration. Nonnegativity and conservation of the number of bacteria, i.e. of the $L^1(\mathbb{T}^1)$-norm, are obvious, the latter implying global existence. □

Convergence to equilibrium: We study the convergence of solutions of the spatially homogeneous problem (2.16) to equilibria of the form (2.14) as $t \to \infty$. We have, however, only partial results in this direction due to two difficulties. The first one is the lack of a third conservation law for general initial data. We shall therefore restrict our attention to *two-group initial data* f_I satisfying (2.15). In this case the conservation of

$$\int_{\mathbb{T}^1_+} f\, d\varphi, \qquad \int_{\mathbb{T}^1_-} f\, d\varphi, \qquad \text{and} \qquad \int_{\mathbb{T}^1} \varphi f\, d\varphi,$$

allows to determine the parameters in (2.14) from the initial data:

$$\rho_+ = \int_{\mathbb{T}^1_+} f_I\, d\varphi, \qquad \rho_- = \int_{\mathbb{T}^1_-} f_I\, d\varphi, \qquad \varphi_+ = \frac{1}{\rho_+ + \rho_-}\left(\int_{\mathbb{T}^1_+} \varphi f_I\, d\varphi + \int_{\mathbb{T}^1_-} \varphi^\downarrow f_I\, d\varphi\right).$$

Note that $\varphi_+ \in \mathbb{T}^1_+$ is an average angle where, however, angles in $\mathbb{T}^1_-$ are mapped to $\mathbb{T}^1_+$ by reversal.

First, we state a preliminary result on the decay of the variance

$$V[f] := \int_{\mathbb{T}^1_+} (\varphi - \varphi_+)^2 f\, d\varphi$$

for the even more restricted case of *one-group initial data* supported in $\mathbb{T}^1_+ = (\pi/4, 3\pi/4)$, where only alignment collisions occur.

Lemma 2.2. *Let $f_I \in L^1_+(\mathbb{T}^1)$ with $supp(f_I) \subset \mathbb{T}^1_+$ and let f be a solution of (2.16). Then*
a) for Maxwellian myxos, i.e. $b(\varphi, \varphi_*) \equiv 1$,

$$V[f(\cdot,t)] = e^{-t\rho_+/2} V[f_I],$$

b) and for rod shaped myxobacteria, i.e. $b(\varphi, \varphi_*) = |\sin(\varphi - \varphi_*)|$,

$$\frac{1}{\rho_+}\left(M_{1,I}^{-1} + 2t\right)^{-2} \leq V[f(\cdot,t)] \leq \left(V[f_I]^{-1/2} + \kappa t\right)^{-2},$$

with

$$M_{1,I} := \int_{\mathbb{T}^1_+} |\varphi - \varphi_+| f_I\, d\varphi, \qquad \kappa = \frac{\sqrt{\rho_+}}{4\pi}.$$

Remark 2.3. *The result of Lemma 2.2 b) corresponds to Haff's law [20] for the spatially homogeneous dissipative Boltzmann equation, stating that the variance of the distribution decays like t^{-2}. There the degeneracy of the collision cross section is the same as here. Our proof follows along the lines of [2].*

Proof. For the computation of the time derivative of the variance along solutions of (2.16) the formula (2.9) with $\psi(\varphi) = \mathbb{1}_{\mathbb{T}^1_+}(\varphi)(\varphi-\varphi_+)^2$ can be used:

$$\frac{dV[f]}{dt} = -\frac{1}{4}\int_{\mathbb{T}^1_+}\int_{\mathbb{T}^1_+} b(\varphi,\varphi_*) f f_* (\varphi-\varphi_*)^2 d\varphi_* d\varphi \,. \tag{2.17}$$

a) We compute

$$\frac{dV[f]}{dt} = -\frac{1}{4}\int_{\mathbb{T}^1_+}\int_{\mathbb{T}^1_+} f f_* (\varphi-\varphi_+ +\varphi_+-\varphi_*)^2 d\varphi_* d\varphi = -\frac{\rho_+}{2}\int_{\mathbb{T}^1_+} f(\varphi-\varphi_+)^2 d\varphi = -\frac{\rho_+}{2}V[f]\,.$$

b) Since $|\varphi-\varphi_*| \le \pi/2$ in the right hand side of (2.17), we have

$$b(\varphi,\varphi_*) = |\sin(\varphi-\varphi_*)| \ge \frac{2}{\pi}|\varphi-\varphi_*|\,,$$

and therefore, using the Jensen inequality twice,

$$\begin{aligned}
&\int_{\mathbb{T}^1_+}\int_{\mathbb{T}^1_+} b(\varphi,\varphi_*) f f_* (\varphi-\varphi_*)^2 d\varphi_* d\varphi \ge \frac{2}{\pi}\int_{\mathbb{T}^1_+} f\left(\int_{\mathbb{T}^1_+} f_* |\varphi-\varphi_*|^3 d\varphi_*\right) d\varphi \\
&\ge \frac{2\rho_+}{\pi}\int_{\mathbb{T}^1_+} f\left|\int_{\mathbb{T}^1_+}\frac{f_*}{\rho_+}(\varphi-\varphi_*)d\varphi_*\right|^3 d\varphi = \frac{2\rho_+}{\pi}\int_{\mathbb{T}^1_+} f\,|\varphi-\varphi_+|^3\,d\varphi \\
&\ge \frac{2\rho_+^2}{\pi}\left(\int_{\mathbb{T}^1_+}\frac{f}{\rho_+}(\varphi-\varphi_+)^2\,d\varphi\right)^{3/2} = \frac{2\sqrt{\rho_+}}{\pi}\left(V[f]\right)^{3/2}\,,
\end{aligned}$$

giving

$$\frac{dV[f]}{dt} \le -\frac{\sqrt{\rho_+}}{2\pi}V[f]^{3/2}\,,$$

implying the upper bound by solving the corresponding differential equation. A lower bound is first derived for

$$M_1[f](t) := \int_{\mathbb{T}^1_+}|\varphi-\varphi_+| f\,d\varphi\,.$$

We again use (2.9), now with $\psi(\varphi) = \mathbb{1}_{\mathbb{T}^1_+}(\varphi)|\varphi-\varphi_+|$:

$$\frac{dM_1[f]}{dt} = -\frac{1}{2}\int_{\mathbb{T}^1_+}\int_{\mathbb{T}^1_+}|\sin(\varphi-\varphi_*)| f f_* \left(|\varphi-\varphi_+|+|\varphi_*-\varphi_+|-|\varphi+\varphi_*-2\varphi_+|\right)d\varphi_* d\varphi\,.$$

With the elementary inequalities (see also [2, equ. (3.3)] for the second)

$$(|a|+|b|-|a+b|)|\sin(a-b)| \le (|a|+|b|-|a+b|)|a-b| \le 4|a|\,|b|\,,$$

we obtain

$$\frac{dM_1[f]}{dt} \ge -2M_1[f]^2\,,$$

implying

$$M_1[f](t) \ge \left(M_{1,I}^{-1}+2t\right)^{-1}\,.$$

An application of the Cauchy-Schwarz inequality $M_1[f]^2 \le \rho_+ V[f]$ concludes the proof. □

Lemma 2.2 can be interpreted as a convergence result with respect to the *Wasserstein distance* [37]. In particular, for $f, g \in \mathcal{P}(\mathbb{T}^1)$ (the space of probability measures), the Wasserstein distance with quadratic cost is defined by

$$W_2^{\mathbb{T}^1}(f,g) := \inf_{\pi \in \Pi(f,g)} \left(\iint_{\mathbb{T}^1 \times \mathbb{T}^1} \mathrm{dist}_{\mathbb{T}^1}(\varphi_1, \varphi_2)^2 \, d\pi(\varphi_1, \varphi_2) \right)^{1/2},$$

where $\Pi(f,g) \subset \mathcal{P}(\mathbb{T}^1 \times \mathbb{T}^1)$ is the set of all transference plans π, satisfying $\pi(\cdot, \mathbb{T}^1) = f$, $\pi(\mathbb{T}^1, \cdot) = g$. We shall also use the straightforward extension of the definition to pairs of measures with the same total mass, not necessarily equal to one. It is well known that for $g(\varphi) = m\delta(\varphi - \hat{\varphi})$ the only possible transference plan is $\pi = (f \otimes g)/m$ and therefore

$$W_2^{\mathbb{T}^1}(f,g)^2 = \int_{\mathbb{T}^1} \mathrm{dist}_{\mathbb{T}^1}(\varphi, \hat{\varphi})^2 f \, d\varphi \,,$$

implying for distributions with support $\mathbb{T}^1_+$ as in Lemma 2.2 that $V[f] = W_2^{\mathbb{T}^1}(f, f_\infty)^2$.

Since for the two-group case we are dealing with distributions, which are the sums of two point masses, we shall need the following result.

Lemma 2.4. *Let $f, g \in \mathcal{P}(\mathbb{T}^1)$, $\mathrm{supp}(f)$, $\mathrm{supp}(g) \subset \mathbb{T}^1_+ \cup \mathbb{T}^1_-$, $f(\mathbb{T}^1_\pm) = g(\mathbb{T}^1_\pm)$. Then*

$$W_2^{\mathbb{T}^1}(f,g)^2 = W_2^{\mathbb{T}^1_+}(f,g)^2 + W_2^{\mathbb{T}^1_-}(f,g)^2 \,,$$

where on the right hand side f, g denote the restrictions to $\mathbb{T}^1_+$ and, respectively, $\mathbb{T}^1_-$.

Remark 2.5. *The result is actually a rather obvious consequence of the fact that the distance between points within $\mathbb{T}^1_\pm$ is never larger than the distance between a point in $\mathbb{T}^1_+$ and a point in $\mathbb{T}^1_-$, with the consequence that there always exists an optimal transference plan transferring only within the two groups.*

Proof. We only give a proof for the case where f and g are sums of point measures, since the result then follows by a density argument. So let

$$f = \sum_{i=1}^M f_i \delta_{\varphi_i} \,, \qquad g = \sum_{j=1}^N g_j \delta_{\psi_j} \,.$$

A transference plan is then determined by a matrix $\pi \in \mathbb{R}^{M \times N}$ with nonnegative entries, such that

$$\sum_{j=1}^N \pi_{ij} = f_i \,, \qquad \sum_{i=1}^M \pi_{ij} = g_j \,.$$

The statement of the lemma means that there exists an optimal π such that

$$\pi_{ij} > 0 \qquad \Longleftrightarrow \qquad \varphi_i, \psi_j \in \mathbb{T}^1_+ \quad \text{or} \quad \varphi_i, \psi_j \in \mathbb{T}^1_- \,. \tag{2.18}$$

Let now π be a general transference plan and assume that there exists (i,j) such that $\varphi_i \in \mathbb{T}^1_+$, $\psi_j \in \mathbb{T}^1_-$, $\pi_{ij} > 0$. This means that some mass is transferred from $\mathbb{T}^1_+$ to $\mathbb{T}^1_-$. Since the total masses are the same in both groups, the mass balance requires that also some mass is transferred from $\mathbb{T}^1_-$ to $\mathbb{T}^1_+$, i.e. there exists (i_*, j_*) such that $\varphi_{i_*} \in \mathbb{T}^1_-$, $\psi_{j_*} \in \mathbb{T}^1_+$, $\pi_{i_* j_*} > 0$.

The idea is that in this situation the transference plan can be improved by moving mass $m := \min\{\pi_{ij}, \pi_{i_*j_*}\}$ in a cheaper way by the changes

$$\pi_{ij} \to \pi_{ij} - m\,, \quad \pi_{i_*j_*} \to \pi_{i_*j_*} - m\,, \quad \pi_{ij_*} \to \pi_{ij_*} + m\,, \quad \pi_{i_*j} \to \pi_{i_*j} + m\,.$$

This means that the contribution

$$m\left(\mathrm{dist}_{\mathbb{T}^1}(\varphi_i, \psi_j)^2 + \mathrm{dist}_{\mathbb{T}^1}(\varphi_{i_*}, \psi_{j_*})^2\right) \geq \frac{m\pi^2}{2}$$

to the total cost is replaced by

$$m\left((\varphi_i - \psi_{j_*})^2 + (\varphi_{i_*} - \psi_j)^2\right) \leq \frac{m\pi^2}{2}\,,$$

and in the improved transference plan either π_{ij} or $\pi_{i_*j_*}$ is replaced by zero. Iterating the procedure, an improved transference plan satisfying (2.18) is reached in finitely many steps. □

For the two-group case with equilibrium f_∞ given in (2.14), it seems natural to examine the evolution of the Wasserstein distance

$$W_2^{\mathbb{T}^1}(f, f_\infty)^2 = \int_{\mathbb{T}^1_+} (\varphi - \varphi_+)^2 f\, d\varphi + \int_{\mathbb{T}^1_-} (\varphi - \varphi_+ + \pi)^2 f\, d\varphi\,.$$

For the computation of its time derivative along solutions of (2.16) the formulas (2.9), (2.10) with $\psi(\varphi) = \mathbb{1}_{\mathbb{T}^1_+}(\varphi)(\varphi - \bar\varphi_+)^2 + \mathbb{1}_{\mathbb{T}^1_-}(\varphi)(\varphi - \bar\varphi_-)^2$ can be used:

$$\begin{aligned}\frac{d}{dt} W_2^{\mathbb{T}^1}(f, f_\infty)^2 \;&=\; -\frac{1}{4}\int_{\mathbb{T}^1_+}\int_{\mathbb{T}^1_+} b(\varphi, \varphi_*) f f_* (\varphi - \varphi_*)^2 d\varphi_* d\varphi \\ &\quad -\frac{1}{4}\int_{\mathbb{T}^1_-}\int_{\mathbb{T}^1_-} b(\varphi, \varphi_*) f f_* (\varphi - \varphi_*)^2 d\varphi_* d\varphi \leq 0\,.\end{aligned}$$

Note that the reversal collisions do not contribute to the right hand side which vanishes, whenever concentration is reached in both groups, even when the two concentration angles are not opposite each other. Therefore it is not possible to derive a differential inequality for $W_2^{\mathbb{T}^1}(f, f_\infty)$ as in the proof of Lemma 2.2.

We have been able to overcome this problem only for Maxwellian myxos, where we construct a Lyapunov function of the form

$$\mathcal{H}[f] = W_2^{\mathbb{T}^1}(f, \bar f)^2 + \gamma W_2^{\mathbb{T}^1}(\bar f, f_\infty)^2\,,$$

with $\gamma > 0$, and where $\bar f$ denotes the partial equilibrium

$$\bar f(\varphi, t) = \rho_+ \delta(\varphi - \bar\varphi_+(t)) + \rho_- \delta(\varphi - \bar\varphi_-(t))\,, \qquad \text{with } \bar\varphi_\pm(t) := \frac{1}{\rho_\pm}\int_{\mathbb{T}^1_\pm} \varphi f(\varphi, t) d\varphi\,.$$

This implies

$$W_2^{\mathbb{T}^1}(f, \bar f)^2 = \int_{\mathbb{T}^1_+} (\varphi - \bar\varphi_+)^2 f\, d\varphi + \int_{\mathbb{T}^1_-} (\varphi - \bar\varphi_-)^2 f\, d\varphi\,,$$

and

$$W_2^{\mathbb{T}^1}(\bar f, f_\infty)^2 = \rho_+(\bar\varphi_+ - \varphi_+)^2 + \rho_-(\bar\varphi_- - \varphi_+^\downarrow)^2 = \frac{\rho_+\rho_-}{\rho_+ + \rho_-}(\bar\varphi_+ - \bar\varphi_- - \pi)^2\,, \tag{2.20}$$

where the second equality is due to the conservation law (2.13), i.e.,

$$\rho_+\bar\varphi_+ + \rho_-\bar\varphi_- = \rho_+\varphi_+ + \rho_-\varphi_+^\downarrow\,.$$

For the time derivative of the first contribution we obtain, similarly to (2.19), but now with $b \equiv 1$,

$$\begin{aligned}\frac{d}{dt}W_2^{\mathbb{T}^1}(f,\bar f)^2 &= -\frac14\int_{\mathbb{T}^1_+}\int_{\mathbb{T}^1_+} ff_*(\varphi-\varphi_*)^2 d\varphi_* d\varphi - \frac14\int_{\mathbb{T}^1_-}\int_{\mathbb{T}^1_-} ff_*(\varphi-\varphi_*)^2 d\varphi_* d\varphi\\ &\quad +2\rho_+\rho_-(\bar\varphi_+ - \bar\varphi_- - \pi)^2\,,\end{aligned}$$

where the nonnegative term in the second line results from the reversal collisions. The time derivative of the second contribution is not influenced by alignment collisions:

$$\frac{d}{dt}W_2^{\mathbb{T}^1}(\bar f, f_\infty)^2 = -2\rho_+\rho_-(\bar\varphi_+ - \bar\varphi_- - \pi)^2\,,$$

from which, together with (2.20), exponential decay of $W_2^{\mathbb{T}^1}(\bar f, f_\infty)^2$, the reversal part of our Lyapunov function follows. Finally, the identity

$$\int_{\mathbb{T}^1_\pm}\int_{\mathbb{T}^1_\pm} ff_*(\varphi-\varphi_*)^2 d\varphi_* d\varphi = 2\rho_\pm\int_{\mathbb{T}^1_\pm} f(\varphi-\bar\varphi_\pm)^2 d\varphi$$

implies

$$\begin{aligned}\frac{d\mathcal{H}[f]}{dt} &= -\frac{\rho_+}{2}\int_{\mathbb{T}^1_+} f(\varphi-\bar\varphi_+)^2 d\varphi - \frac{\rho_-}{2}\int_{\mathbb{T}^1_-} f(\varphi-\bar\varphi_-)^2 d\varphi\\ &\quad -2(\gamma-1)\rho_+\rho_-(\bar\varphi_+ - \bar\varphi_- - \pi)^2 \le 0\,,\end{aligned}$$

for $\gamma \ge 1$. It is easily seen that with the choice $\gamma = 8/7$ we have

$$\frac{d\mathcal{H}[f]}{dt} \le -2\lambda\mathcal{H}[f]\,, \qquad \text{with } \lambda = \frac14\min\{\rho_+,\rho_-\}\,. \tag{2.21}$$

Theorem 2.6. *Let $f_I \in L^1_+(\mathbb{T}^1)$ with $\mathrm{supp}(f_I) \subset \mathbb{T}^1_+ \cup \mathbb{T}^1_-$, and let f be a solution of (2.16). Then for Maxwellian myxos, i.e. $b(\varphi,\varphi_*) \equiv 1$, there exists $C > 0$, such that*

$$W_2^{\mathbb{T}^1}(f(\cdot,t), f_\infty) \le Ce^{-\lambda t}\,, \qquad \forall\, t \ge 0\,,$$

with f_∞ defined in (2.14) and λ as in (2.21).

Proof. After using (2.21), it only remains to use the triangle inequality for the Wasserstein distance to obtain $W_2^{\mathbb{T}^1}(f, f_\infty)^2 \le 2\mathcal{H}[f]$. □

2.5 Numerical Simulations

Discretization: The results of the preceding section will be illustrated by numerical simulations of the spatially homogeneous model (2.16). Discretization in the angle direction is based on an equidistant grid

$$\varphi_k = \frac{(k-n)\pi}{n}\,, \qquad k = 0,\dots,2n\,,$$

with an even number of grid points, guaranteeing that the grid is invariant under reversal collisions, i.e., with φ_k also $\varphi_k^\downarrow = \varphi_{k+n}$ is a grid point. Similarly, only those alignment collisions between discrete

angles will be allowed, which produce post-collisional angles belonging to the grid. This is facilitated by rewriting the alignment collision operator (2.8) as

$$Q_{AL}(f,f) = 2\int_{\mathbb{T}^{AL}_{\to\varphi}} b(\tilde{\varphi},\varphi_*)(\tilde{f}f_* - f\tilde{f}_*)d\varphi_*\,,$$

with $\tilde{\varphi} = 2\varphi - \varphi_*$, $\tilde{\varphi}_* = 2\varphi_* - \varphi$, before discretization. Note that in this form mass conservation is obvious since $b(\tilde{\varphi},\varphi_*) = b(\tilde{\varphi}_*,\varphi)$, and the grid is invariant under the map $(\varphi,\varphi_*) = (\varphi_k,\varphi_{k_*}) \mapsto (\tilde{\varphi},\tilde{\varphi}_*) = (\varphi_{2k-k_*},\varphi_{2k_*-k})$. Finally, we always choose n odd to avoid the angle $\pi/2$ between grid angles and, thus, the ambiguity between alignment and reversal collisions.

Solutions of (2.16) are approximated at grid points by

$$f^n(t) := (f_1(t),\dots,f_{2n}(t)) \approx (f(\varphi_1,t),\dots,f(\varphi_{2n},t))\,,$$

extended periodically by $f_{k+2n}(t) = f_k(t)$. This straightforwardly leads to the discrete model

$$\frac{df_k}{dt} = Q^n(f^n,f^n)_k\,,$$

with

$$Q^n(f^n,f^n)_k := \frac{2\pi}{n}\sum_{|k_*-k|<n/4} b_{2k-k_*,k_*}(f_{2k-k_*}f_{k_*} - f_k f_{2k_*-k}) + \frac{\pi}{n}\sum_{|k_*-k|>n/2} b_{k,k_*}(f_{k+n}f_{k_*+n} - f_k f_{k_*})\,,$$

and $b_{k,k_*} := b(\varphi_k,\varphi_{k_*})$.

For the time discretization the *explicit Euler scheme* is used, such that the total mass is conserved by the discrete scheme, which has been implemented in MATLAB.

Numerical simulations with two group initial conditions: Simulations have been carried out with $n = 201$ and with the time step $\Delta t = 0.1$. In the first rows of Figures 2.3, 2.4, 2.6, density is color coded as a function of φ (vertically) and t (horizontally). The plots in the second rows show snapshots of the distribution function f at different times.

Although we only provide a proof for Maxwellian myxos, we expect solutions of (2.16) with initial data satisfying (2.15) to converge to the equilibrium f_∞, given by (2.14), also for rod shaped myxobacteria. This conjecture is supported by the simulation results depicted in Figures 2.3, 2.4.

On the left side of Figure 2.3 the initial distribution is uniform within both $\mathbb{T}^1_+$ and $\mathbb{T}^1_-$, but with zero mass outside. The equilibrium angle is given by $\varphi_+ = \frac{\pi}{2}$. The initial data on the right side are similar, but with no mass in intervals around $\pi/2$ and $-\pi/2$, which again causes $\varphi_+ = \frac{\pi}{2}$.

In the left part of Figure 2.4 the initial data are supported in $\mathbb{T}^1_+$, therefore excluding reversal collisions. The discretization preserves the mass conservation in both $\mathbb{T}^1_+$ and $\mathbb{T}^1_-$ separately. This is the situation of Lemma 2.2 b). The decay estimate for the variance as t^{-2} (Haff's law) is demonstrated by the left part of Figure 2.5. The simulation has also been carried out for Maxwellian myxos, demonstrating the exponential decay of the variance in this case (Figure 2.5, right). The right part of Figure 2.4 shows an example, where the average directions $\bar{\varphi}_\pm$ within the groups change significantly.

Instability of constant steady states: In Figure 2.6 we consider small perturbations of a constant steady state. On the left side we start with a random perturbation and see mass concentrating at unpredictable directions φ_+ and $\varphi_+^\downarrow$. On the right side we considered a perturbation at one random point $\hat{\varphi}$. We see convergence to f_∞, with equilibrium angle $\varphi_+ = \hat{\varphi}$. Both simulations illustrate instability of the uniform distribution on $\mathbb{T}^1$.

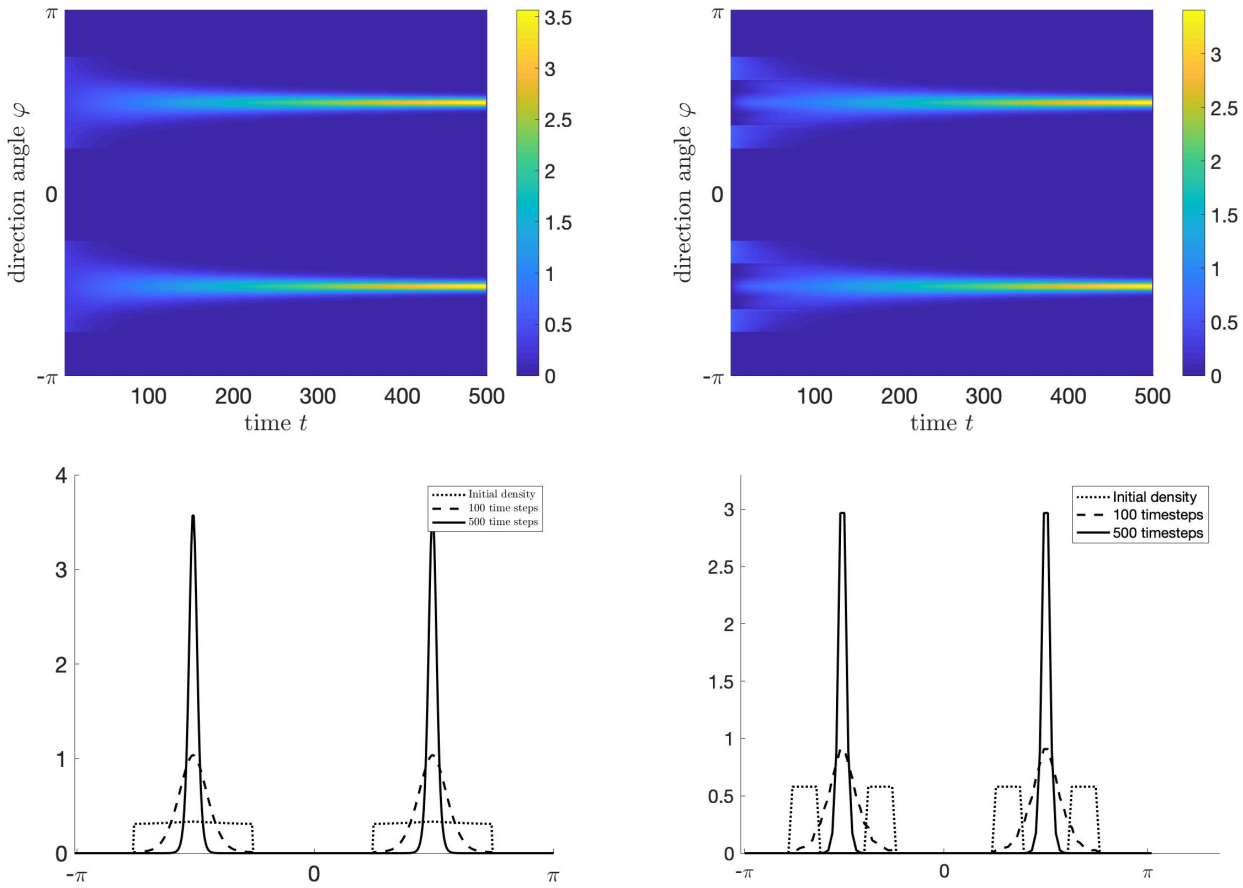

Figure 2.3: Two group initial conditions with the same mass in $\mathbb{T}^1_+$ and $\mathbb{T}^1_-$; rod shaped bacteria. *Left:* uniform distributions within $\mathbb{T}^1_+$ and $\mathbb{T}^1_-$. *Right:* vacuum around $\pm\pi/2$.

2.6 Formal macroscopic limit

For the simulation of spatial pattern formation phenomena kinetic transport models pose significant numerical challenges and contain often unnecessary information on microscopic lengths and time scales. Therefore such simulations are often based on macroscopic models. For myxobacteria colonies macroscopic models have been formulated both by a direct continuum approach [19, 22, 23, 24] and based on microscopic or kinetic descriptions [5, 10, 18]. This section is concerned with the formal macroscopic limit of the kinetic model (2.7) to demonstrate which features of other models are reproduced. Similarities can also be found with models for the interaction of microtubules by motor proteins [4] and for granular gases assuming nonelastic collisions [11, 25, 35]. In the latter case the macroscopic limit is often combined with the assumption of weakly inelastic collisions, leading to an energy balance equation describing the cooling of the gas [11, 35]. Since the model (2.7) corresponds to the other extreme of *sticky particles*, the macroscopic limit already involves the passage to zero temperature.

We investigate the behavior at macroscopic position and time scales by introducing the rescaling $x \to \frac{x}{\varepsilon}$, $t \to \frac{t}{\varepsilon}$, with a Knudsen number $\varepsilon \ll 1$ in (2.7):

$$\partial_t f^\varepsilon + \omega \cdot \nabla_x f^\varepsilon = \frac{1}{\varepsilon} Q(f^\varepsilon, f^\varepsilon)\,.$$

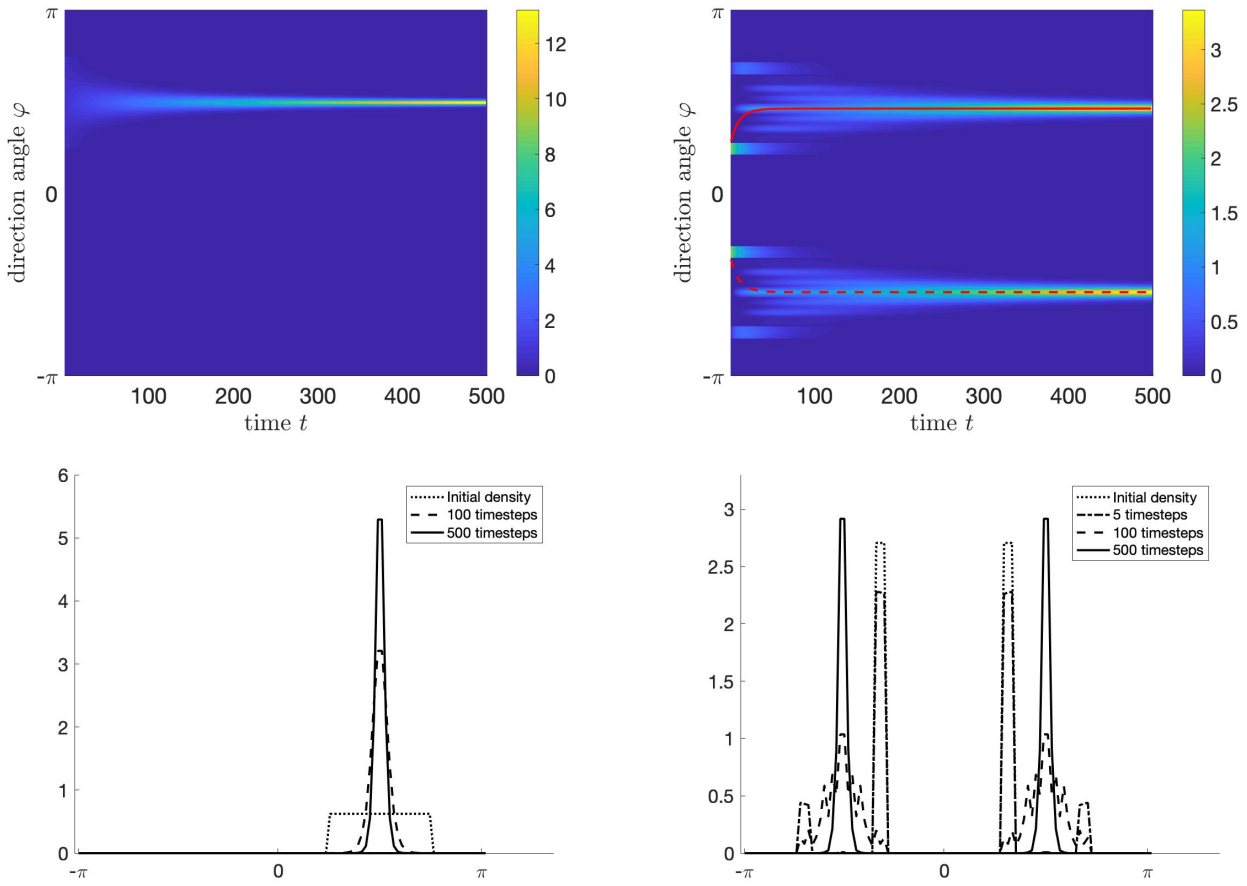

Figure 2.4: *Left:* initial condition with uniform distribution in $\mathbb{T}^1_+$ and vacuum everywhere else. *Right:* initially two concentrated patches at a distance somewhat bigger than $\pi/2$ (yellow at the left end). Outer stripes created by reversal, then fill-in by alignment, followed by concentration towards opposite directions. The mean angles $\bar{\varphi}_+$ (red line) and $\bar{\varphi}_-$ (dotted red line) in the two groups change significantly.

Formally, the convergence $f^\varepsilon \to f$ as $\varepsilon \to 0$ implies, by (2.14),

$$f(x,\varphi,t) = \rho_+(x,t)\delta(\varphi - \varphi_+(x,t)) + \rho_-(x,t)\delta\left(\varphi - \varphi_+(x,t)^\downarrow\right) .$$

In Section 2.3 we have seen that in general the collision operator only allows for two independent collision invariants $\psi(\varphi) = 1$ and $\psi(\varphi) = \varphi$, providing only two conservation laws

$$\partial_t \int_{\mathbb{T}^1} f\psi \, d\varphi + \nabla_x \cdot \int_{\mathbb{T}^1} \omega f \psi \, d\varphi = 0 \,,$$

for the three unknowns ρ_+, ρ_-, and φ_+. However, assuming two group initial data (see again Section 2.3), the mass within the group is a third conserved quantity, closing the macroscopic limit system:

$$\begin{aligned}
&\partial_t \rho_+ + \nabla_x \cdot (\rho_+ \omega(\varphi_+)) = 0 \,, \\
&\partial_t \rho_- - \nabla_x \cdot (\rho_- \omega(\varphi_+)) = 0 \,, \\
&\partial_t((\rho_+ + \rho_-)\varphi_+) + \nabla_x \cdot ((\rho_+ - \rho_-)\varphi_+ \omega(\varphi_+)) = 0 \,.
\end{aligned}$$

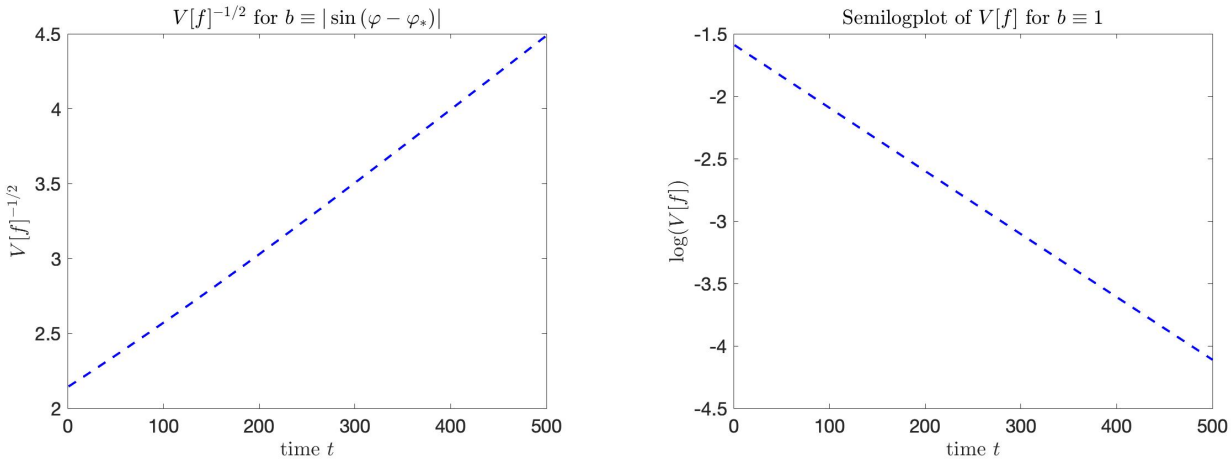

Figure 2.5: *Left:* The evolution of the inverse square root of the variance $V[f]$ from the simulation depicted on the left side of Figure 2.4, supporting the validity of Haff's law for rod shaped myxos. *Right:* Semi-log plot of $V[f]$ for a simulation with the same initial data, but for Maxwellian myxos, demonstrating exponential decay to equilibrium as shown in Lemma 2.2 a).

Expanding the derivatives, it can also be written as

$$\begin{aligned}
&\partial_t \rho_+ + \omega \cdot \nabla_x \rho_+ + \rho_+ \omega^\perp \cdot \nabla_x \varphi_+ = 0\,,\\
&\partial_t \rho_- - \omega \cdot \nabla_x \rho_- - \rho_- \omega^\perp \cdot \nabla_x \varphi_+ = 0\,,\\
&\partial_t \varphi_+ + \frac{\rho_+ - \rho_-}{\rho_+ + \rho_-} \omega \cdot \nabla_x \varphi_+ = 0\,,
\end{aligned}$$

showing that for $\rho_+, \rho_- > 0$ the system is strictly hyperbolic with characteristic velocities ω, $-\omega$, $\frac{\rho_+ - \rho_-}{\rho_+ + \rho_-}\omega$. Although the system is nonlinear, all three characteristic fields are linearly degenerate. On the other hand, the special case $\rho_- = 0$ leads to

$$\begin{aligned}
&\partial_t \rho_+ + \omega \cdot \nabla_x \rho_+ + \rho_+ \omega^\perp \cdot \nabla_x \varphi_+ = 0\,,\\
&\partial_t \varphi_+ + \omega \cdot \nabla_x \varphi_+ = 0\,,
\end{aligned}$$

a non-strictly hyperbolic system with the same structure as the equations for pressureless gas dynamics, derived as macroscopic limit of the dissipative Boltzmann equation [25].
Furthermore, comparing the equation for φ_+ in (2.22) with the macroscopic one for the equilibrium angle in [18], we see that they only differ by a pressure term proportional to $(\rho_+ - \rho_-)\omega^\perp \cdot \nabla_x \varphi_+$ not occurring in our case. Considering the limit of vanishing diffusion in [18] this term vanishes, which reveals the fact that the two different microscopic models provide the same macroscopic equations. The models in [5] and [10] are quite different. They consider only one macroscopic density, coupled with a nematic polarization vector and an order parameter in [5], and with a mean velocity with variable speed in [10].

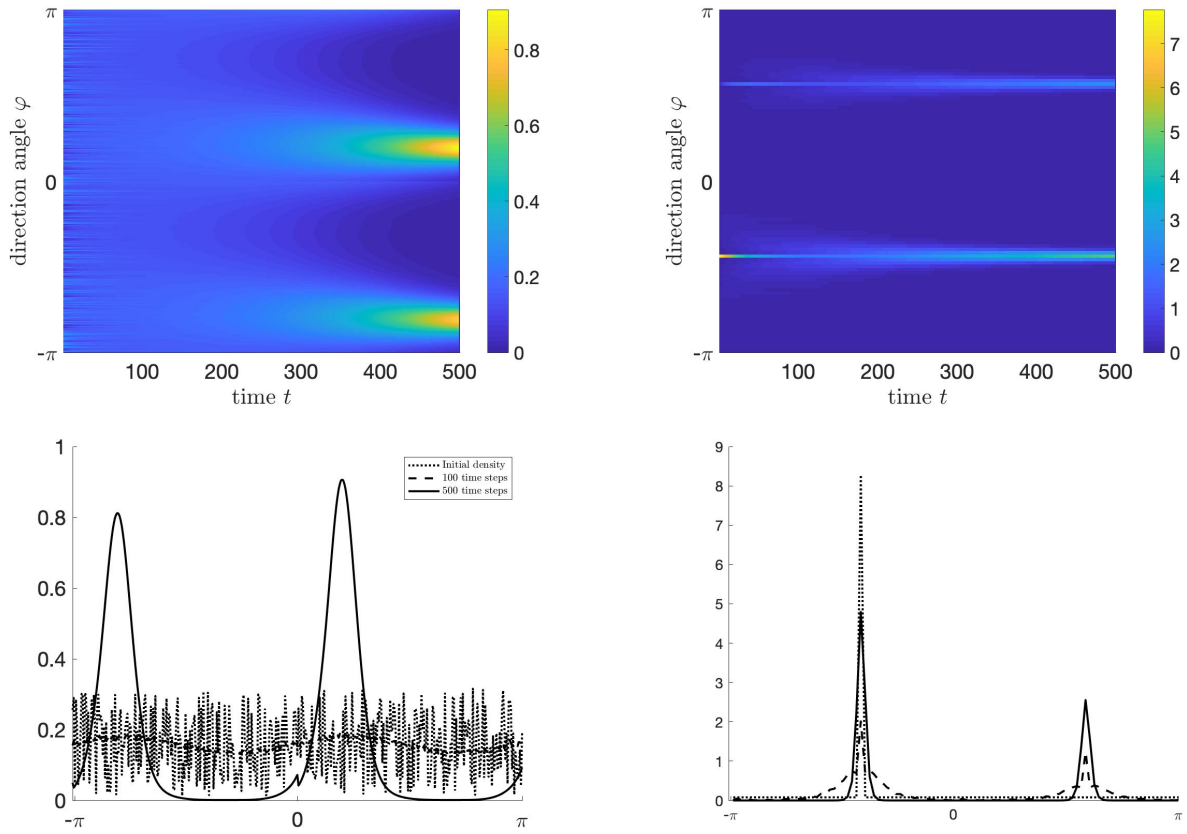

Figure 2.6: Instability of constant positive steady states. *Left:* random initial perturbation, leading to an unpredictable equilibrium direction. *Right:* initial perturbation at one direction, which eventually becomes the equilibrium direction. Note that this differs from the simulations in Figure 2.4, left, by the fact that a positive state is perturbed, and therefore reversal collisions are active.

Acknowledgments

This work has been supported by the Austrian Science Fund (FWF) project F65 *Taming Complexity in Partial Differential Systems*. C.S. acknowledges support by the Austrian Science Fund (grant no. W1245), by the Fondation Sciences Mathématiques de Paris, and by Paris Science et Lettres. S.H. acknowledges support via FWF project T-764. The authors also acknowledge the comments of an anonymous referee, who pointed out a significant number of references.

Bibliography

[1] R.J. Alonso, *Existence of global solutions to the Cauchy problem for the inelastic Boltzmann equation with near-vacuum data,* JSTOR 58 (2009), pp. 999–1022.

[2] R. J. Alonso, V. Bagland, Y. Cheng, B. Lods, *One-Dimensional Dissipative Boltzmann Equation: Measure Solutions, Cooling Rate, and Self-Similar Profile,* SIAM J. Math. Anal. 50 (2015), pp. 1278–1321.

[3] R.J. Alonso, B. Lods, *Two proofs of Haff's law for dissipative gases: The use of entropy and the weakly inelastic regime,* J. Math. Anal. Appl. 397 (2013), pp. 260–275.

[4] I.S. Aranson, L.S. Tsimring, *Pattern formation of microtubules and motors: inelastic interaction of polar rods,* Phys. Rev. E Stat. Nonlin. Soft Matter Phys. 71 (2005), 050901.

[5] A. Baskaran, M.C. Marchetti, *Enhanced Diffusion and Ordering of Self-Propelled Rods,* Phys. Rev. Lett. 101 (2008), 268101.

[6] A. Baskaran, M.C. Marchetti, *Nonequilibrium statistical mechanics of self propelled hard rods,* J. Stat. Mech. 2010 (2010), P04019.

[7] D. Benedetto, M. Pulvirenti, *On the one-dimensional Boltzmann equation for granular flows,* M2AN 35 (2001), pp. 899–905.

[8] E. Ben-Naim, P.L. Krapivsky, *Alignment of rods and partition of integers,* Phys. Rev. E Stat. Nonlin. Soft Matter Phys. 73 (2006), 031109.

[9] E. Bertin, M. Droz, G. Grégoire, *Boltzmann and hydrodynamic description for self-propelled particles.* (2006-08-02), Physical Review E. 74 (2): 022101.

[10] E. Bertin, M. Droz, G. Gregoire, *Hydrodynamic equations for self-propelled particles: microscopic derivation and stability analysis,* J. Phys. A: Math. Theor. 42 (2009), 445001.

[11] A.V. Bobylev, J.A.Carrillo, I.M. Gamba, *On Some Properties of Kinetic and Hydrodynamic Equations for Inelastic Interactions,* J. Stat. Phys. 98 (2000), pp. 743–773.

[12] A.V. Bobylev, C. Cercignani, *Self-Similar Asymptotics for the Boltzmann Equation with Inelastic and Elastic Interactions,* J. Stat. Phys. 110 (2003), pp. 333–375.

[13] L. Boltzmann, *Weitere Studien über das Wärmegleichgewicht unter Gasmolekülen,* Sitzungsberichte Akad. Wiss., Vienna, part II, 66 (1872), pp. 275–370.

[14] J. Carrillo, G. Toscani, *Contractive probability metrics and asymptotic behavior of dissipative kinetic equations*, Riv. Mat. Univ. Parma (7) 6 (2007), pp. 75–198.

[15] E. Carlen, M. C. Carvalho, P. Degond, B. Wennberg, *A Boltzmann model for rod alignment and schooling fish,* Nonlinearity 28 (2015), pp. 1783–1804.

[16] C. Cercignani, R. Illner, M. Pulvirenti, *The Mathematical Theory of Dilute Gases*, Springer-Verlag, New York, 1994.

[17] P. Degond, A. Frouvelle, G. Raoul, *Local stability of perfect alignment for a spatially homogeneous kinetic model,* J. Stat. Phys. 157 (2014), pp. 84–112.

[18] P. Degond, A. Manhart, H. Yu, *A continuum model of nematic alignment of self-propelled particles,* DCDS-B 22 (2017), pp. 1295–1327.

[19] P. Degond, A. Manhart, H. Yu, *An age-structured continuum model for myxobacteria,* M3AS 28 (2018), pp. 1737–1770.

[20] P. Haff, *Grain flow as a fluid-mechanical phenomenon,* J. Fluid Mech. 134 (1983), pp. 401–30.

[21] J. Hodgkin, D. Kaiser, *Genetics of gliding motility in Myxococcus xanthus (Myxobacterales): two gene systems control movement,* Mol. Gen. Genet. 171 (1979), pp. 177–191.

[22] O. A. Igoshin, A. Mogilner, R. D. Welch, D. Kaiser, G. Oster, *Pattern formation and traveling waves in myxobacteria: Theory and modeling,* PNAS December 18, 2001 98 (26) 14913-14918

[23] O. A. Igoshin, G. Oster, *Rippling of myxobacteria,* Math. Biosci. 188 (2004), pp. 221–233.

[24] O. A. Igoshin, R. Welch, D. Kaiser, and G. Oster, *Waves and aggregation patterns in myxobacteria*, PNAS 101 (2004), pp. 4256–4261.

[25] P.-E. Jabin, T. Rey, *Hydrodynamic limit of granular gases to pressureless Euler in dimension 1,* Quart. Appl. Math. 75 (2017), 155–179.

[26] Y. Jiang, O. Sozinova, M. Alber, *On modeling complex collective behavior in myxobacteria*, Adv. in Complex Syst. 9 (2006), pp. 353–367.

[27] L. Jelsbak, L. Sogaard-Andersen, *The cell surface-associated intercellular C-signal induces behavioral changes in individual Myxococcus xanthus cells during fruiting body morphogenesis,* PNAS 96 (1999), pp. 5031–5036.

[28] S. Kim, D. Kaiser, *C-factor: A cell-cell signaling protein required for fruiting body morphogenesis of M. xanthus,* Cell 61 (1990), pp. 19–26.

[29] O. E. Lanford, *Time evolution of large classical systems,* Lect. Notes Phys. 38 (1975), pp. 1–111.

[30] E. M. F. Mauriello, T. Mignot, Z. Yang, D. R. Zusman, *Gliding Motility Revisited: How Do the Myxobacteria Move without Flagella?,* Microbiol. Mol. Biol. Rev. 74 (2010), pp. 229–249.

[31] S. Mischler, C. Mouhot, M. Rodriguez Ricard, *Cooling Process for Inelastic Boltzmann Equations for Hard Spheres, Part I: The Cauchy Problem,* J. Stat. Phys. 124 (2006), pp. 655–702.

[32] S. Mischler, C. Mouhot, *Cooling Process for Inelastic Boltzmann Equations for Hard Spheres, Part II: Self-Similar Solutions and Tail Behavior,* J. Stat. Phys. 124 (2006), pp. 703–746.

[33] B. Nan, D. R. Zusman, *Uncovering the Mystery of Gliding Motility in the Myxobacteria,* Annu. Rev. Genet. 45 (2011), pp. 21–39.

[34] B. Sager, D. Kaiser, *Intercellular C-signaling and the traveling waves of Myxococcus,* Genes Dev. 8 (1994), pp. 2793–2804.

[35] G. Toscani, *Hydrodynamics from the dissipative Boltzmann equation,* in: G. Capriz, P.M. Mariano, P. Giovine (eds), Mathematical Models of Granular Matter, Lect. Notes in Math. 1937, Springer, Berlin–Heidelberg, 2008.

[36] I. Tristani, *Boltzmann equation for granular media with thermal force in a weakly inhomogeneous setting,* J. Functional Anal. 270 (2016), pp. 1922–1970.

[37] C. Villani, *Topics in Optimal Transportation,* Graduate Studies in Math. 58, AMS, 2003.

[38] D. Wall, D. Kaiser, *Type IV pili and cell motility,* Mol. Microbiol. 32 (1999), pp. 1–10.

[39] R. Welch, D. Kaiser, *Cell behavior in traveling wave patterns of myxobacteria,* PNAS 98 (2001), pp. 14907–14912.

[40] C. Wolgemuth, E. Hoiczyk, D. Kaiser, G. Oster, *How myxobacteria glide,* Curr. Biol. 12 (2002), pp. 369–377.

3 Kinetic Model for Myxobacteria with Directional Diffusion

I come from Detroit where it's rough and
I'm not a smooth talker.

Eminem

Contents

3.1 Introduction **53**
3.2 Decay to the uniform equilibrium **56**
3.2.1 Spectral stability by hypocoercivity 56
3.2.2 Nonlinear stability of the uniform equilibrium 60
3.3 Existence and Stability of Equilibria for the Spatially Homogeneous Equation **62**
3.3.1 Bifurcation Analysis 62
3.3.2 Existence of Equilibria for Small Diffusivity 66
3.4 Numerical Simulations **69**

This chapter consist of an article together with C. Schmeiser, which is close to submission.

3.1 Introduction

The aim of this work is to investigate a model for the dynamics of myxobacteria colonies moving on flat substrates. Existence and uniqueness of solutions is studied and in a second step existence of equilibria as well as their bifurcation behavior. The work is completed with numerical simulations showing the investigated behavior.

The equation of interest is the kinetic transport equation for the distribution function $f(x, \varphi, t) \geq 0$, where $x \in \mathbb{T}^2, \varphi \in \mathbb{T}^1$ and $t \geq 0$ introduced in [31], which was extended with a diffusion term in velocity direction and is of the form

$$\partial_t f + \omega(\varphi) \cdot \nabla_x f = \mu \partial_\varphi^2 f + Q(f, f). \tag{3.1}$$

The velocity is given by $\omega(\varphi) = (\cos\varphi, \sin\varphi)$ and $\mathbb{T}^1$, $\mathbb{T}^2$ denotes the one-dimensional flat torus of length 2π resp. the two-dimensional torus with area $4\pi^2$. The positive constant μ describes the intensity of diffusivity with respect to movement direction. The collision operator is of the form

$$Q(f, g) = 2 \int_{\mathbb{T}^{AL}_{\to\varphi}} b(\tilde{\varphi}, \varphi_*) \tilde{f} g_* d\varphi_* + \int_{\mathbb{T}^{REV}_{\varphi}} b(\varphi^\downarrow, \varphi_*^\downarrow) f^\downarrow g_*^\downarrow d\varphi_* - \int_{\mathbb{T}^1} b(\varphi, \varphi_*) f g_* d\varphi_* \,, \tag{3.2}$$

where

$$\mathbb{T}^{REV}_{\varphi} := \left(\varphi + \frac{\pi}{2}, \varphi + \frac{3\pi}{2}\right), \qquad \mathbb{T}^{AL}_{\to\varphi} = \left(\varphi - \frac{\pi}{4}, \varphi + \frac{\pi}{4}\right),$$

and

$$\tilde{\varphi} := 2\varphi - \varphi_*, \qquad \varphi^{\downarrow} = \varphi + \pi, \qquad \varphi^{\downarrow}_* = \varphi_* + \pi.$$

The model describes movement along trajectories governed by *Brownian motion* in velocity direction, interrupted by hard binary collisions with *collision cross-section* $b(\varphi, \varphi_*)$, which quantifies the collision frequency and depends on the shape of the bacteria. In this work we consider two possible types of the collision kernel b: On one hand we take $b(\varphi, \varphi_*) = |\omega_* \cdot \omega^{\perp}| = |\sin(\varphi - \varphi_*)|$, which is a consequence of the rod shape of the bacteria. It gives the rate of collisions between bacteria with directions φ and φ_*. On the other hand, assuming instead bacteria with circular shape, yields a collision rate independent from the movement direction. By analogy to a similar simplification of the gas dynamics' Boltzmann equation [17], we use the name *'Maxwellian myxos'* for this imagined species, modeled by (3.2) with $b(\varphi, \varphi_*) \equiv 1$. We may note at this point that in both cases $b(\varphi, \varphi_*) = b(\varphi^{\downarrow}, \varphi^{\downarrow}_*)$ holds. As usual, sub- and super-scripts on f indicate evaluation at φ with the same sub- and super-scripts. The collision operator (3.2) consists of a loss term and two different gain terms describing two different types of collisions:

- *Alignment:* $(\tilde{\varphi}, \varphi_*) \to (\varphi, \varphi)$ with $\varphi = (\tilde{\varphi} + \varphi_*)/2$, if two myxobacteria moving in directions $\tilde{\varphi}$ and φ_* meet at an angle smaller than $\pi/2$. The factor 2 is due to the fact that an alignment collision produces 2 myxobacteria with the same direction. The set $\mathbb{T}^{AL}_{\to\varphi}$ describes all angles φ_*, which can produce the angle φ upon collision.
- *Reversal:* $(\varphi, \varphi_*) \to (\varphi^{\downarrow}, \varphi^{\downarrow}_*)$, if two myxobacteria with directions φ and φ_* meet at an angle larger than $\pi/2$. The set $\mathbb{T}^{REV}_{\varphi}$ describes all angles φ_* such that a collision involving φ can produce the angle $\varphi^{\downarrow}$.

Let us further mention the in [31] introduced and investigated kinetic equation for myxobacteria colonies without directional diffusion (i.e. $\mu = 0$)

$$\partial_t f + \omega(\varphi) \cdot \nabla_x f = Q(f, f), \tag{3.3}$$

describing bacteria ensembles with individuals following straight runs with constant velocity interrupted by the binary collisions explained above. Its properties will serve as motivation for dynamics we expect in (3.1) in the small diffusion regime. In both (3.1) and (3.3) the total mass is conserved and denoted by

$$M := \int_{\mathbb{T}^1 \times \mathbb{T}^2} f(x, \varphi, t)\, \mathrm{d}\varphi \mathrm{d}x.$$

Throughout all of this paper, we denote the *uniform distribution* by

$$f_0 := \frac{M}{2\pi},$$

which defines an equilibrium for both (3.1) and (3.3). Investigations in the no diffusion-case show that f_0 is unstable and under special conditions convergence of the solution to the measure equilibrium

$$f_\infty(\varphi) := \rho_+ \delta(\varphi - \varphi_+) + \rho_- \delta(\varphi - \varphi^{\downarrow}_+) \tag{3.4}$$

could be proved for the spatially homogeneous equation. Here, $\varphi_+ \in \mathbb{T}^1_+$ describes a mean angle, where the average is computed after mapping angles in $\mathbb{T}^1_-$ to $\mathbb{T}^1_+$ by reversal. These observations give

rise to the assumption that for small μ the uniform equilibrium f_0 will also be unstable for (3.1) and other equilibria will occur.

In [11] a similar model, also of Boltzmann-type but just describing alignment interactions, was introduced as binary collision counterpart of the Vicsek model for swarm dynamics, which on the other hand is based on nonlocal alignment interactions between agents [44]. It was investigated further in [12] as well as in [16], where additionally the case of Brownian forcing between binary interactions was considered. Before, such a diffusive kinetic equation modelling alignment between agents was also already introduced and studied in [8].

The structure of this paper will be the following: Section 3.2 is dedicated to proving global existence of a solution subject to initial condition sufficiently close the uniform equilibrium f_0 as well es exponential decay towards this steady state, both in dependence of the diffusivity resp. the total mass. This result relies on a perturbative approach including the proof of spectral stability of the equilibrium before extending it to the nonlinear framework, close to equilibrium. We want to mention at this point that the theory for the dissipative Boltzmann equation is much less developed than the one of the conservative Boltzmann equation, which is due to the lack of a-priory estimates given by an entropy. Global existence results for the spatially inhomogeneous Cauchy problem in the inelastic case are only known for near vacuum data [1] (i.e. the collisions do not have much impact on the dynamics) inspired by the method using Kaniel & Shinbrot iterates [35]. More recently in [42] existence in the spatially inhomogeneous framework for inelastic collisions could be established without the closeness to vacuum restriction. Further, theory in the one-dimensional situation, where grazing collisions are almost elastic, can be found in [7]. Another important work in the one dimensional case has been done in [33], carrying out the rigorous macroscopic limit towards pressureless gas dynamics. Much more results have been established in an homogeneous framework, see e.g. [28] and [40] for investigations on the existence and uniqueness of solutions. Besides work on the Cauchy problem, a wide amount of results on existence and further properties of self-similar profiles for diffusively excited inelastic hard sphere models have been obtained. Among them to mention [13], [28] and [37, 38, 39] for the case of a constant coefficient of restitution, while we refer the reader to [3] for considerations on the non-constant case.

All of this stands in contrast to the case for the conservative Boltzmann equation, where the existence of solutions, known as *renormalized solutions* was proved by DiPerna and Lions in 1989 [22], used and developed further ever since then. Other methods arising from a perturbative approach and spectral study of the linearized operator where developed earlier, starting from Hilbert in the early 20th century [30], Grad in the late 50' [25, 26] and later also Ukai [43] using semigroup theory to establish global solutions for the Boltzmann equation.

In the first part of Section 3.3 we investigate stability of the uniform steady state f_0 in the dependence of the diffusivity and total mass of the system, using bifurcation theory [18] via Fourier series expansion of the uniform equilibrium. We establish to show occurrence of a supercritical pitchfork bifurcation. Although the calculations remain formal, it does provide new insights in the behavior of the model, while being accurate with already existing results. Indeed, in [16] a rigorous proof of existence of a pitchfork bifurcation in the noisy version of a Boltzmann-type alignment model for swarming behavior is stated. In the second part, we investigate the stationary, spatially homogeneous equation for existence of non-uniform solutions, i.e. spatially homogeneous equilibria different form the constant one. A result proving the existence of an approximations of such a solution is stated in the case of Mawellian myxos, i.e. with constant collision kernel $b \equiv 1$.

In Section 3.4 numerical simulations for the spatially homogeneous equation can be found, giving evidence for the bifurcation results obtained in Section 3.3.

3.2 Decay to the uniform equilibrium

The aim of this section is to establish existence and uniqueness of solutions of (3.1), as well as asymptotic stability of the uniform equilibrium. This can only be expected under the assumption of large enough diffusivity μ compared to the total mass M.

Theorem 3.1. *Let $f_I \in H^2_{x,\varphi}(\mathbb{T}^2\times\mathbb{T}^1)$, $f_I \geq 0$, and let μ/M be large enough with $M = \int_{\mathbb{T}^2\times\mathbb{T}^1} f_I \mathrm{d}\varphi\mathrm{d}x$. Let furthermore $\|f_I - f_0\|_{H^2_{x,\varphi}(\mathbb{T}^2\times\mathbb{T}^1)}$ be small enough with $f_0 = M/(2\pi)$. Then equation (3.1) subject to the initial condition $f(t=0) = f_I$ has a unique global solution $f \in C([0,\infty), H^2_{x,\varphi}(\mathbb{T}^2\times\mathbb{T}^1))$, satisfying*

$$\|f(t) - f_0\|_{H^2_{x,\varphi}(\mathbb{T}^2\times\mathbb{T}^1)} \leq Ce^{-\lambda t}\|f_I - f_0\|_{H^2_{x,\varphi}(\mathbb{T}^2\times\mathbb{T}^1)}\,, \qquad C,\lambda > 0\,.$$

The rest of this section is dedicated to the proof of Theorem 3.1. The first step will be a proof of spectral stability by an application of the *L^2-hypocoercivity method* of [23]. Then this result will be extended to an H^2-setting in order to be able to control the quadratic nonlinearities of the collision operator.

3.2.1 Spectral stability by hypocoercivity

Following the notation of [23], we write the linearization of (3.1) around $f_0 = M/(2\pi)$ in the abstract form

$$\partial_t f + Tf = Lf + Q_M f\,, \tag{3.5}$$

with the dissipative operator $L := \mu\partial^2_\varphi$, the conservative transport operator $T := \omega(\varphi)\cdot\nabla_x$, and the linearized collision operator $Q_M f := Q(f_0, f) + Q(f, f_0)$, treated as a perturbation. The linear operators T, L, and Q_M are closed on the Hilbert space

$$\mathcal{H} := \left\{ f \in L^2(\mathbb{T}^2\times\mathbb{T}^1) : \int_{\mathbb{T}^2\times\mathbb{T}^1} f \mathrm{d}\varphi\mathrm{d}x = 0 \right\},$$

and $L + Q_M - T$ generates the strongly continuous semigroup $e^{(L+Q_M-T)t}$ on $\mathcal{H}$. The scalar product and the norm on $\mathcal{H}$ will be denoted by $\langle\cdot,\cdot\rangle$ and, respectively, $\|\cdot\|$. The orthogonal projection to the nullspace $\mathcal{N}(L)$ of L is given by the average with respect to the angle:

$$\Pi f := \frac{1}{2\pi}\int_{\mathbb{T}^1} f \mathrm{d}\varphi\,.$$

The decay to equilibrium relies on two coercivity properties:

Microscopic coercivity:

$$-\langle Lf, f\rangle = \mu\int_{\mathbb{T}^2\times\mathbb{T}^1} (\partial_\varphi f)^2 \mathrm{d}\varphi\mathrm{d}x \geq \mu\|f - \Pi f\|^2\,,$$

where the last inequality is the Poincaré inequality on $\mathbb{T}^1$ with optimal Poincaré constant 1.

Macroscopic coercivity:

$$\|T\Pi f\|^2 = \pi\int_{\mathbb{T}^2} |\nabla_x \Pi f|^2 \mathrm{d}x \geq 8\pi^3\int_{\mathbb{T}^2} (\Pi f)^2 \mathrm{d}x = 4\pi^2\|\Pi f\|^2\,,$$

where now the Poincaré inequality on $\mathbb{T}^2$ with optimal Poincaré constant $8\pi^2$ has been used. The macroscopic coercivity constant $4\pi^2$ can be seen as a lower bound for the spectrum of the symmetric operator $(T\Pi)^* T\Pi$ on $\mathcal{N}(L)$.

Diffusive macroscopic limit: The method of [23] relies on an algebraic property, which guarantees that the macroscopic limit, when the dissipative operator L dominates the transport operator T, is diffusive:

$$\Pi T \Pi = 0\,. \tag{3.6}$$

It is easily verified in our situation. The macroscopic limit of (3.5) without the perturbation ($Q_M = 0$) is the heat equation on $\mathbb{T}^2$.

The modified entropy: A natural entropy for the unperturbed version of (3.5) is given by the square of the norm:

$$\frac{d}{dt}\frac{\|f\|^2}{2} = \langle Lf, f\rangle + \langle Q_M f, f\rangle\,.$$

The semidefiniteness of the dissipation $\langle Lf, f\rangle$, which vanishes on $\mathcal{N}(L)$, can be remedied by introducing the modified entropy (see [23])

$$H[f] := \frac{1}{2}\|f\|^2 + \varepsilon\langle Af, f\rangle\,,$$

with an appropriately chosen small parameter $\varepsilon > 0$, with the operator

$$A = (1 + (T\Pi)^* T\Pi)^{-1}(T\Pi)^*\,.$$

It has been shown in [23, Lemma 1] that under the assumption (3.6), A and TA are bounded operators with

$$\|Af\| \le \frac{1}{2}\|(1-\Pi)f\|\,, \qquad \|TAf\| \le \|(1-\Pi)f\|\,. \tag{3.7}$$

For $\varepsilon < 1$, the bound on A implies the equivalence inequalities

$$\frac{1-\varepsilon}{2}\|f\|^2 \le H[f] \le \frac{1+\varepsilon}{2}\|f\|^2\,. \tag{3.8}$$

The time derivative of the modified entropy is written as

$$\frac{d}{dt}H[f] = -D[f]\,, \tag{3.9}$$

where the dissipation is given by

$$\begin{aligned} D[f] := &-\langle Lf, f\rangle + \varepsilon\langle AT\Pi f, f\rangle + \varepsilon\langle AT(1-\Pi)f, f\rangle - \varepsilon\langle ALf, f\rangle - \varepsilon\langle TAf, f\rangle \\ &- \langle Q_M f, f\rangle - \varepsilon\langle AQ_M f, f\rangle\,. \end{aligned} \tag{3.10}$$

We want to note here that the terms $-\varepsilon\langle Af, Lf\rangle$ and $-\varepsilon\langle Af, Q_M f\rangle$ are not represented in the formulation of $D[f]$, since they vanish due to the easily checked properties $A = \Pi A$ as well as

$$Q_M = (1-\Pi)Q_M(1-\Pi)\,, \tag{3.11}$$

which the linearized collision operator

$$\begin{aligned} Q_M f \;=\; & 2f_0 \int_{\mathbb{T}^{AL}_{\to\varphi}} b(\tilde{\varphi}, \varphi_*)(\tilde{f} + f_*)\mathrm{d}\varphi_* + f_0 \int_{\mathbb{T}^{REV}_{\varphi}} b(\varphi^{\downarrow}, \varphi_*^{\downarrow})(f^{\downarrow} + f_*^{\downarrow})\mathrm{d}\varphi_* \\ & - f_0 \int_{\mathbb{T}^1} b(\varphi, \varphi_*)(f + f_*)\mathrm{d}\varphi_* \end{aligned}$$

inherits from Q due to mass conservation. Coercivity is provided by the first two terms as a combination of microscopic and macroscopic coercivity and of the observation that $AT\Pi$ can be interpreted as the application of the map $z \mapsto z/(1+z)$ to the operator $(T\Pi)^*T\Pi$:

$$-\langle Lf, f\rangle + \varepsilon\langle AT\Pi f, f\rangle \geq \mu\|(1-\Pi)f\|^2 + \varepsilon\frac{4\pi^2}{1+4\pi^2}\|\Pi f\|^2 . \tag{3.12}$$

It remains to show that the last five terms in (3.10) can be controlled by the first two. We start with the last term of the first line. The property $A = \Pi A$ and (3.6) imply $TA = (1-\Pi)TA$ and therefore, with (3.7),

$$|\langle TAf, f\rangle| = |\langle TAf, (1-\Pi)f\rangle| \leq \|(1-\Pi)f\|^2 . \tag{3.13}$$

The operator AT is bounded if and only if its adjoint is bounded which, after using the self-adjointness of Π and the skew-symmetry of T, can be written as

$$(AT)^* = -T^2\Pi[1 + (T\Pi)^*(T\Pi)]^{-1} .$$

Let us define $g := [1 + (T\Pi)^*(T\Pi)]^{-1}f$, giving

$$(AT)^* f = -T^2\Pi g .$$

Furthermore, the definition of g is equivalent to $g - \Pi(v \cdot \nabla_x(v \cdot \nabla_x \Pi g)) = f$. After applying Π on both sides and using the notation $\rho_g := \Pi g$ and $\rho_f := \Pi f$, the equation reads

$$\rho_g - \frac{1}{2}\Delta_x \rho_g = \rho_f .$$

Testing against $\Delta_x \rho_g$ implies $\|\Delta_x \rho_g\|_{L^2_x} \leq 2\|\rho_f\|_{L^2_x}$. Therefore

$$\|(AT)^* f\|^2 = \|T^2\rho_g\|^2 \leq \pi\|\nabla_x^2 \rho_g\|^2_{L^2_x} = \pi\|\Delta_x \rho_g\|^2_{L^2_x} \leq 4\pi\|\rho_f\|^2_{L^2_x} = 2\|\Pi f\|^2 ,$$

implying

$$|\langle AT(1-\Pi)f, f\rangle| = |\langle (1-\Pi)f, (AT)^* f\rangle| \leq \sqrt{2}\,\|\Pi f\|\,\|(1-\Pi)f\| . \tag{3.14}$$

Since, by a straightforward computation, $\Pi TL = -\mu\Pi T$ we have $AL = -\mu A$ and, thus,

$$|\langle ALf, f\rangle| = \mu|\langle Af, \Pi f\rangle| \leq \frac{\mu}{2}\,\|\Pi f\|\,\|(1-\Pi)f\| . \tag{3.15}$$

Finally, we deal with the perturbation terms. Using $0 \leq b \leq 1$ we easily conclude

$$(Q_M f)f \leq f_0|f|\left(6\int_{\mathbb{T}^1}|f_*|d\varphi_* + \pi|f^{\downarrow}|\right) ,$$

and therefore, with (3.11) and with the Cauchy-Schwarz inequality,

$$\langle Q_M f, f\rangle \leq 13\pi f_0\|(1-\Pi)f\|^2 = \frac{13}{2}M\|(1-\Pi)f\|^2 . \tag{3.16}$$

Similarly,

$$|Q_M f| \leq f_0\left(6\int_{\mathbb{T}^1}|f_*|d\varphi_* + \pi|f^{\downarrow}| + 2\pi|f|\right) ,$$

implying

$$\|Q_M f\| \leq f_0\left(6\sqrt{2\pi}\|f\| + 3\pi\|f\|\right) = 3M\left(2\sqrt{\frac{2}{\pi}} + 1\right)\|f\| .$$

Combining this with (3.7), $A = \Pi A$, and with (3.11) gives

$$|\langle AQ_M f, f\rangle| \leq 3M\left(\sqrt{\frac{2}{\pi}} + \frac{1}{2}\right)\|\Pi f\|\|(1-\Pi)f\| . \tag{3.17}$$

Hypocoercivity: Using our results (3.12), (3.13), (3.14), (3.15), (3.16), (3.17) in (3.9), (3.10) gives

$$\begin{aligned}\frac{d}{dt}H[f] \;\leq\; &-\left(\mu-\frac{13}{2}M-\varepsilon\right)\|(1-\Pi)f\|^2-\varepsilon\frac{8\pi^3}{1+8\pi^3}\|\Pi f\|^2\\ &+\varepsilon\left(\sqrt{2}+\frac{\mu}{2}+3M\left(\sqrt{\frac{2}{\pi}}+\frac{1}{2}\right)\right)\|\Pi f\|\,\|(1-\Pi)f\|\,.\end{aligned}$$

Obviously for $\mu > 13M/2$ (as requested in Theorem 3.1) and for ε small enough, the right hand side is negative definite and controls $\|f\|^2 = \|\Pi f\|^2 + \|(1-\Pi)f\|^2$. With (3.8) we obtain the existence of $\lambda > 0$, such that

$$\frac{d}{dt}H[f] \leq -2\lambda H[f]\,,$$

and therefore exponential decay of the modified entropy and also of $\|f\|$ by another application of (3.8). This proves spectral stability of the uniform equilibrium in L^2.

Theorem 3.2. *Let $\mu/M > 13/2$. Then there exist positive constants λ and C, such that for any initial datum $f_I \in \mathcal{H}$, we have*

$$\|e^{t(L+Q_M-T)}f_I\| \leq Ce^{-\lambda t}\|f_I\|\,, \qquad t \geq 0\,.$$

This result can easily be extended to the Sobolev space $H^2(\mathbb{T}^2\times\mathbb{T}^1)\cap\mathcal{H}$, which is continuously imbedded in $L^\infty(\mathbb{T}^2\times\mathbb{T}^1)$ and, thus, an algebra. The procedure will only be outlined in the following.

Note that $f \in H^2(\mathbb{T}^2\times\mathbb{T}^1)\cap\mathcal{H}$ implies that the partial derivatives of f lie in $\mathcal{H}$. Therefore Theorem 3.2 immediately carries over to the pure x-derivatives, since the coefficients in (3.5) are x-independent and the x-derivatives thus solve the same equation. If there is also differentiation with respect to φ on the other hand, we have to proceed recursively. The following crucial, but technical observation that the collision operator Q factorizes when derived with respect to φ, will be used throughout the following considerations.

Lemma 3.3. *Let $h_1, h_2 \in H^2(\mathbb{T}^2\times\mathbb{T}^1)$, we observe that*

$$\partial_\varphi Q(h_1,h_2) = Q(\partial_\varphi h_1, h_2) + Q(h_1, \partial_\varphi h_2),$$

and hence also

$$\partial_\varphi^2 Q(h_1,h_2) = Q(\partial_\varphi^2 h_1, h_2) + 2Q(\partial_\varphi h_1, \partial_\varphi h_2) + Q(h_1, \partial_\varphi^2 h_2)$$

i.e. the collision operator $Q(h_1,h_2)$ behaves like a pointwise product with respect to the φ-derivative.

Proof. This property can be seen easily by rewriting the collision operator in the form

$$Q(h_1,h_2) = \int_{\mathbb{T}^1} b_{AL}(\varphi-\varphi_*)\tilde{h}_1 h_{2*}\,\mathrm{d}\varphi_* + \int_{\mathbb{T}^1} b_{REV}(\varphi-\varphi_*)h_1^\downarrow h_{2*}^\downarrow\,\mathrm{d}\varphi_* - \int_{\mathbb{T}^1} b(\varphi-\varphi_*)h_1 h_{2*}\,\mathrm{d}\varphi_*\,,$$

where we defined

$$b_{AL}(\varphi-\varphi_*) := b(\tilde{\varphi},\varphi_*)\mathbb{1}_{\mathbb{T}^{AL}_{\to\varphi}}(\varphi_*) = b(\tilde{\varphi},\varphi_*)\mathbb{1}_{\{\cos(2(\cdot))>0\,\&\,\cos(\cdot)>0\}}(\varphi-\varphi_*)$$

and

$$b_{REV}(\varphi-\varphi_*) := b(\varphi^\downarrow,\varphi_*^\downarrow)\mathbb{1}_{\mathbb{T}^{REV}_{\varphi}}(\varphi_*) = b(\varphi^\downarrow,\varphi_*^\downarrow)\mathbb{1}_{\{\cos(\cdot)<0\}}(\varphi-\varphi_*)\,,$$

with the crucial observation that b_{AL}, b_{REV} and b depend on the difference $\varphi-\varphi_*$. Deriving the collision operator with respect to φ while using integration by parts to avoid the occurrence of derivatives of the collision kernel gives the desired result. □

The first φ-derivative, $g := \partial_\varphi f$, solves the equation

$$\begin{aligned}\partial_t g + (T-L)g &= -\omega(\varphi)^\perp \cdot \nabla_x f + 2f_0 \int_{\mathbb{T}^{AL}_{\to\varphi}} b(\tilde\varphi,\varphi_*)(\tilde g + g_*)\mathrm{d}\varphi_* \\ &\quad + f_0 \int_{\mathbb{T}^{REV}_{\varphi}} b(\varphi^\downarrow,\varphi_*^\downarrow)(g^\downarrow + g_*^\downarrow)\mathrm{d}\varphi_* - f_0 \int_{\mathbb{T}^1} b(\varphi,\varphi_*)(g+g_*)\mathrm{d}\varphi_*\,,\end{aligned}$$

with $(\omega_1,\omega_2)^\perp = (-\omega_2,\omega_1)$. The first term on the right hand side comes from the φ-dependence of the coefficient in the transport term, whereas the remaining terms are $\partial_\varphi(Q_M f)$, which is derived by first using the above Lemma 3.3 before linearizing around the uniform equilibrium f_0.

By Theorem 3.2 and by the argument above, exponential decay of the first term on the right hand side is already known. The remaining three terms are given by Q_M applied to g and therefore can be treated as a perturbation of $L-T$ as in the proof of Theorem 3.2. For this step again property (3.11) is important. As a consequence, exponential decay of g follows from the variation-of-constants formula for μ large enough. The derivatives $\nabla_x\partial_\varphi f$ (with second order x-derivatives in the inhomogeneity) and $\partial_\varphi^2 f$ (with $\nabla_x f$ and $\nabla_x\partial_\varphi f$ in the inhomogeneity) are treated analogously, proving the following result.

Corollary 3.4. *For μ/M large enough there exist positive constants λ and C, such that for any initial datum $f_I \in H^2(\mathbb{T}^2\times\mathbb{T}^1)\cap\mathcal{H}$, we have*

$$\|e^{t(L+Q_M-T)}f_I\|_{H^2(\mathbb{T}^2\times\mathbb{T}^1)} \le Ce^{-\lambda t}\|f_I\|_{H^2(\mathbb{T}^2\times\mathbb{T}^1)}\,,\qquad t\ge 0\,.$$

Remark 3.5. *The exponential rate constant λ in Corollary 3.4 has to be chosen a little smaller than in Theorem 3.2 because of resonance in the inhomogeneous equations like (3.18). Otherwise an additional factor t^2 would appear as a result of the two-stage recursion process needed for estimating $\partial_\varphi^2 f$. Also the ratio μ/M might have to be larger than in Theorem 3.2.*

3.2.2 Nonlinear stability of the uniform equilibrium

This section is devoted to the proof of Theorem 3.1. We introduce the perturbation

$$h := f - f_0 \in H^2(\mathbb{T}^2\times\mathbb{T}^1)\cap\mathcal{H}\,,$$

satisfying, with the notation introduced above,

$$\partial_t h + Th = Lh + Q_M h + Q(h,h)\,,\qquad h(t=0) = f_I - f_0\,,$$

and consider the mild formulation

$$h(t) = e^{t(L+Q_M-T)}(f_I-f_0) + \int_0^t e^{(t-s)(L+Q_M-T)}Q(h(s),h(s))\mathrm{d}s\,.$$

For the estimation of the semigroup, Corollary 3.4 will be used, and apart from that we need estimates of the quadratic collision operator.

Lemma 3.6. *Let $h_1,h_2\in H^2(\mathbb{T}^2\times\mathbb{T}^1)\cap\mathcal{H}$. Then $Q(h_1,h_2)\in H^2(\mathbb{T}^2\times\mathbb{T}^1)\cap\mathcal{H}$ and there exists a constant $\bar Q$ such that*

$$\|Q(h_1,h_2)\|_{H^2(\mathbb{T}^2\times\mathbb{T}^1)} \le \bar Q\,\|h_1\|_{H^2(\mathbb{T}^2\times\mathbb{T}^1)}\|h_2\|_{H^2(\mathbb{T}^2\times\mathbb{T}^1)}\,.$$

Proof. Because of the Sobolev inequality

$$\|h\|_{L^\infty(\mathbb{T}^2\times\mathbb{T}^1)}+\|\nabla_x h\|_{L^4(\mathbb{T}^2\times\mathbb{T}^1)}+\|\partial_\varphi h\|_{L^4(\mathbb{T}^2\times\mathbb{T}^1)}\leq c_S\|h\|_{H^2(\mathbb{T}^2\times\mathbb{T}^1)}\,, \tag{3.19}$$

it will be sufficient to find estimates in terms of the L^∞-norms of h_1 and h_2 or of the L^4-norms of the first order derivatives. We start with the observation

$$|Q(h_1,h_2)|\leq 4\|h_1\|_{L^\infty(\mathbb{T}^2\times\mathbb{T}^1)}\int_{\mathbb{T}^1}|h_2|\mathrm{d}\varphi\,,$$

implying

$$\|Q(h_1,h_2)\|\leq 8\pi\,\|h_1\|_{L^\infty(\mathbb{T}^2\times\mathbb{T}^1)}\|h_2\|\,, \tag{3.20}$$

and similarly,

$$\|Q(h_1,h_2)\|\leq \sqrt{8\pi+33\pi^2}\,\|h_1\|\|h_2\|_{L^\infty(\mathbb{T}^2\times\mathbb{T}^1)}\,,$$

Alternatively it is, by the convolution structure of the collision terms, straightforward to show

$$\int_{\mathbb{T}^1}Q(h_1,h_2)^2\mathrm{d}\varphi\leq 6\pi\int_{\mathbb{T}^1}h_1^2\mathrm{d}\varphi\int_{\mathbb{T}^1}h_2^2\mathrm{d}\varphi\,,$$

with the consequence

$$\|Q(h_1,h_2)\|\leq\sqrt{12\pi}\|h_1\|_{L^4(\mathbb{T}^2\times\mathbb{T}^1)}\|h_2\|_{L^4(\mathbb{T}^2\times\mathbb{T}^1)}\,. \tag{3.21}$$

By elliptic regularity, we may use the equivalent norm $\|h\|_*=\|h\|+\|\Delta_x h\|+\|\partial_\varphi^2 h\|$ on $H^2(\mathbb{T}^2\times\mathbb{T}^1)$. We have

$$\begin{aligned}\|\Delta_x Q(h_1,h_2)\| &\leq \|Q(\Delta_x h_1,h_2)\|+\|Q(h_1,\Delta_x h_2)\|+2\|Q(\nabla_x h_1,\nabla_x h_2)\|\\ &\leq \sqrt{8\pi+33\pi^2}\,\|\Delta_x h_1\|\|h_2\|_{L^\infty(\mathbb{T}^2\times\mathbb{T}^1)}+8\pi\,\|h_1\|_{L^\infty(\mathbb{T}^2\times\mathbb{T}^1)}\|\Delta_x h_2\|\\ &\quad+\sqrt{12\pi}\|\nabla_x h_1\|_{L^4(\mathbb{T}^2\times\mathbb{T}^1)}\|\nabla_x h_2\|_{L^4(\mathbb{T}^2\times\mathbb{T}^1)}\\ &\leq c_S(\sqrt{8\pi+33\pi^2}+8\pi+c_S\sqrt{12\pi})\|h_1\|_{H^2(\mathbb{T}^2\times\mathbb{T}^1)}\|h_2\|_{H^2(\mathbb{T}^2\times\mathbb{T}^1)}\,,\end{aligned}$$

where we have used (3.20)–(3.21) as well as (3.19). It remains to estimate $\partial_\varphi^2 Q(h_1,h_2)$. Due to the property stated in Lemma 3.3 we can estimate analogously to the above,

$$\|\partial_\varphi^2 Q(h_1,h_2)\|\leq c_S(\sqrt{8\pi+33\pi^2}+8\pi+c_S\sqrt{12\pi})\|h_1\|_{H^2(\mathbb{T}^2\times\mathbb{T}^1)}\|h_2\|_{H^2(\mathbb{T}^2\times\mathbb{T}^1)}\,,$$

completing the proof. □

Lemma 3.6 implies local Lipschitz continuity of Q, considered as a map on $H^2(\mathbb{T}^2\times\mathbb{T}^1)\cap\mathcal{H}$ and therefore local existence and uniqueness of a mild solution. Corollary 3.4 and Lemma 3.6 imply

$$\|h(t)\|_{H^2(\mathbb{T}^2\times\mathbb{T}^1)}\leq Ce^{-\lambda t}\|f_I-f_0\|_{H^2(\mathbb{T}^2\times\mathbb{T}^1)}+C\bar{Q}\int_0^t e^{\lambda(s-t)}\|h(s)\|^2_{H^2(\mathbb{T}^2\times\mathbb{T}^1)}\mathrm{d}s\,.$$

It is easily checked that for

$$\|f_I-f_0\|_{H^2(\mathbb{T}^2\times\mathbb{T}^1)}\leq\frac{\lambda}{4C^2\bar{Q}}\,,$$

Picard iteration preserves the inequality

$$\|h(t)\|_{H^2(\mathbb{T}^2\times\mathbb{T}^1)}\leq 2Ce^{-\lambda t}\|f_I-f_0\|_{H^2(\mathbb{T}^2\times\mathbb{T}^1)}\,,$$

completing the proof of Theorem 3.1.

3.3 Existence and Stability of Equilibria for the Spatially Homogeneous Equation

This section focuses on finding nonuniform, *spatially homogeneous* equilibria of (3.1), i.e. stationary solutions of the equation

$$\begin{aligned} &\partial_t f = \mu \partial_\varphi^2 f + Q(f,f), \quad \varphi \in \mathbb{T}^1,\ t>0, \\ &f(\varphi,0) = f_I(\varphi), \quad \varphi \in \mathbb{T}^1, \end{aligned} \tag{3.22}$$

and further investigate their stability. We expect the uniform distribution f_0 to be a stable equilibrium for sufficiently large diffusion and hope to find other stable equilibria in the collision dominating regime. Therefore, we aim to find a concrete diffusion parameter μ^*, which defines the threshold from which on the uniform equilibrium becomes stable.

We approach this problem form two sides. On one hand, in Section 3.3.1 we find a branch of constant homogeneous solutions different from the uniform one, which are existing for sufficiently small but moderate diffusion. We perform the corresponding computations in a formal way, with the remark that they can easily be made rigorous following the theory for bifurcations from a simple eigenvalue by Crandall and Rabinowitz, [18].
On the other hand, in Section 3.3.2, our aim is to show existence of a stationary solution to (3.22) for $\mu \ll 1$, which can be seen as regularization of the measure solution $f_\infty(\varphi) := \rho_+ \delta(\varphi - \varphi+) + \rho_- \delta(\varphi - \varphi^\downarrow)$, which is a stable equilibrium of the model without directional diffusion (3.3), i.e. $\mu = 0$. In [31] this problem was discussed and it could be shown that for a constant collision kernel and special initial conditions the spatially homogeneous solution decays exponentially to f_∞ in the *Wasserstein space* $\mathcal{P}(\mathbb{T}^1)$.

3.3.1 Bifurcation Analysis

We start with analyzing the stability of $f_0 = \frac{M}{2\pi}$ by linearizing the problem (3.22) around f_0. We search for stationary, spatially homogeneous solutions close to f_0 and set

$$f = f_0 + \varepsilon f^*,$$

for a small parameter $\varepsilon > 0$ and a perturbation function f^* satisfying

$$\int_{\mathbb{T}^1} f^*(\varphi)\, \mathrm{d}\varphi = 0,$$

in order to be consistent with mass conservation. We plug $f = f_0 + \varepsilon f^*$ into (3.22), which gives due to $Q(f_0, f_0) = 0$

$$\varepsilon \partial_t f^* = \varepsilon \mu f^{*''} + \varepsilon Q(f_0, f^*) + \varepsilon Q(f^*, f_0) + \varepsilon^2 Q(f^*, f^*),$$

where the prime now denotes the derivative with respect to φ. Looking at order ε, we obtain the *linearized equation for the perturbation* f^*

$$\begin{aligned} &\partial_t f^* = \mu f^{*''} + Q_M(f^*), \\ &\int_{\mathbb{T}^1} f^*\, \mathrm{d}\varphi = 0, \quad f^*(\varphi) = f^*(-\varphi),\ \forall \varphi \in \mathbb{T}^1, \end{aligned} \tag{3.23}$$

where, as in Section 3.2, Q_M describes the linearization of Q around f_0 defined as

$$Q_M(f) := Q(f_0, f) + Q(f, f_0).$$

Since we expect our solution to be in $L^2(\mathbb{T}^1)$, we make the *Fourier series* ansatz for the function f^* and write

$$\begin{aligned} f^*(\varphi) &= \sum_{n\geq 1} a_n \cos(n\varphi) + \sum_{n\geq 1} b_n \sin(n\varphi) \\ &= \sum_{n\geq 1} a_n \sin(n\varphi + \pi/2) + \sum_{n\geq 1} b_n \sin(n\varphi) \end{aligned} \tag{3.24}$$

We calculate $-\mu f^{*''} + Q_M f^*$ in order to obtain equations for the Fourier modes. Indeed, plugging (3.24) into (3.23) we see that the operator $\mu\partial_\varphi^2 \cdot + Q_M(\cdot)$ is diagonal in $L^2(\mathbb{T}^1)$ with respect to the basis $\{\cos(n\,\cdot), \sin(n\,\cdot)\}_{n\geq 0}$ and we obtain the following evolution equations for the Fourier modes

$$\begin{pmatrix} \dot{a}_n \\ \dot{b}_n \end{pmatrix} = \lambda_n(\mu, f_0) \begin{pmatrix} a_n \\ b_n \end{pmatrix}$$

where $\{\lambda_n(\mu, f_0)\}_{n\geq 1}$ describe the eigenvalues to the eigenfucntions $\{\sin(n\cdot)\}_{n\geq 1}$ resp. $\{\cos(n\cdot)\}_{n\geq 1}$, which can be computed explicitly and are given by

$$\lambda_1(\mu, f_0) = -\mu + \frac{f_0}{3}\left(1 - 8\sin(\pi/4)\right),$$

$$\lambda_2(\mu, f_0) = -4\mu + \frac{2f_0}{3},$$

$$\lambda_n(\mu, f_0) = -n^2\mu + 2f_0\left(\frac{4n\sin(n\pi/4) - 8}{n^2 - 4} + \frac{n\sin(n\pi/2) + (-1)^n}{n^2 - 1} + (-1)^n - 2\right).$$

For $n \neq 2$ we observe strict negativity of the eigenvalues, independent from the value of μ, i.e. $\lambda_n < 0, \forall \mu > 0$. Other than that, the second eigenvalue λ_2 passes zero for changing diffusion constant:

$$\lambda_2(\mu) = -4\mu + \frac{2f_0}{3} \quad \begin{cases} > 0 & \text{for } \mu < \frac{f_0}{6} \\ < 0 & \text{for } \mu > \frac{f_0}{6} \end{cases}$$

At the critical value

$$\mu = \mu^* := \frac{f_0}{6} \tag{3.25}$$

we have $\lambda_2 = 0$. These observations reveal the following linear stability result for the uniform equilibrium f_0:
The uniform equilibrium is linearly stable for $\mu > \mu^*$, while for $\mu < \mu^*$ the f_0 becomes an unstable equilibrium, since the critical eigenvalue λ_2 is positive. The point (μ^*, f_0) is a *bifurcation point*, where a branch of new stationary solutions emerge, which close left to the bifurcation point is of the form

$$f(\varphi) = f_0 + \varepsilon f^*(\varphi) = f_0 + \varepsilon a \sin(2\varphi + \pi/2) + \varepsilon b \sin(2\varphi),$$

for some small parameter $\varepsilon << 1$. We renamed the second Fourier modes $a := a_2$ and $b := b_2$. The rotational symmetry of the problem (3.22) causes $\ker\left(\partial_\varphi^2 \cdot + Q_M(\cdot)\right)$ to be two dimensional, spanned by $\{\sin(2\cdot), \cos(2\cdot)\}$. Since we are able to express one direction with respect to the other, we will only focus on the sin-part of the $\left(\ker\left(\partial_\varphi^2 \cdot + Q_M(\cdot)\right)\right)$, which corresponds to fixing f^* at 0, i.e. $f^*(0) = 0$ in this case.

Determining the type of Bifurcation: The *flip-symmetry* in our equation indicates the occurrence of a *pitchfork bifurcation*. Having in mind that in the no-diffusion-regime the equilibrium $f_\infty(\varphi) := \rho_+\delta_{\varphi_+}(\varphi) + \rho_-\delta_{\varphi_-}(\varphi)$, consisting of two Dirac-deltas with masses concentrated exactly opposite of each other, is stable (see [31]), we also expect to find stable, non-constant equilibria, with two peaks exactly opposite from each other for small values of μ. Therefore, we search left of μ^* and make the ansatz

$$\begin{aligned} \mu &= \mu^* - \delta, \\ f(\varphi) &= f_0 + \sqrt{\delta} f^*(\varphi) + \delta g(\varphi) + \mathcal{O}\left(\delta^{\frac{3}{2}}\right), \end{aligned} \tag{3.26}$$

for $\delta := \varepsilon^2 > 0$ and

$$f^*(\varphi) := b \sin(2\varphi),$$

with Fourier mode $a \in \mathbb{R}$ to be determined. Due to *mass conservation* the perturbation g also fulfills

$$\int_{\mathbb{T}^1} g(\varphi, t)\, \mathrm{d}\varphi = 0.$$

Plugging (3.26) into (3.22) yields, after dividing by $\sqrt{\delta}$,

$$\begin{aligned} \partial_t f^* + \sqrt{\delta}\partial_t g =& \mu^* \partial_\varphi^2 f^* + Q_M(f^*) + \sqrt{\delta}\left(\mu^* \partial_\varphi^2 g + Q(f^*, f^*) + Q_M(g)\right) \\ &+ \delta\left(-\partial_\varphi^2 f^* + Q(f^*, g) + Q(g, f^*)\right) + \delta^{\frac{3}{2}}\left[-\partial_\varphi^2 g + Q(g, g)\right]. \end{aligned}$$

$\underline{\delta \in \mathcal{O}(1)}$: Ignoring terms up from order $\sqrt{\delta}$, we get the following equation

$$\partial_t f^* = \mu^* f^{*\prime\prime} + Q_M(f^*) = 0,$$

which of course was matter of investigation while considering the linearized equation in the chapter before. Hence, we already know that $f^* \in \ker\left(\mu^*\partial_\varphi^2 \cdot + Q_M(\cdot)\right)$, which gives the shape of the non-uniform stationary solutions emerging at μ^* close to the bifurcation point. The constant b determines how these branch of nonuniform solutions look like.
$\underline{\mathcal{O}(\sqrt{\delta})}$: In order to obtain information on these unknowns, we go up to higher order in the stationary version of problem (3.3.1) and compare coefficients of $\sqrt{\delta}$.

$$0 = \mu^* g'' + Q(f^*, f^*) + Q_M(g).$$

The second term on the right hand side, i.e. collision operator applied to f^*, can be computed in terms of b, which yields

$$Q(f^*, f^*) = -\frac{4}{3} b^2 \cos(4\varphi).$$

Next we search for a *solvability condition*, which we want to apply to the equation above in order to get rid of its dependence on the unknown g. This is equivalent to searching for left-eigenvectors to the eigenvalue 0 of the already known operator $\mu^*\partial_\varphi^2 \cdot + Q_M(\cdot)$. One can see easily that it is symmetric, from which we conclude that the solvability condition is given by multiplication of $\sin(2\varphi)$, which is spanning the nullspace of $\mu^*\partial_\varphi^2 \cdot + L \cdot$ after we turned off the rotational symmetry of (3.22), and integration over $\mathbb{T}^1$. Carrying out these computations yields

$$\begin{aligned} 0 &= \int_{\mathbb{T}^1} \sin(2\varphi)(\mu^*\partial_\varphi^2 g + Q_M(g) + Q(f^*, f^*))\, \mathrm{d}\varphi \\ &= -\frac{4}{3} b^2 \int_{\mathbb{T}^1} \sin(2\varphi)\cos(4\varphi) = 0, \end{aligned}$$

which gives no information about b. But from (3.3.1)

$$\mu^* g'' + Q_M(g) = \frac{4}{3} b^2 \cos(4\varphi)$$

we can calculate g in terms of b again using the Fourier series Ansatz

$$g(\varphi) = \sum_{n\geq 1, n\neq 2} a_n \cos(n\varphi) + \sum_{n\geq 1, n\neq 2} b_n \sin(n\varphi).$$

Having in mind that the operator $\mu^* \partial_\varphi^2 \cdot + Q_M(\cdot)$ is diagonal with respect to the basis $\{\cos(n\,\cdot), \sin(n\,\cdot)\}_{n\geq 0}$ and using the formula for the eigenvalue λ_4, we obtain

$$\frac{4}{3} b^2 = -16 \left(\mu^* + \frac{f_0}{5}\right) a_4,$$

which is equivalent to

$$a_4 = -\frac{b^2}{12(\mu^* + \frac{f_0}{5})}.$$

Therefore, g can be expressed as

$$g(\varphi) = -\frac{cb^2}{2} \cos(4\varphi),$$

where we defined $c := (6(\mu^* + \frac{f_0}{5}))^{-1} > 0$ for simplicity.
$\underline{\mathcal{O}(\delta)}$: We we compare coefficients in (3.3.1) of the next higher order of δ and obtain

$$0 = -f^{*''} + Q(f^*, g) + Q(g, f^*).$$

Using the expressions of f^* and g, we calculate the terms of the above equation and obtain

$$0 = \left(4b - \frac{3cb^3}{10}\right) \sin(2\varphi).$$

Now, we again want to apply our *solvability condition* in order to get information on b. By multiplication with $\sin(2\,\cdot)$ and integrating over $\mathbb{T}^1$ yields after division by π

$$0 = 4b - \frac{3c}{10} b^3.$$

From here, one can already recognize easily that this equation for b describes the normal form of a *supercritical pitchfork bifurcation*. The solution $b = 0$ refers to the uniform equilibrium, while the two nonzero solutions to $b^2 = \frac{40}{3c}$ give rise to two branches of non-constant equilibria, symmetric around f_0. Linear stability of these branches left of μ^* is proved by investigating the eigenvalues λ_n, $n \neq 2$, for the operator on the right-hand-side of (3.3.1). For $n \neq 4$, the eigenvalues are again of the form

$$\lambda_n = -n^2 \mu^* + 2 f_0 \left(\frac{4n \sin(n\pi/4) - 8}{n^2 - 4} + \frac{n \sin(n\pi/2) + (-1)^n}{n^2 - 1} + (-1)^n - 2 \right),$$

and strictly negative, as we proved above. For the case $n = 4$ we have

$$\lambda_4 = -\left(16\mu^* + f_0 \frac{16}{5} + \frac{4}{3} b^2\right) < 0.$$

Hence, the branches of equilibria $f(\varphi) = f_0 \pm \sqrt{\delta \frac{40}{3c}} \sin(2\varphi)$, $\delta \ll 1$, are *linearly stable* and we can conclude that at $\mu = \mu^*$ a *supercritical pitchfork bifurcation* occurs, see Figure 3.1.

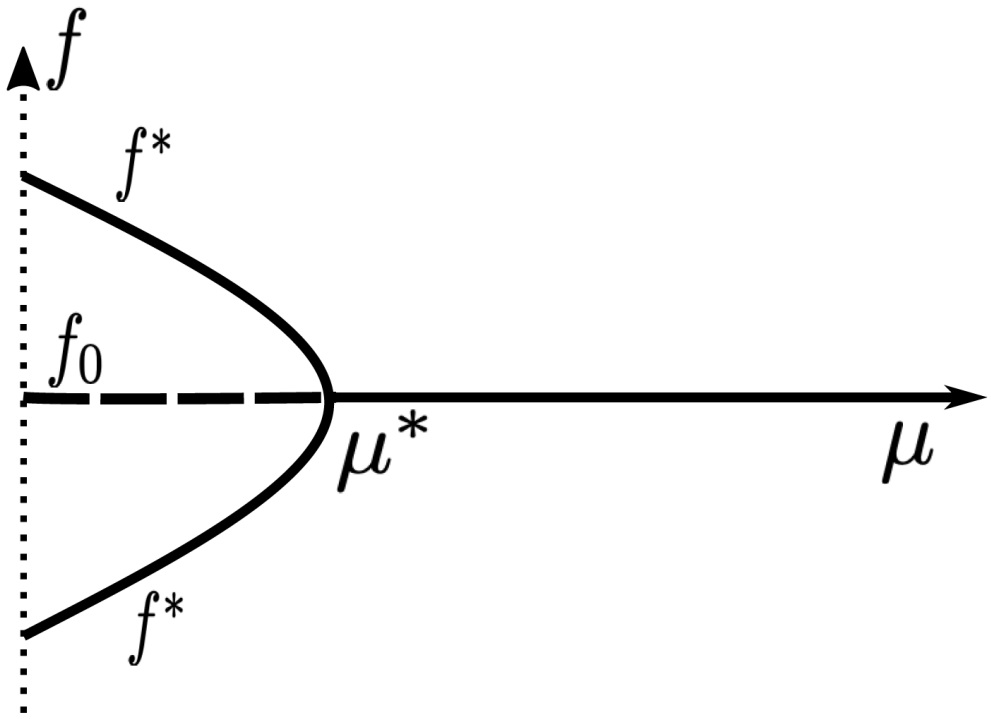

Figure 3.1: Bifurcation diagram of a supercritical pitchfork bifurcation with branches to the left; solid lines represent stable points, while dotted line represents unstable ones

Remark 3.7. *The above calculations were carried out for* $b(\varphi, \varphi_*) = |\sin(\varphi - \varphi_*)|$*, modelling the case of rod-shaped myxobacteria. We want to mention here that our method yields the same type of bifurcation result for Maxwellian myxos, i.e.* $b \equiv 1$*. Although qualitative analogous, the bifurcation point at which the pitchfork bifurcation happens is in this case given by*

$$\mu^* = f_0 \left(1 - \frac{\pi}{4}\right) = \frac{M}{2} \left(\frac{1}{\pi} - 1\right).$$

3.3.2 Existence of Equilibria for Small Diffusivity

Having in mind that $f_\infty(\varphi) := \rho_+ \delta(\varphi - \varphi_+) + \rho_- \delta(\varphi - \varphi_+^\downarrow)$ as in (3.4) is a stationary, homogeneous (measure) solution to the kinetic equation for myxobacteria (3.3) (see [31]), we now want to investigate existence of equilibria for (3.1) with very small directional diffusion, i.e. $\mu \ll 1$, which we expect to find close to f_∞. The bifurcation result from the above Section 3.3.1, which formally shows existence of nonuniform π-symmetric solutions for sufficiently small μ, suggest that nonuniform equilibria have the form of two equally weighted peaks, which are with distance π apart. Therefore, different from the problem without diffusion (3.3), where the equilibrium f_∞ could possibly consist of two different weighted Dirac deltas situated opposite from each other, we expect the equilibrium for the equation with directional diffusion to be symmetric. In fact, performing numerical simulations (see Section 3.4) we could observe that in the presence of directional diffusion no asymmetrical equilibrium can be reached. More precisely, simulations show that wo exactly opposite, but differently weighted peaks

are destroyed by diffusion, which equals them out.
For the search of such equilibria we restrict ourselves to the case of 'Maxwellian myxos', whose dynamics are characterized by the collision operator Q with constant collision kernel $b(\varphi, \varphi_*) \equiv 1$. This can be seen as an analogy to a similar simplification of the gas dynamics Boltzmann equation known as 'Maxwellian molecules' [17]. For $\varphi \in \mathbb{T}^1$, $t > 0$ equation (3.22) then has the following simple form

$$\partial_t f(\varphi) = \mu \partial_\varphi^2 f(\varphi) + 2 \int_{\varphi - \frac{\pi}{4}}^{\varphi + \frac{\pi}{4}} f(2\varphi - \varphi_*) f(\varphi_*) \, \mathrm{d}\varphi_* + f(\varphi + \pi) \int_{\varphi - \frac{\pi}{2}}^{\varphi + \frac{\pi}{2}} f(\varphi_*) \, \mathrm{d}\varphi_* - M f(\varphi). \tag{3.27}$$

Motivated by the discussions above, we seek for an equilibrium which is π-symmetric and regularizes the measure equilibrium concentrated around 0 and π with equally weighted peaks, i.e.

$$f_\infty(\varphi) = \frac{M}{2} \delta(\varphi) + \frac{M}{2} \delta(\varphi - \pi).$$

Therefore, we aim to find a solution to (3.27) with significant values only close to 0 and π and investigate its behavior close to these values separately. We introduce the local variables:

- $\xi := \varphi \sqrt{\frac{M}{2\mu}}$ close to 0,
- $\eta := (\varphi - \pi) \sqrt{\frac{M}{2\mu}}$ close to π.

Now, we make the symmetry ansatz

$$F(\xi) := \frac{1}{2} \sqrt{\frac{32\mu}{M^3}} f\left(\xi \sqrt{\frac{2\mu}{M}} \right) = \frac{1}{2} \sqrt{\frac{32\mu}{M^3}} f(\varphi) \tag{3.28}$$

equivalent to

$$f(\varphi) = \sqrt{\frac{M^3}{32\mu}} \left[F\left(\varphi \sqrt{\frac{M}{2\mu}} \right) + F\left((\varphi - \pi) \sqrt{\frac{M}{2\mu}} \right) \right] = \sqrt{\frac{M^3}{32\mu}} \left[F(\xi) + F(\eta) \right] = 2 \sqrt{\frac{M^3}{32\mu}} F(\xi),$$

having in mind that $F(\xi) \searrow 0$ for $\xi \to \pm\infty$ should hold. Plugging now (3.28) into the stationary version of (3.27), the equation for F reads

$$0 = F''(\xi) + 2 \int_{\xi - \frac{\pi}{4}\sqrt{\frac{M}{2\mu}}}^{\xi + \frac{\pi}{4}\sqrt{\frac{M}{2\mu}}} F(2\xi - \xi_*) F(\xi_*) \, \mathrm{d}\xi_* + F(\eta) - 2F(\xi),$$

where the primes denote derivatives with respect to ξ. After approximating the integral with an integral over $\mathbb{R}$, since we consider solutions which decay to zero for $|\xi| \to \infty$, as well the symmetry assumption $F(\eta) = F(\xi)$ we obtain the following equation for F

$$0 = F''(\xi) + 2 \int_{\mathbb{R}} F(2\xi - \xi_*) F(\xi_*) \, \mathrm{d}\xi_* - F(\xi). \tag{3.29}$$

Fixed-point argument The question now has simplified to searching for functions F that fulfill (3.29). Having in mind to apply a fixed-point argument we write

$$G(\xi) := -2 \int_{\mathbb{R}} F(2\xi - \xi_*) F(\xi_*) \, \mathrm{d}\xi_*,$$

with which the equation in (3.29) can be reformulated as

$$F'' - F = G.$$

For solving this ODE, we take G as given datum and find that the solution is given by

$$F(\xi) = -\frac{1}{2}\int_{\mathbb{R}} e^{-|\xi-\xi_*|}G(\xi_*)\,\mathrm{d}\xi_*.$$

Having in mind (3.3.2), a solution to (3.29) has therefore to fulfill the equation

$$F(\xi) = \int_{\mathbb{R}}\int_{\mathbb{R}} e^{-|\xi-\xi_*|}F(2\xi_* - \tilde{\xi})F(\tilde{\xi})\,\mathrm{d}\tilde{\xi}\,\mathrm{d}\xi_*.$$

Our aim now is to prove that the mapping

$$\mathcal{S}:\mathcal{B}\to\mathcal{B},\quad F\overset{\mathcal{S}}{\mapsto}\int_{\mathbb{R}}\int_{\mathbb{R}} e^{-|\xi-\xi_*|}F(2\xi_* - \tilde{\xi})F(\tilde{\xi})\,\mathrm{d}\tilde{\xi}\,\mathrm{d}\xi_* \tag{3.30}$$

with

$$\mathcal{B} := \Big\{F\in B_1(L^1(\mathbb{R})) :\ \int_{\mathbb{R}}\xi^2F(\xi)\,\mathrm{d}\xi \le 4\Big\}.$$

has a fixed-point. First, we make the following observations:

1. Calculating the L^1-norm of $G(F)$ yields

$$\|G(F)\|_{L^1} = 2\int_{\mathbb{R}}\int_{\mathbb{R}} F(2\xi-\xi_*)F(\xi_*)\,\mathrm{d}\xi_*\,\mathrm{d}\xi = \int_{\mathbb{R}}\int_{\mathbb{R}} F(\hat{\xi})F(\xi_*)\,\mathrm{d}\xi_*\,\mathrm{d}\hat{\xi} = \|F\|_{L^1}^2,$$

   and therefore for $\mathcal{S}(F)$ we obtain

$$\begin{aligned}\|\mathcal{S}(F)\|_{L^1} &= \frac{1}{2}\int_{\mathbb{R}}\int_{\mathbb{R}} e^{-|\xi-\xi_*|}G(F)(\xi_*)\,\mathrm{d}\xi_*\,\mathrm{d}\xi\\ &= \frac{1}{2}\int_{\mathbb{R}}\int_{\mathbb{R}} e^{-|\xi|}G(F)(\xi_*)\,\mathrm{d}\xi_*\,\mathrm{d}\xi = \|G(F)\|_{L^1} = \|F\|_{L^1}^2.\end{aligned}$$

2. The L^∞-norm of $\mathcal{S}(F)$ can be estimated as follows

$$\begin{aligned}\|\mathcal{S}(F)\|_{L^\infty} &= \sup_{\xi\in\mathbb{R}}\int_{\mathbb{R}}\int_{\mathbb{R}} e^{-|\xi-\xi_*|}F(2\xi_*-\tilde{\xi})F(\tilde{\xi})\,\mathrm{d}\tilde{\xi}\,\mathrm{d}\xi_*\\ &\le \sup_{\xi}\int_{\mathbb{R}}\int_{\mathbb{R}} F(2\xi_*-\tilde{\xi})F(\tilde{\xi})\,\mathrm{d}\tilde{\xi}\,\mathrm{d}\xi_* = \frac{1}{2}\|F\|_1^2.\end{aligned}$$

3. Further, we calculate for the variance

$$\begin{aligned}&\int_{\mathbb{R}}\xi^2\mathcal{S}(F)(\xi)\,\mathrm{d}\xi = \int_{\mathbb{R}}\int_{\mathbb{R}}\int_{\mathbb{R}}\xi^2 e^{-|\xi-\xi_*|}F(2\xi_*-\tilde{\xi})F(\tilde{\xi})\,\mathrm{d}\tilde{\xi}\,\mathrm{d}\xi_*\,\mathrm{d}\xi\\ &= -\frac{1}{2}\int_{\mathbb{R}} e^{-|\xi|}\,\mathrm{d}\xi\int_{\mathbb{R}}\xi_*^2G(F)(\xi_*)\,\mathrm{d}\xi_* - \int_{\mathbb{R}}\int_{\mathbb{R}}\xi_*\xi e^{-|\xi_*|}G(F)(\xi_*)\,\mathrm{d}\xi_*\,\mathrm{d}\xi + \frac{1}{2}\|G(F)\|_1\int_{\mathbb{R}}\xi^2e^{-|\xi|}\,\mathrm{d}\xi\\ &= -\int_{\mathbb{R}}\xi_*^2G(F)(\xi_*)\,\mathrm{d}\xi_* + 2\|G(F)\|_1.\end{aligned}$$

In order to obtain also a formulation for F, we further write

$$\int_{\mathbb{R}} \xi^2 \mathcal{S}(F)(\xi)\,\mathrm{d}\xi = 2\int_{\mathbb{R}}\int_{\mathbb{R}} \xi^2 F(2\xi-\xi_*)F(\xi_*)\,\mathrm{d}\xi_*\,\mathrm{d}\xi + 2\|F\|_1^2$$
$$= \frac{1}{4}\int_{\mathbb{R}}\int_{\mathbb{R}} (\hat{\xi}+\xi_*)^2 F(\hat{\xi})F(\xi_*)\,\mathrm{d}\xi_*\,\mathrm{d}\hat{\xi} + 2\|F\|_1^2 = \frac{1}{2}\int_{\mathbb{R}} \xi^2 F(\xi)\,\mathrm{d}\xi + 2\|F\|_1^2,$$

where we used that the integrals with integrand containing the product $\xi\xi_*$ vanish since F, G as well as $e^{-|\cdot|}$ are even functions.

With this ingredients we can prove the following theorem:

Theorem 3.8. *The fixed-point equation (3.29) has a positive solution $F \in \mathcal{B}$, i.e. satisfying*

$$\int_{\mathbb{R}} F(\xi)\,\mathrm{d}\xi = 1 \text{ and } \int_{\mathbb{R}} \xi^2 F(\xi)\,\mathrm{d}\xi \le 4.$$

Proof. In the following we show the existence of a solution to (3.29) by finding a fixed-point of the mapping (3.30), using *Schauder fixed-point theorem*.
From 1. and 3. one can easily deduce that $\mathcal{S}: \mathcal{B} \to \mathcal{B}$ holds. The continuity of the mapping $\mathcal{S}$ follows immediately from its integral representation.
Boundedness of $\mathcal{S}(\mathcal{B})$ follows from observation 1., while due to estimate 2. we can calculate for a set $A \subset \mathbb{R}$ and $F \in \mathcal{B}$

$$\int_A |\mathcal{S}(F)(\xi)|\,\mathrm{d}\xi \le |A|\|\mathcal{S}(F)\|_{L^\infty(\mathbb{R})} \le \frac{|A|}{2}\|F\|_{L^1(\mathbb{R})} \le \frac{|A|}{2},$$

which implies *uniform integrability* of the set $\mathcal{S}(\mathcal{B})$. Furthermore, due to the bounded variance 3. we are able to deduce that $\mathcal{S}(\mathcal{B})$ is *tight*. Due to the *Dunford-Pettis* criterion we obtain from the uniform integrability and tightness that $\mathcal{S}(\mathcal{B})$ is weakly relatively compact in $L^1(\mathbb{R})$. This concludes the proof, since we now have all ingredients for applying Schauder fixed-point theorem. □

Remembering the derivation of the fixed-point equation (3.29), its solution F can be seen as symmetric *approximate solution* to the stationary problem (3.27). Up to this point, we just have a formal approximation for symmetric equilibria in the small diffusion regime. The validity of this approximation remains an open problem.

3.4 Numerical Simulations

Discretization: The results of the preceding Section 3.3 will be illustrated by numerical simulations of the spatially homogeneous model (3.22). Discretization in velocity direction $\varphi \in \mathbb{T}^1$ is based on an equidistant grid

$$\varphi_k = \frac{(k-n)\pi}{n}, \qquad k = 0, \dots, 2n,$$

with an even number of grid points, guaranteeing that the grid is invariant under reversal collisions, i.e., with φ_k also $\varphi_k^{\downarrow} = \varphi_{k+n}$ is a grid point. Similarly, only those alignment collisions between discrete angles will be allowed, which produce post-collisional angles belonging to the grid.
Solutions of (3.22) are approximated at grid points by

$$f^n(t) := (f_0(t), \dots, f_{2n}(t)) \approx (f(\varphi_0, t), \dots, f(\varphi_{2n}, t)),$$

extended periodically by $f_{k+2n}(t) = f_k(t)$. We consider collision operator Q with collision kernel $b(\varphi, \varphi_*) = |\sin(\varphi - \varphi_*)|$ and rewrite it by splitting also the loss term into its alignment and reversal part, which results in the following representation of (3.2)

$$Q(f,f) = 2\int_{\mathbb{T}^{AL}_{\to\varphi}} b(\tilde{\varphi},\varphi_*)(\tilde{f}f_* - f\tilde{f}_*)d\varphi_* + \int_{\mathbb{T}^{REV}_{\varphi}} b(\varphi,\varphi_*)(f^{\downarrow}f_*^{\downarrow} - ff_*)d\varphi_*\,,$$

with $\tilde{\varphi} = 2\varphi - \varphi_*$, $\tilde{\varphi}_* = 2\varphi_* - \varphi$, before discretization. Note that in this form mass conservation is obvious since $b(\tilde{\varphi},\varphi_*) = b(\tilde{\varphi}_*,\varphi)$, and the grid is invariant under the map $(\varphi,\varphi_*) = (\varphi_k,\varphi_{k_*}) \mapsto (\tilde{\varphi},\tilde{\varphi}_*) = (\varphi_{2k-k_*},\varphi_{2k_*-k})$. Finally, we always choose n odd to avoid the angle $\pi/2$ between grid angles and, thus, the ambiguity between alignment and reversal collisions. Accordingly, the discrete representation of the collision operator is then of the form

$$Q^n(f^n,f^n)_k := \frac{2\pi}{n}\sum_{|k_*-k|<n/4} b_{2k-k_*,k_*}(f_{2k-k_*}f_{k_*} - f_kf_{2k_*-k}) + \frac{\pi}{n}\sum_{|k_*-k|>n/2} b_{k,k_*}(f_{k+n}f_{k_*+n} - f_kf_{k_*})\,,$$

with $b_{k,k_*} := b(\varphi_k,\varphi_{k_*})$. For the diffusion term we use the following finite difference discretization

$$\begin{aligned} f_k^{n''} &:= \frac{n^2}{\pi^2}(f_{k-1} - 2f_k + f_{k+1})\,, \quad k \notin \{0,2n\},\\ f_0^{n''} &:= \frac{n^2}{\pi^2}(f_{2n} - 2f_0 + f_1)\,,\\ f_{2n}^{n''} &:= \frac{n^2}{\pi^2}(f_{2n-1} - 2f_{2n} + f_0)\,. \end{aligned}$$

Combining this straightforwardly leads to the discrete model

$$\frac{df_k}{dt} = \mu f^{n''} + Q^n(f^n,f^n)_k\,.$$

Time discretization is done by using the *explicit Euler scheme*, such that the total mass is conserved by the discrete scheme, which has been implemented in MATLAB.
Simulations have been carried out with $n = 51$, the time stepsize Δt as well as the number of time steps are chosen accordingly. The solution f has been normalized with respect to the L^1-norm. Therefore, the value of the diffusion constant at the bifurcation point, μ^*, is the same for all of the following simulations and can be calculated explicitly (see (3.25))

$$\mu^* = \frac{1}{12\pi} \approx 0.0265.$$

Simulations in the bifurcation regime: Hereinafter we aim to illustrate the bifurcation result from Section 3.3.1 on one hand with simulations showing convergence to the uniform equilibirum f_0 for $\mu > \mu^*$ and convergence to the nonuniform equilibirum for $\mu < \mu^*$.
The plots show the distribution function f at three different times: Initial distribution at $t = 0$ (small dotted, red), at an intermediate time $t \in (0, t_{END})$ (dashed, blue) as well as close to equilibrium $t = t_{END}$ (solid line, black).
In Figure 3.2 we see the effect of different strong diffusion starting with randomly distributed initial conditions. On the left we chose $\mu = 0.02$ and performed 25000 time steps each of size $\Delta t = 0.01$. The solution converges to the nonuniform steady state with peaks centered around two unpredictable, but always opposite points. The plot on the right side shows simulations for a bigger diffusion constant, namely $\mu = 0.03$. After 2500 timesteps of size $\Delta t = 0.1$ the constant equilibrium is reached.

In Figure 3.3 one can see dynamics for different diffusion intensities starting with data close to the uniform equilibrium, where a small perturbation at a random point was added. On the left, again the choice $\mu = 0.02$ was made, which leads to convergence of the solution to the nonuniform equilibrium. This state was reached after 25000 timesteps of size $\Delta t = 0.01$. On the right side one can observe that with $\mu = 0.03$ diffusion is strong enough such that the solution converges to the constant steady state. 2500 time steps with size $\Delta t = 0.1$ were carried out.

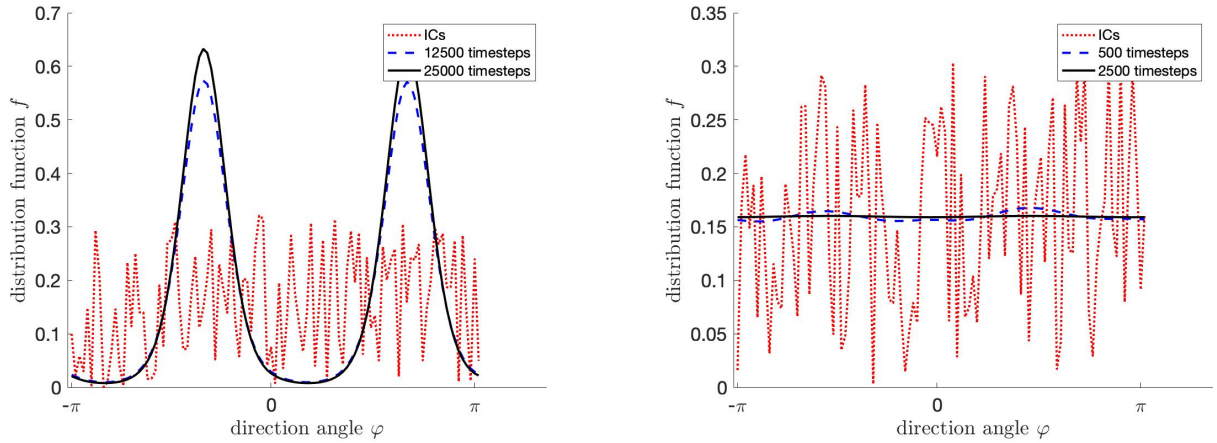

Figure 3.2: Random distributed initial conditions.
Left: With sufficiently small diffusivity ($\mu = 0.02$) the solution converges to the nonuniform equilibrium with peaks at predictable positions. *Right:* Under presence of strong diffusion ($\mu = 0.03$) the random initial distribution equals out to the constant steady state $f_0 = \frac{1}{2\pi}$.

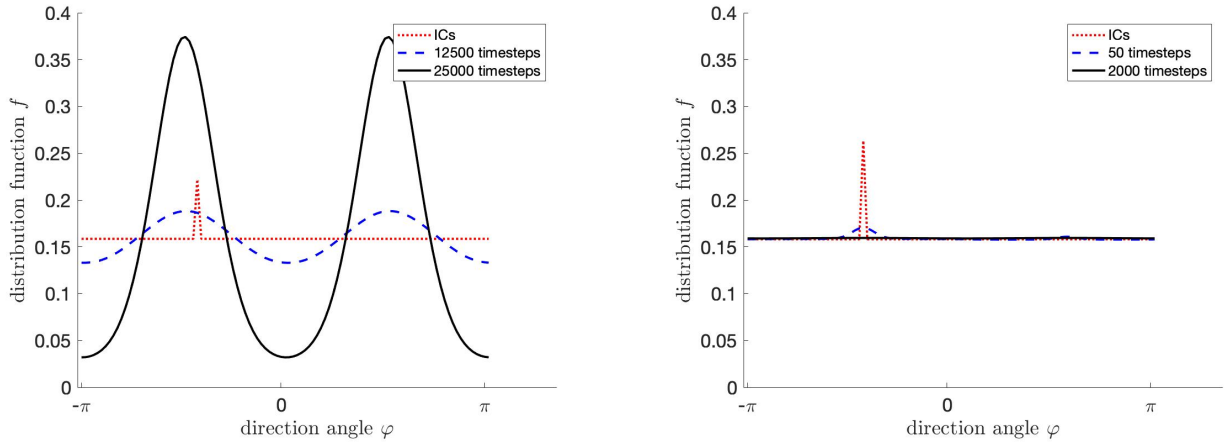

Figure 3.3: Uniform distributed initial condition, perturbed at a random point.
Left: Convergence to the symmetric nonuniform equilibrium for weak diffusion ($\mu = 0.02$). *Right:* Convergence to the uniform equilibrium for diffusion being strong enough ($\mu = 0.03$).

Simulations in the small diffusion regime: In the following, simulations are presented for very weak diffusion in velocity direction, mimicking the regime investigated in Section 3.3.2. The value for

diffusion constant was chosen as $\mu = 0.001$. For even smaller μ the necessity of numerical calculations with very expansive costs makes it unpractical. In our moderate small regime we could observe emergence of equally weighted peaks, even if staring with initial data very close to the nonuniform equilibrium, i.e. opposite peaks, but weighted differently (see especially, Figure 3.5). In Figures 3.4 and 3.4 we presented the simulation result in three different plots. In the up left corner the distribution function f is color coded w.r.t. the angle φ (vertical axis) and time t (horizontal axis). The graphic in the up right part shows f plotted against φ at three different times: Initial distribution at $t = 0$ (small dotted, red), at an intermediate time $t \in (0, t_{END})$ (dashed, blue) as well as close to equilibrium $t = t_{END}$ (solid line, black). The plot in the second row shows the masses in the positive $\|f\|_{L^1([0,\pi])}$ (dashed, red) and negative $\|f\|_{L^1([-\pi,0])}$ (small dotted, blue) part of the torus approaching each other with time. The black, solid, vertical lines indicate the times at which the graph of f is displayed in the up right corner of the figure.
In Figure 3.4 initial conditions of the form

$$f_I(\varphi) = \frac{2}{7\pi} \begin{cases} 1 & \text{for } \varphi \in [-3\pi/4, \pi/4] \\ 6 & \text{for } \varphi \in [\pi/4, 3\pi/4] \end{cases}$$

as well as diffusivity constant $\mu = 0.001$ were chosen. A number of 50000 timesteps with size $\Delta t = 0.1$ were performed. The solution approximates two equally weighted, smooth peaks around $-\frac{\pi}{2}$ and $\frac{\pi}{2}$. One can further observe that the concentration of angles due to the alignment part of the collision operator takes place on a faster time scale than the equalization of the masses of the emerging peaks. Moreover, we can conclude that the equalization of masses is only caused by the presence of diffusion, since velocity reversal doesn't have any effect in this case (see [31]).
Different from this, in Figure 3.5, one can observe that starting with initial conditions given by

$$f_I(\varphi) = \begin{cases} 1 & \text{for } \varphi = \frac{\pi}{2} \\ 7 & \text{for } \varphi = -\frac{3\pi}{4} \end{cases},$$

where mass is concentrated at two Diracs, not exactly opposite from each other, additionally to the diffusion, also this time with intensity $\mu = 0.001$ and the alignment also the reversal part of Q is acting. A number of 12500 timesteps of size $\Delta t = 0.01$ were performed. Again one can observe the solution converging to the symmetric equilibrium with peaks centered exactly opposite from each other.

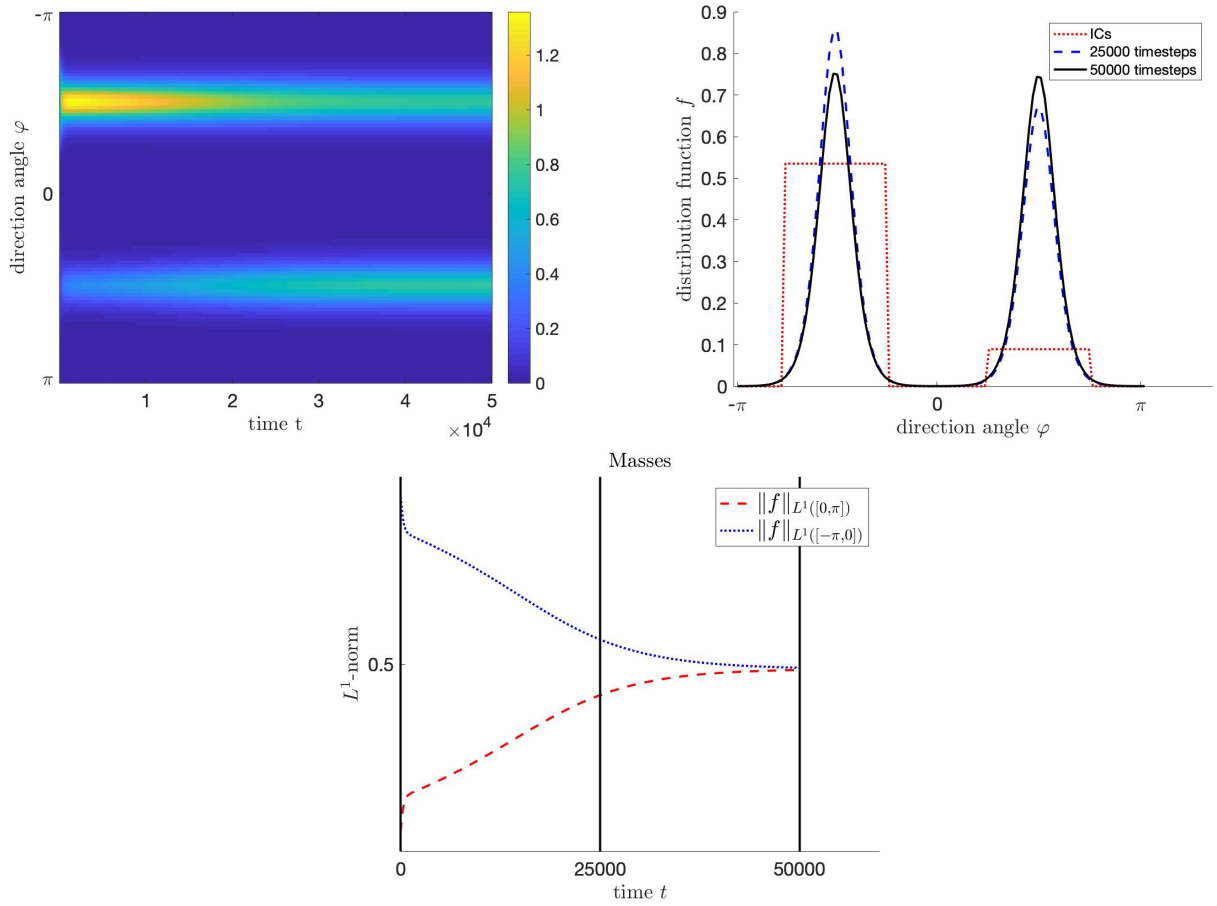

Figure 3.4: Initial conditions with different mass in $\mathbb{T}^1_+ := [-3\pi/4, -\pi/4]$ and $\mathbb{T}^1_- := [\pi/4, 3\pi/4]$, diffusion constant $\mu = 0.001$.
Up left: f color coded as a function of φ with respect to time. *Up right:* Distribution function plotted at three different times: Initial distribution at $t = 0$ (small dotted red), at $t = 25000$ (dashed blue) and at the end of the simulation at $t = 50000$ (solid, black). *Down:* Masses of f in the positive part of $\mathbb{T}^1$ (dashed, red) and in the negative part of $\mathbb{T}^1$ (small dotted, blue) plotted separately.

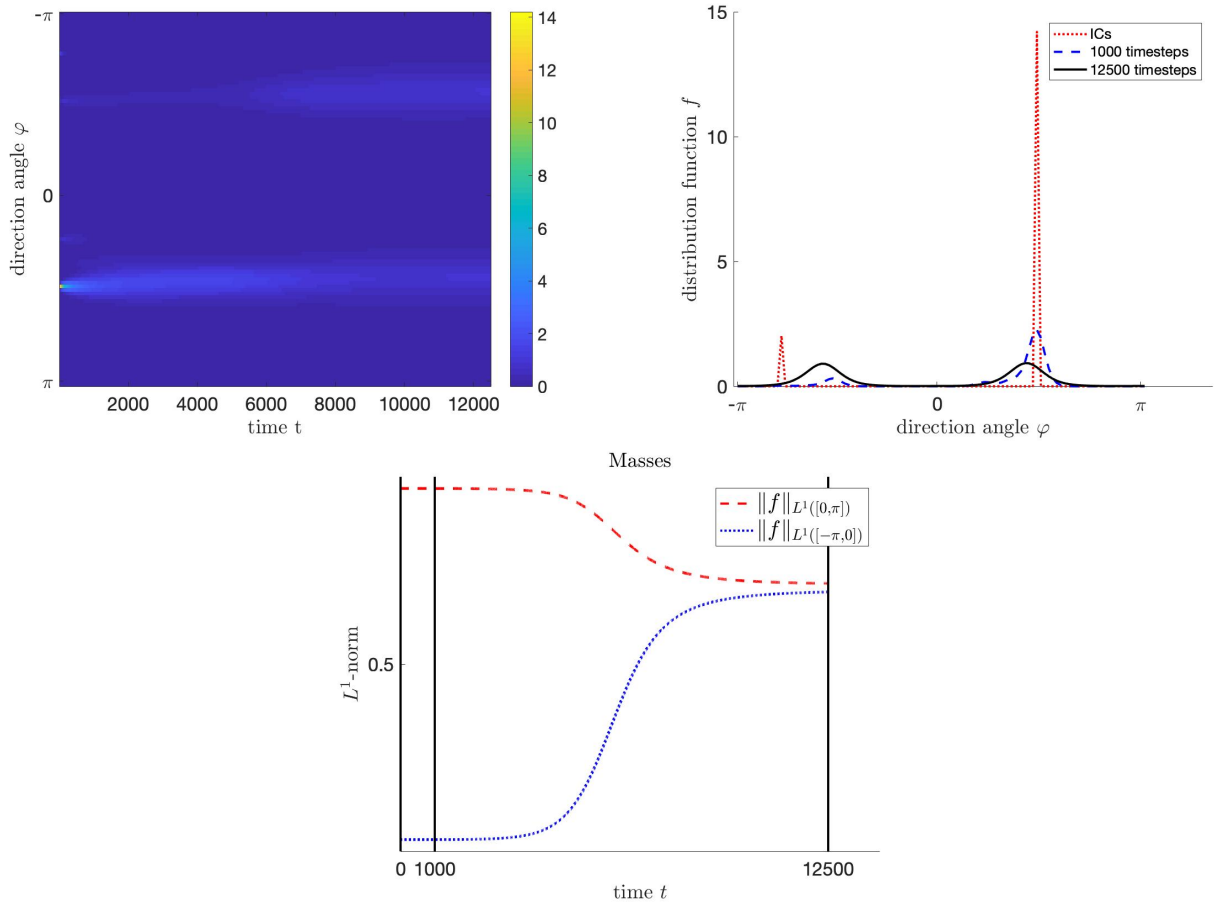

Figure 3.5: Initial conditions consisting of differently weighted Diracs concentrated at $-\frac{3\pi}{2}$ and $\frac{\pi}{2}$, diffusion constant $\mu = 0.001$.
Up left: f color coded as a function of φ with respect to time. *Up right:* Distribution function plotted at three different times: Initial distribution at $t = 0$ (small dotted, red), at $t = 100$ (dashed, blue) and at the end of the simulation at $t = 25000$ (solid, black). *Down:* Masses of f in the positive part of $\mathbb{T}^1$ (dashed, red) and in the negative part of $\mathbb{T}^1$ (small dotted, blue) plotted separately.

Remark 3.9. *These observations as well as the bifurcation analysis in Section 3.3 gives rise to the following conjecture, which already motivated the ansatz (3.28) in Section 3.3.2: We expect the solution always to converge to a symmetric equilibrium. In the case for sufficiently strong diffusion, it is the uniform equilibrium f_0, while for small diffusion it will be two smooth peaks, exactly with distance π apart from each other. To be more precise, we write f in the form $f = \rho_+ f_+ + \rho_- f_-$, i.e. splitting it up in its contributions on the positive and negative part of $\mathbb{T}^1$ with notation*

$$f_\pm(\varphi, t) := \frac{f(\varphi, t)}{\rho} \mathbb{1}_{\varphi \gtrless 0}(\varphi), \quad \text{and} \quad \rho_\pm(t) := \int_{\varphi \gtrless 0} f(\varphi, t)\, \mathrm{d}\varphi,$$

where we expect

$$|\rho_+(t) - \rho_-(t)| \to 0 \quad \text{for } t \to \infty.$$

This is due to interplay between the reversal operator and the diffusion. While the reversal collision operator has a symmetrizing effect (see Chapter 4), the diffusion distributes mass over the torus such

that the domain of the reversal operator is big enough. We aim to rigorously proof this conjecture by performing exponential asymptotics.

Bibliography

[1] R.J. Alonso, *Existence of global solutions to the Cauchy problem for the inelastic Boltzmann equation with near-vacuum data,* JSTOR 58 (2009), pp. 999–1022.

[2] R.J. Alonso, V. Bagland, Y. Cheng, B. Lods, *One-Dimensional Dissipative Boltzmann Equation: Measure Solutions, Cooling Rate, and Self-Similar Profile*, SIAM J. Math. Anal. (2018), 50, pp. 1278-1321.

[3] R. J. Alonso, and B. Lods, *Uniqueness and regularity of steady states of the Boltzmann equation for viscoelastic hard-spheres driven by a thermal bath.* Commun. Math. Sci. 11, 4 (2013), 851–906.

[4] K. Asano, S. Ukai, *On the Cauchy problem of the Boltzmann equation with a soft potential.* Publ. RIMS, Kyoto Univ. 18, 57-99 (1982).

[5] A. Baskaran, M.C. Marchetti, *Nonequilibrium statistical mechanics of self propelled hard rods,* J. Stat. Mech. 2010 (2010), P04019.

[6] E. Bertin, M. Droz, G. Gregoire, *Hydrodynamic equations for self-propelled particles: microscopic derivation and stability analysis,* J. Phys. A: Math. Theor. 42 (2006), 445001.

[7] D. Benedetto, M. Pulvirenti, On the one-dimensional Boltzmann equation for granular flows, M2AN 35 (2001), pp. 899–905.

[8] E. Ben-Naim, P.L. Krapivsky, *Alignment of rods and partition of integers,* Phys. Rev. E Stat. Nonlin. Soft Matter Phys. 73 (2006), 031109.

[9] A.V. Bobylev, C. Cercignani, *Self-Similar Asymptotics for the Boltzmann Equation with Inelastic and Elastic Interactions,* J. Stat. Phys. 110 (2003), pp. 333–375.

[10] A. V. Bobylev, J. A. Carrillo, I. Gamba, *On Some Properties of Kinetic and Hydrodynamic Equations for Inelastic Interactions*, J. Statist. Phys (2000), 98, pp. 743–773.

[11] E. Bertin, M. Droz, G. Gregoire, *Boltzmann and hydrodynamic description for self-propelled particles,* (2006) Phys. Rev. E 74 022101

[12] E. Bertin, M. Droz, G. Gregoire, *Hydrodynamic equations for self-propelled particles: microscopic derivation and stability analysis,* J. Phys. A: Math. Theor. 42 (2006), 445001.

[13] A. V. Bobylev, I. M. Gamba, V. A, Panferov, *Moment inequalities and high-energy tails for Boltzmann equations with inelastic interactions.* J. Statist. Phys. 116, 5-6 (2004), 1651–1682.

[14] L. Boltzmann, *Weitere Studien über das Wärmegleichgewicht unter Gasmolekülen,* Sitzungsberichte Akad. Wiss., Vienna, part II, 66 (1872), pp. 275–370.

[15] J. Carrillo, G. Toscani, *Contractive probability metrics and asymptotic behavior of dissipative kinetic equations*, Riv. Mat. Univ. Parma (7) 6 (2007), pp. 75–198.

[16] E. Carlen, M. C. Carvalho, P. Degond, B. Wennberg, *A Boltzmann model for rod alignment and schooling fish,* Nonlinearity 28 (2015), pp. 1783–1804.

[17] C. Cercignani, R. Illner, M. Pulvirenti, *The Mathematical Theory of Dilute Gases*, Springer-Verlag, New York, 1994.

[18] M. G. Crandall, P. H. Rabinowitz, *Bifurcation from simple eigenvalues*, Journal of Functional Analysis, 8, Issue 2, October 1971, pp 321–340.

[19] P. Degond, A. Frouvelle, G. Raoul, *Local stability of perfect alignment for a spatially homogeneous kinetic model,* J. Stat. Phys. 157 (2014), pp. 84–112.

[20] P. Degond, A. Manhart, H. Yu, *A continuum model of nematic alignment of self-propelled particles,* DCDS-B 22 (2017), pp. 1295–1327.

[21] P. Degond, A. Manhart, H. Yu, *An age-structured continuum model for myxobacteria,* M3AS 28 (2018), pp. 1737–1770.

[22] R. J. DiPerna and P. L. Lions, *On the Cauchy Problem for Boltzmann Equations: Global Existence and Weak Stability*, Annals of Mathematics, Second Series, 130, No. 2 (Sep., 1989), pp. 321-366

[23] J. Dolbeault, C. Mouhot, C. Schmeiser, *Hypocoercivity for linear kinetic equations conserving mass,* Trans. AMS 367 (2015), pp. 3807-3828.

[24] I.M. Gamba, V. Panferov & C. Villani, *On the Boltzmann Equation for Diffusively Excited Granular Media,* Communications in Mathematical Physics volume 246, pages503–541(2004)

[25] H. Grad, *Principles of the kinetic theory of gases.* In Handbuch der Physik, Bd. 12, Thermodynamik der Gase. Springer-Verlag, Berlin, 1958, pp. 205–294.

[26] H. Grad, *Asymptotic theory of the Boltzmann equation. II. In Rarefied Gas Dynamics*, (Proc. 3rd Internat. Sympos., Palais de l'UNESCO, Paris, 1962), Vol. I. Academic Press, New York, 1963, pp. 26–59.

[27] M. P. Gualdani, S. Mischler, and C. Mouhot, *Factorization for non-symmetric operators and exponential H-theorem.* http://hal.archives-ouvertes.fr/ccsd-00495786 (2013).

[28] I.M. Gamba, V. Panferov, C. Villani, *On the Boltzmann equation for diffusively excited granular media.* Commun. Math. Phys. 246, 503-541 (2004).

[29] P. Haff, *Grain flow as a fluid-mechanical phenomenon,* J. Fluid Mech. 134 (1983), pp. 401–30.

[30] D. Hilbert, *Begründung der kinetischen Gastheorie.* Math. Ann. 72, 4 (1912), 562–577.

[31] S. Hittmeir, L. Kanzler, A. Manhart, C. Schmeiser, *Kinetic modelling of colonies of myxobacteria,* Kinetic and Related Models 14, Number 1, (2021), pp. 1–24, doi:10.3934/krm.2020046

[32] J. Hodgkin, D. Kaiser, *Genetics of gliding motility in Myxococcus xanthus (Myxobacterales): two gene systems control movement,* Mol. Gen. Genet. 171 (1979), pp. 177–191.

[33] P.-E. Jabin, T. Rey, *Hydrodynamic limit of granular gases to pressureless Euler in dimension 1,* Quart. Appl. Math. 75 (2017), 155–179.

[34] Y. Jiang, O. Sozinova, M. Alber, *On modeling complex collective behavior in myxobacteria*, Adv. in Complex Syst. 9 (2006), pp. 353–367.

[35] S. Kaniel, M. Shinbrot, *The Boltzmann equation, uniqueness and local existence.* Commun. Math. Phys. 58, 65-84 (1978).

[36] O. E. Lanford, *Time evolution of large classical systems,* Lect. Notes Phys. 38 (1975), pp. 1–111.

[37] S. Mischler, C. Mouhot, *Cooling Process for Inelastic Boltzmann Equations for Hard Spheres,* Part II: Self-Similar Solutions and Tail Behavior, J. Stat. Phys. 124 (2006), pp. 703–746.

[38] S. Mischler, C. Mouhot, *Stability, convergence to self-similarity and elastic limit for the Boltzmann equation for inelastic hard spheres.* Comm. Math. Phys. 288, 2 (2009), 431–502.

[39] S. Mischler, C. Mouhot, *Stability, convergence to the steady state and elastic limit for the Boltzmann equation for diffusively excited granular media.* Discrete Contin. Dyn. Syst. 24, 1 (2009), 159–185.

[40] S. Mischler, C. Mouhot & M. Rodriguez Ricard, *Cooling Process for Inelastic Boltzmann Equations for Hard Spheres, Part I: The Cauchy Problem,* Journal of Statistical Physics volume 124, pages655–702(2006)

[41] G. Toscani, *Hydrodynamics from the dissipative Boltzmann equation,* in: G. Capriz, P.M. Mariano, P. Giovine (eds), Mathematical Models of Granular Matter, Lect. Notes in Math. 1937, Springer, Berlin–Heidelberg, 2008.

[42] I. Tristani, *Boltzmann equation for granular media with thermal force in a weakly inhomogeneous setting,* Journal of Functional Analysis, Volume 270, Issue 5, 2016, Pages 1922-1970, SSN 0022-1236.

[43] S. Ukai, *On the existence of global solutions of mixed problem for non-linear Boltzmann equation.* Proc. Japan Acad. 50 (1974), 179–184.

[44] T. Vicsek, A. Czirok, E. Ben-Jacob, I. Cohen, and O. Shochet. *Novel type of phase transition in a system of self-driven particles.* Phys. Rev. Lett., 75(6):12261229, 1995.

[45] C. Villani, *Hypocoercivity,* Mem. Amer. Math. Soc., 202(950): iv+141, 2009

4 Reversal Collision Dynamics

Symmetry is what we see at a glance; based on the fact that there is no reason for any difference.

Blaise Pascal

Contents

4.1 Introduction **81**
4.2 Properties of the collision operator **82**
4.3 Asymptotic behavior **83**
4.4 Reversal collisions on the torus $\mathbb{T}^1$ **90**
4.5 Numerical simulations **91**

This chapter contains results of an ongoing collaboration with A. Frouvelle and C. Schmeiser.

4.1 Introduction

We study *reversal collision dynamics* on a *compact metric space* $\mathcal{S}$, which is endowed with a symmetric structure that allows to define an *inclusion* $x^\downarrow$ for all $x \in \mathcal{S}$ as well as a symmetric measure dx. Further, we assume that $B_r(x) \subset B_R(y)$ implies $d(x,y) \geq R - r$, for $0 < r < R$. For a subset $\mathcal{T} \subset \mathcal{S}$ we define $\mathcal{T}^\downarrow := \left\{ x^\downarrow \in \mathcal{S} : \, x \in \mathcal{T} \right\}$. The dynamics are given by the following kinetic equation

$$\begin{aligned} &\partial_t f = \int_{x* \in \mathcal{C}[x]} b(x, x_*) \left(f^\downarrow f_*^\downarrow - f f_* \right) dx_* =: Q_{REV}(f,f), \quad x \in \mathcal{S},\, t > 0 \\ &f(x,0) = f_I(x), \quad x \in \mathcal{S}, \end{aligned} \tag{4.1}$$

which describes the evolution of the distribution function $f = f(x,t)$ of the dynamical states of individual particles $x \in \mathcal{S}$, undergoing reversal collisions

$$(x, x_*) \longrightarrow (x^\downarrow, x_*^\downarrow).$$

As usual in kinetic theory, we use the notation $f^\downarrow = f(x^\downarrow, t)$ and $f_* = f(x_*, t)$. As the *set of collision partners* for $x \in \mathcal{S}$ we define

$$\mathcal{C}[x] := \left\{ x_* \in \mathcal{S} : \, x_* \in B_\alpha(x^\downarrow) \right\},$$

for a constant $\alpha > 0$. Obviously it holds

$$x^\downarrow \in \mathcal{C}[x], \;\text{ and }\; \mathcal{C}[x^\downarrow] = \mathcal{C}[x]^\downarrow.$$

Although we allow the *collision kernel* b be quite general, we have to make the following symmetry assumption

$$b(x, x_*) = b(x_*, x) = b(x^\downarrow, x_*) = b(x_*^\downarrow, x),$$

as well as boundedness from below away from zero, i.e. $b(x, x_*) \geq b_0 > 0$, for all $x, x_* \in \mathcal{S}$. Further, we suppose normalization of the initial mass, i.e.

$$\int_{\mathcal{S}} f_I \, \mathrm{d}x = 1.$$

Remark 4.1. *For the case $\mathcal{S} = \mathbb{T}^1$, $d(\cdot, \cdot)$ defining the distance between two angles on the torus and $\alpha = \frac{\pi}{2}$ this simplifies to*

$$\partial_t f = \int_{d(\varphi, \varphi_*) > \frac{\pi}{2}} b(\varphi, \varphi_*) \left(f^\downarrow f_*^\downarrow - f f_* \right) d\varphi_*, \tag{4.2}$$

which corresponds to the spatially homogeneous kinetic model for myxobacteria (2.16) (Chapter 2), where just reversal collisions between bacteria are considered.

4.2 Properties of the collision operator

In this section, we summarize results directly obtained from the structure of the collision operator Q_{REV}.

Weak formulation and conservation laws: For a suitable test-function $\psi = \psi(x)$ the *weak formulation* of the reversal-collision operator has the from

$$\int_{\mathcal{S}} Q_{REV}(f, f)\psi \, \mathrm{d}x = \frac{1}{2} \int_{\mathcal{S}} \int_{\mathcal{C}[x]} b(x, x_*) f f_* \left(\psi^\downarrow + \psi_*^\downarrow - \psi - \psi_* \right) \mathrm{d}x_* \mathrm{d}x. \tag{4.3}$$

Choosing $\psi \equiv 1$ in (4.3) we immediately obtain *mass conservation*, i.e.:

$$\int_{\mathcal{S}} f \, \mathrm{d}x = \int_{\mathcal{S}} f_I \, \mathrm{d}x \equiv 1.$$

For taking $\psi(x) = \delta(x - x_0) + \delta(x^\downarrow - x_0)$ with $x_0 \in \mathcal{S}$ fixed but arbitrary, we can further observe easily that the right-hand-side of (4.3) vanishes.

At each point $x \in \mathcal{S}$ we define the average $\tilde{f}$ of f at x and its opposite $x^\downarrow$ by

$$\tilde{f}(x) := \frac{f(x) + f(x^\downarrow)}{2},$$

which is symmetric by definition. Further, if we choose $\psi(x_*) = \frac{1}{2} \left(\delta(x_* - x) + \delta(x_*^\downarrow - x) \right)$ in (4.3) we immediately observe that

$$\partial_t \tilde{f} = \partial_t \int_{\mathcal{S}} f\psi \, \mathrm{d}x_* = \int_{\mathcal{S}} Q_{REV}(f, f)\psi \, \mathrm{d}x_* = 0,$$

and therefore time-independence of $\tilde{f}$, which implies

$$\tilde{f} = \frac{f_I + f_I^\downarrow}{2}.$$

This also yields

$$\int_{\mathcal{S}} \tilde{f}\, dx = \frac{1}{2}\left(\int_{\mathcal{S}} f\, dx + \int_{\mathcal{S}} f^{\downarrow}\, dx\right) = 1.$$

By rewriting the collision operator we obtain for the time evolution of f in terms of $\tilde{f}$

$$\partial_t f = -2\int_{\mathcal{C}[x]} b(x, x_*)\Big(\tilde{f}_*(f - \tilde{f}) + \tilde{f}(f_* - \tilde{f}_*)\Big)\, \mathrm{d}x_*. \tag{4.4}$$

We further observe that this describes a linear problem for $f - \tilde{f}$, since the average $\tilde{f}$ is a function fully determined by the initial conditions. The evolution of $g := f - \tilde{f}$ is therefore given by

$$\partial_t g = -2\int_{\mathcal{C}[x]} b(x, x_*)\Big(\tilde{f}_* g + \tilde{f} g_*)\Big)\, \mathrm{d}x_* =: Q^L_{REV} g. \tag{4.5}$$

Existence and uniqueness of solutions: Existence and uniqueness in $L^1(\mathcal{S})$ will be shown by the *Picard theorem* under the additional assumption of a bounded collision kernel, since then the collision operator can be shown to be Lipschitz continuous.

Theorem 4.2. *Let $b \in L^\infty(\mathcal{S}\times\mathcal{S})$ and $f_I \in L^1(\mathcal{S})$. Then (4.1) has a unique global solution $f \in C([0,\infty), L^1_+(\mathcal{S}))$.*

Proof. We use the linear representation (4.5) of the collision operator. Let therefore $g_1, g_2 \in L^1(\mathcal{S})$. Straight forward estimation gives:

$$\begin{aligned}\|Q^L_{REV} g_1 - Q^L_{REV} g_2\|_{L^1(\mathcal{S})} &\le -2\int_{\mathcal{S}}\int_{\mathcal{C}[x]} b(x, x_*)|\tilde{f}_* g_1 + \tilde{f} g_{1*} - \tilde{f}_* g_2 - \tilde{f} g_{2_*}|\, dx_* dx \\ &\le 2\|b\|_{L^\infty(\mathcal{S}\times\mathcal{S})}\|g_1 - g_2\|_{L^1(\mathcal{S})},\end{aligned}$$

hence global Lipschitz continuity of Q^L_{REV}. Therefore a unique local solution exists by *Picard iteration*. Nonnegativity and conservation of the mass are obvious, the latter implying global existence of a solution g to (4.5) and hence existence of a solution f for the original problem (4.1). □

4.3 Asymptotic behavior

In order to get information about the asymptotic behavior of the solution f to (4.1) we make the following preliminary observations:
We first denote by $\mathcal{K}$ the support of $\tilde{f}$ regarding the definition coming from measure theory

$$\mathcal{K} := \operatorname{supp}(\tilde{f}) := \left\{x \in \mathcal{S} : \int_{B_\varepsilon(x)} \tilde{f}\, dx > 0,\ \forall \varepsilon > 0\right\},$$

which is compact, since it is a closed subspace of the compact space $\mathcal{S}$. We further define

$$h(x) := \frac{f(x) - \tilde{f}(x)}{\tilde{f}(x)}, \quad \text{for a.e. } x \in \mathcal{K} \tag{4.6}$$

and notice that $h \in [-1, 1]$ is bounded a.e. and hence well-defined in $L^1(\mathcal{S})$. Moreover, h fulfills the important property

$$\int_{\mathcal{S}} h\tilde{f}\, dx = 0.$$

The normalized quadratic distance from the average is then defined as

$$\mathcal{H}[f] = \frac{1}{2}\int_{\mathcal{S}} h^2 \tilde{f}\, dx = \frac{1}{2}\int_{\mathcal{S}}\int_{\mathcal{S}} \tilde{f}\tilde{f}'(h-h')^2\, dx'dx. \tag{4.7}$$

Computing its time-derivative, we obtain using (4.4)

$$\begin{aligned}\frac{\mathrm{d}}{\mathrm{d}t}\mathcal{H}[f] &= -2\int_{\mathcal{S}} h \int_{\mathcal{C}[x]} b(x,x_*)\left((f-\tilde{f})\tilde{f}_* + (f_*-\tilde{f}_*)\tilde{f}\right)\, dx_*dx \\ &= -2\int_{\mathcal{S}}\int_{\mathcal{C}[x]} b(x,x_*)h(h+h_*)\tilde{f}\tilde{f}_*\, dx_*dx \\ &= -\int_{\mathcal{S}}\int_{\mathcal{C}[x]} b(x,x_*)(h+h_*)^2\tilde{f}\tilde{f}_*\, dx_*dx =: -\mathcal{D}[f],\end{aligned} \tag{4.8}$$

where the last equality is due to symmetry. From here we can see that

$$\mathcal{D}[f] = 0 \quad \Leftrightarrow \quad h(x) + h(x_*) = 0, \quad \text{for a.e. } x, x_* \in \mathcal{K} \text{ s.t. } x_* \in \mathcal{C}[x], \tag{4.9}$$

which will be our equilibrium condition. We further notice that $\mathcal{H}$ is *coercive*. Indeed, due to Jensen inequality we have

$$\mathcal{H}[f] \geq \frac{1}{2}\|f-\tilde{f}\|^2_{L^1(\mathcal{S})}. \tag{4.10}$$

General framework for cells on $\mathcal{S}$: We suppose to have a finite covering of $\mathcal{S}$ by measurable subsets $\{\mathcal{T}_k\}_k$ and by $\rho_k := \int_{\mathcal{T}_k}\tilde{f}\,dx$ we denote their associated masses w.r.t. $\tilde{f}$.

Definition 4.3. *1. Let $\mathcal{T} \subset \mathcal{S}$, then*

$$\mathcal{C}[\mathcal{T}] := \{x_* \in \mathcal{S} : x_* \in B_\alpha(x^\downarrow), \forall x \in \mathcal{T}\} = \bigcap_{x\in\mathcal{T}} \mathcal{C}[x]$$

defines the set of common collision partners *of all elements in $\mathcal{T}$.*

2. We say that two subsets $\mathcal{T}_j$ and $\mathcal{T}_k$ are linked*, iff*

$$\rho_k, \rho_j, \rho^*_{j,k} > 0, \quad \text{where } \rho^*_{j,k} := \int_{\mathcal{C}[\mathcal{T}_j\cup\mathcal{T}_k]} \tilde{f}\, dx.$$

We want to note that if two subsets are linked, their set of common collision partners is of positive mass. This relation defines a *finite graph* $\mathcal{G} = \{\mathcal{V}, \mathcal{E}\}$, with vertices $\mathcal{V} := \{\mathcal{T}_k : \rho_k > 0\}_k$ and edges $\mathcal{E} := \{(\mathcal{T}_j, \mathcal{T}_k) : \mathcal{T}_j \text{ and } \mathcal{T}_k \text{ are linked.}\}$. Furthermore, we note the important property

$$\int_{\mathcal{T}_j\cup\mathcal{T}_k}\int_{\mathcal{T}^*_{j,k}} (h+h_*)^2\tilde{f}\tilde{f}_*\, dx_*dx \leq \int_{\mathcal{T}_j\cup\mathcal{T}_k}\int_{x_*\in\mathcal{C}[x]} (h+h_*)^2\tilde{f}\tilde{f}_*\, dx_*dx, \tag{4.11}$$

with $\mathcal{T}^*_{j,k} := \mathcal{C}[\mathcal{T}_j \cup \mathcal{T}_k]$. With this ingredient, we are able to proof the following theorem:

Theorem 4.4. *We suppose to have a covering $\{\mathcal{T}_k\}_k$ of $\mathcal{S}$ such that the graph $\mathcal{G}$ defined by this covering is connected. Then there exists a constant $c > 0$ such that we have exponential decay of $\mathcal{H}$ along the solution f to (4.1)*

$$\mathcal{H}[f(\cdot,t)] \leq e^{-ct}\mathcal{H}[f_I].$$

Proof. By splitting the integration domain $\mathcal{S}\times\mathcal{S}$ regarding the subsets $\{\mathcal{T}_k\}_k$, we rewrite (4.7), i.e.

$$\mathcal{H}[f] \le \sum_{j,k} \frac{1}{2}\int_{\mathcal{T}_j}\int_{\mathcal{T}_k} \tilde{f}\tilde{f}'(h-h')^2\,dx_*dx =: \frac{1}{2}\sum_{j,k}\mathcal{H}_{j,k}[f]$$

and estimate each component $\mathcal{H}_{j,k}[f]$ separately. Since $\mathcal{T}_j$ and $\mathcal{T}_k$ are connected, we find a path $\{j=i_0,i_1,\dots,i_n=k\}$ such that $\mathcal{T}_{i_{l-1}}$ and $\mathcal{T}_{i_l}$ are linked for $1\le l\le n$. We write $\mathcal{H}_{j,k}[f]$ as *telescopic sum* in l:

$$\begin{aligned}\mathcal{H}_{j,k}[f] &= \frac{1}{2}\int_{\mathcal{T}_{i_0}}\int_{\mathcal{T}_{i_n}} \tilde{f}_{i_0}\tilde{f}_{i_n}\left(\sum_{l=1}^{n}\left(h_{i_{l-1}}-h_{i_l}\right)\right)^2 dx_{i_0}dx_{i_n} \\ &\le \frac{n}{2}\int_{\mathcal{T}_{i_0}}\int_{\mathcal{T}_{i_n}} \tilde{f}_{i_0}\tilde{f}_{i_n}\sum_{l=1}^{n}\left(h_{i_{l-1}}-h_{i_l}\right)^2 dx_{i_0}dx_{i_n},\end{aligned} \tag{4.12}$$

where we use the notation h_{i_l}, f_{i_l} for h resp. f evaluated at a points in $\mathcal{T}_{i_l}$. We estimate for $1\le l\le n$

$$\left(h_{i_{l-1}}-h_{i_l}\right)^2 \le 2\left((h_{i_{l-1}}+h^*_{i_{l-1},i_l})^2+(h_{i_l}+h^*_{i_{l-1},i_l})^2\right), \tag{4.13}$$

where we write $h^*_{i_{l-1},i_l}$ for h evaluated at points in $\mathcal{T}^*_{i_{l-1},i_l}$. We multiply (4.13) now with $\tilde{f}$ evaluated at $x_{i_{l-1}}\in\mathcal{T}_{i_{l-1}}$, $x_{i_l}\in\mathcal{T}_{i_l}$ and $x_*\in\mathcal{T}^*_{i_{l-1},i_l}$ before integrating over $\mathcal{T}_{i_{l-1}}\times\mathcal{T}_{i_l}\times\mathcal{T}^*_{i_{l-1},i_l}$ and obtain, by noting that $\rho^*_{i_{l-1},i_l}>0$ since $\mathcal{T}_{i_{l-1}}$ and $\mathcal{T}_{i_l}$ are linked,

$$\int_{\mathcal{T}_{i_{l-1}}\times\mathcal{T}_{i_l}}(h_{i_{l-1}}-h_{i_l})^2\tilde{f}_{i_{l-1}}\tilde{f}_{i_l}\,dx_{i_{l-1}}dx_{i_l} \le 2\frac{\rho_{i_{l-1}}-\rho_{i_l}}{\rho^*_{i_l,i_{l-1}}}\int_{x\in\mathcal{T}_{i_l}\cup\mathcal{T}_{i_{l-1}}}\int_{x_*\in\mathcal{T}^*_{i_{l-1},i_l}}(h+h_*)^2\tilde{f}\tilde{f}_*\,dx_*dx.$$

Using (4.11) we can further estimate

$$\int_{\mathcal{T}_{i_{l-1}}\times\mathcal{T}_{i_l}}(h_{i_{l-1}}-h_{i_l})^2\tilde{f}_{i_{l-1}}\tilde{f}_{i_l}\,dx_{i_{l-1}}dx_{i_l} \le 2\frac{\rho_{i_{l-1}}-\rho_{i_l}}{\rho^*_{i_l,i_{l-1}}}\int_{\mathcal{T}_{i_l}\cup\mathcal{T}_{i_{l-1}}}\int_{x_*\in\mathcal{C}[x]}(h+h_*)^2\tilde{f}\tilde{f}_*\,dx_*dx.$$

If we now multiply (4.12) by $\tilde{f}$ evaluated at all the points x_{i_l} for $1\le l\le n$ and using the last inequality, we obtain

$$\begin{aligned}\left(\prod_{m=1}^{n}\rho_{i_m}\right)\mathcal{H}_{j,k}[f] &\le n\sum_{l=1}^{n}\int_{\prod_{m=0}^{n}\mathcal{T}_{i_l}}\left(\prod_{m=1}^{n}\tilde{f}_{i_m}\right)(h_{i_{l-1}}-h_{i_l})^2\prod_{m=0}^{n}dx_{i_m} \\ &\le n\sum_{l=1}^{n}\frac{\prod_{m\neq i_{l-1},i_l}\rho_{i_m}(\rho_{i_{l-1}}+\rho_{i_l})}{\rho^*_{i_l,i_{l-1}}}\int_{\mathcal{T}_{i_l}\cup\mathcal{T}_{i_{l-1}}}\int_{x_*\in\mathcal{C}[x]}(h+h_*)^2\tilde{f}\tilde{f}_*\,dx_*dx.\end{aligned}$$

The desired result is obtained by combining this estimate with (4.8), using $b>b_0$ and performing Gronwall's estimate. □

We now aim to use this abstract result to prove exponential convergence to equilibrium for our solution f to (4.1). In order to provide the setting needed for Theorem 4.4 and characterize the equilibrium we make the following definition.

Definition 4.5. *1. We say x and y are* connected *and write*

$$x\longleftrightarrow y :\Leftrightarrow \exists x_*\in\mathcal{K}\quad s.t\quad x*\in\mathcal{C}[x]\cap\mathcal{C}[y].$$

This relation defines the graph $\Gamma=(\mathcal{V},\mathcal{E})$, where $\mathcal{V}=\mathcal{K}$ and the edges given by $E:=\{(x,y)\in\mathcal{K}\times\mathcal{K}:\ x\longleftrightarrow y\}$

2. *Let $\gamma > 0$ and $x, y \in \mathcal{K}$. We say x and y are* γ-connected *and write*

$$x \longleftrightarrow_\gamma y \quad :\Leftrightarrow \exists x_* \in \mathcal{K} : \; B_\gamma(x_*) \subset \mathcal{C}[x] \cap \mathcal{C}[y].$$

Also this relation defines a graph $\Gamma^\gamma = \{V, E^\gamma\}$ associated to the initial conditions with vertices $V := \mathcal{K}$ and edges $E^\gamma := \{(x, y) \in \mathcal{K} \times \mathcal{K} : \; x \longleftrightarrow_\gamma y\}$.

Looking at the dissipation $\mathcal{D}$ and at the equilibrium condition (4.9) we can make the following observation

Lemma 4.6. *If $\mathcal{D}[f] = 0$, then h is a.e. constant on connected components of Γ.*

Proof. Assume $x_j \longleftrightarrow x_k$, then by definition $\exists \; x_* \in \mathcal{K}$ s.t. $x_* \in \mathcal{C}[x_j] \cap \mathcal{C}[x_k]$, which together with (4.9) implies

$$h(x_j) - h(x_k) = h(x_j) + h(x_*) - h(x_*) - h(x_k) = 0, \quad \text{almost surely.}$$

□

The graph associated to the initial conditions is connected: We assume that $\exists \gamma > 0$ such that Γ^γ is connected. We choose a finite covering of $\mathcal{S}$ by $\{\mathcal{T}_k\}_{1 \le k \le n}$ with $\mathcal{T}_k := B_{\gamma/2}(x_k)$, with $x_k \in \mathcal{K}$ such that $x_1, \dots, x_n$ is a connected subgraph of Γ^γ. This is possible by first choosing a finite covering, which can be done since $\mathcal{K}$ is compact, and then adding possibly missing connecting paths.

Lemma 4.7. *If $x_j \longleftrightarrow_\gamma x_k$ then $\mathcal{T}_j$ and $\mathcal{T}_k$ are linked.*

Proof. Let $x_j \longleftrightarrow_\gamma x_k$, therefore $\exists x_* \in \mathcal{K}$ with $B_\gamma(x_*) \subset B_\alpha(x_j^\downarrow) \cap B_\alpha(x_k^\downarrow)$. Let $x \in \mathcal{T}_j \cup \mathcal{T}_k$. W.l.o.g. assume $x \in \mathcal{T}_j = B_{\gamma/2}(x_j)$. For any $y \in B \in B_\gamma(x_*)$ we have

$$d(x^\downarrow, y) \le d(y, x_*) + d(x_*, x_j^\downarrow) + d(x_j^\downarrow, x^\downarrow) = d(y, x_*) + d(x_*, x_j^\downarrow) + d(x_j, x) < \frac{\gamma}{2} + (\alpha - \gamma) + \frac{\gamma}{2},$$

which implies $B_{\gamma/2}(x_*) \subset C[x]$ and therefore

$$B_{\gamma/2}(x_*) \subset C[\mathcal{T}_j \cup \mathcal{T}_k].$$

The claim follows by noticing that the mass of $B_{\gamma/2}(x_*)$ is positive, since $x_* \in \mathcal{K}$. □

As a direct consequence from the above lemma and Theorem 4.4 and the coercivity property of the entropy (4.10) we can state the following Corollary:

Corollary 4.8. *Assume that $\exists \gamma > 0$ such that the graph Γ^γ defined in Definition 4.5 is connected. Then $\mathcal{H}$ defined as in (4.7) decays exponentially along solutions f to (4.1), i.e.*

$$\mathcal{H}[f] \le \mathcal{H}[f_I] e^{-ct},$$

for a constant $c > 0$, which implies exponential decay of f to the symmetric equilibrium $\tilde{f}$, i.e.

$$\|f - \tilde{f}\|_{L^1(\mathcal{S})} \le \sqrt{2\mathcal{H}[f_I]} e^{-ct/2}, \quad t > 0.$$

The graph associated to the initial conditions has more connected components: Since $\mathcal{S}$ and therefore, since it is closed, also $\mathcal{K}$ is compact, Γ form Definition 4.5, 1.) has a finite number of connected components $N \geq 1$, denoted by $\{\Gamma^i\}_{i\in\{1,\dots,N\}}$ with their corresponding set of vertices $\mathcal{V}^i$. We make the following observations:

Lemma 4.9. *For any $x, y \in \mathcal{K}$ it holds*

$$x \longleftrightarrow y \;\Leftrightarrow\; x^{\downarrow} \longleftrightarrow y^{\downarrow}.$$

Proof. Regarding Definition 4.5 ct that $\exists x* \in \mathcal{K}$ s.t. $x_* \in B_\alpha(x^{\downarrow}) \wedge x_* \in B_\alpha(y^{\downarrow})$ implies due to symmetry $x_*^{\downarrow} \in B_\alpha(x) \wedge x_*^{\downarrow} \in B_\alpha(y)$, which implies $x^{\downarrow} \longleftrightarrow y^{\downarrow}$, since also $x*^{\downarrow} \in \mathcal{K}$. □

Lemma 4.10. *Let Γ^i be a connected component of Γ and $x \in \mathcal{V}^i$ arbitrary. Let $\Gamma^{i\downarrow}$ be the component which contains $x^{\downarrow}$. Then $y^{\downarrow} \in \mathcal{V}^{i\downarrow}$ for all $y \in \mathcal{V}^i$.*

Proof. Since $x, y \in \mathcal{V}^i$ there exists a connecting path $x = x_{i_0}, \dots, x_{i_n} = y$ with $x_{i_{l-1}} \longleftrightarrow x_{i_l}$, for $l \in \{1, \dots, n\}$. This implies due to Lemma 4.9 $x^{\downarrow}_{i_{l-1}} \longleftrightarrow x^{\downarrow}_{i_l}$, for $l \in \{1, \dots, n\}$, with which we found a path connecting $x^{\downarrow}$ and $y^{\downarrow}$. □

Lemma 4.11. *For all $x \in \mathcal{V}^i$ it holds that $\mathcal{C}[x] \cap \mathcal{V}^j = \emptyset$, whenever $\Gamma^j \neq \Gamma^{i\downarrow}$.*

Proof. Assume $\exists z \in \mathcal{C}[x] \cap \mathcal{V}^j$. By definition of $\mathcal{C}[x]$ this implies $z \in B_\alpha(x^{\downarrow})$, which leads to $x^{\downarrow} \longleftrightarrow z$, which is a contradiction. □

This last observation implies that elements in $\mathcal{V}^i$ only interact with elements of $\mathcal{V}^{i\downarrow}$. Therefore, for $x_i \in \mathcal{V}^i$, our model (4.1) reads

$$\partial_t f_i = \int_{\mathcal{V}^{i\downarrow} \cap \mathcal{C}[x_i]} b(x_i, x*) \left(f_i^{\downarrow} f_*^{\downarrow} - f_i f_* \right) dx_*.$$

By choosing $\psi \equiv \mathbb{1}_{\mathcal{V}^i}$ in (4.3) one can see easily that mass is conserved in each component. We use the following notation

$$\rho_i := \int_{\mathcal{V}^i} f \, dx, \quad \rho_i^{\downarrow} := \int_{\mathcal{V}^{i\downarrow}} f \, dx, \quad i \in \{1, \dots, N\}. \tag{4.14}$$

Obviously $\sum_{i=1}^N \rho_i = 1$ has to hold. Further, we have

$$\int_{\mathcal{V}^i} \tilde{f} \, dx = \int_{\mathcal{V}^{i\downarrow}} \tilde{f} \, dx = \frac{\rho_i + \rho_i^{\downarrow}}{2}. \tag{4.15}$$

Considering Lemma 4.6, we see that the dissipation $\mathcal{D}$ is already zero a.e., if

$$f(x) = (1 + c_i)\tilde{f}(x), \quad x \in \mathcal{V}^i, \quad i \in \{1, \dots, N\}, \tag{4.16}$$

for constants $c_i \in \mathbb{R}$, which gives us the candidate for the equilibrium. For the case $\Gamma^i = \Gamma^{i\downarrow}$ we have $c_i = -c_i = 0$ and we are in the one-component case like in the last section. Using (4.14) and (4.15), we obtain $c_i = -c_i^{\downarrow} = \frac{\rho_i - \rho_i^{\downarrow}}{\rho_i + \rho_i^{\downarrow}}$, where we again use the $\downarrow$-notation for the quantities corresponding to the opposite connected component. In order to construct a suitable Lyapunov functional for the more-component case we precede analogous to the two-component case. We first define

$$h_i(x) := \frac{1}{\tilde{f}(x)} \left(f(x) - 2\frac{\rho_i}{\rho_i + \rho_i^{\downarrow}} \tilde{f}(x) \right), \quad \text{for } x \in \mathcal{V}_i, \quad i \in \{1, \dots, N\},$$

which can also be written in terms of h (4.6)

$$h(x) = h_i(x) + \frac{\rho_i - \rho_i^{\downarrow}}{\rho_i + \rho_i^{\downarrow}}, \quad \text{for } x \in \mathcal{V}^i.$$

The normalized quadratic distance from the equilibrium (4.16) w.r.t. each component of Γ is then defined as

$$\bar{\mathcal{H}}[f] = \sum_{i=1}^{N} \mathcal{H}_i[f],$$

with

$$\mathcal{H}_i[f] := \frac{1}{2} \int_{\mathcal{V}^i} h_i^2 \tilde{f} \, \mathrm{d}x. \tag{4.17}$$

Computing its time-derivative we obtain using (4.4)

$$\begin{aligned}
\frac{\mathrm{d}}{\mathrm{d}t}\mathcal{H}_i[f] &= \int_{\mathcal{V}^i} h_i \partial_t f \, \mathrm{d}x = -2 \int_{\mathcal{V}^i} \int_{\mathcal{V}^{i\downarrow} \cap \mathcal{C}[x]} b(x, x_*) \left(\tilde{f}_*(f - \tilde{f}) + \tilde{f}(f_* - \tilde{f}_*) \right) h_i \, dx_* dx \\
&= -2 \int_{\mathcal{V}^i} \int_{\mathcal{V}^{i\downarrow} \cap \mathcal{C}[x]} b(x, x_*) \left(\tilde{f}_*(f - \tilde{f}) + \tilde{f}(f_* - \tilde{f}_*) \right) \left(h - \frac{\rho_i - \rho_i^{\downarrow}}{\rho_i + \rho_i^{\downarrow}} \right) dx_* dx.
\end{aligned}$$

Pairwise adding contributions from opposite components Γ^i and $\Gamma^{i\downarrow}$ of Γ, we obtain

$$\begin{aligned}
\frac{\mathrm{d}}{\mathrm{d}t} \left(\mathcal{H}_i[f] + \mathcal{H}_i^{\downarrow}[f] \right) &= \left[\int_{\mathcal{V}^i} h_i \partial_t f \, \mathrm{d}x + \int_{\mathcal{V}^{i\downarrow}} h_i^{\downarrow} \partial_t f \, \mathrm{d}x \right] \\
&= -2 \left[\int_{\mathcal{V}^i} \int_{\mathcal{V}^{i\downarrow} \cap \mathcal{C}[x]} b(x, x_*) \left(\tilde{f}_*(f - \tilde{f}) + \tilde{f}(f_* - \tilde{f}_*) \right) h_i \, dx_* dx \right. \\
&\quad \left. + \int_{\mathcal{V}^{i\downarrow}} \int_{\mathcal{V}^i \cap \mathcal{C}[x]} b(x, x_*) \left(\tilde{f}_*(f - \tilde{f}) + \tilde{f}(f_* - \tilde{f}_*) \right) h_i^{\downarrow} \, dx_* dx \right] \\
&= -2 \left[\int_{\mathcal{V}^i} \int_{\mathcal{V}^{i\downarrow} \cap \mathcal{C}[x]} b(x, x_*) \left(\tilde{f}_*(f - \tilde{f}) + \tilde{f}(f_* - \tilde{f}_*) \right) \left(h - \frac{\rho_i - \rho_i^{\downarrow}}{\rho_i + \rho_i^{\downarrow}} \right) dx_* dx \right. \\
&\quad \left. + \int_{\mathcal{V}^i} \int_{\mathcal{V}^{i\downarrow} \cap \mathcal{C}[x]} b(x, x_*) \left(\tilde{f}_*(f - \tilde{f}) + \tilde{f}(f_* - \tilde{f}_*) \right) \left(h + \frac{\rho_i - \rho_i^{\downarrow}}{\rho_i + \rho_i^{\downarrow}} \right) dx_* dx \right] \\
&= -2 \int_{\mathcal{V}^i} \int_{\mathcal{V}^{i\downarrow} \cap \mathcal{C}[x]} b(x, x_*) \tilde{f} \tilde{f}_* (h + h_*) \, dx_* dx,
\end{aligned}$$

where we first performed the coordinate change $x \to x^{\downarrow}, x_* \to x_*^{\downarrow}$ and used the symmetry properties Lemma 4.9 and Lemma 4.10. From here we can conclude

$$\frac{\mathrm{d}}{\mathrm{d}t}\bar{\mathcal{H}}[f] = -\mathcal{D}[f], \tag{4.18}$$

and therefore, that the dissipation of $\bar{\mathcal{H}}$ coincides with the one from $\mathcal{H}$. Moreover, we can see that $\bar{\mathcal{H}}$ serves as Lyapunov functional. Further, we notice, again by applying Jensen inequality, that

$$\mathcal{H}_i[f] \geq \frac{1}{\rho_i + \rho_i^{\downarrow}} \|f - \tilde{f}\|_{L(\mathcal{V}^i)},$$

and therefore that $\bar{\mathcal{H}}[f]$ controls the L^1-distance of f to $\tilde{f}$ by

$$\bar{\mathcal{H}}[f] \geq \sum_{i=1}^{n} \frac{1}{\rho_i + \rho_i^{\downarrow}} \|f - \tilde{f}\|^2_{L^1(\mathcal{S})}. \tag{4.19}$$

Also here we try to establish a convergence rate for the decay of $\bar{\mathcal{H}}$ by first observing

$$\int_{\mathcal{V}^i} h_i \tilde{f}\, dx = 0 = \int_{\mathcal{V}^{i\downarrow}} h_i \tilde{f}\, dx,$$

obtained by straight forward computations. Next, we use these identities in order to reformulate and estimate $\bar{\mathcal{H}}$, which will be done component-wise:

$$\begin{aligned}
\mathcal{H}_i[f] &= \frac{1}{2}\int_{\mathcal{V}^i} h_i^2 \tilde{f}\, \mathrm{d}x = \frac{1}{2}\int_{\mathcal{V}^i} \left(h_i - \frac{2}{\rho_i + \rho_i^{\downarrow}} \int_{\mathcal{V}^i} h_i' \tilde{f}'\, dx' \right)^2 \tilde{f}\, dx \\
&= \frac{1}{2}\int_{\mathcal{V}^i} \left(\int_{\mathcal{V}^i} (h_i - h_i') \frac{2}{\rho_i + \rho_i^{\downarrow}} \tilde{f}'\, dx' \right)^2 \tilde{f}\, dx \\
&\leq \frac{1}{2}\int_{\mathcal{V}^i} \int_{\mathcal{V}^i} (h_i - h_i')^2 \frac{2}{\rho_i + \rho_i^{\downarrow}} \tilde{f}'\, dx' \tilde{f}\, dx \\
&= \frac{1}{\rho_i + \rho_i^{\downarrow}} \int_{\mathcal{V}^i} \int_{\mathcal{V}^i} (h - h')^2 \tilde{f}' \tilde{f}\, dx' dx,
\end{aligned}$$

where in the second line we could use *Jensen's inequality*, since $\frac{2}{\rho_i+\rho_i^{\downarrow}}\tilde{f}$ is a measure on $\mathcal{V}^i$. In the last inequality we rewrote h_i again in terms of h. We now have all ingredients to formulate the convergence result, which will be a Corollary from Theorem 4.4 and Corollary 4.8 by using the result on each connected component of Γ separately. Convergence in $L^1(\mathcal{S})$ follows by the coercivity property (4.19) of $\mathcal{H}_i[f]$, $i \in \{1, \dots, N\}$.

Corollary 4.12. *There exists a constant $c > 0$ such that for the solution f to (4.1) we have*

$$\bar{\mathcal{H}}[f(\cdot, t)] \leq e^{-ct} \bar{\mathcal{H}}[f_I],$$

for all $t > 0$, which implies exponential decay of f to $\frac{2\rho_i}{\rho_i+\rho_i^{\downarrow}}\tilde{f}$ on each connected component of the graph Γ, i.e.

$$\|f - \tilde{f}\|_{L^1(\mathcal{V}^i)} \leq \sqrt{(\rho_i + \rho_i^{\downarrow})\mathcal{H}_i[f_I]}\, e^{-ct/2}, \quad i = \{1, \dots, N\}.$$

Proof. In order to be able to perform the Gronwall estimate in (4.18) we need to find the proper inequalities for each of the terms

$$\int_{\mathcal{V}^i} \int_{\mathcal{V}^i} (h - h')^2 \tilde{f}' \tilde{f}\, dx' dx,$$

similar as in the proof of Theorem 4.4, but restricted to the integration domain $\mathcal{V}^i$. The Definition 4.5 2.) of the graph allows to find a constant $\gamma_i > 0$ for all its connected components such that $\Gamma^i = \Gamma^{\gamma_i}$ regarding Definition 4.5 2.). We now choose a finite covering $B_{\frac{\gamma_i}{2}}(x_1), \dots, B_{\frac{\gamma_i}{2}}(x_n)$ of $\mathcal{V}_i$, such that $x_1, \dots, x_n$ are the edges of a connected subgraph of Γ^i regarding Definition 4.5. This is possible by first choosing a finite covering $B_{\frac{\gamma_i}{4}}(x_1^*), \dots, B_{\frac{\gamma_i}{4}}(x_m^*)$ of $\mathcal{K}$, since $\mathcal{K}$ is compact, an then extracting the balls $\{B_{\frac{\gamma_i}{4}}(x_{il}^*)\}_{l=1}^n$, which contain at least one $x_l \in \mathcal{V}_i$. The set $B_{\frac{\gamma_i}{2}}(x_1), \dots, B_{\frac{\gamma_i}{2}}(x_n)$ is then a finite covering og $\mathcal{V}^i$, where $x_{l-1} \longleftrightarrow_{\gamma_i} x_l$ can be obtained by adding possible missing points. From Lemma 4.7 we can conclude that $B_{\frac{\gamma_i}{2}}(x_{l-1})$ and $B_{\frac{\gamma_i}{2}}(x_l)$ are linked whenever $x_{l-1} \longleftrightarrow_{\gamma_i} x_l$. The claim follows now by applying Theorem 4.4 and estimate (4.19). □

4.4 Reversal collisions on the torus $\mathbb{T}^1$

For the setting in Remark 4.1, we can characterize the asymptotic behavior of the solution f to (4.2) completely. The the definition of the edges of the graph Γ associated to the initial conditions f_I reads:

Definition 4.13. *Let $\varphi_1, \varphi_2 \in \mathcal{K}$. We say that*

$$\varphi_1 \text{ is connected to } \varphi_2 \text{ and write } \varphi_1 \longleftrightarrow \varphi_2 :\Leftrightarrow \exists \varphi_* \in \mathcal{K} : \ d(\varphi_1, \varphi_*) \geq \frac{\pi}{2} \text{ and } d(\varphi_2, \varphi_*) \geq \frac{\pi}{2}.$$

It is easy to see that the graph Γ has the following properties:

Lemma 4.14. *For $\varphi_1, \varphi_2 \in \mathcal{K}$ it holds:*

$$d(\varphi_1, \varphi_2) \leq \frac{\pi}{2} \Rightarrow \varphi_1 \longleftrightarrow \varphi_2.$$

Proof. Since $\pi = d\left(\varphi_1, \varphi_1^{\downarrow}\right) = d(\varphi_1, \varphi_2) + d\left(\varphi_1^{\downarrow}, \varphi_2\right) < \frac{\pi}{2} + d\left(\varphi_1^{\downarrow}, \varphi_2\right)$ we can deduce $d\left(\varphi_1^{\downarrow}, \varphi_2\right) > \frac{\pi}{2}$. Taking $\varphi_* = \varphi_1^{\downarrow}$ we found a $\varphi_* \in \Omega$ such that $d(\varphi_1, \varphi_*) \geq \frac{\pi}{2}$ and $d(\varphi_2, \varphi_*) \geq \frac{\pi}{2}$. □

Lemma 4.15. *Γ has at most 2 connected components.*

Proof. Assume Γ_1, Γ_2 and Γ_3 are three different connected components of Γ and let $\varphi_1 \in \Gamma_1$, $\varphi_2 \in \Gamma_2$ as well as $\varphi_3 \in \Gamma_3$. Since φ_1, φ_2 and φ_3 are pairwise not connected, it holds:

$$d(\varphi_1, \varphi_3) < \frac{\pi}{2} \ \vee \ d(\varphi_2, \varphi_3) < \frac{\pi}{2},$$

which is a contradiction to Lemma 4.14. □

Lemma 4.16. *If Γ has two connected components Γ_1 and Γ_2, then*

$$\varphi \in \Gamma_1 \Rightarrow \varphi^{\downarrow} \in \Gamma_2.$$

Proof. Contrary, let us assume $\varphi, \varphi^{\downarrow} \in \Gamma_1$. Furthermore, let $\varphi_2 \in \Gamma_2$. Then $\varphi, \varphi^{\downarrow}$ and φ_2 can be located in 3 possible ways.
Either $d(\varphi, \varphi_2) < \frac{\pi}{2}$, or $d(\varphi^{\downarrow}, \varphi_2) < \frac{\pi}{2}$, which, again thanks to Lemma 4.14, both lead to contradiction $\varphi \longleftrightarrow \varphi_2$ or $\varphi^{\downarrow} \longleftrightarrow \varphi_2$.
Or they can be located such that $d(\varphi, \varphi_2) = d(\varphi^{\downarrow}, \varphi_2) = \frac{\pi}{2}$, which implies that $\varphi \longleftrightarrow \varphi_2$, as well as $\varphi^{\downarrow} \longleftrightarrow \varphi_2$, both contradicting the assumption. □

Lemma 4.17. *If Γ has 2 connected components Γ_1, Γ_2 and $\varphi, \varphi_* \in \Gamma_1$ (resp. Γ_2) such that $d(\varphi, \varphi_*) \geq \frac{\pi}{2}$, then $d(\varphi, \varphi_*) = \frac{\pi}{2}$.*

Proof. If $d(\varphi, \varphi_*) > \frac{\pi}{2}$, then $d(\varphi, \varphi_*^{\downarrow}) < \frac{\pi}{2}$, which, by Lemma 4.14 implies $\varphi \longleftrightarrow \varphi_*^{\downarrow}$. This together with Lemma 4.16 contradicts our assumption of Γ having two different connected components. □

Remark 4.18. *The graph associated to $f_I := \{\varphi, \varphi + \pi/2, \varphi^{\downarrow}, \varphi + 3\pi/2\}$, for $\varphi \in \mathbb{T}^1$ has therefore only one connected component.*

With this characterization of the graph Γ we are able to state the asymptotic behavior as follows, which then directly follows from the results in Section 4.3:

Corollary 4.19. *1. If Γ has one connected component, then $\mathcal{H}$ (4.7), the quadratic distance of from f, solution to (4.2), to the average $\tilde{f}$ converges to zero exponentially fast, i.e. $\exists c > 0$ such that*

$$\mathcal{H}[f(\cdot,t)] \leq e^{-ct}\mathcal{H}[f_I].$$

2. If Γ has two connected components Γ_1, Γ_2, then the quadratic distance of from f, solution to (4.2), to the weighted average $2\rho_i\tilde{f}$ converges to zero on each component Γ_i exponentially fast, i.e. $\exists c_i > 0$ such that

$$\mathcal{H}_i[f(\cdot,t)] \leq e^{-c_i t}\mathcal{H}_i[f_I], \quad i \in \{1,2\},$$

for $\mathcal{H}_i$ defined as in (4.17), which in this special setting is of the form

$$\mathcal{H}_i[f(t)] = \frac{1}{2}\int_{\mathcal{V}^i} \frac{(f - 2\rho_i\tilde{f})^2}{\tilde{f}}\, d\varphi \quad i \in \{1,2\}.$$

Remark 4.20. *Convergence in norm again is implied by the coercivity property of $\mathcal{H}$ (4.10) in the one-component case reps. $\mathcal{H}_i$, $i \in \{1,\dots,n\}$ (4.19) in the two-component case.*

4.5 Numerical simulations

Discretization: The results of the preceding section will be illustrated by numerical simulations for the simple problem (4.2) on the torus with $b \equiv 1$. Discretization is based on an equidistant grid

$$\varphi_k = \frac{(k-n)\pi}{n}, \qquad k = 0,\dots,2n,$$

with an even number of grid points, guaranteeing that the grid is invariant under the reversal collisions, i.e., with φ_k also $\varphi_k^{\downarrow} = \varphi_{k+n}$ is a grid point. Solutions of (4.2) are approximated at grid points by

$$f^n(t) := (f_1(t),\dots,f_{2n}(t)) \approx (f(\varphi_1,t),\dots,f(\varphi_{2n},t)),$$

extended periodically by $f_{k+2n}(t) = f_k(t)$. This straightforwardly leads to the discrete model

$$\frac{df_k}{dt} = Q^n_{REV}(f^n,f^n)_k,$$

with

$$Q^n_{REV}(f^n,f^n)_k := \frac{\pi}{n}\sum_{|k_*-k|>n/2} b_{k,k_*}(f_{k+n}f_{k_*+n} - f_k f_{k_*}),$$

and $b_{k,k_*} := b(\varphi_k,\varphi_{k_*})$. For the *time discretization* the *explicit Euler scheme* is used, such that the total mass is conserved by the discrete scheme, which has been implemented in MATLAB.

Γ **has one connected component:** Simulations have been carried out with grid-size n =201. The left row of Figures 4.1, 4.3 show snapshots of the distribution function f at different times together with the symmetric equilibrium $\tilde{f}$. In the second row the total mass $\int_{\mathbb{T}^1} f\,dx = 1$ as well as $\int_{-\pi}^{0} f\,dx$ and $\int_0^{\pi} f\,dx$ are plotted against time. In Figure 4.2 displays the log-plot of $\mathcal{H}[f]$ belonging to the simulations of Figure 4.1, which shows its exponential decay.
In Figure 4.1 we started with asymmetric data, positive everywhere, which makes it clear that the associated graph Γ has only one connected component and hence the solution converges to the symmetric equilibrium $\tilde{f}$ by Corollary 4.19, 1.). For this simulation the time-stepsize was chosen as $k = 0.01$ for

1000 time-steps.
Figure 4.3 shows the evolution with initial conditions chosen positive from in the intervals $(-3\pi/4, -\pi/4)$ and $(\pi/4, 3\pi/4)$, although weighted differently. Furthermore, a perturbation in the interval $[-\pi/4, \pi/4]$ was added, which serves as connecting point for the else wise not connected graph. Also here convergence to the symmetric equilibrium $\tilde{f}$ can be observed. For this simulation the time-stepsize was chosen as $k = 0.1$ for 5000 time-steps.

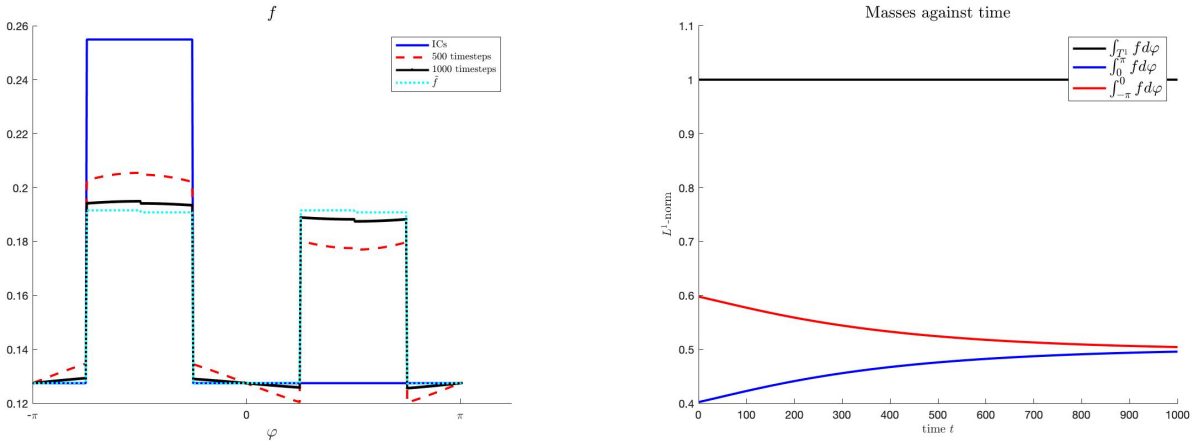

Figure 4.1: Initial conditions positive everywhere, Γ has one connected component. *Left:* Initial condition (solid dark blue), f after 500 time-steps (dashed red), f after 1000 time-steps (solid black) and $\tilde{f}$ (dotted light blue). *Right:* Total mass conservation (black), masses of the positive (dark blue) and negative (red) part of the torus are different initially, but converge to the same value.

Γ **has two connected components:** For the simulations corresponding to Figure 4.4 initial data only positive in the intervals $(-3\pi/4, -\pi/4)$ and $(\pi/4, 3\pi/4)$ was chosen. This causes the graph Γ to have two connected components Γ_-, supported in $(-\pi, 0)$ and Γ_+, supported in $(0, \pi)$. The masses in $\mathcal{V}_\pm$ were chosen differently.
Again, the left part of Figure 4.4 shows snapshots of the distribution function f at different times together with the equilibrium

$$\bar{f} = 2 \begin{cases} \tilde{f} \int_{-\pi}^0 f \, dx, & \varphi \in (-\pi, 0] \\ \tilde{f} \int_0^\pi f \, dx, & \varphi \in [0, \pi]. \end{cases}$$

In the second row the total mass $\int_{\mathbb{T}^1} f \, dx = 1$ as well as $\int_{-\pi}^0 f \, dx$ and $\int_0^\pi f \, dx$ are plotted against time, which shows mass conservation in $\mathcal{V}_\pm$.
The simulation was carried out for $k = 0.01$ and 250 time-steps.

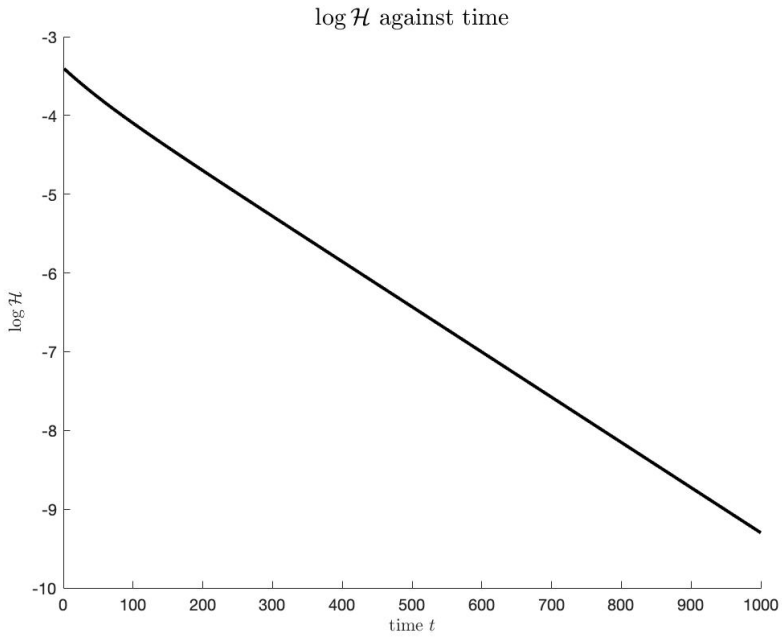

Figure 4.2: log-plot of the Lyapunov functional $\mathcal{H}$ corresponding to the simulations of Figure 4.1, showing exponential decay.

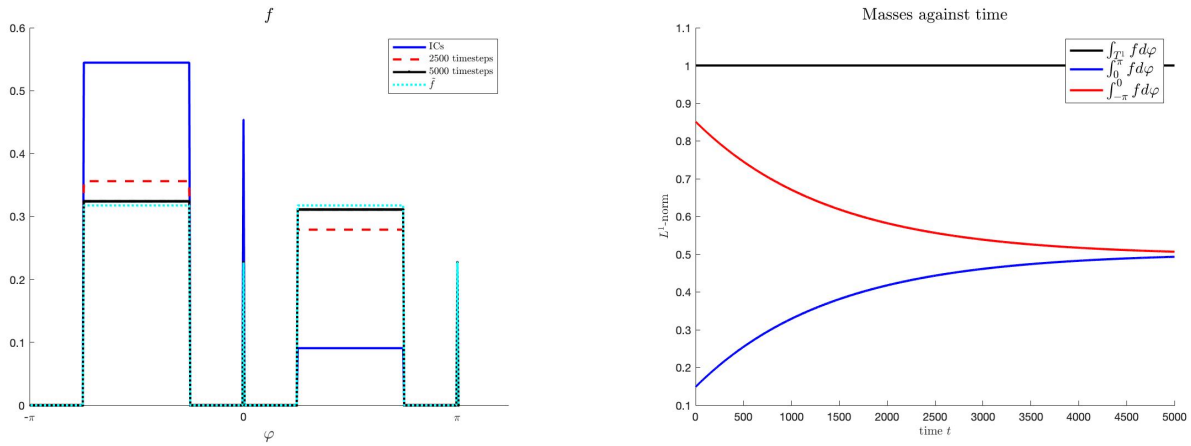

Figure 4.3: Initial conditions supported on $(-3\pi/4, -\pi/4)$ and $(\pi/4, 3\pi/4)$, as well as in a very small interval contained in $(-\pi/4, \pi/4)$. Γ has one connected component. *Left:* Initial condition (solid dark blue), f after 2500 time-steps (dashed red), f after 5000 time-steps (solid black) and the equilibrium $\tilde{f}$ (dotted light blue). *Right:* Total mass conservation (black), masses of the positive (dark blue) and negative (red) part of the torus, which are also conserved quantities.

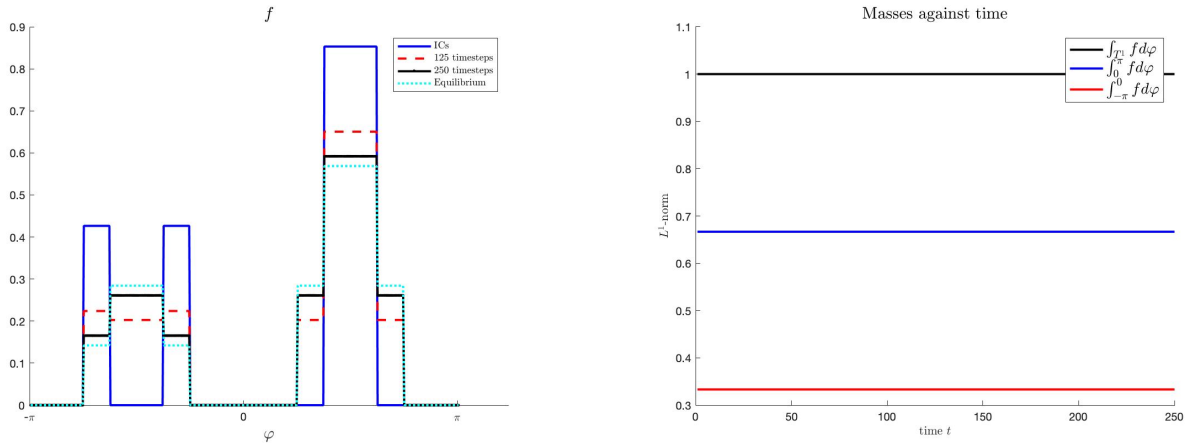

Figure 4.4: Initial conditions supported on $(-3\pi/4, -\pi/4)$ and $(\pi/4, 3\pi/4)$, vacuum else. Γ has two connected components Γ_- with $\mathcal{V}_- \subset (-\pi, 0)$ and Γ_+ with $\mathcal{V}_+ \subset (0, \pi)$. *Left:* Initial condition (solid dark blue), f after 125 time-steps (dashed red), f after 250 time-steps (solid black) and the equilibrium (dotted light blue). *Right:* Total mass conservation (black), masses of the positive (dark blue) and negative (red) part of the torus, which are different initially, but converge to the same value.

5 A Kinetic Model for Non-instantaneous Binary Collisions

'How long is forever?'
'Sometimes, just one second.'

Lewis Carroll ('Alice's Adventures in Wonderland')

Contents

5.1 Introduction . . . 95
5.2 Kinetic Equation for Time-resolved Alignment Collisions with Stochastic Collisions Dynamics . . . 96
5.2.1 Conservation laws and equilibria . . . 98
5.2.2 Existence and uniqueness of solutions . . . 101
5.2.3 Convergence to equilibrium . . . 103
5.2.4 Instantaneous limit . . . 105
5.3 Kinetic Equation for Time-resolved Alignment Collisions with Deterministic Collisions Dynamics . . . 113
5.3.1 Conservation laws and equilibria . . . 115
5.3.2 Instantaneous limit . . . 116

This chapter contains results of an ongoing collaboration with C. Schmeiser and V. Tora. The first part consists of an article close to submission, while in the second part preliminary results of ongoing work are stated.

5.1 Introduction

The main aim of this work is to derive and investigate a kinetic model for an assemble of particles undergoing binary, *non-instantaneous*, alignment collisions. The motivation to study such dynamics was inspired by the fact that the assumption of instantaneous interactions between two agents, standard in kinetic theory, is in some context not an accurate description of reality, especially when it comes to the modelling of biological phenomena. A first idea to introduce a kinetic model for non-instantaneous collisions can be found in [25], which was inspired by heavy-ion reactions, involving scatterings, which is shown not to happen in an instant [16]. The model is of Boltzmann-type, where the non-instantaneity of the collisions is encoded in a time-delay in the involved scattering matrix. This novel concept was not investigated much further and -to our best knowledge- no more modelling attempts were made to overcome this simplification of particle interactions.

The common approach in kinetic theory is modelling interactions between agents via a *jump process* on the microscopic level. More precisely, the dynamics at the individual based level are determined by

interactions, happening between particles at a random time with a specific rate and causing jumps from their pre-collisional states to their post-collisional ones. The collision-process itself is not described and assumed to happen in an instant.

In contrast to this, we aim to model also the collision process itself, for which's duration we therefore will assume a positive time. The dynamics of the whole assemble of particles will be split up into the ones for *single particles* as well as, since we just consider *binary collisions* for the moment, *pairs of particles*, which are in a collision process. The assumption that only interactions between two agents can happen is accurate in a framework where the interaction process is instantaneous. This is the case since, e.g., for hard collisions between particles in rarefied gases, it was proved that the amount of non-binary interactions happening at each time is negligible from a probabilistic point of view [15]. In the framework of non-instantaneous particles this does not apply, since generally speaking, there is no reason why the probability of a third particle hitting a pair of colliding particles would differ from the one of two single agents colliding. Nevertheless, as a first modelling attempt for the sake of simplification, we restrict ourselves to dynamics just involving binary collisions.

In this chapter we consider two cases of time-resolved binary interactions between agents, modeled by an alignment potential. On one hand, in Section 5.2 collisions between agents are assumed to be determined by two *Poisson processes*. A collision of two individuals happens at a specific rate λ, which makes $\frac{1}{\lambda}$ that average waiting time for a collision to happen, and ends with rate γ, whereas $\frac{1}{\gamma}$ describes the average duration of collision. Therefore, the interaction ends before the alignment process of the involved individuals is complete. On the other hand, in Section 5.3 the rate at which interactions happen is modeled the same but the collision itself is assumed to be fully deterministic and only ends when the alignment process is completed.

The main objectives analyzing the proposed models was proving existence and uniqueness of a solution, determining equilibria and showing convergence of the solution towards them. Further, carrying out the instantaneous limit in the equations, both formally and rigorously, is of interest. This is the case since by letting the collision time go to zero, we should be able to recover a traditional kinetic equation modelling instantaneous alignment collisions. Another important aim of this Chapter is to compare the dynamics of this time-resolved stochastic and time-resolved deterministic collision dynamics. While in the model for stochastic collisions treated in Section 5.2 we were able to complete the full analysis, with the model with deterministic alignment dynamics in Section 5.3 difficulties arise due to the singularity caused by the non-invertibility of the alignment collisions.

5.2 Kinetic Equation for Time-resolved Alignment Collisions with Stochastic Collisions Dynamics

We assume an assemble of particles moving freely in $\mathbb{R}^2$ interrupted by *binary, "non-instantaneous" collisions* following stochastic processes. Each particle is described by its position $x \in \mathbb{R}^2$ and a property $\varphi \in \mathbb{R}$. We suppose that the times at which a binary collision between two particles happens as well as the duration of such a collision are modeled by *Poisson processes* in the following way.

- Let $\lambda > 0$ be the rate of collision events, therefore $\frac{1}{\lambda}$ describes the average waiting time of particles in free flight until a collision takes place.
- Let further $\gamma > 0$ be the rate of splitting of a pair of particles, which are in collision. The factor $\frac{1}{\gamma}$ then has the meaning of an average duration of a collision process.

We suppose the following collision-dynamics. Let $t_c > 0$ be the time at which two particles, with pre-collisional states φ and φ_*, meet.

Pre-collisional: $\varphi = \varphi(t_c)$ and $\varphi_* = \varphi_*(t_c)$

In-collision: Let $s \in [t_c,\, t_c + t_\gamma]$. We denote the states of the two involved particles during a collision with $\tilde{\varphi}(s)$ and $\tilde{\varphi}_*(s)$, which can be calculated as

$$\tilde{\varphi}(s) = \frac{\varphi + \varphi_*}{2} + e^{-s+t_c}\frac{\varphi - \varphi_*}{2},$$
$$\tilde{\varphi}_*(s) = \frac{\varphi + \varphi_*}{2} + e^{-s+t_c}\frac{\varphi_* - \varphi}{2}.$$

For the duration of the collision we assume $t_\gamma \sim E(\gamma)$, i.e. being an exponentially distributed random variable with parameter γ. Therefore having expected time a collision takes is $\frac{1}{\gamma}$. One can see easily that the Hamiltonian for these dynamics are given by

$$\begin{pmatrix}\dot{\varphi}\\ \dot{\varphi}_*\end{pmatrix} = V(\varphi, \varphi_*) \quad \text{with} \quad V(\varphi, \varphi_*) := \frac{1}{2}\begin{pmatrix}\varphi_* - \varphi\\ \varphi - \varphi_*\end{pmatrix}. \tag{5.1}$$

Post-collisional: As usual in kinetic theory, we denote the post-collisional states with a prime. Therefore, the states after collision φ' and φ'_* are given by

$$\varphi' = \tilde{\varphi}\,(t_c + t_\gamma) = \frac{\varphi + \varphi_*}{2} + e^{-t_\gamma}\frac{\varphi - \varphi_*}{2},$$
$$\varphi'_* = \tilde{\varphi}_*\,(t_c + t_\gamma) = \frac{\varphi + \varphi_*}{2} + e^{-t_\gamma}\frac{\varphi_* - \varphi}{2},$$

The transition form pre-collisional states to post-collisional ones is invertible and it holds

$$\varphi = \frac{1}{2}\left(\left(1 + e^{t_\gamma}\right)\varphi' + \left(1 - e^{t_\gamma}\right)\varphi'_*\right),$$
$$\varphi_* = \frac{1}{2}\left(\left(1 - e^{t_\gamma}\right)\varphi' + \left(1 + e^{t_\gamma}\right)\varphi'_*\right).$$

Having now the collision process set, we aim to formulate a kinetic model describing the above introduced dynamics of the particles, which results in two distinct-coupled partial differential equations that concern respectively the evolution of the distribution function of the dynamical states of an individual particle

$$f = f(x, \varphi, t), \quad x \in \mathbb{R}^2, \quad \varphi \in \mathbb{R}, \quad t > 0,$$

and the evolution of the distribution function of the the pairs

$$g = g(x, \varphi, \varphi_*, t), \quad x \in \mathbb{R}^2, \quad \varphi, \varphi_* \in \mathbb{R}, \quad t > 0.$$

whose states at time t and position x are φ and φ_*. The dynamics of the distribution functions f and g are then governed by the following equations

$$\partial_t f + \omega \cdot \nabla_x f = 2\Big(\gamma \int_{\mathbb{R}} g(\varphi, \varphi_*)\,\mathrm{d}\varphi_* - \lambda f(\varphi)\int_{\mathbb{R}} b(\varphi, \varphi_*) f(\varphi_*)\,\mathrm{d}\varphi_*\Big),$$
$$\partial_t g + \nabla \cdot (Vg) = \lambda b(\varphi, \varphi_*) f(\varphi_*) f(\varphi) - \gamma g(\varphi, \varphi_*),$$

with prescribed initial data

$$f(x, \varphi, 0) = f_0(x, \varphi),\ x \in \mathbb{R},\ \varphi \in \mathbb{R}, \quad g(x, \varphi, \varphi_*, 0) = g_0(x, \varphi, \varphi_*),\ x \in \mathbb{R},\ \varphi_*, \varphi_* \in \mathbb{R}.$$

Therefore, being in free flight, particles are transported in the state space regarding $\omega = \omega(\varphi) \in \mathbb{R}^2$, with ω being some function of the particle's property φ. The left-hand-side of the equation for single particles consist of a *gain term* describing the separation of two colliding particles with rate γ from a collision with all possible collision partners φ_*. On the other hand, single particles are lost with collision rate λ by hitting all possible free-flight particles. The non-instantaneous collisions occur in dependence of the *collision-cross-section* $b(\varphi, \varphi_*) = B(|\varphi - \varphi_*|)$, a function we assume to depend only on the difference between the two states. Similar, the drift-term of the g-equation describes how a pair of particles in collision is transported towards the midpoint of the states (φ, φ_*) regarding the potential V. The gain- and the loss-term represent the respective counterpart of the ones in the f-equation.

Spatially homogeneous model: In this work, we will focus on investigating the above introduced model after considering two simplifications. One one hand, we assume the particles moving only along lines in $\mathbb{R}^2$ and therefore the system being spatially homogeneous. On the other hand, we consider *Maxwellian particles*, i.e. the collision-cross-section is constant, especially independent from $|\varphi - \varphi_*|$, and given by

$$b(\varphi, \varphi_*) \equiv 1.$$

The resulting system of coupled equations concerning respectively the evolution of individual bacteria and the evolution of the collision-pairs then has the form:

$$\begin{aligned} \partial_t f &= 2\Big(\gamma \int_{\mathbb{R}} g \, \mathrm{d}\varphi_* - \lambda f \int_{\mathbb{R}} f_* \, \mathrm{d}\varphi_*\Big), \\ \partial_t g + \nabla_{(\varphi,\varphi_*)} \cdot (Vg) &= \lambda f f_* - \gamma g, \end{aligned} \tag{5.2}$$

where as usual in kinetic theory we omitted the arguments and for $t > 0$ denote $f = f(\varphi, t)$, $f_* = f(\varphi_*, t)$ and $g = g(\varphi, \varphi_*, t)$. The model is completed by prescribing initial data

$$f(\varphi, 0) = f_0(\varphi), \ \varphi \in \mathbb{R}, \quad g(\varphi, \varphi_*, 0) = g_0(\varphi, \varphi_*), \ \varphi_*, \varphi_* \in \mathbb{R}.$$

5.2.1 Conservation laws and equilibria

The aim of this section is to establish and investigate ODE systems for the moments up to second order of solutions to (5.2).

Mass: We define the the time-dependent masses of the single particles and the pairs of colliding particles as follows

$$M_f(t) := \int_{\mathbb{R}} f \, \mathrm{d}\varphi \ \text{ and } \ M_g(t) := \int_{\mathbb{R}^2} g \, \mathrm{d}\varphi \, \mathrm{d}\varphi_*.$$

Since the drift-term in the g-equation vanishes due to the *Divergence theorem* one can see immediately from (5.2) that *total mass conservation* holds

$$M := M_f(t) + 2M_g(t) = const. \tag{5.3}$$

In order to investigate the dynamics of $M_f(t)$ and $M_g(t)$ we integrate the first equation of (5.2) over $\mathbb{R}$ and the second equation over $\mathbb{R}^2$, from which we obtain the following system of ordinary differential equations for M_f and M_g:

$$\begin{aligned} \dot{M}_f &= 2\gamma M_g - 2\lambda M_f^2 \\ \dot{M}_g &= \lambda M_f^2 - \gamma M_g. \end{aligned} \tag{5.4}$$

Having in mind mass conservation (5.3), we can reduce (5.4) to the following ODE for M_g

$$\dot{M}_g = F(M_g) := 4\lambda M_g^2 - (4\lambda M + \gamma)M_g + \lambda M^2,$$

equipped with initial condition $M_g(0) = M_{g_0} = \int_{\mathbb{R}^2} g_0 \, \mathrm{d}\varphi_* \mathrm{d}\varphi$. Further we have to take into account that M_g is bounded from above by $\frac{M}{2}$ and from below by zero due to (5.3). Possible equilibria of M_g are found by calculating the roots of the polynomial F, which are given by

$$M_g^{\pm} := \frac{M}{2} + \frac{\gamma}{8\lambda} \pm \frac{1}{8\lambda}\sqrt{8\lambda\gamma M + \gamma^2}.$$

Due to total mass conservation it is clear that just M_g^- is relevant for our dynamics. Moreover, noticing that $F(M_g) > 0$ for $M_g \in [0, M_g^-)$ and $F(M_g) < 0$ for $M_g \in (M_g^-, M/2]$ gives us convergence to $M_g^- := M_{g_\infty}$ for $t \to \infty$. Using again (5.3) to calculate the equilibrium M_{f_∞} of M_f, we obtain from the system (5.4)

$$(M_f(t),\, M_g(t)) \to (M_{f_\infty},\, M_{g_\infty}) = \frac{1}{4\lambda}\left(\sqrt{8\lambda\gamma M + \gamma^2} - \gamma,\, 2M\lambda + \frac{\gamma}{2} - \frac{1}{2}\sqrt{8\lambda\gamma M + \gamma^2}\right), \tag{5.5}$$

for $t \to \infty$.

Mean value: For the time-dependent first moments of f resp g we introduce the notation

$$I_f(t) := \int_{\mathbb{R}} \varphi f \, \mathrm{d}\varphi, \quad I_g(t) := \int_{\mathbb{R}^2} \varphi g \, \mathrm{d}\varphi_* \mathrm{d}\varphi.$$

Again, one can conclude easily that the *total mean*

$$M\varphi_\infty := I_f(t) + 2I_g(t) \tag{5.6}$$

is a conserved quantity of the above system. For obtaining an ODE system for the the single momenta I_f and I_g we multiply (5.2) by φ and again integrate over $\mathbb{R}$ and $\mathbb{R}^2$ respectively, which yields

$$\begin{aligned} \dot{I}_f &= 2\gamma I_g - 2\lambda I_f M_f \\ \dot{I}_g &= \lambda I_f M_f - \gamma I_g. \end{aligned} \tag{5.7}$$

Using our second conservation law, i.e. conservation of the mean (5.6) $M\varphi_\infty = I_f + 2I_g = const.$, we can again reduce the system to a single ODE for I_g, which is given by

$$\dot{I}_g = -(2\lambda M_f + \gamma)I_g + \lambda\varphi_\infty M M_f,$$

with initial conditions $I_g(0) = I_{g_0} := \int_{\mathbb{R}^2} \varphi g_0 \, \mathrm{d}\varphi_* \mathrm{d}\varphi$. Variation of constants yields

$$I_g(t) = e^{-2\lambda\int_0^t M_f \, \mathrm{d}s - \gamma t}\left(I_{g_0} + \lambda\varphi_\infty M \int_0^t e^{2\lambda\int_0^s M_f \, \mathrm{d}r + \gamma s} M_f(s) \, \mathrm{d}s\right)$$

and therefore

$$I_f(t) = \varphi_\infty M - 2e^{-2\lambda \int_0^t M_f \,\mathrm{d}s - \gamma t} \left(I_{g_0} + \lambda \varphi_\infty M \int_0^t e^{2\lambda \int_0^s M_f \,\mathrm{d}r + \gamma s} M_f(s) \,\mathrm{d}s \right),$$

noticing that M_f, the mass of f, is a given bounded function. Directly from the differential equation for I_g we can further see that an equilibrium is reached whenever

$$\bar{I}_g = \lambda M_f \frac{\varphi_\infty M}{2\lambda M_f + \gamma}, \quad \bar{I}_f = \gamma \frac{\varphi_\infty M}{2\lambda M_f + \gamma}.$$

From (5.7) or the ODE describing just the dynamics of I_g one can see that the equilibrium

$$(I_{f_\infty}, I_{g_\infty}) = \frac{2\varphi_\infty M}{\sqrt{8\lambda\gamma M + \gamma^2} + \gamma} \left(\frac{1}{4}\sqrt{8\lambda\gamma M + \gamma^2}, \gamma \right)$$

is linearly stable, where we also considered (5.5).

Variance: Analogously, we define the (relative) variance of f and g separately by

$$V_f(t) := \int_{\mathbb{R}} (\varphi - \varphi_\infty)^2 f \,\mathrm{d}\varphi, \quad V_g(t) := \int_{\mathbb{R}} (\varphi - \varphi_\infty)^2 g \,\mathrm{d}\varphi_* \mathrm{d}\varphi.$$

Investigating the dynamics of the variance we multiply (5.2) by $(\varphi - \varphi_\infty)^2$ before integration over $\mathbb{R}$ and $\mathbb{R}^2$ respectively. Different from the total mass and the mean, the *total variance*

$$\mathcal{V}[f,g] := \int_{\mathbb{R}} (\varphi - \varphi_\infty)^2 f \;\varphi + 2 \int_{\mathbb{R}^2} (\varphi - \varphi_\infty)^2 g \,\mathrm{d}\varphi_* \mathrm{d}\varphi,$$

is decreasing in time. Indeed, computing the time-derivative of $\mathcal{V}[f,g]$ we obtain

$$\frac{\mathrm{d}}{\mathrm{d}t}\mathcal{V}[f,g] = -2 \int_{\mathbb{R}^2} (\varphi - \varphi_*)^2 g \,\mathrm{d}\varphi_* \mathrm{d}\varphi_*, \tag{5.8}$$

a fact that is not surprising, since we deal with alignment collisions, producing concentration of mass at the mean value, see [17, 22]. We further observe that $\mathcal{V}$ stops decaying whenever there are no pairs of particles, i.e. $g = 0$, or if the states are already concentrated along the diagonal $D := \{(\varphi, \varphi_*) \in \mathbb{R}^2 : \varphi = \varphi_*\}$.
The dynamics of the single variances V_f and V_g are given by

$$\begin{aligned} \dot{V}_f &= 2\gamma V_g - 2\lambda M_f V_f \\ \dot{V}_g &= \lambda M_f V_f - \gamma V_g - \int_{\mathbb{R}^2} (\varphi - \varphi_*)^2 g \,\mathrm{d}\varphi_* \mathrm{d}\varphi. \end{aligned}$$

Equilibria: Searching for equilibria of (5.2) we have to take into account the two different effects governing the dynamics. One one hand, we have an exchange between single particles and and pairs of particles, given by the *collision operator* on the right hand side of the system. Functions being uneffected by these collision dynamics, so-called *collision invariants*, can be described by the set of local equilibria

$$Eq := \left\{ (\bar{f}, \bar{g}) : \;\; \lambda \bar{f}\bar{f}^* = \gamma \bar{g} \right\}, \tag{5.9}$$

which we will call *'exchange equilibria'* in the following. One can see immediately that, if the system arrives at the set (5.9), it will not remain there, but instead will be transported away by the drift-term in the g-equation, which produces concentration of mass at a single point, namely the mean value φ_∞ defined in (5.6). Therefore, we observe a *hypocoercivity problem*, where the interplay between the transport towards concentration $\nabla \cdot (Vg)$ and the exchange dynamics is needed to arrive at the *global equilibrium*, given by

$$(f_\infty, g_\infty) := (M_{f_\infty}\delta_{\varphi_\infty}, M_{g_\infty}\delta_{(\varphi_\infty,\varphi_\infty)}), \tag{5.10}$$

with M_{f_∞} and M_{g_∞} as in (5.5).

5.2.2 Existence and uniqueness of solutions

We aim to show existence and uniqueness of a solution to the system (5.2) using a *fixed-point argument*. Therefore, we rewrite (5.2) in *mild formulation* (Peano-formulation) by incorporating the drift

$$\begin{aligned} f(\varphi,t) &= f_0(\varphi) + 2\int_0^t \left(\gamma \int_{\mathbb{R}} g(\varphi,\varphi_*,s)\,\mathrm{d}\varphi_* - \lambda \int_{\mathbb{R}} f(\varphi,s) f(\varphi_*,s)\,\mathrm{d}\varphi_*\right)\,\mathrm{d}s \\ g(\varphi,\varphi_*,t) &= g_0\left(\Phi(t)^0, \Phi_*(t)^0\right) + \int_0^t \left[\lambda f\left(\Phi(t)^s,s\right) f\left(\Phi_*(t)^s,s\right) - (\gamma-1) g\left(\Phi(t)^s,\Phi_*(t)^s,s\right)\right]\,\mathrm{d}s, \end{aligned} \tag{5.11}$$

where the flux of the collision dynamics is given by

$$\begin{aligned} \Phi(s)^t &= \frac{\varphi+\varphi_*}{2} + e^{-s+t}\frac{\varphi-\varphi_*}{2} \\ \Phi_*(s)^t &= \frac{\varphi+\varphi_*}{2} + e^{-s+t}\frac{\varphi_*-\varphi}{2}. \end{aligned}$$

We define the fixed-point mapping as

$$(f(t), g(t)) \mapsto \mathcal{FP}(f(t), g(t)),$$

where $\mathcal{FP}$ is given by

$$\mathcal{FP}(f(t),g(t)) = \begin{pmatrix} f_0 + 2\gamma \int_0^t \int_{\mathbb{R}} g\,\mathrm{d}\varphi_*\,\mathrm{d}s - 2\lambda \int_0^t \int_{\mathbb{R}} f f^*\,\mathrm{d}\varphi_* \\ g_0(\Phi(t)^0, \Phi_*(t)^0) + \lambda \int_0^t f\left(\Phi(t)^s\right) f\left(\Phi_*(t)^s\right)\,\mathrm{d}s - (\gamma-1)\int_0^t g\left(\Phi(t)^s,\Phi_*(t)^s\right)\,\mathrm{d}s \end{pmatrix}.$$

We can prove the following theorem:

Theorem 5.1. *Let $f_0 \in L^1_+(\mathbb{R})$, $g_0 \in L^1_+(\mathbb{R}^2)$. Then (5.11) has a unique global solution $(f,g) \in C([0,\infty);\, L^1(\mathbb{R}) \times L^1(\mathbb{R}^2))$.*

Proof. Let (f,g), $(\tilde f, \tilde g)$ $\in L^1(\mathbb{R}) \times L^1(\mathbb{R}^2)$. In the follwoing, we want to find a Lipschitz estimate for

$$\begin{aligned} &\|\mathcal{FP}(f,g)(t) - \mathcal{FP}(\tilde f,\tilde g)(t)\|_{L^1(\mathbb{R})\times L^1(\mathbb{R}^2)} \\ &\le 2\gamma \int_{\mathbb{R}^2}\int_0^t |g(\varphi,\varphi_*,t) - \tilde g(\varphi,\varphi_*,t)|\,\mathrm{d}s\,\mathrm{d}\varphi\,\mathrm{d}\varphi_* \\ &+ 2\lambda \int_{\mathbb{R}^2}\int_0^t \left|f(\varphi,s)f(\varphi_*,s) - \tilde f(\varphi,s)\tilde f(\varphi_*,s)\right|\,\mathrm{d}s\,\mathrm{d}\varphi\,\mathrm{d}\varphi_* \\ &+ \lambda \int_{\mathbb{R}^2}\int_0^t \left|f\left(\Phi(t)^s,s\right) f\left(\Phi_*(t)^s,s\right) - \tilde f\left(\Phi(t)^s,s\right)\tilde f\left(\Phi_*(t)^s,s\right)\right|\,\mathrm{d}s\,\mathrm{d}\varphi\,\mathrm{d}\varphi_* \\ &+ |\gamma-1| \int_{\mathbb{R}^2}\int_0^t \left|g\left(\Phi(t)^s,\Phi_*(t)^s,s\right) - \tilde g\left(\Phi(t)^s,\Phi_*(t)^s,s\right)\right|\,\mathrm{d}s\,\mathrm{d}\varphi\,\mathrm{d}\varphi_* \\ &= \int_0^t (I + II + III + IV)\,\mathrm{d}s, \end{aligned}$$

and deal with each term separately in order to obtain L^1-estimates, uniform in time.

$$I = 2\gamma \|g - \tilde{g}\|_{L^1(\mathbb{R}^2)}.$$

For the following three terms we have to use on one hand total mass conservation (5.3) as well as the simple estimate $2|ab - \tilde{a}\tilde{b}| \leq |a - \tilde{a}||b + \tilde{b}| + |a + \tilde{a}||b - \tilde{b}|$, for $a, b > 0$.

$$\begin{aligned} II &= 2\lambda \int_{\mathbb{R}^2} \left| f(\varphi, s) f(\varphi_*, s) - \tilde{f}(\varphi, s) \tilde{f}(\varphi_*, s) \right| \, \mathrm{d}\varphi \, \mathrm{d}\varphi_* \\ &\leq 4M\lambda \int_{\mathbb{R}} \left| f(\varphi, s) - \tilde{f}(\varphi, s) \right| \, \mathrm{d}\varphi \\ &= 4M\lambda \|f - \tilde{f}\|_{L^1(\mathbb{R})} \end{aligned}$$

Next we estimate term III as follows

$$III \leq \lambda \int_{\mathbb{R}^2} \left| f\left(\Phi(t)^s\right) f\left(\Phi_*(t)^s\right) - \tilde{f}\left(\Phi(t)^s\right) \tilde{f}\left(\Phi_*(t)^s\right) \right| \, \mathrm{d}\varphi \, \mathrm{d}\varphi_*.$$

After performing the coordinate change $(\Phi(t)^s, \Phi_*(t)^s) \mapsto (\varphi, \varphi_*)$ with Jacobian determinant e^{-t+s} we obtain

$$\begin{aligned} III &\leq \lambda e^{s-t} \int_{\mathbb{R}^2} \left| f(\varphi, s) f(\varphi_*, s) - \tilde{f}(\varphi, s) \tilde{f}(\varphi_*, s) \right| \, \mathrm{d}\varphi \, \mathrm{d}\varphi_* \\ &\leq 2\lambda M e^{s-t} \int_{\mathbb{R}^2} |f(\varphi, s) - \tilde{f}(\varphi, s)| \, \mathrm{d}\varphi \\ &\leq 2\lambda M \|f - \tilde{f}\|_{L^1(\mathbb{R})}, \end{aligned}$$

since $s < t$. After first performing the coordinate change and then estimating the last term yields

$$\begin{aligned} IV &= |\gamma - 1| \int_{\mathbb{R}^2} \int_0^t |g(\varphi, \varphi_*, s) - \tilde{g}(\varphi, \varphi_*, s)| \, \mathrm{d}s \, \mathrm{d}\varphi \, \mathrm{d}\varphi_* \\ &= |\gamma - 1| \|g - \tilde{g}\|_{L^1(\mathbb{R}^2)} \end{aligned}$$

Combining these estimates of the terms I-IV for fixed but arbitrary $t > 0$ provide the following estimate for the fixed-point mapping $\mathcal{S}$:

$$\begin{aligned} &\|\mathcal{FP}(f, g)(t) - \mathcal{FP}(\tilde{f}, \tilde{g})(t)\|_{L^1(\mathbb{R}) \times L^1(\mathbb{R} \times \mathbb{R})} \\ &\qquad \leq \max\{6M\lambda, 2\gamma + |\gamma + 1|\} \int_0^t \|(f, g) - (\tilde{f}, \tilde{g})\|_{L^1(\mathbb{R}) \times L^1(\mathbb{R}^2)} \, \mathrm{d}s, \end{aligned}$$

which yields

$$\begin{aligned} &\|\mathcal{FP}(f, g) - \mathcal{FP}(\tilde{f}, \tilde{g})\|_{C\left([0,t];\, L^1(\mathbb{R}) \times L^1(\mathbb{R}^2)\right)} \\ &\qquad \leq t \max\{6M\lambda, 2\gamma + |\gamma + 1|\} \|(f, g) - (\tilde{f}, \tilde{g})\|_{C\left([0,t];\, L^1(\mathbb{R}) \times L^1(\mathbb{R}^2)\right)}. \end{aligned}$$

Choosing first t small enough in order to make $\mathcal{S}$ a contraction and then apply Banach's fixed-point theorem gives a unique solution $(f, g) \in C([0, t];\ L^1(\mathbb{R}) \times L^1(\mathbb{R}^2))$. Starting now from t and iterating this argument finally yields global existence and therefore a solution

$$(f, g) \in C([0, \infty);\ L^1(\mathbb{R}) \times L^1(\mathbb{R}^2)).$$

□

5.2.3 Convergence to equilibrium

We study the convergence of solutions of the spatially homogeneous problem (5.2) to equilibria of the form (5.10) as $t \to \infty$. As already indicated in Section 5.2.1, due to the hypocoercivity structure of the problem it is that we need both the effects of exchange and drift in order to find an apropraite *entropy functional*.

Exchange dynamics: We first consider the exchange between single particles f and collision-pairs g only. The corresponding system has the form

$$\begin{aligned} \partial_t f &= 2\Big(\gamma \int_{\mathbb{R}} g \,\mathrm{d}\varphi_* - \lambda f M_f\Big), \\ \partial_t g &= \lambda f f_* - \gamma g, \end{aligned} \tag{5.12}$$

whose equilibria are given by the set Eq defined in (5.9). Inspired by the Boltzmann's H-theorem, we define the following logarithmic entropy

$$\mathcal{H}_{ex}[f,g] := \int_{\mathbb{R}} (\ln(f) - 1) f \,\mathrm{d}\varphi + \int_{\mathbb{R}^2} \left(\ln\left(\frac{\gamma g}{\lambda}\right) - 1\right) g \,\mathrm{d}\varphi_* \,\mathrm{d}\varphi. \tag{5.13}$$

Computing the time-derivative of $\mathcal{H}_{ex}$ along solutions to (5.13), we obtain

$$\begin{aligned} \frac{\mathrm{d}}{\mathrm{d}t}\mathcal{H}_{ex}[f,g] &= \int_{\mathbb{R}} \ln(f)\partial_t f \,\mathrm{d}\varphi + \int_{\mathbb{R}^2} \ln\left(\frac{\gamma g}{\lambda}\right)\partial_t g \,\mathrm{d}\varphi_* \,\mathrm{d}\varphi \\ &= 2\gamma \int_{\mathbb{R}^2} \ln(f) g \,\mathrm{d}\varphi_* \,\mathrm{d}\varphi - 2\lambda \int_{\mathbb{R}^2} \ln(f) f f_* \,\mathrm{d}\varphi_* \,\mathrm{d}\varphi \\ &+ \lambda \int_{\mathbb{R}^2} \ln\left(\frac{\gamma g}{\lambda}\right) f f_* \,\mathrm{d}\varphi_* \,\mathrm{d}\varphi - \gamma \int_{\mathbb{R}^2} \ln\left(\frac{\gamma g}{\lambda}\right) g \,\mathrm{d}\varphi_* \,\mathrm{d}\varphi \\ &= \int_{\mathbb{R}^2} \Big(\gamma g - \lambda f f_*\Big) \ln(f f_*) \,\mathrm{d}\varphi_* \,\mathrm{d}\varphi + \int_{\mathbb{R}^2} \Big(\lambda f f_* - \gamma g\Big) \ln\left(\frac{\gamma g}{\lambda b}\right) \,\mathrm{d}\varphi_* \,\mathrm{d}\varphi \\ &= \int_{\mathbb{R}^2} \Big(\gamma g - \lambda f f_*\Big) \ln\left(\frac{\lambda f f_*}{\gamma g}\right) \,\mathrm{d}\varphi_* \,\mathrm{d}\varphi \leq 0. \end{aligned}$$

Moreover, we can see easily that

$$\frac{\mathrm{d}}{\mathrm{d}t}\mathcal{H}_{ex}[f,g] \equiv 0 \quad \Leftrightarrow \quad \lambda f f^* = \gamma g, \quad \forall \varphi, \varphi_* \in \mathbb{R}.$$

Therefore, we found with $\mathcal{H}_{ex}$ a quantity for the system (5.12), which is decaying in time until the dynamics hit the set of local equilibria Eq.
Incorporating now also the drift term in the equation for g, which causes concentration of mass at the mean value φ_∞, makes it clear that the logarithmic entropy (5.13) will not work in this case. Indeed, computing it's time derivative along a solution (f,g) yields

$$\frac{\mathrm{d}}{\mathrm{d}t}\mathcal{H}_R[f,g] = \int_{\mathbb{R}^2} \Big(\gamma g - \lambda f f_*\Big) \ln\left(\frac{\lambda f f_*}{\gamma g}\right) \,\mathrm{d}\varphi_* \,\mathrm{d}\varphi + M_g(t),$$

where the blowing up factor $M_g(t)$ comes from the drift term $\nabla \cdot (Vg)$. In order to control $M_g(t)$ we modify the logarithmic entropy to

$$\mathcal{H}[f,g,t] := \int_{\mathbb{R}} (\ln(f) - 1) f \,\mathrm{d}\varphi + \int_{\mathbb{R}^2} \left(\ln\left(\frac{\gamma g}{\lambda}\right) - 1\right) g \,\mathrm{d}\varphi_* \,\mathrm{d}\varphi - \int_0^t M_g(s) \,\mathrm{d}s. \tag{5.14}$$

Performing basic computations, one can see that

$$\mathcal{H}[f,g,t] = \int_{\mathbb{R}} \left[\ln\left(\exp\left(-\frac{1}{M}\int_0^t M_g(s)\,\mathrm{d}s \right) f \right) - 1 \right] f \,\mathrm{d}\varphi + \int_{\mathbb{R}^2} \left[\ln\left(\frac{\gamma}{\lambda} \exp\left(-\frac{2}{M}\int_0^t M_g(s)\,\mathrm{d}s \right) g \right) - 1 \right] g \,\mathrm{d}\varphi_* \,\mathrm{d}\varphi$$

which, together with the fact that we expect convergence to Dirac deltas of the form (5.10), motivates to introduce the following *change of coordinates* $(\varphi, \varphi_*) \mapsto (\psi, \psi_*)$ given by

$$\psi = exp\left(\frac{1}{M}\int_0^t M_g(s)\,\mathrm{d}s \right)(\varphi - \varphi_\infty), \quad \psi_* = exp\left(\frac{1}{M}\int_0^t M_g(s)\,\mathrm{d}s \right)(\varphi_* - \varphi_\infty), \tag{5.15}$$

$$f(\varphi,t) = exp\left(\frac{1}{M}\int_0^t M_g(s)\,\mathrm{d}s \right)\tilde{f}(\psi,t), \quad g(\varphi,\varphi_*,t) = exp\left(\frac{2}{M}\int_0^t M_g(s)\,\mathrm{d}s \right)\tilde{g}(\psi,\psi_*,t). \tag{5.16}$$

We further notice that the masses remain unaffected by this coordinate transform

$$M_{\tilde{f}}(t) := \int_{\mathbb{R}} \tilde{f}(\psi,t)\,\mathrm{d}\psi = M_f(t) \text{ as well as } M_{\tilde{g}}(t) := \int_{\mathbb{R}^2} g(\psi,\psi_*,t)\,\mathrm{d}\psi_*\,\mathrm{d}\psi = M_g(t). \tag{5.17}$$

Computing now the time-derivative of $\mathcal{H}[f,g,t]$ (5.14) along a solution (f,g) to the problem (5.2) we obtain

$$\frac{\mathrm{d}}{\mathrm{d}t}\mathcal{H}[f(t),g(t),t] = \int_{\mathbb{R}^2} \left(\gamma\tilde{g} - \lambda\tilde{f}\tilde{f}_* \right) \ln\left(\frac{\lambda\tilde{f}\tilde{f}_*}{\gamma\tilde{g}} \right) \mathrm{d}\psi_*\,\mathrm{d}\psi \le 0,$$

which yields decay to the set of local equilibria Eq, since we can see easily from (5.16) that

$$\gamma\tilde{g} = \lambda\tilde{f}\tilde{f}_* \quad \forall \varphi, \varphi_* \in \mathbb{R} \quad \Leftrightarrow \quad (f,g) \in Eq$$

holds.

In order to obtain decay to the global equilibrium (5.10) we now combine the last result for the logarithmic entropy with the decay of the variance established in (5.8). We define the total *entropy functional* by

$$\mathcal{E}[f,g,t] := \mathcal{V}[f,g] + \mathcal{H}[f,g,t],$$

whose time derivative along solutions to (5.2) is decreasing in the following way

$$\frac{\mathrm{d}}{\mathrm{d}t}\mathcal{E}[f,g,t] = -\int_{\mathbb{R}^2} (\varphi - \varphi_*)^2 g \,\mathrm{d}\varphi_*\mathrm{d}\varphi - \int_{\mathbb{R}^2} (\lambda f f_* - \gamma g) \ln\left(\frac{\lambda f f_*}{\gamma g} \right) \mathrm{d}\varphi_*\mathrm{d}\varphi \le 0.$$

Furthermore, we have that

$$\frac{\mathrm{d}}{\mathrm{d}t}\mathcal{E}[f,g,t] = 0 \quad \Leftrightarrow \quad g(\varphi,\varphi_*) = 0,\ \forall \varphi \neq \varphi_* \in \mathbb{R} \ \wedge\ \lambda f(\varphi) f(\varphi_*) = \gamma g(\varphi,\varphi_*),\ \forall \varphi,\varphi_* \in \mathbb{R},$$

which implies

$$\forall \varphi \neq \varphi_* :\ f(\varphi) = 0 \vee f(\varphi_*) = 0 \ \Rightarrow\ \exists\, \tilde{\varphi} \text{ s.t. } f = M_f \delta_{\tilde{\varphi}}.$$

Since the mean value φ_∞ is a conserved quantity (see (5.6)), this implies

$$f(\varphi) = M_f \delta_{\varphi_\infty}(\varphi), \quad \varphi \in \mathbb{R},$$

from which we can further deduce

$$g(\varphi,\varphi_*) = M_g \delta_{(\varphi_\infty,\varphi_\infty)}(\varphi,\varphi_*), \quad \varphi,\varphi_* \in \mathbb{R}.$$

All together, we have that $\mathcal{E}$ is decreasing and stops decreasing as soon as the equilibrium

$$(f_\infty, g_\infty) := \left(M_{f_\infty}\delta_{\varphi_\infty},\ M_{g_\infty}\delta_{(\varphi_\infty,\varphi_\infty)} \right)$$

is reached, where M_{f_∞}, M_{g_∞} are determined explicitly by (5.5).

Weak convergence to equilibrium: The construction of the coordinate change (5.15), (5.16) indicates already convergence of f and g towards Dirac deltas for large time. Indeed, we can prove the following result:

Theorem 5.2 (Weak convergence to equilibrium)**.** *Let $(f(t), g(t)), t \geq 0$ be the solution to (5.2). Then*

$$(f(t), g(t)) \longrightarrow \left(M_{f_\infty}\delta_{\varphi_\infty}, M_{g_\infty}\delta_{(\varphi_\infty,\varphi_\infty)}\right), \quad \text{for} \quad t \to \infty, \tag{5.18}$$

in the sense of distributions, where the weights M_{f_∞} and M_{g_∞} are given by (5.5).

Proof. For smooth and bounded test-functions $h_1, h_2 \in \mathcal{C}_b^\infty$ we aim to show

$$\begin{aligned} \int_{\mathbb{R}} f(\varphi,t)h_1(\varphi)\,\mathrm{d}\varphi &\overset{t\to\infty}{\longrightarrow} M_{f_\infty}h_1(\varphi_\infty), \\ \int_{\mathbb{R}^2} g(\varphi,\varphi_*,t)h_2(\varphi,\varphi_*)\,\mathrm{d}\varphi_*\mathrm{d}\varphi &\overset{t\to\infty}{\longrightarrow} M_{g_\infty}h_2(\varphi_\infty,\varphi_\infty), \end{aligned} \tag{5.19}$$

which this is equivalent to (5.18). We use the coordinate change (5.15) and (5.16) to compute

$$\begin{aligned} &\int_{\mathbb{R}} f(\varphi,t)h_1(\varphi)\,\mathrm{d}\varphi = \int_{\mathbb{R}} \tilde{f}(\psi,t)h_1\left(\exp\left(-\frac{1}{M}\int_0^t M_g(s)\,\mathrm{d}s\right)\psi + \varphi_\infty\right)\mathrm{d}\psi, \\ &\int_{\mathbb{R}^2} g(\varphi,\varphi_*,t)h_2(\varphi,\varphi_*)\,\mathrm{d}\varphi \\ &= \int_{\mathbb{R}^2} \tilde{g}(\psi,\psi_*,t)h_2\left(\exp\left(-\frac{2}{M}\int_0^t M_g(s)\,\mathrm{d}s\right)\psi + \varphi_\infty, \exp\left(-\frac{2}{M}\int_0^t M_g(s)\,\mathrm{d}s\right)\psi_* + \varphi_\infty\right)\mathrm{d}\psi\mathrm{d}\psi_*. \end{aligned}$$

We first notice that

$$h_1\left(\exp\left(-\frac{1}{M}\int_0^t M_g(s)\,\mathrm{d}s\right)\psi + \varphi_\infty\right) \overset{t\to\infty}{\longrightarrow} h_1(\varphi_\infty),$$

$$h_2\left(\exp\left(-\frac{2}{M}\int_0^t M_g(s)\,\mathrm{d}s\right)\psi + \varphi_\infty, \exp\left(-\frac{2}{M}\int_0^t M_g(s)\,\mathrm{d}s\right)\psi_* + \varphi_\infty\right) \overset{t\to\infty}{\longrightarrow} h_2(\varphi_\infty,\varphi_\infty)$$

for every $\psi \in \mathbb{R}$. Further we use the relations (5.17) and (5.3) for concluding L^1-boundedness of $\tilde{f}$ and $\tilde{g}$ for all times $t \geq 0$. Moreover, due to (5.5) we further observe

$$M_{\tilde{f}}(t) = M_f(t) \overset{t\to\infty}{\longrightarrow} M_{f_\infty},$$

$$M_{\tilde{g}}(t) = M_g(t) \overset{t\to\infty}{\longrightarrow} M_{g_\infty}$$

from which (5.19) and hence the claim follows.

□

5.2.4 Instantaneous limit

In this section we tackle the question about deriving an instantaneous collision model from (5.2) by performing the limit where the average collision-time goes to zero. We start with the assumption that the collision dynamics are much faster than the free flight dynamics under which we introduce the small parameter $\varepsilon << 1$ and perform the scaling

$$g \mapsto \varepsilon g,\ \gamma \mapsto \varepsilon^{-1}\gamma,\ V \mapsto \varepsilon^{-1}V.$$

We obtain the singular perturbed problem of the from

$$\begin{aligned} \partial_t f &= 2\Big(\gamma \int_{\mathbb{R}} g \, \mathrm{d}\varphi_* - \lambda M_f f\Big), \\ \varepsilon \partial_t g + \nabla \cdot (Vg) &= \lambda f f^* - \gamma g. \end{aligned} \tag{5.20}$$

The formal limit $\varepsilon \to 0$ of this singular perturbed problem yields

$$\begin{aligned} \partial_t f &= 2\Big(\gamma \int_{\mathbb{R}} g \, \mathrm{d}\varphi_* - \lambda M_f f\Big), \\ \nabla \cdot (Vg) &= \lambda f f^* - \gamma g, \end{aligned} \tag{5.21}$$

where the equation for particles pairs in collision is not time dependent, allowing us to compute g explicitly and incorporate it into the right hand side of the f-equation with the aim to obtain an alignment collision operator.
We use (5.1) and write the second equation of (5.21) as

$$\frac{1}{2}(\varphi_* - \varphi)\partial_\varphi g(\varphi, \varphi_*) + \frac{1}{2}(\varphi - \varphi_*)\partial_{\varphi_*} g(\varphi, \varphi_*) = (1-\gamma) g(\varphi, \varphi_*) + \lambda f(\varphi) f(\varphi_*),$$

which has a singularity on the manifold $\Gamma := \Big\{(\varphi, \varphi_*) \in \mathbb{R}^2 : \ \varphi = \varphi_*\Big\}$.

Solving the ODE for g: In (5.21), we perform the following coordinate transformation

$$p = \frac{1}{2}(\varphi + \varphi_*)\,, \qquad q = \frac{1}{2}(\varphi - \varphi_*)\,,$$

giving

$$-q\partial_q g = (1-\gamma) g + \lambda f(p+q) f(p-q)\,,$$

an equation symmetric under $q \to -q$. Noting that $|q|^{\gamma-1}$ solves the homogeneous equation and is not integrable, we obtain by variation of constants

$$\begin{aligned} g &= \lambda |q|^{\gamma-1} \int_{|q|}^{\infty} |q'|^{-\gamma} f(p+q') f(p-q') \, \mathrm{d}q' \\ &= 2^{1-\gamma} \lambda |\varphi - \varphi_*|^{\gamma-1} \int_{|\varphi-\varphi_*|/2}^{\infty} |q'|^{-\gamma} f\left(\frac{\varphi+\varphi_*}{2} + q'\right) f\left(\frac{\varphi+\varphi_*}{2} - q'\right) \mathrm{d}q'\,, \end{aligned} \tag{5.22}$$

as the only solution having a chance to be integrable. In the integral $\int g \, d\varphi_*$ we introduce the new coordinates

$$u = q' + \frac{\varphi_* - \varphi}{2}\,, \qquad v = q' - \frac{\varphi_* - \varphi}{2}\,,$$

satisfying $|\varphi - \varphi_*| = |u - v|$ and

$$q' > \frac{|\varphi - \varphi_*|}{2} \qquad \Leftrightarrow \qquad u, v > 0\,.$$

Therefore, we obtain

$$\int_{-\infty}^{\infty} g(\varphi, \varphi_*) d\varphi_* = 2\lambda \int_0^{\infty} \int_0^{\infty} |u-v|^{\gamma-1} |u+v|^{-\gamma} f(\varphi+u) f(\varphi-v) \mathrm{d}u \, \mathrm{d}v\,.$$

Inserting this into the governing equation for the single particles f, yields the following kinetic model

$$\partial_t f = 4\gamma\lambda \int_0^{\infty} \int_0^{\infty} |u-v|^{\gamma-1} |u+v|^{-\gamma} f(\varphi+u) f(\varphi-v) \mathrm{d}u \, \mathrm{d}v - 2\lambda f \int_{\mathbb{R}} f_* \, \mathrm{d}\varphi_*. \tag{5.23}$$

Weak formulation: The right-hand-side of (5.23) defines the *collision operator* and is denoted by

$$\begin{aligned} Q(f,f)(\varphi) &= G(f,f)(\varphi) - L(f,f)(\varphi) \\ &= 4\gamma\lambda \int_0^\infty \int_0^\infty |u-v|^{\gamma-1}|u+v|^{-\gamma} f(\varphi+u)f(\varphi-v)\,\mathrm{d}u\,\mathrm{d}v \\ &\quad - 2\lambda f(\varphi)\int_{\mathbb{R}} f(\varphi_*)\,\mathrm{d}\varphi_*, \end{aligned}$$

for every $\varphi \in \mathbb{R}$. The weak formulation of the collision operator is obtained by first integrating against a test-function $h = h(\varphi)$ and then performing coordinate changes as well as using symmetrization arguments. More precisely we write

$$\begin{aligned} \int_{\mathbb{R}} Q(f,f)h(\varphi)\mathrm{d}\varphi &= 4\lambda\gamma \int_{\mathbb{R}}\int_0^\infty \int_0^\infty |u-v|^{\gamma-1}|u+v|^{-\gamma} f(\varphi+u)f(\varphi-v)h(\varphi)\mathrm{d}u\,\mathrm{d}v\,\mathrm{d}\varphi \\ &\quad - 2\lambda \int_{\mathbb{R}^2} f(\varphi)f(\varphi_*)h(\varphi)\mathrm{d}\varphi_*\,\mathrm{d}\varphi \end{aligned}$$

and calculate the gain and the loss-term separately. In the *gain-term* we perform the coordinate change

$$x = \varphi + \frac{u-v}{2} \in \mathbb{R}, \quad y = \frac{u+v}{2} \in [0,\infty), \quad z = \frac{u-v}{u+v} \in [-1,1],$$

with Jacobian $D_{(u,v,\varphi)\to(x,y,z)} = 2y$, which yields

$$\begin{aligned} \int_{\mathbb{R}} G(f,f)h(\varphi)\mathrm{d}\varphi &= 4\lambda\gamma \int_{\mathbb{R}}\int_0^\infty \int_0^\infty |u-v|^{\gamma-1}|u+v|^{-\gamma} f(\varphi+u)f(\varphi-v)h(\varphi)\mathrm{d}u\,\mathrm{d}v\,\mathrm{d}\varphi \\ &= 4\lambda\gamma \int_{\mathbb{R}}\int_0^\infty \int_{-1}^1 |z|^{\gamma-1} f(x+y)f(x-y)h(x-zy)\mathrm{d}z\,\mathrm{d}y\,\mathrm{d}x \\ &= 2\lambda\gamma \int_{\mathbb{R}^2}\int_{-1}^1 |z|^{\gamma-1} f(x+y)f(x-y)h(x-zy)\mathrm{d}z\,\mathrm{d}y\,\mathrm{d}x, \end{aligned}$$

where the last equality is due to symmetry of $(x,y,z) \leftrightarrow (x,-y,-z)$. Starting from this formulation, we further introduce the new coordinates

$$\varphi = x + y \in \mathbb{R}, \quad \text{and} \quad \varphi_* = x - y \in \mathbb{R},$$

whose corresponding Jacobian is given by $D_{(x,y)\to(\varphi,\varphi_*)} = \frac{1}{2}$. The gain term in weak formulation then has the shape

$$\int_{\mathbb{R}} G(f,f)h(\varphi)\mathrm{d}\varphi = \lambda\gamma \int_{\mathbb{R}^2}\int_{-1}^1 |z|^{\gamma-1} h\Big(\frac{\varphi+\varphi_*}{2} + z\frac{\varphi_*-\varphi}{2}\Big) f(\varphi_*)f(\varphi)\mathrm{d}z\,\mathrm{d}\varphi_*\,\mathrm{d}\varphi.$$

In the *loss term* we use the usual symmetrization argument and obtain

$$\int_{\mathbb{R}} L(f,f)h(\varphi)\mathrm{d}\varphi = \lambda \int_{\mathbb{R}^2} f(\varphi)f(\varphi_*)(h(\varphi)+h(\varphi_*))\mathrm{d}\varphi_*\,\mathrm{d}\varphi.$$

Putting the contributions from the gain- and the loss term together we are able to write the *weak formulation of the collision operator* as

$$\begin{aligned} &\int_{\mathbb{R}} Q(f,f)h(\varphi)\mathrm{d}\varphi \\ &= \lambda \int_{\mathbb{R}^2} f(\varphi)f(\varphi_*)\left(\gamma\int_{-1}^1 |z|^{\gamma-1} h\Big(\frac{\varphi+\varphi_*}{2} + z\frac{\varphi_*-\varphi}{2}\Big)\mathrm{d}z - h(\varphi) - h(\varphi_*)\right)\mathrm{d}\varphi_*\,\mathrm{d}\varphi. \end{aligned} \tag{5.24}$$

Conservation laws: Choosing the test-function h in the weak formulation (5.24) accordingly, we can deduce the following conservation laws:
For $h \equiv 1$ in (5.24) we obtain

$$\int_{\mathbb{R}} Q(f,f)\mathrm{d}\varphi = \lambda \int_{\mathbb{R}^2} ff_* \left(2\gamma \int_0^1 z^{\gamma-1}\mathrm{d}z - 2 \right) \mathrm{d}\varphi_* \, \mathrm{d}\varphi = 0,$$

by using

$$\int_{-1}^1 |z|^{\gamma-1}\mathrm{d}z = 2\int_0^1 z^{\gamma-1}\mathrm{d}z = \frac{2}{\gamma}.$$

This observation yields that the *mass of the system*

$$M = M_f := \int_{\mathbb{R}} f\mathrm{d}\varphi \equiv const$$

is constant with respect to time.
Similar calculations yield for $h(\varphi) = \varphi, \forall \varphi \in \mathbb{R}$

$$\begin{aligned}\int_{\mathbb{R}} Q(f,f)\varphi\mathrm{d}\varphi &= \lambda \int_{\mathbb{R}^2} ff_* \left(\gamma \int_{-1}^1 |z|^{\gamma-1} \left(\frac{\varphi+\varphi_*}{2} + z\frac{\varphi_*-\varphi}{2} \right) \mathrm{d}z - \varphi_* - \varphi \right) \mathrm{d}\varphi_* \, \mathrm{d}\varphi \\ &= \lambda \int_{\mathbb{R}^2} ff_* \left(\gamma(\varphi+\varphi_*) \int_0^1 z^{\gamma-1}\mathrm{d}z + \frac{\gamma}{2}(\varphi_*-\varphi) \int_{-1}^1 z|z|^{\gamma-1}\mathrm{d}z - \varphi_* - \varphi \right) \mathrm{d}\varphi_* \, \mathrm{d}\varphi \\ &= 0,\end{aligned}$$

due to the same argument as above and the observation that

$$\int_{-1}^1 z|z|^{\gamma-1}\mathrm{d}z = 0.$$

This shows that also the *mean value*

$$\int_{\mathbb{R}} \varphi f \mathrm{d}\varphi := M\varphi_\infty$$

is a conserved quantity.
Last, we choose $h(\varphi) = (\varphi - \varphi_\infty)^2, \forall \varphi \in \mathbb{R}$ in (5.24), which yields

$$\begin{aligned}&\int_{\mathbb{R}} Q(f,f)(\varphi-\varphi_\infty)^2\mathrm{d}\varphi \\ &= \lambda \int_{\mathbb{R}^2} ff_* \left(\gamma \int_{-1}^1 |z|^{\gamma-1} \left(\frac{\varphi+\varphi_*}{2} + z\frac{\varphi_*-\varphi}{2} - \varphi_\infty \right)^2 \mathrm{d}z - (\varphi-\varphi_\infty)^2 - (\varphi_*-\varphi_\infty)^2 \right) \mathrm{d}\varphi_* \, \mathrm{d}\varphi \\ &= \lambda \int_{\mathbb{R}^2} ff_* \left(\frac{\Big((\varphi-\varphi_\infty)+(\varphi_*-\varphi_\infty)\Big)^2}{2} + \frac{\gamma}{\gamma+2}\frac{(\varphi-\varphi_*)^2}{2} - (\varphi-\varphi_\infty)^2 - (\varphi_*-\varphi_\infty)^2 \right) \mathrm{d}\varphi_* \, \mathrm{d}\varphi \\ &= \lambda \int_{\mathbb{R}^2} ff_* \left(-\frac{\Big((\varphi-\varphi_\infty)-(\varphi_*-\varphi_\infty)\Big)^2}{2} + \frac{\gamma}{\gamma+2}\frac{(\varphi-\varphi_*)^2}{2} \right) \mathrm{d}\varphi_* \, \mathrm{d}\varphi \\ &= -\frac{\lambda}{\gamma+2} \int_{\mathbb{R}^2} (\varphi-\varphi_*)^2 ff_* \mathrm{d}\varphi_* \, \mathrm{d}\varphi \le 0.\end{aligned}$$

First, one can deduce from this formulation that $Q(f,f)(\varphi)=0$ implies either $f(\varphi)=0$ or $f(\varphi_*)=0$ for all $\varphi_* \neq \varphi$, from which one can further conclude that an equilibrium can only be concentrated at one point, i.e.

$$f_\infty = \delta_{\varphi_\infty}$$

which is given by the *mean value* $\varphi_\infty := \frac{1}{M}\int_{\mathbb{R}} \varphi f \mathrm{d}\varphi$ due to conservation of the first moment.
By

$$\mathcal{V}[f] := \int_{\mathbb{R}} (\varphi - \varphi_\infty)^2 f \mathrm{d}\varphi$$

we define the (relative) *variance* of the system. In the following we compute the time derivative along a solution trajectory. We obtain

$$\begin{aligned}
\frac{\mathrm{d}}{\mathrm{d}t}\mathcal{V}[f] &= \int_{\mathbb{R}} Q(f,f)(\varphi-\varphi_\infty)^2 \mathrm{d}\varphi = -\frac{\lambda}{\gamma+2}\int_{\mathbb{R}^2}(\varphi-\varphi_*)^2 f f_* \mathrm{d}\varphi_* \,\mathrm{d}\varphi \\
&= -\frac{\lambda}{\gamma+2}\int_{\mathbb{R}^2}((\varphi-\varphi_\infty)-(\varphi_*-\varphi_\infty))^2 f f_* \mathrm{d}\varphi_* \,\mathrm{d}\varphi \\
&= -\frac{2\lambda M}{\gamma+2}\int_{\mathbb{R}}(\varphi-\varphi_\infty)^2 f \mathrm{d}\varphi_* + \left(\frac{2\lambda}{\gamma+2}\int_{\mathbb{R}}(\varphi-\varphi_\infty) f \,\mathrm{d}\varphi\right)^2 \\
&= -\frac{2\lambda M}{\gamma+2}\mathcal{V}[f],
\end{aligned}$$

which shows *exponential* decay of $\mathcal{V}$ in time. The variance only stops decreasing if $f(\varphi)=f(\varphi_*)$ for all $\varphi \neq \varphi_* \in \mathbb{R}$, which means $f \equiv \delta_{\varphi_\infty}$.

Existence and uniqueness of solutions:

Theorem 5.3. *Equipped with initial conditions $f_I \in L^1_+(\mathbb{R})$, the model (5.23) has a unique global solution $f \in C\Big([0,\infty); L^1_+(\mathbb{R})\Big)$.*

Proof. Let $f,h \in L^1(\mathbb{R})$ with $\|f\|_{L^1(\mathbb{R})}, \|h\|_{L^1(\mathbb{R})} \leq M$. In the following we aim to show Lipschitz-continuity of the collision operator Q by estimating

$$\|Q(f,f)-Q(h,h)\|_{L^1(\mathbb{R})} \leq \|G(f,f)-G(h,h)\|_{L^1(\mathbb{R})} + \|L(f,f)-L(h,h)\|_{L^1(\mathbb{R})},$$

where we will treat the *gain-* and *loss-term* separately.

$$\begin{aligned}
&\|G(f,f)-G(h,h)\|_{L^1(\mathbb{R})} \\
&\quad\leq 4\lambda\gamma\int_{\mathbb{R}}\int_0^\infty\int_0^\infty \left|\frac{u-v}{u+v}\right|^{\gamma-1}\frac{1}{u+v}\left|f(\varphi+u)f(\varphi-v)-h(\varphi+u)h(\varphi-v)\right| \mathrm{d}u\,\mathrm{d}v\,\mathrm{d}\varphi \\
&\quad= 4\lambda\gamma\int_{\mathbb{R}}\int_0^\infty\int_0^\infty \left|\frac{u-v}{u+v}\right|^{\gamma-1}\frac{1}{u+v}|f(\varphi+u)||f(\varphi-v)-h(\varphi-v)| \,\mathrm{d}u\,\mathrm{d}v\,\mathrm{d}\varphi \\
&\quad+ 4\lambda\gamma\int_{\mathbb{R}}\int_0^\infty\int_0^\infty \left|\frac{u-v}{u+v}\right|^{\gamma-1}\frac{1}{u+v}|h(\varphi-v)||f(\varphi+u)-h(\varphi+u)| \,\mathrm{d}u\,\mathrm{d}v\,\mathrm{d}\varphi.
\end{aligned}$$

Performing now the coordinate transformation

$$x = \varphi + \frac{u-v}{2} \in \mathbb{R}, \quad y = \frac{u+v}{2} \in [0,\infty), \quad z = \frac{u-v}{u+v} \in [-1,1],$$

we obtain

$$\begin{aligned}\|G(f,f)-G(h,h)\|_{L^1(\mathbb{R})}&\\ &\leq 4\gamma\lambda\int_{\mathbb{R}}\int_0^\infty\int_{-1}^1 z^{\gamma-1}|f(x+y)||f(x-y)-h(x-y)|\,\mathrm{d}z\,\mathrm{d}y\,\mathrm{d}x\\ &+4\gamma\lambda\int_{\mathbb{R}}\int_0^\infty\int_{-1}^1 z^{\gamma-1}|h(x-y)||f(x+y)-h(x+y)|\,\mathrm{d}z\,\mathrm{d}y\,\mathrm{d}x.\end{aligned}$$

After making use of the symmetry $y\leftrightarrow -y$ as well as performing yet another coordinate change

$$\varphi = x+y\in\mathbb{R},\quad \text{and}\quad \varphi_* = x-y\in\mathbb{R},$$

the right hand side of the above estimate can be reformulated as

$$\begin{aligned}\|G(f,f)-G(h,h)\|_{L^1(\mathbb{R})}&\\ &\leq \lambda\int_{\mathbb{R}^2}\left(|f(\varphi)||f(\varphi_*)-h(\varphi_*)|+|h(\varphi_*)||f(\varphi)-h(\varphi_*)|\right)\mathrm{d}\varphi_*\,\mathrm{d}\varphi,\end{aligned}$$

where also the identity

$$\int_{-1}^1 z^{\gamma-1}\,\mathrm{d}z = \frac{2}{\gamma}$$

was taken into account. From assumption $\|f\|_{L^1(\mathbb{R})},\|h\|_{L^1(\mathbb{R})}\leq M$ we can conclude

$$\|G(f,f)-G(h,h)\|_{L^1(\mathbb{R})}\leq 2\lambda M\|f-h\|_{L^1(\mathbb{R})}.$$

Estimating the loss-term yields

$$\begin{aligned}\|L(f,f)-L(h,h)\|_{L^1(\mathbb{R})}&\leq 2\lambda\int_{\mathbb{R}^2}|f(\varphi)f(\varphi_*)-h(\varphi)h(\varphi_*)|\,\mathrm{d}\varphi_*\,\mathrm{d}\varphi\\ &=2\lambda\int_{\mathbb{R}^2}\left(|f(\varphi)||f(\varphi_*)-h(\varphi_*)|+|h(\varphi_*)||f(\varphi)-h(\varphi)|\right)\mathrm{d}\varphi_*\,\mathrm{d}\varphi\\ &\leq 4\lambda M\|f-g\|_{L^1(\mathbb{R})},\end{aligned}$$

from which together with the estimate of the gain-term we can conclude the desired Lipschitz estimate of the whole collision operator

$$\|Q(f,f)-Q(h,h)\|_{L^1(\mathbb{R})}\leq 6M\lambda\|f-h\|_{L^1(\mathbb{R})}.$$

Therefore, a unique local solution exists by Picard iteration. Maintenance of positivity as well as mass conservation are obvious, where the latter implies global existence. □

Rigorous instantaneous limit:

Theorem 5.4 (Rigorous instantaneous limit)**.** *Let $(f_\varepsilon,g_\varepsilon)$, be the solution to (5.20). Then*

$$(f_\varepsilon,g_\varepsilon)\longrightarrow(f,g),\quad \textit{for } \varepsilon\to 0 \tag{5.25}$$

in the sense of distributions, where (f,g) is the solution to (5.21).

Proof. We start from the scaled equations (5.20)

$$\partial_t f_\varepsilon = 2\gamma \int_{\mathbb{R}} g_\varepsilon \, \mathrm{d}\varphi_* - 2\lambda M_{f_\varepsilon} f_\varepsilon,$$
$$\varepsilon \partial_t g_\varepsilon + \nabla_{(\varphi,\varphi_*)} \cdot (V g_\varepsilon) = \lambda f_\varepsilon f_{\varepsilon *} - \gamma g_\varepsilon,$$

where we denote its solution by $(f_\varepsilon, g_\varepsilon)$. We aim to rigorously prove convergence in the sense of distributions of

$$(f_\varepsilon, g_\varepsilon) \longrightarrow (f, g), \qquad \text{as } \varepsilon \to 0,$$

where (f, g) is the solution to (5.23) with g given by (5.22). We first make the following observations on the masses M_{f_ε} and M_{g_ε}:
From total mass conservation

$$M_{f_\varepsilon} + 2\varepsilon M_{g_\varepsilon} = M = const.$$

we obtain boundedness of $M_{f_\varepsilon} \leq M$, independent of ε. Further, by integrating the equation for g_ε over $\mathbb{R}^2$ we obtain

$$\dot{M}_{g_\varepsilon} = \frac{\lambda}{\varepsilon} M_{f_\varepsilon}^2 - \frac{\gamma}{\varepsilon} g_\varepsilon \leq \frac{\lambda}{\varepsilon} M^2 - \frac{\gamma}{\varepsilon} M_{g_\varepsilon},$$

from which we can conclude

$$M_{g_\varepsilon} \leq e^{-\frac{\gamma t}{\varepsilon}} M_{g_0} + \frac{\lambda M^2}{\gamma} \left(1 - e^{-\frac{\gamma t}{\varepsilon}}\right) \leq M_{g_0} + \frac{\lambda M^2}{\gamma},$$

and hence, also boundedness of M_{g_ε} independent of ε. Moreover, from the uniform bound on g_ε we can conclude convergence

$$M_{f_\varepsilon} = M - 2\varepsilon M_{g_\varepsilon} \to M, \quad \text{for} \quad \varepsilon \to 0. \tag{5.26}$$

Similarly we observe the following for the variances:

$$V_{f_\varepsilon} \leq V_{f_\varepsilon} + 2\varepsilon V_{g_\varepsilon} \searrow 0, \qquad \text{for } t \to \infty,$$

due to (5.8). For investigating V_{g_ε} we multiply the equation of g_ε by $(\varphi - \varphi_\infty)^2$ and integrate w.r.t φ and φ_*.

$$\dot{V}_{g_\varepsilon} = -\int_{\mathbb{R}^2} (\varphi - \varphi_*)^2 g_\varepsilon \, \mathrm{d}\varphi_* \mathrm{d}\varphi + \frac{\lambda}{\varepsilon} M_{f_\varepsilon} V_{f_\varepsilon} - \frac{\gamma}{\varepsilon} V_{g_\varepsilon} \leq \frac{\lambda}{\varepsilon} M V_0 - \frac{\gamma}{\varepsilon} V_{g_\varepsilon},$$

from which we can conclude

$$V_{g_\varepsilon} \leq e^{-\frac{\gamma t}{\varepsilon}} V_{g_0} + \frac{\lambda M V_0}{\gamma} \left(1 - e^{-\frac{\gamma t}{\varepsilon}}\right) \leq V_{g_0} + \frac{\lambda M V_0}{\gamma},$$

where we used the notation $V_0 := V_{f_0} + 2\varepsilon V_{g_0}$.
Due to the boundedness of the masses as well as variances we know that $\{\frac{f_\varepsilon}{M_{f_\varepsilon}}\}_\varepsilon$ and $\{\frac{g_\varepsilon}{M_{g_\varepsilon}}\}_\varepsilon$ are *tight sets* of probability measures on $\mathcal{P}(\mathbb{R})$ and $\mathcal{P}(\mathbb{R}^2)$. Due to *Prokhorov's theorem* [27] this is equivalent to weak sequentially compactness of $\frac{f_\varepsilon}{M_{f_\varepsilon}}$ and $\frac{g_\varepsilon}{M_{g_\varepsilon}}$, which implies that there exist sequences, denoted by $\{\varepsilon_n\}_n$, with $\varepsilon_n \to 0$ for $n \to \infty$, and a probability measures $\frac{f}{M}$ on $\mathcal{P}(\mathbb{R})$ and $\frac{g}{M}$ on $\mathcal{P}(\mathbb{R}^2)$, such that $\left\{\frac{f_{\varepsilon_n}}{M_{f_{\varepsilon_n}}}\right\}_n \overset{n\to\infty}{\rightharpoonup} \frac{f}{M}$ and $\left\{\frac{g_{\varepsilon_n}}{M_{g_{\varepsilon_n}}}\right\}_n \overset{n\to\infty}{\rightharpoonup} \frac{g}{M}$, i.e.

$$\frac{1}{M_{f_{\varepsilon_n}}} \int_{\mathbb{R}} f_{\varepsilon_n}(\varphi) h_1(\varphi) \, \mathrm{d}\varphi \longrightarrow \frac{1}{M} \int_{\mathbb{R}} f(\varphi) h_1(\varphi) \, \mathrm{d}\varphi,$$

and

$$\frac{1}{M_{g_{\varepsilon_n}}}\int_{\mathbb{R}^2} g_{\varepsilon_n}(\varphi,\varphi_*)h_2(\varphi,\varphi_*)\,\mathrm{d}\varphi_*\mathrm{d}\varphi \longrightarrow \frac{1}{\tilde{M}}\int_{\mathbb{R}^2} g(\varphi,\varphi_*)h_2(\varphi,\varphi_*)\,\mathrm{d}\varphi_*\mathrm{d}\varphi,$$

for all bounded, continuous test functions h_1 on $\mathbb{R}$, h_2 on $\mathbb{R}^2$. By $\tilde{M}$ we denoted the limit of M_{g_ε} for $\varepsilon \to 0$. By matters of simplicity, the above mentioned subsequences will again be denoted as $\{\frac{f_\varepsilon}{M_{f_\varepsilon}}\}_\varepsilon$ and $\{\frac{g_\varepsilon}{M_{g_\varepsilon}}\}_\varepsilon$. Next, we need to show that the limit (f,g) also fulfills (5.21) in a weak sense, i.e.

$$2\int_{\mathbb{R}}\left(\gamma\int_{\mathbb{R}} g_\varepsilon(\varphi,\varphi_*)\,\mathrm{d}\varphi_* - \lambda M_{f_\varepsilon} f_\varepsilon(\varphi)\right)h_1(\varphi)\,\mathrm{d}\varphi \overset{\varepsilon\to 0}{\longrightarrow} 2\int_{\mathbb{R}}\left(\gamma\int_{\mathbb{R}} g(\varphi,\varphi_*)\,\mathrm{d}\varphi_* - \lambda M f(\varphi)\right)h_1(\varphi)\,\mathrm{d}\varphi, \tag{5.27}$$

and

$$\int_{\mathbb{R}^2}\left(-\nabla_{(\varphi,\varphi_*)}\cdot(Vg_\varepsilon)(\varphi,\varphi_*) + \lambda f_\varepsilon(\varphi_*)f_\varepsilon(\varphi) - \gamma g + \varepsilon(\varphi,\varphi_*)\right)h_2(\varphi,\varphi_*)\,\mathrm{d}\varphi\mathrm{d}\varphi_* \overset{\varepsilon\to 0}{\longrightarrow}$$
$$\int_{\mathbb{R}^2}\left(-\nabla_{(\varphi,\varphi_*)}\cdot(Vg)(\varphi,\varphi_*) + \lambda f(\varphi_*)f(\varphi) - \gamma g(\varphi,\varphi_*)\right)h_2(\varphi,\varphi_*)\,\mathrm{d}\varphi\mathrm{d}\varphi_*.$$

The fact that we can interpret $h_1(\varphi) = \tilde{h}_1(\varphi,\varphi_*)$ as bounded continuous test-function in both variables allows us to go to the limit in the gain-term of (5.27). For the loss term we have to use (5.26).
We let $\varepsilon \to 0$ in the g_ε-equation. While the passage to the limit in the loss-term is straight forward, for the gain-term we first have to restrict ourselves to test-functions which factorize, i.e.

$$h_2(\varphi,\varphi_*) = h_2^1(\varphi)h_2^2(\varphi_*), \quad \forall\varphi,\varphi_*\in\mathbb{R}, \tag{5.28}$$

with h_2^1 and h_2^2 are bounded continuous functions on $\mathbb{R}$. Indeed, for such test-functions we have

$$\lambda\int_{\mathbb{R}^2} f_\varepsilon(\varphi)f_\varepsilon(\varphi_*)h_2(\varphi,\varphi_*)\,\mathrm{d}\varphi_*\mathrm{d}\varphi = \lambda M_{f_\varepsilon}^2\int_{\mathbb{R}}\frac{f_\varepsilon(\varphi)}{M_{f_\varepsilon}}h_2^2(\varphi)\,\mathrm{d}\varphi\int_{\mathbb{R}}\frac{f_\varepsilon(\varphi_*)}{M_{f_\varepsilon}}h_2^2(\varphi_*)\,\mathrm{d}\varphi_*.$$

Due to Prokhorov's theorem convergence of the two factors hold

$$\int_{\mathbb{R}}\frac{f_\varepsilon(\varphi)}{M_{f_\varepsilon}}h_2^1(\varphi)\,\mathrm{d}\varphi \overset{\varepsilon\to 0}{\longrightarrow}\int_{\mathbb{R}}\frac{f(\varphi)}{M}h_2^1(\varphi)\,\mathrm{d}\varphi,$$
$$\int_{\mathbb{R}}\frac{f_\varepsilon(\varphi)}{M_{f_\varepsilon}}h_2^2(\varphi)\,\mathrm{d}\varphi \overset{\varepsilon\to 0}{\longrightarrow}\int_{\mathbb{R}}\frac{f(\varphi)}{M}h_2^2(\varphi)\,\mathrm{d}\varphi,$$

which implies, together with $M_{f_\varepsilon}\to M$ as $\varepsilon\to 0$,

$$\begin{aligned}\lambda\int_{\mathbb{R}^2} f_\varepsilon(\varphi)f_\varepsilon(\varphi_*)h_2(\varphi,\varphi_*)\,\mathrm{d}\varphi_*\mathrm{d}\varphi &\overset{\varepsilon\to 0}{\longrightarrow}\lambda\int_{\mathbb{R}} f(\varphi)h_2^1(\varphi)\,\mathrm{d}\varphi\int_{\mathbb{R}} f(\varphi_*)h_2^2(\varphi_*)\,\mathrm{d}\varphi_*\\ &=\lambda\int_{\mathbb{R}^2} f(\varphi)f(\varphi_*)h_2(\varphi,\varphi_*)\,\mathrm{d}\varphi_*\mathrm{d}\varphi.\end{aligned}$$

We now consider test-functions of the form:

$$h_2(\varphi,\varphi_*) = h_2^1(\varphi) + h_2^2(\varphi_*), \quad \forall\varphi,\varphi_*\in\mathbb{R}, \tag{5.29}$$

with h_2^1 and h_2^2 are bounded continuous functions on $\mathbb{R}$, which yields

$$\begin{aligned}&\lambda\int_{\mathbb{R}^2} f_\varepsilon(\varphi)f_\varepsilon(\varphi_*)h_2(\varphi,\varphi_*)\,\mathrm{d}\varphi_*\mathrm{d}\varphi\\ &= \lambda M_{f_\varepsilon}\left(\int_{\mathbb{R}^2}\frac{f_\varepsilon(\varphi)f_\varepsilon(\varphi_*)}{M_{f_\varepsilon}}h_2^1(\varphi)\,\mathrm{d}\varphi\,\mathrm{d}\varphi_* + \int_{\mathbb{R}^2}\frac{f_\varepsilon(\varphi)f_\varepsilon(\varphi_*)}{M_{f_\varepsilon}}h_2^2(\varphi_*)\,\mathrm{d}\varphi\mathrm{d}\varphi_*\right)\\ &\overset{\varepsilon\to 0}{\longrightarrow}\lambda\int_{\mathbb{R}^2} f(\varphi)f(\varphi_*)h_2(\varphi,\varphi_*)\,\mathrm{d}\varphi_*\mathrm{d}\varphi..\end{aligned}$$

We further consider polynomials on a compact set K of $\mathbb{R}^2$ as test-functions which are a subset of continuous and bounded function and whose general expression is given by

$$p(\varphi,\varphi_*)=\sum_{n=0}^{k_1}\sum_{m=0}^{k_2}a_{n,m}\varphi^n\varphi_*^m \qquad a_{n,m}\in\mathbb{R},\ \varphi,\varphi_*\in K$$

These are combinations of test-functions of the form (5.28) and (5.29) with $h_2^1(\varphi)=\varphi^n$ and $h_2^2(\varphi_*)=\varphi_*^m$.
Therefore, for any polynomial $p(\varphi,\varphi_*)\in\mathcal{P}(K\subset\mathbb{R}^2,\mathbb{R})$

$$\lambda\int_{\mathbb{R}^2}f_\varepsilon(\varphi)f_\varepsilon(\varphi_*)p(\varphi,\varphi_*)\,\mathrm{d}\varphi_*\mathrm{d}\varphi\overset{\varepsilon\to0}{\longrightarrow}\lambda\int_{\mathbb{R}^2}f(\varphi)f(\varphi_*)p(\varphi,\varphi_*)\,\mathrm{d}\varphi_*\mathrm{d}\varphi.$$

As a consequence of the *Stone-Weierstrass Theorem* we have that the algebra of all polynomials in $\mathcal{P}(K\subset\mathbb{R}^2,\mathbb{R})$ is dense in $\mathcal{C}(K\subset\mathbb{R}^2,\mathbb{R})$ w.r.t. supremum norm. Thus, any function
$h_2(\varphi,\varphi_*)\in\mathcal{C}(K\subset\mathbb{R}^2,\mathbb{R})$ can be approximated by polynomials, which is implying that the convergence

$$\int_{\mathbb{R}^2}f_\varepsilon(\varphi)f_\varepsilon(\varphi_*)h_2(\varphi,\varphi_*)\,\mathrm{d}\varphi\overset{\varepsilon\to0}{\longrightarrow}\int_{\mathbb{R}^2}f(\varphi)h_2(\varphi,\varphi_*)\,\mathrm{d}\varphi,\qquad\forall h_2\in\mathcal{C}_c^0(\mathbb{R}^2)$$

follows by a density argument. Next, we consider the drift term:

$$\begin{aligned}&\int_{\mathbb{R}^2}\nabla_{(\varphi,\varphi_*)}\cdot(Vg_\varepsilon)(\varphi,\varphi_*)h_2(\varphi,\varphi_*)\,\mathrm{d}\varphi_*\mathrm{d}\varphi=-\int_{\mathbb{R}^2}(Vg_\varepsilon)(\varphi,\varphi_*)\nabla h_2(\varphi,\varphi_*)\,\mathrm{d}\varphi_*\mathrm{d}\varphi\\&=\frac12\int_{\mathbb{R}^2}g_\varepsilon(\varphi,\varphi_*)(\varphi-\varphi_*)(\partial_{\varphi_*}h_2(\varphi,\varphi_*)-\partial_\varphi h_2(\varphi,\varphi_*))\,\mathrm{d}\varphi_*\mathrm{d}\varphi,\end{aligned}$$

where in the first equality we performed integration by parts. We consider test-functions h_2, which together with their fist partial derivatives multiplied by linear polynomials are in $\mathcal{C}_c^0(\mathbb{R}^2)$, which is fulfilled if, for example, we take a test-function h_2 from the *Schwartz space* $\mathcal{S}(\mathbb{R}^2)$. Therefore, h_2, $(\varphi-\varphi_*)\partial_{\varphi_*}h_2$ and $-(\varphi-\varphi_*)\partial_\varphi h_2$ are bounded and continuous, we have due to Prokhorov's theorem

$$\begin{aligned}&\int_{\mathbb{R}^2}\nabla_{(\varphi,\varphi_*)}\cdot(Vg_\varepsilon)(\varphi,\varphi_*)h_2(\varphi,\varphi_*)\,\mathrm{d}\varphi_*\mathrm{d}\varphi\\&=\frac12\int_{\mathbb{R}^2}g_\varepsilon(\varphi,\varphi_*)(\varphi-\varphi_*)(\partial_{\varphi_*}h_2(\varphi,\varphi_*)-\partial_\varphi h_2(\varphi,\varphi_*))\,\mathrm{d}\varphi_*\mathrm{d}\varphi,\\&\overset{\varepsilon\to0}{\longrightarrow}\frac12\int_{\mathbb{R}^2}g(\varphi,\varphi_*)(\varphi-\varphi_*)(\partial_{\varphi_*}h_2(\varphi,\varphi_*)-\partial_\varphi h_2(\varphi,\varphi_*))\,\mathrm{d}\varphi_*\mathrm{d}\varphi\\&=\int_{\mathbb{R}^2}\nabla_{(\varphi,\varphi_*)}\cdot(Vg)(\varphi,\varphi_*)h_2(\varphi,\varphi_*)\,\mathrm{d}\varphi_*\mathrm{d}\varphi\end{aligned}$$

From the observation $\mathcal{C}_c^\infty(\mathbb{R}^2)\subset\mathcal{C}_c^0(\mathbb{R}^2)$ and $\mathcal{C}_c^\infty(\mathbb{R}^2)\subset\mathcal{S}(\mathbb{R}^2)$ we can finally conclude (5.25), which closes the proof. □

5.3 Kinetic Equation for Time-resolved Alignment Collisions with Deterministic Collisions Dynamics

Similar to the model introduced and investigated in Section 5.2, we aim to derive equations describing particles performing binary alignment collisions, this time right away in a spatially homogeneous environment. The difference will be that this time we will not allow randomness in the collision

dynamics themselves. Indeed, on one hand we still assume the collision events to to take place following a Poisson-process with rate $\lambda > 0$, but the collisions themselves are deterministic in the sense that two colliding particles φ, φ_* approach their midpoint $\frac{\varphi+\varphi_*}{2}$ with constant speed 1. The collision ends as soon as the midpoint is reached. According to this, we define the collision potential

$$V(\varphi, \varphi_*) := \frac{1}{2}\begin{pmatrix}\operatorname{sgn}(\varphi_* - \varphi)\\ \operatorname{sgn}(\varphi - \varphi_*)\end{pmatrix}, \quad \varphi \neq \varphi_*. \tag{5.30}$$

The dynamics are then given by the following system of equations

$$\begin{aligned}\partial_t f &= S_f - 2\lambda M_f f, \quad \varphi \in \mathbb{R}\\ \partial_t g + \nabla \cdot (Vg) &= \lambda f f^*, \quad (\varphi, \varphi_*) \in \mathbb{R}^2 \setminus D\end{aligned}$$

where again f describes the distribution function of the single particles with mass $M_f := \int_{\mathbb{R}} f \,\mathrm{d}\varphi$ and g the one for the pairs of particles in collision with mass $M_g := \int_{\mathbb{R}^2} g \,\mathrm{d}\varphi_*\mathrm{d}\varphi$.. Further, we denote by D the diagonal in $\mathbb{R}^2$, i.e. $D := \{(\varphi, \varphi_*) \in \mathbb{R}^2 : \varphi = \varphi_*\}$. The source term S_f arises from the outflow and has to be computed out of mass balance, since the total mass of the system

$$M = \int_{\mathbb{R}} f \,\mathrm{d}\varphi + 2\int_{\mathbb{R}^2} g \,\mathrm{d}\varphi_*\mathrm{d}\varphi$$

also has to be a conserved quantity in this case. Derivation w.r.t. time gives

$$\begin{aligned}\frac{\mathrm{d}}{\mathrm{d}t}M &= \int_{\mathbb{R}} S_f \,\mathrm{d}\varphi - 2\int_{\mathbb{R}^2} \nabla \cdot (Vg) \,\mathrm{d}\varphi_*\mathrm{d}\varphi\\ &= \int_{\mathbb{R}} S_f \,\mathrm{d}\varphi - 2\left(\int_{D_+} (V_+ g) \cdot \nu_+ \,\mathrm{d}S + \int_{D_-} (V_- g) \cdot \nu_- \,\mathrm{d}S\right),\end{aligned}$$

where $D_\pm$ describes the limit approaching the diagonal D from above resp. below and $\nu_\pm$ denotes the corresponding unit outward normal. One can see easily that

$$\nu_+ = \frac{1}{\sqrt{2}}\begin{pmatrix}1\\-1\end{pmatrix}, \quad \nu_- = \frac{1}{\sqrt{2}}\begin{pmatrix}-1\\1\end{pmatrix}$$

as well as

$$V_+ := \lim_{(\varphi,\varphi_*)\to D_+} V(\varphi, \varphi_*) = \frac{1}{\sqrt{2}}\nu_+, \quad V_- := \lim_{(\varphi,\varphi_*)\to D_-} V(\varphi, \varphi_*) = \frac{1}{\sqrt{2}}\nu_-$$

has to hold. Since the diagonal can be parametrized by φ with functional determinant $\sqrt{2}$, we can further calculate

$$\begin{aligned}\frac{\mathrm{d}}{\mathrm{d}t}M &= \int_{\mathbb{R}} S_f \,\mathrm{d}\varphi - 2\sqrt{2}\left(\int_{\mathbb{R}} (V_+ \cdot \nu_+) g(\varphi, \varphi) \,\mathrm{d}\varphi + \int_{\mathbb{R}} (V_- \cdot \nu_-) g(\varphi, \varphi) \,\mathrm{d}\varphi\right)\\ &= \int_{\mathbb{R}} S_f \,\mathrm{d}\varphi - 2\int_{\mathbb{R}} (g_+(\varphi, \varphi) + g_-(\varphi, \varphi)) \,\mathrm{d}\varphi,\end{aligned}$$

where we denote by $g_\pm$ the limit

$$g_\pm(\tilde{\varphi}) := \lim_{(\varphi,\varphi_*)\to D_\pm(\tilde{\varphi},\tilde{\varphi})} g(\varphi, \varphi_*).$$

Since we assume g to be symmetric, we have $g_+ = g_- =: \bar{g}$. From here we can conclude that the gain-term for the single particles has to be of the shape

$$S_f(\varphi) = 4\bar{g}(\varphi), \quad \varphi \in \mathbb{R}.$$

Therefore, the *deterministic model for time-resolved binary alignment collisions* is given by

$$\begin{aligned}\partial_t f &= 4\bar{g} - 2\lambda M_f f, \quad \varphi \in \mathbb{R}\\ \partial_t g + \nabla \cdot (Vg) &= \lambda f f^*, \quad (\varphi, \varphi_*) \in \mathbb{R}^2 \setminus D.\end{aligned} \tag{5.31}$$

5.3.1 Conservation laws and equilibria

We first observe that the *total mass*

$$M := \int_{\mathbb{R}} f \,\mathrm{d}\varphi + 2 \int_{\mathbb{R}^2} g \,\mathrm{d}\varphi \mathrm{d}\varphi_* \tag{5.32}$$

is conserved by construction. Further, we can see easily that the *mean value*

$$I := \int_{\mathbb{R}} \varphi f \,\mathrm{d}\varphi + 2 \int_{\mathbb{R}^2} \varphi g \,\mathrm{d}\varphi \mathrm{d}\varphi_*$$

is conserved by the equation. Indeed, if we calculate its time-derivative we obtain

$$\begin{aligned}\frac{\mathrm{d}}{\mathrm{d}t} I(t) &= 4 \int_{\mathbb{R}} \varphi \bar{g}(\varphi) \,\mathrm{d}\varphi - 2 \int_{\mathbb{R}^2} \varphi \nabla \cdot (Vg)(\varphi, \varphi_*) \,\mathrm{d}\varphi_* \mathrm{d}\varphi \\ &= 4 \int_{\mathbb{R}} \varphi \bar{g}(\varphi) \,\mathrm{d}\varphi - \left(\int_{D_+} \varphi \,(V_+ g) \cdot \nu_+ \,\mathrm{d}S + \int_{D_-} \varphi \,(V_- g) \cdot \nu_- \,\mathrm{d}S \right) = 0,\end{aligned}$$

where we used the same arguments and notation as in the derivation of the model. This allows us to define the mean

$$\varphi_\infty := \frac{I}{M}.$$

Similarly, we define the *total (relative) variance* of the system by

$$\mathcal{V}[f, g](t) := \int_{\mathbb{R}} (\varphi - \varphi_\infty)^2 f \,\mathrm{d}\varphi + 2 \int_{\mathbb{R}^2} (\varphi - \varphi_\infty)^2 g \,\mathrm{d}\varphi \mathrm{d}\varphi_*.$$

Computing the time-derivative yields

$$\begin{aligned}\frac{\mathrm{d}}{\mathrm{d}t} \mathcal{V}(t) &= 4 \int_{\mathbb{R}} (\varphi - \varphi_\infty)^2 \bar{g}(\varphi) \,\mathrm{d}\varphi - \int_{\mathbb{R}^2} \left[(\varphi - \varphi_\infty)^2 + (\varphi_* - \varphi_\infty)^2 \right] \nabla \cdot (Vg)(\varphi, \varphi_*) \,\mathrm{d}\varphi_* \mathrm{d}\varphi \\ &= 4 \int_{\mathbb{R}} (\varphi - \varphi_\infty)^2 \bar{g}(\varphi) \,\mathrm{d}\varphi + 2 \int_{\mathbb{R}^2} \begin{pmatrix} \varphi - \varphi_\infty \\ \varphi_* - \varphi_\infty \end{pmatrix} \cdot \begin{pmatrix} \operatorname{sgn}(\varphi_* - \varphi) \\ \operatorname{sgn}(\varphi - \varphi_*) \end{pmatrix} g(\varphi, \varphi_*) \,\mathrm{d}\varphi_* \mathrm{d}\varphi \\ &\quad - 4 \int_{\mathbb{R}} (\varphi - \varphi_\infty)^2 \bar{g}(\varphi) \,\mathrm{d}\varphi \\ &= -2 \int_{\mathbb{R}^2} |\varphi - \varphi_*| g(\varphi, \varphi_*) \,\mathrm{d}\varphi_* \mathrm{d}\varphi,\end{aligned}$$

i.e. decay of variance. One further notices that, as in the previous model, the variance stops decaying as soon as g, the function of pairs of particles in a collision, is only concentrated on the diagonal, i.e.

$$g(\varphi, \varphi_*) = 0, \quad \text{for all} \quad \varphi \neq \varphi_*.$$

The difference to the previous model with collisions modeled by a stochastic process is, that the decay does not involve the quadratic factor $(\varphi - \varphi_*)^2$, but the linear one $|\varphi - \varphi_*|$. This is due to the fact that we chose the potential in such a way that the mean-value of two colliding particles is reached with constant speed 1 during a collision.

Since we deal with an alignment model, we again expect mass concentrated at a single point for $t \to \infty$, given by the mean value φ_∞. One can easily verify that

$$(f_\infty(\varphi), g_\infty(\varphi, \varphi_*)) := \left(M_{f_\infty} \delta_{\varphi_\infty}(\varphi), \, \frac{\lambda M_{f_\infty}^2}{2} \delta_\varphi(\varphi_*) \delta_{\varphi_\infty}(\varphi) \right),$$

with

$$M_{f_\infty} = -\frac{1}{2\lambda} + \sqrt{\frac{1}{4\lambda^2} + \frac{1}{\lambda}}$$

given by total mass conservation (5.32)

$$M = M_{f_\infty} + 2M_{g_\infty},$$

is an equilibrium of the system (5.31).

5.3.2 Instantaneous limit

Under the assumption that the collision dynamics are much faster than the free flight dynamics, we introduce the small parameter $\varepsilon \ll 1$. Performing the scaling

$$V \mapsto \frac{1}{\varepsilon} V, \quad g \mapsto \varepsilon g,$$

yields the singular perturbed problem

$$\begin{aligned} \partial_t f &= 4\bar{g} - 2\lambda M_f f, \\ \varepsilon \partial_t g + \nabla \cdot (Vg) &= \lambda f f^*. \end{aligned}$$

The formal limit $\varepsilon \to 0$ of this singular perturbed problem leads to the system

$$\begin{aligned} \partial_t f &= 4\bar{g} - 2\lambda M_f f, \\ \nabla \cdot (Vg) &= \lambda f f^*. \end{aligned}$$

As in section 5.2.4 the time-independence of the g-equation allows us to solve it explicitly for given f in order to incorporate it into the f-equation for single particles. Using (5.30) we can write the second equation from (5.31) as

$$\operatorname{sgn}(\varphi_* - \varphi)\partial_\varphi g + \operatorname{sgn}(\varphi - \varphi_*)\partial_{\varphi_*} g = 2\lambda f f^*,$$

which can be transformed to

$$\partial_q g = -2\lambda \operatorname{sgn}(q) f(p+q) f(p-q),$$

via introducing the new coordinates

$$q = \frac{\varphi - \varphi_*}{2}, \quad \text{and} \quad p = \frac{\varphi + \varphi_*}{2}.$$

Integrating this ODE from $|q|$ to ∞ yields

$$g(p,q) = 2\lambda \int_{|q|}^{\infty} f(p+q') f(p-q') \, \mathrm{d}q'$$

and after rewriting it in the old coordinates one obtains the following formula for g

$$g(\varphi, \varphi_*) = 2\lambda \int_{\frac{|\varphi - \varphi_*|}{2}}^{\infty} f\left(\frac{\varphi + \varphi_*}{2} + q'\right) f\left(\frac{\varphi + \varphi_*}{2} - q'\right) \mathrm{d}q'. \tag{5.33}$$

The limit of (5.33) for $(\varphi, \varphi_*) \to D$ is given by

$$\bar{g}(\varphi) = 2\lambda \int_0^\infty f\left(\varphi + q'\right) f\left(\varphi - q'\right)\, \mathrm{d}q'$$

Plugging this into the equation for f yields the following *instantaneous alignment model arising from deterministic collision dynamics*:

$$\begin{aligned}
\partial_t f &= Q_d(f,f) = G_d(f,f) - L_d(f,f) \\
&:= 2\lambda \left[4 \int_0^\infty f(\varphi + q') f(\varphi - q')\, \mathrm{d}q' - Mf \right] \\
&= 2\lambda \left[2 \int_{\mathbb{R}} f(\varphi + q') f(\varphi - q')\, \mathrm{d}q' - Mf \right] \\
&= 2\lambda \left[2 \int_{\mathbb{R}} f(2\varphi + \varphi_*) f(\varphi_*)\, \mathrm{d}\varphi_* - Mf \right],
\end{aligned} \tag{5.34}$$

where from the middle to the last line we made first use of the fact that the gain term is symmetric w.r.t q' in order to the grid of the additional factor 2 and second performed the coordinate change $\varphi_* = \varphi + q'$. We denoted the collision operator by Q_d, quadratic in f and consisting of its gain-term, G_d, and loss-term, L_d. We observe that the model obtained after performing the instantaneous limit corresponds to the usual midpoint/alignment-model, recent matter of investigation in [17,22] and with additional noise term in [14].

Weak formulation and properties of the collision operator: Also here, the *weak formulation* of Q_d is obtained by first multiplying it with a suitable test-function h before integrating it over $\mathbb{R}$. Doing this yields

$$\begin{aligned}
&\int_{\mathbb{R}} Q_d(f,f)(\varphi) h(\varphi)\, \mathrm{d}\varphi = \int_{\mathbb{R}} G_d(f,f)(\varphi) h(\varphi)\, \mathrm{d}\varphi - \int_{\mathbb{R}} L_d(f,f)(\varphi) h(\varphi)\, \mathrm{d}\varphi \\
&= 2\lambda \left[2 \int_{\mathbb{R}^2} f(\varphi' + q') f(\varphi' - q') h(\varphi')\, \mathrm{d}q' \mathrm{d}\varphi' - \int_{\mathbb{R}^2} f(\varphi) f(\varphi_*) h(\varphi)\, \mathrm{d}\varphi_* \mathrm{d}\varphi \right] \\
&= 2\lambda \left[\int_{\mathbb{R}^2} f f^* \left(h\left(\frac{\varphi + \varphi_*}{2} \right) - \frac{h(\varphi) + h(\varphi_*)}{2} \right) \mathrm{d}\varphi_* \mathrm{d}\varphi \right],
\end{aligned} \tag{5.35}$$

where in the integral with the gain-term the transform $(\varphi' + q', \varphi' - q') \to (\varphi, \varphi_*)$ was performed and the change in the loss-term is due to symmetrization.
Choosing $h \equiv 1$ in (5.35), we can deduce immediately that *mass conservation*

$$M := \int_{\mathbb{R}} f\, \mathrm{d}\varphi = const.$$

has to hold. Further, by setting $h(\varphi) = \varphi$, we obtain that the *mean value* of the system (5.34) has to be a conserved quantity, i.e.

$$M\varphi_\infty := \int \varphi f\, \mathrm{d}\varphi = const.$$

Again, we define the *variance of the system* by

$$\mathcal{V}[f](t) := \int_{\mathbb{R}} (\varphi - \varphi_*)^2 f\, \mathrm{d}\varphi.$$

Computing its time-derivative by choosing $h(\varphi) = (\varphi - \varphi_\infty)^2$ in (5.35), we see that it *decays exponentially*:

$$\frac{\mathrm{d}}{\mathrm{d}t}\mathcal{V}[f](t) = -\frac{\lambda}{2}\int_{\mathbb{R}^2}(\varphi-\varphi_*)^2 f f_* \,\mathrm{d}\varphi_*\mathrm{d}\varphi = -\lambda M \int_{\mathbb{R}}(\varphi-\varphi_\infty)^2 f \,\mathrm{d}\varphi = -\lambda M \mathcal{V}[f].$$

Existence and uniqueness of solutions to the instantaneous limit problem: Using the standard method of performing uniform Lipschitz-estimates on the collision operator Q_d before applying the Picard-Lipschitz theorem allows us to obtain existence of unique solutions in L^1, global in time.

Theorem 5.5. *Let $f_I \in L^1_+(\mathbb{R})$, then the model (5.34) has a unique global solution $f \in C\Big([0,\infty); L^1_+(\mathbb{R})\Big)$.*

Proof. Let $f, h \in L^1(\mathbb{R})$ with $\|f\|_{L^1(\mathbb{R})}, \|h\|_{L^1(\mathbb{R})} \leq M$. In the following we aim to show Lipschitz-continuity of the collision operator Q_d by estimating

$$\|Q_d(f,f) - Q_d(h,h)\|_{L^1(\mathbb{R})} \leq \|G_d(f,f) - G_d(h,h)\|_{L^1(\mathbb{R})} + \|L_d(f,f) - L_d(h,h)\|_{L^1(\mathbb{R})},$$

where we will treat the *gain-* and *loss-term* separately.

$$\|G(f,f) - G(h,h)\|_{L^1(\mathbb{R})} \leq 2\lambda \int_{\mathbb{R}^2} |f(2\varphi-\varphi_*)f(\varphi_*) - h(2\varphi-\varphi_*)h(\varphi_*)| \,\mathrm{d}\varphi_*\mathrm{d}\varphi$$

Performing now the coordinate transform $2\varphi - \varphi_* \mapsto \varphi$ in the φ-integral, we obtain

$$\begin{aligned}
\|G_d(f,f) - G_d(h,h)\|_{L^1(\mathbb{R})} &\leq \lambda \int_{\mathbb{R}^2} |f(\varphi)f(\varphi_*) - h(\varphi)h(\varphi_*)| \,\mathrm{d}\varphi_*\mathrm{d}\varphi \\
&\leq \lambda \int_{\mathbb{R}^2} \Big(|f(\varphi_*) - h(\varphi_*)| f(\varphi) + |f(\varphi) - h(\varphi)| h(\varphi_*) \Big) \,\mathrm{d}\varphi_*\mathrm{d}\varphi \\
&\leq 2\lambda M \|f - h\|_{L^1(\mathbb{R})}.
\end{aligned}$$

Estimating the loss-term is trivial

$$\|L_d(f,f) - L_d(h,h)\|_{L^1(\mathbb{R})} \leq 2\lambda M \|f-h\|_{L^1(\mathbb{R})},$$

which gives in total

$$\|Q_d(f,f) - Q_d(h,h)\|_{L^1(\mathbb{R})} \leq 4\lambda M \|f-h\|_{L^1(\mathbb{R})},$$

which gives the desired Lipschitz-estimate for the collision operator Q_d. The existence of a unique solution to (5.34) follows by Picard-iteration. It is obvious that positivity as well as mass is conserved, where from the last global existence follows. □

Bibliography

[1] R.J. Alonso, *Existence of global solutions to the Cauchy problem for the inelastic Boltzmann equation with near-vacuum data,* JSTOR 58 (2009), pp. 999–1022.

[2] R. J. Alonso, V. Bagland, Y. Cheng, B. Lods, *One-Dimensional Dissipative Boltzmann Equation: Measure Solutions, Cooling Rate, and Self-Similar Profile,* SIAM J. Math. Analysis 2015, Vol. 50, pp. 1278-1321

[3] R.J. Alonso, B. Lods, *Two proofs of Haff's law for dissipative gases: The use of entropy and the weakly inelastic regime,* Journal of Mathematical Analysis and Applications, Volume 397, Issue 1, 1 January 2013, Pages 260-275

[4] I.S. Aranson, L.S. Tsimring, *Pattern formation of microtubules and motors: inelastic interaction of polar rods,* Phys Rev E Stat Nonlin Soft Matter Phys. 2005 May;71(5 Pt 1):050901.

[5] A. Baskaran, M.C. Marchetti, *Enhanced Diffusion and Ordering of Self-Propelled Rods,* Phys. Rev. Lett. 101, 268101 – Published 22 December 2008

[6] A. Baskaran, M.C. Marchetti, *Nonequilibrium statistical mechanics of self propelled hard rods,* J. Stat. Mech. 2010 (2010), P04019.

[7] D. Benedetto, M. Pulvirenti, *On the one-dimensional Boltzmann equation for granular flows,* ESAIM: Mathematical Modelling and Numerical Analysis - Modélisation Mathématique et Analyse Numérique, Volume 35 (2001) no. 5, pp. 899-905.

[8] E. Ben-Naim, P.L. Krapivsky, *Alignment of rods and partition of integers,* Phys Rev E Stat Nonlin Soft Matter Phys. 2006 Mar;73(3 Pt 1):031109.

[9] E. Bertin, M. Droz, G. Gregoire, *Hydrodynamic equations for self-propelled particles: microscopic derivation and stability analysis,* J. Phys. A: Math. Theor. 42 (2006), 445001.

[10] A.V. Bobylev, J.A.Carrillo, I.M. Gamba, *On Some Properties of Kinetic and Hydrodynamic Equations for Inelastic Interactions,* Journal of Statistical Physics 98, 743–773 (2000).

[11] A.V. Bobylev, C. Cercignani, *Self-Similar Asymptotics for the Boltzmann Equation with Inelastic and Elastic Interactions,* Journal of Statistical Physics 110, 333–375 (2003).

[12] L. Boltzmann, *Weitere Studien über das Wärmegleichgewicht unter Gasmolekülen,* Sitzungsberichte Akad. Wiss., Vienna, part II, 66 (1872), pp. 275–370.

[13] J. Carrillo, G. Toscani, *Contractive probability metrics and asymptotic behavior of dissipative kinetic equations*, Riv. Mat. Univ. Parma (7) 6 (2007), pp. 75–198.

[14] E. Carlen, M. C. Carvalho, P. Degond, B. Wennberg, *A Boltzmann model for rod alignment and schooling fish,* Nonlinearity 28 (2015), pp. 1783–1804.

[15] C. Cercignani, R. Illner, M. Pulvirenti, *The Mathematical Theory of Dilute Gases*, Springer-Verlag, New York, 1994.

[16] P. Danielewicz and S. Pratt, *Delays Associated with Elementary Processes in Nuclear Reaction Simulations* Phys. Rev. C 53, 249 (1996).

[17] P. Degond, A. Frouvelle, G. Raoul, *Local stability of perfect alignment for a spatially homogeneous kinetic model,* J. Stat. Phys. 157 (2014), pp. 84–112.

[18] P. Degond, A. Manhart, H. Yu, *A continuum model of nematic alignment of self-propelled particles,* DCDS-B 22 (2017), pp. 1295–1327.

[19] P. Degond, A. Manhart, H. Yu, *An age-structured continuum model for myxobacteria,* M3AS 28 (2018), pp. 1737–1770.

[20] R.J. DiPerna, P-L. Lions, *On the Cauchy problem for Boltzmann equations: Global existence and weak stability*, Ann. Math., 130, (1989), 321–366.

[21] P. Haff, *Grain flow as a fluid-mechanical phenomenon,* J. Fluid Mech. 134 (1983), pp. 401–30.

[22] S. Hittmeir, L. Kanzler, A. Manhart, C. Schmeiser, *Kinetic modelling of colonies of myxobacteria,* Kinetic and Related Models, doi:10.3934/krm.2020046

[23] P.-E. Jabin, T. Rey, *Hydrodynamic limit of granular gases to pressureless Euler in dimension 1,* Quart. Appl. Math. 75 (2017), 155–179.

[24] O. E. Lanford, *Time evolution of large classical systems,* Lect. Notes Phys. 38 (1975), pp. 1–111.

[25] P. Lipavsky, V. Spicka, K. Morawetz, *Non-instant collisions and two concepts of quasiparticles,* February 1999, Physical review. E, Statistical physics, plasmas, fluids, and related interdisciplinary topics 59(2)

[26] S. Mischler, C. Mouhot, M. Rodriguez Ricard, *Cooling Process for Inelastic Boltzmann Equations for Hard Spheres, Part I: The Cauchy Problem,* Journal of Statistical Physics volume 124, pages 655–702 (2006)

[27] V. Y. Prokhorov, (1965) *Convergence of random processes and limit theorems in probability theory,* Theory of Probability & Its Applications. 1 (2): 157–214. doi:10.1137/1101016

[28] G. Toscani, *Hydrodynamics from the dissipative Boltzmann equation,* Mathematical Models of Granular Matter, Lect. Notes in Math. 1937, Springer, Berlin–Heidelberg, 2008.

[29] I. Tristani, *Boltzmann equation for granular media with thermal force in a weakly inhomogeneous setting,* Journal of Functional Analysis, Volume 270, Issue 5, 1 March 2016, pp. 1922-1970

[30] C. Villani, *Topics in Optimal Transportation,* Graduate Studies in Math. 58, AMS, 2003.